

UNIVERSITY OF LJUBLJANA
BIOTECHNICAL FACULTY

Angelika VIŽINTIN

**ALTERNATIVE PULSE WAVEFORMS IN
ELECTROPORATION-BASED TECHNOLOGIES**

DOCTORAL DISSERTATION

Ljubljana, 2022

UNIVERSITY OF LJUBLJANA
BIOTECHNICAL FACULTY

Angelika VIŽINTIN

**ALTERNATIVE PULSE WAVEFORMS IN ELECTROPORATION-
BASED TECHNOLOGIES**

DOCTORAL DISSERTATION

**ALTERNATIVNE OBLIKE PULZOV V TEHNOLOGIJAH Z
ELEKTROPORACIJO**

DOKTORSKA DISERTACIJA

Ljubljana, 2022

Based on the Statute of the University of Ljubljana and the decision of the Biotechnical Faculty senate, as well as the decision of the Commission for Doctoral Studies of the University of Ljubljana adopted on December 8, 2020, it has been confirmed that the candidate meets the requirements for pursuing a PhD in the interdisciplinary doctoral programme in Biosciences, Scientific Field Cell Sciences. Prof. Dr. Damijan Miklavčič is appointed as supervisor and Dr. Mounir Tarek as co-advisor.

Doctoral dissertation was conducted at the Laboratory of Biocybernetics, Faculty of Electrical Engineering, University of Ljubljana.

Commission for assessment and defense:

President: Prof. Dr. Marko KREFT
University of Ljubljana, Biotechnical Faculty, Department of Biology

Member: Prof. Dr. Gregor SERŠA
Institute of Oncology Ljubljana

Member: Izr. Prof. Dr. Jure DERGANČ
University of Ljubljana, Faculty of Medicine

Date of defense: 22nd December 2022

Angelika Vižintin

KEY WORDS DOCUMENTATION

DN Dd

DC UDC 576.32(043.3)

CX electroporation, cell survival, membrane permeabilization, metal release, electrochemotherapy

AU VIŽINTIN, Angelika

AA MIKLAVČIČ, Damijan (supervisor), TAREK, Mounir (co-advisor)

PP SI-1000 Ljubljana, Jamnikarjeva 101

PB University of Ljubljana, Biotechnical Faculty, Interdisciplinary Doctoral Programme in Biosciences, Scientific Field Cell Sciences

PY 2022

TI ALTERNATIVE PULSE WAVEFORMS IN ELECTROPORATION-BASED TECHNOLOGIES

DT Doctoral dissertation

NO X, 105 p., 0 tab., 3 fig., 2 ann., 160 ref.

LA en

AI en/sl

AB The aim of this study was to compare standard eight 100 μ s pulses with alternative pulse waveforms (namely nanosecond and short high-frequency biphasic (H-FIRE) pulses) at different levels important for electroporation-based applications (extent of electrochemical reactions, time required for cell membrane resealing, decrease of cell survival and intracellular accumulation of chemotherapeutic agent after electrochemotherapy). By measuring the release of metal ions from the electrodes after electroporation, we confirmed the hypothesis that the use of H-FIRE and nanosecond pulses reduces electrochemical reactions even when the parameters of the electric field (amplitude, pause between pulses, ...) are adjusted to have the same biological effect as with longer monophasic pulses. Our second hypothesis, that electroporation of cells with different pulse shapes leading to comparable permeabilization of the cell membrane results in comparable oxidation of cellular components, could neither be confirmed nor refuted because it was shown that Click-iT Lipid Peroxidation Imaging Kit - Alexa Fluor 488 is not a suitable method for measuring lipid peroxidation in the first hours after electroporation. Our results show that nanosecond pulses with appropriately chosen parameters are suitable for use in electrochemotherapy with cisplatin and bleomycin, as they cause the same decrease in cell survival as with the standard eight 100 μ s pulses. We confirmed the hypothesis that electroporation with nanosecond pulses increases the amount of chemotherapeutic agent in the cell and consequently increases its cytotoxic effect.

KLJUČNA DOKUMENTACIJSKA INFORMACIJA

ŠD	Dd
DK	UDK 576.32(043.3)
KG	elektroporacija, celično preživetje, permeabilizacija membrane, sproščanje kovin, nanosekundni pulzi, elektrokemoterapija
AV	VIŽINTIN, Angelika
SA	MIKLAVČIČ, Damijan (mentor), TAREK, Mounir (somentor)
KZ	SI-1000 Ljubljana, Jamnikarjeva 101
ZA	Univerza v Ljubljani, Biotehniška fakulteta, Interdisciplinarni doktorski študijski program Bioznanosti, znanstveno področje Znanosti o celici
LI	2022
IN	ALTERNATIVNE OBLIKE PULZOV V TEHNOLOGIJAH Z ELEKTROPORACIJO
TD	Doktorska disertacija
OP	X, 105 str., 0 pregl., 3 sl., 2 pril., 160 vir.
IJ	en
JJ	en/sl

AI Cilj študije je bil primerjati standardnih osem 100 μ s pulzov z alternativnimi oblikami pulzov (in sicer nanosekundnimi in kratkimi visokofrekvenčnimi bipolarnimi (H-FIRE) pulzi) na različnih ravneh pomembnih za aplikacije, ki temeljijo na elektroporaciji (obseg elektrokemijskih reakcij, čas za zaceljenje celične membrane, zmanjšanje preživetja celic in znotrajcelično kopičenje kemoterapevtika po elektrokemoterapiji). Z merjenjem sproščanja kovinskih ionov z elektrod po elektroporaciji smo potrdili hipotezo, da uporaba H-FIRE in nanosekundnih pulzov zmanjšuje elektrokemijske reakcije tudi, ko so parametri električnega polja (amplituda, pavza med pulzi, ...) prilagojeni tako, da imajo enak biološki učinek kot daljši monopolarni pulzi. Naše druge hipoteze, da elektroporacija celic z različnimi oblikami pulzov, ki vodijo v primerljivo permeabilizacijo celične membrane, povzroči primerljivo oksidacijo celičnih komponent, nismo mogli niti potrditi niti ovreči, ker se je izkazalo, da Click-iT Lipid Peroxidation Imaging Kit - Alexa Fluor 488 ni ustrezna metoda za merjenje lipidne peroksidacije v prvih urah po elektroporaciji. Naši rezultati kažejo, da so nanosekundni pulzi s primerno izbranimi parametri primerni za uporabo v elektrokemoterapiji s cisplatinom in bleomicinom, saj povzročijo enako zmanjšanje celičnega preživetja kot z uporabo standardnih osmih 100 μ s pulzov. Potrdili smo hipotezo, da elektroporacija z nanosekundnimi pulzi poveča količino kemoterapevtika v celici in posledično poveča tudi njegov citotoksični učinek.

TABLE OF CONTENTS

	KEY WORDS DOCUMENTATION	III
	KLJUČNA DOKUMENTACIJSKA INFORMACIJA	IV
	TABLE OF CONTENTS	V
	TABLE OF CONTENTS OF SCIENTIFIC WORKS	VII
	LIST OF FIGURES	VIII
	LIST OF ANNEXES	IX
	ABBREVIATIONS AND SYMBOLS	X
1	PRESENTATION OF THE PROBLEM AND HYPOTHESES	1
1.1	ELECTROCHEMOTHERAPY	8
1.2	AIMS OF THE STUDY	9
1.3	RESEARCH HYPOTHESES	10
2	SCIENTIFIC WORKS	12
2.1	PUBLISHED SCIENTIFIC WORKS	12
2.1.1	Effect of interphase and interpulse delay in high-frequency irreversible electroporation pulses on cell survival, membrane permeabilization and electrode material release	12
2.1.2	Electroporation with nanosecond pulses and bleomycin or cisplatin results in efficient cell kill and low metal release from electrodes	27
2.1.3	Nanosecond electric pulses are equally effective in electrochemotherapy with cisplatin as microsecond pulses	40
2.2	REMAINING LINKING SCIENTIFIC WORK	51
2.2.1	Survival-permeabilization curves of B16F1 cells	51
2.2.2	Lipid peroxidation after electroporation	54
3	DISCUSSION AND CONCLUSIONS	58
3.1	DISCUSSION	58
3.1.1	Determination of equiefficient pulses	58
3.1.2	Release of metal from electrodes	61
3.1.3	Cell membrane resealing and lipid peroxidation	64
3.1.4	Electrochemotherapy with nanosecond pulses	66
3.2	CONCLUSIONS	72
4	SUMMARY (POVZETEK)	75
4.1	SUMMARY	75

4.2	POVZETEK	84
5	REFERENCES	94
	ACKNOWLEDGEMENTS	
	ZAHVALA	
	PRILOGE	

TABLE OF CONTENTS OF SCIENTIFIC WORKS

Vižintin A., Vidmar J., Ščančar J., Miklavčič D. 2020. Effect of interphase and interpulse delay in high-frequency irreversible electroporation pulses on cell survival, membrane permeabilization and electrode material release. *Bioelectrochemistry*, 134: 107523, doi: 10.1016/j.bioelechem.2020.107523: 14 p.

Vižintin A., Marković S., Ščančar J., Miklavčič D. 2021. Electroporation with nanosecond pulses and bleomycin or cisplatin results in efficient cell kill and low metal release from electrodes. *Bioelectrochemistry*, 140: 107798, doi: 10.1016/j.bioelechem.2021.107798: 12 p.

Vižintin A., Marković S., Ščančar J., Kladnik J., Turel I., Miklavčič D. 2022. Nanosecond electric pulses are equally effective in electrochemotherapy with cisplatin as microsecond pulses. *Radiology and Oncology*, 56, 3: 326–335

LIST OF FIGURES

Figure 1: Schematic representation of the mechanisms of electroporation. Figure adapted from (Kotnik and others, 2019).	4
Figure 2: Cell survival (triangles, dashed line) and cell membrane permeabilization (circles, solid line) of B16F1 cells after electroporation with (A) twenty-five 200 ns pulses with 10 Hz repetition rate, (B) one hundred 200 ns pulses with 10 Hz repetition rate, (C) one 400 ns pulse, (D) one hundred 400 ns pulses with 10 Hz repetition rate, (E) one 550 ns pulse, (F) twenty-five 550 ns pulses with 10 Hz repetition rate, (G) one hundred 550 ns pulses with 10 Hz repetition rate at different electric field strengths (E).	53
Figure 3: Lipid peroxidation of CHO cells measured with the Click-iT Lipid Peroxidation Imaging Kit - Alexa Fluor 488.	57

LIST OF ANNEXES

Annex A: Consent from publishers for the re-publication of the article entitled effect of interphase and interpulse delay in high-frequency irreversible electroporation pulses on cell survival, membrane permeabilization and electrode material release

Annex B: Consent from publishers for the re-publication of the article entitled Effect of interphase and interpulse delay in high-frequency irreversible electroporation pulses on cell survival, membrane permeabilization and electrode material release

ABBREVIATIONS AND SYMBOLS

ANOVA	analysis of variance
CHO	Chinese hamster ovary
cisplatin	cis-diamminedichloroplatinum (II)
DAMP	damage-associated molecular pattern
DMEM	Dulbecco's Modified Eagle Medium
EDTA	ethylenediaminetetraacetic acid
ESOP	Standard Operating Procedures of Electrochemotherapy
H-FIRE	high-frequency irreversible electroporation
MTS	3-(4,5-dimethylthiazol-2-yl)-5-(3-carboxymethoxyphenyl)-2-(4-sulfophenyl)-2H-tetrazolium
PBS	phosphate buffered saline
ROS	reactive oxygen species
SOD2	superoxide dismutase 2

1 PRESENTATION OF THE PROBLEM AND HYPOTHESES

Electroporation (also called electroporabilization or pulsed electric field treatment) is the phenomenon of increased cell membrane permeabilization due to exposure of cells/tissues to short high-voltage electric pulses which allows transmembrane transport of otherwise impermeant molecules (Kotnik et al., 2019). Electroporation is universal: it applies to all cell types (eukaryotic, bacterial, and archaeal) in any cell arrangement (in suspension, adherent to the surface, in clusters, or in tissue). Apart from cells it can also be observed in any other bilayer membrane system such as planar lipid bilayers, lipid vesicles, and polymeric vesicles (Rems and Miklavčič, 2016).

The current explanation of electroporation is based on the formation of water pores in the lipid bilayer as the main underlying mechanism. Molecular dynamics simulations indicate that the formation of the pore starts with the orientation of the polar molecules (water molecules, membrane phospholipids, ...) in the direction of the electric field. The orientation of polar molecules occurs very rapidly, in the range of a few picoseconds and is followed in the next microseconds by the redistribution of charges (ions in the intracellular and extracellular solution) so that they accumulate on both sides of the membrane (Tieleman, 2004; Tarek, 2005).

Water molecules oriented in the direction of the electric field connect together by hydrogen bonding to form small clusters. These clusters, called water fingers, grow in size and gradually penetrate the hydrophobic core of the lipid bilayer from the intracellular and extracellular sides until they come together and connect the two sides, forming a water column. Phospholipids in contact with the water molecules reorient by turning their polar heads toward the water column to “shield” the nonpolar tails from water molecules. The reorientation of the phospholipids stabilizes the pore, allowing more water molecules (and other polar molecules) to enter the water column (Tieleman, 2004; Tarek, 2005). When the electric field is no longer present, the pores begin to close. The closing of the pores occurs in reverse order to the analogous phases of pore formation (Kotnik et al., 2019).

While the time required for pore formation decreases exponentially with increasing electric field strength, the time required for pore closure is virtually independent of the electric field strength that triggered their formation - pore closure in lipid bilayers always takes a few tens to a few hundreds of nanoseconds in molecular dynamics simulations, suggesting that the pores are not stable (Levine and Vernier, 2010; Bennett et al., 2014). The estimated time required for the pores to close in the simulations is, however, several orders of magnitude shorter than the experimentally determined time required for membrane resealing (i.e., the time during which increased transmembrane transport is observed). In experiments,

increased permeability of the cell membrane was still observed minutes to hours after the electric field was no longer present, even when using pulses with a duration of only a few nanoseconds (Lopez et al., 1988; Teissié and Rols, 1994; Pakhomov et al., 2009) and was noted that it is temperature dependent (Teissié and Rols, 1994; Pakhomov et al., 2007b, 2007a; Pucihar et al., 2008; Muralidharan et al., 2021).

Electroporation pulses trigger the formation of extracellular and intracellular reactive oxygen species (ROS) (Gabriel and Teissié, 1994, 1995; Maccarrone et al., 1995b, 1995a; Nuccitelli et al., 2013). Oxidation of lipids due to exposure to electrical pulses, as those used in electroporation, alters the composition and properties of both lipid bilayers and cell membranes. Chemical changes in membrane lipids, particularly peroxidation, could explain the longer-lasting increased permeability of cell membranes observed experimentally after electroporation.

Lipid peroxidation is the oxidative degradation of lipids. It involves the formation and degradation of dioxygen adducts of unsaturated lipids called lipid hydroperoxides. The reaction is initiated by a strong oxidant (e.g., a hydroxyl radical) that sequesters the weakly bound allylic hydrogen from the lipid. Further degradation of hydroperoxides (the primary products of lipid peroxidation) produces many secondary products, e.g. aldehydes, ketones, alcohols, hydrocarbons, esters, furans, lactones, peroxides. The presence of oxidized lipids decreases the lipid order and leads to the lateral expansion and thinning of the bilayer, lowers the phase transition temperature, alters the hydration of the bilayer, increases the mobility of lipids and the frequency of flip-flop of lipids, affects the lateral phase organization, and promotes the formation of structural defects in membranes. Therefore, bilayers with oxidized lipids are significantly more permeable and conductive than non-oxidized bilayers (Sabatini et al., 2006; Wong-Ekkabut et al., 2007; Vernier et al., 2009; Runas and Malmstadt, 2015; Rems et al., 2019). It has been shown that the ROS concentration and extent of lipid peroxidation increase with increasing electric field intensity, pulse duration and pulse number in bacterial, plant, and animal cells, as well as in liposomes, and that lipid peroxidation is associated with increased cell membrane permeability, time required for membrane resealing, and cell damage (Benov et al., 1994; Gabriel and Teissié, 1994, 1995; Maccarrone et al., 1995b, 1995a; Breton and Mir, 2018).

Hydroperoxides (primary products of lipid peroxidation) are stable enough to be present in the lipid bilayer for some time after oxidation. In molecular dynamics simulations, even a small amount (about 1%) of hydroperoxides affects the conductivity of the bilayer. However, the increase in conductivity, i.e., permeability of the lipid bilayer to ions, due to the presence of hydroperoxides alone is too small to fully explain the experimentally determined values (Rems et al., 2019). On the other hand, phospholipids with aldehyde groups on acyl tails

(secondary products of phospholipid peroxidation) disrupt the lipid bilayer more than hydroperoxides. In both experiments and molecular dynamics simulations, a significant increase in membrane permeability was observed due to the presence of phospholipids with aldehyde groups, as well as the spontaneous organization of aldehydes into pores (Wong-Ekkabut et al., 2007; Cwiklik and Jungwirth, 2010; Lis et al., 2011; Boonnay et al., 2015; Runas and Malmstadt, 2015; Van der Paal et al., 2016; Wiczew et al., 2021). The pores formed as a result of the presence of lipid peroxidation products are not the same as those in a non-oxidized lipid bilayer under the influence of an electric field. In molecular dynamics simulations, pores formed from lipid peroxidation products with aldehyde groups remained open for several microseconds, and in the presence of cholesterol even longer – for the entire duration of the simulation (i.e. 5 μ s) (Wiczew et al., 2021).

Evidence for the effect of electroporation on proteins and its role in increasing membrane permeability can also be found in the literature. Electroporation causes reversible disruption of the three-dimensional filamentous structures of actin, tubulin, and intermediate filaments, but not degradation of monomeric proteins of cytoskeleton. Cytoskeletal proteins (actin filaments, intermediate filaments and microtubules) and related proteins affect membrane permeability - the formation and expansion of membrane pores and membrane resealing after electroporation (Graybill and Davalos, 2020). Submicrosecond pulses cause the opening of voltage-gated calcium channels via a mechanism that involves no formation of pore in the lipid part of the membrane, no heating, and no membrane depolarization via voltage-gated sodium channels (Craviso et al., 2010; Semenov et al., 2015; Burke et al., 2017). Microsecond pulses have been shown to open the Na⁺/K⁺-ATPase. In molecular dynamics simulations, pore formation was observed in the voltage-sensing domains of various voltage-gated channels when electric fields that induce electroporation were used (Rems et al., 2020; Ruiz-Fernández et al., 2021). Unfolding of the voltage-sensing domain and stabilization of the pore by membrane lipid heads followed the formation of the pore. Interestingly, such pores remained stable even significantly longer than pores formed in the lipid part of the membrane. It was concluded that the protein channel cannot spontaneously refold to its original conformation in case of a major perturbation of its native conformation (Rems et al., 2020).

Formation of pores in the lipid part of the membrane, chemical changes in membrane lipids and modulation of protein structure and function are all generally recognized as underlying mechanisms of increased membrane permeability observed during electroporation (Figure 1), however, they are not the only effects of electroporation on cells. Electroporation causes also influx of Ca²⁺ into the cytoplasm from the extracellular space and from internal stores, efflux of ATP and K⁺ from the cell, depolarization, osmotic imbalance and cell swelling, release of damage-associated molecular pattern (DAMP) molecules, activation of

various signaling pathways, changes in gene expression and synthesis of proteins, which activates various repair mechanisms, and can induce cell death, among other effects. All these changes in the permeabilized cell membrane, as well as all subsequent processes that are still active even when the increased permeability of the cell membrane is no longer observed, are referred to as the electroporome (Sözer et al., 2017)

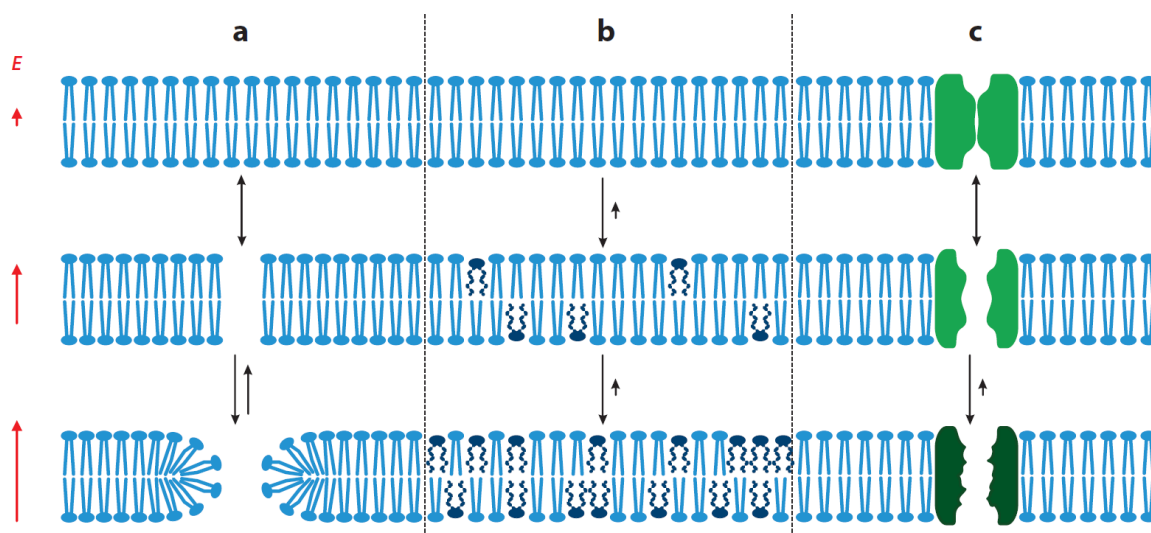


Figure 1: Schematic representation of the mechanisms of electroporation. (a) Formation of aqueous pores in the lipid bilayer due to the presence of an electric field. The process is shown here in only two stages for simplicity. First, a water column is formed. Second, the adjacent phospholipids reorient so that their polar heads face the water columns and form a metastable pore. (b) Electric pulses cause chemical changes in membrane lipids, including lipid peroxidation. This increases the permeability of the bilayer to water, ions, and other small molecules. (c) Electrically induced modulation of membrane protein structure and function is illustrated here for a voltage-gated channel. Electroporation causes opening of the channel and changes its native structure so that the channel can no longer perform its function. The electric field (E) is represented by red line arrows on the left side of the image, where the length of the line arrows corresponds to the electric field strength (i.e., the amplitude of the electric pulse(s)). The black line arrows represent the transition rate (the shorter the line arrow, the slower the transition rate) and are not drawn to scale for the three mechanisms of electroporation presented. Figure adapted from Kotnik and others, 2019.

Electroporation is used in various applications including (but not limited to) cell transfection/transformation, extraction of biomolecules and juices, inactivation of microorganisms in water and liquid foods, biomass drying, increasing freezing tolerance in the process of cryopreservation, cell fusion, tissue ablation and electrochemotherapy (Mahnič-Kalamiza et al., 2014; Kotnik et al., 2015; Geboers et al., 2020). Due to the wide range of applications, the goal of electroporation varies and depends on specific application. For example, in cell transfection/transformation or electrochemotherapy, the goal is to achieve high cell permeabilization and cell survival so that the desired molecule (a plasmid or chemotherapeutic agent) can enter the cells (Gehl, 2003). These applications are based on

reversible electroporation, i.e., when the cell membrane is only temporarily permeabilized and its integrity is eventually restored, and the cell survives. However, in applications such as tissue ablation or inactivation of microorganisms based on irreversible electroporation (i.e., pulse-induced cell death), electroporation should result in low survival of target cells (e.g. cancer cells or arrhythmogenic cells in the myocardium) or microorganisms (e.g., in water treatment or food pasteurization) (Jiang et al., 2015; Kotnik et al., 2015; Sugrue et al., 2019). In *in vitro* studies, the efficacy of electroporation is usually expressed either by the percentage of electroporated cells, the uptake of a particular molecule into the electroporated cells, or the cell survival (Pucihar et al., 2011). The efficacy of electroporation depends on several biophysical parameters: cell parameters defining cell geometry (cell shape and size) and their environment (osmotic pressure, temperature, conductivity of the medium, ...), and electric field parameters (pulse shape, electric field strength and direction, pulse/phase duration, interphase and interpulse delay, number of pulses/bursts, pulse/burst repetition frequency, ...). Cell parameters vary considerably between different cell types, media, tissues and organs and usually cannot be controlled *in vivo*. Therefore, in most cases, the efficacy of electroporation is controlled by the parameters of the electric field, which should be optimized for the specific cells, tissues, media, etc. being treated, as well as by the geometry and placement of the electrodes, which should ensure that the entire treated mass is exposed to a sufficiently high electric field (Reberšek and Miklavčič, 2010). Optimization of pulse parameters for electroporation is mainly performed empirically, while numerical modeling is used to support electrode/treatment chamber design and treatment planning in terms of optimization of electrode positioning and electric field parameter selection (Gerlach et al., 2008; Miklavčič et al., 2010; Županič et al., 2012). Efforts to optimize electroporation protocols are limited by the lack of understanding of the underlying mechanisms of membrane permeabilization and by the large number of variables (pulse parameters, biological differences, positioning of electrodes, ...).

Similar electroporation outcomes can be obtained using pulses with different parameters, i.e., equiefficient pulses. For example, using multiple shorter pulses at higher electric field strengths gives the same outcome as measured after electroporation with a longer pulse at a lower electric field strength (Pucihar et al., 2011). However, finding the right combination of pulse parameters for equiefficient pulses turned out to be a difficult task, as relying on simple relations between pulse parameters, such as using pulses with the same energy or total energized time, proved to be inefficient (Rols and Teissié, 1998; Canatella et al., 2001). Various authors attempted to identify the mathematical relationships between the pulse parameters of equiefficient pulses with a variety of functional dependencies between the pulse parameters, ranging from simple mathematical functions to more complicated mathematical expressions. The relatively large set of different mathematical formulas is due to the fact that the relationships between the parameters were determined in different

intervals of the pulse parameters and using different approaches – some were obtained experimentally, while others were derived from the theory of electroporation. Most studied only the relation between the pulse duration and amplitude, while some also explored the dependence of pulse amplitude on the number of pulses (Pucihar et al., 2011). Of the various pulse parameters, the effect of the delay between pulses, i.e., the pulse repetition rate, is one of the least understood (Pakhomova et al., 2011).

The pulses used in electroporation have a wide range of parameters. The oldest concept for generating electroporation pulses is the capacitor discharge circuit for generating exponentially decaying electric pulses. Later, square wave pulse generators were introduced to better control the electric field parameters. Pulse generators can also be designed to generate biphasic pulses (Reberšek and Miklavčič, 2011). In the early 2000s, new pulse generators were developed to produce nanosecond pulses with very high electric fields (Schoenbach et al., 2001). Pulses with shorter duration and biphasic pulses require the use of higher electric field strengths and/or a higher number of pulses to produce the same biological effect as longer duration pulses or monophasic pulses, respectively (Arena et al., 2011; Pucihar et al., 2011; Sano et al., 2014; Sweeney et al., 2016). Nevertheless, nanosecond and high-frequency biphasic pulses with a pulse duration of only a few microseconds have recently attracted a great deal of research interest because they mitigate several limitations that exist in conventional micro-millisecond range electroporation. Nanosecond pulses penetrate more easily into the cell interior, and have more profound effects on organelles than longer pulses of micro- and millisecond duration (Schoenbach et al., 1997, 2001; White et al., 2004; Tekle et al., 2005; Batista Napotnik et al., 2012; Nuccitelli et al., 2020). The use of pulses with high electric field strength but very short duration means that the energy transferred from the pulses to the treated area is very low and results in low heating (Schoenbach et al., 2001), minimizing the possibility of thermal damage, which is very important for sparing delicate structures in and around the treated area (Cornelis et al., 2020). Electroporation with nanosecond pulses showed induction of apoptosis and antitumor activity (Beebe et al., 2002; Nuccitelli et al., 2006). The excitation thresholds appear to be higher than the electroporation thresholds with nanosecond pulses (Rogers et al., 2004; Long et al., 2011; Pakhomov and Pakhomova, 2020; Kim et al., 2021; Gudvangen et al., 2022), implying that shortening the pulse duration to nanosecond pulses could reduce pulse-induced neuromuscular stimulation, which is an undesirable side effect in medical electroporation-based applications. Also, high-frequency biphasic pulses with pulse durations in the range of a few microseconds, known by the acronym H-FIRE which stands for high-frequency irreversible electroporation, have shown reduced muscle contractions compared with monophasic pulses (Arena et al., 2011; Siddiqui et al., 2016; Yao et al., 2017; Dong et al., 2018; Ringel-Scaia et al., 2019; Cvetkoska et al., 2022) and also appear to limit the likelihood of cardiac interference (O'Brien et al., 2019). Shortening the pulse duration and/or

using biphasic pulses limits electrochemical reactions that accompany the flow of electric current between the electrodes and the electrolyte (Kotnik et al., 2001; Morren et al., 2003; Saulis et al., 2015).

The electric field in electroporation procedures is established by delivering electric pulses through electrodes in contact with the medium/tissue. Electrodes for electroporation procedures are most often made of metal - for medical applications, electrodes made of stainless steel are usually used, in the food industry, electrodes are most often made of stainless steel, followed by titanium and platinum, while for research purposes the use of aluminum cuvettes is common (Breton and Mir, 2012; Pataro and Ferrari, 2020). When high-voltage electric pulses are delivered to cells in suspension, tissue or other medium (e.g. milk, orange juice, beer, ...), electrochemical reactions occur at the electrode-electrolyte interface. These electrochemical reactions lead to electrolysis of water, corrosion and fouling of the electrodes, generation of radicals, extreme local transient pH changes and even longer lasting changes in the pH of the entire treated solution, chemical changes in the treated product, evolution of gas bubbles and release of metal ions from the electrodes (Saulis et al., 2015; Pataro and Ferrari, 2020). The metal ions released from the electrodes during electroporation have various effects on the treated cells and products. They can precipitate nucleic acids and proteins in solutions (Stapulionis, 1999; Kooijmans et al., 2013) and affect the taste and mouthfeel of the treated beer (Evrendilek et al., 2004). Loomis-Husselbee et al. (1991) showed that Al^{3+} ions released from electrodes during electroporation affect the biochemistry of the exposed cells, namely it causes the conversion of inositol 1,3,4,5-tetrakisphosphate into inositol 1,4,5-trisphosphate, which then induces the release of Ca^{2+} from the internal stores of electroporated cells. To date, few studies have examined the effects of metal ions released from electrodes on electroporated and non-electroporated cells. However, certain metals ($\text{Fe}^{2+}/\text{Fe}^{3+}$, Ni^{2+}) have been reported to have a stronger effect on the viability of electroporated cells compared to non-electroporated cells (Kotnik et al., 2001; Košir et al., 2021). Released metal ions may also affect the methods we use to monitor electroporation, e.g., monitoring cell membrane permeabilization after electroporation with calcein, as metal ions (e.g. Fe^{3+} and Cu^{2+}) can form complexes with fluorescent dyes and quench their fluorescence (Pliquett and Gusbeth, 2000).

Experimental evidence is available showing that shortening the pulse duration limits electrochemical reactions and electrode corrosion (Friedrich et al., 1998; Morren et al., 2003), and that contamination with released metal ions can be largely reduced by using biphasic pulses instead of monophasic pulses (Kotnik et al., 2001). Therefore, it has been suggested that pulses with lower amplitudes, shorter pulse durations, or biphasic pulses could be used to reduce the extent of electrochemical reactions (Saulis et al., 2015). However, it remains unclear whether shortening the pulse duration and/or using biphasic

pulses while increasing the voltage (and/or number of pulses used) to achieve the same biological effect still reduces the electrochemical reactions.

1.1 ELECTROCHEMOTHERAPY

Electrochemotherapy is a local treatment of cancer that combines the use of membrane-permeabilizing high-voltage electric pulses delivered to the tumor with some standard chemotherapeutic agents with high intrinsic cytotoxicity for which the plasma membrane is a barrier to reach their intracellular target. The electric pulses are customarily delivered in trains of eight monophasic pulses of 100 μ s duration with 1 Hz or 5 kHz pulse repetition rate. The two most commonly used chemotherapeutic agents in electrochemotherapy are bleomycin and *cis*-diamminedichloroplatinum (II) (cisplatin) (Marty et al., 2006).

Electrochemotherapy entered medical practice after the publication of the European Standard Operating Procedures of Electrochemotherapy (ESOPE) for the treatment of cutaneous and subcutaneous tumors in 2006 (Mir et al., 2006). Its introduction into clinical trials and later into clinical practice was made possible by extensive basic research on mechanisms of action, selection of appropriate pulse parameters, screening of suitable drugs, *in vivo* studies on various animal models etc. Several mechanisms of action have been identified; the dominant one is believed to be the increased intracellular accumulation of the chemotherapeutic agent due to increased permeability of the cell membrane caused by the electric pulses (Miklavčič et al., 2014). Several fold potentiation of the cytotoxicity of bleomycin and cisplatin has been demonstrated *in vitro* (Mir et al., 1991; Jaroszeski et al., 2000) and confirmed *in vivo* in various animal tumor models and patients (Heller et al., 1995; Hyacinthe et al., 1999; Jaroszeski et al., 1997; Serša et al., 1995, Serša et al., 1998). Other mechanisms of electrochemotherapy have also been identified, including vascular effects and involvement of the immune response. Electrochemotherapy induces cell death of tumor vascular endothelial cells, resulting in decreased blood flow to the tumor (vascular disrupting effect) and also has a vasoconstrictor effect (known as “vascular lock”), which leads to a prolonged retention of the chemotherapeutic agent in the tumors due to reduced blood washout (Miklavčič et al., 2014). A local immune response has been shown to be necessary for a therapeutic effect following electrochemotherapy: electrochemotherapy causes the release of DAMPs and leads to immunological cell death, and T cells have been shown to be a crucial mediator of the local and systemic effects of electrochemotherapy (Bendix et al., 2022).

In the last fifteen years, the number of electrochemotherapy treatments for superficial tumors has sharply increased – for example, the consolidated indications for treatment with electrochemotherapy include superficial metastatic melanoma, skin tumors of the head and

neck, breast cancer, and Kaposi's sarcoma. New indications have also been added, such as deep-seated malignancies, treatment of skin metastases from visceral or hematologic malignancies, vulvar cancer, and some noncancer skin lesions (capillary vascular malformations and keloids) (Campana et al., 2019). Electrochemotherapy has gained broad acceptance primarily because of solid evidence of its mechanisms of action, efficacy in various tumor types, and its simplicity (it is easy to learn). Numerous studies have demonstrated its efficacy, tolerability, and high patient satisfaction. However, some side effects have also been reported - the most commonly reported are muscle contractions and unpleasant sensations (which can even be painful), mainly attributed the stimulation of peripheral nerves by the electric pulses (Kendler et al., 2013; Gehl et al., 2018). To overcome this limitation, new pulse protocols are being explored in electrochemotherapy, including high-frequency biphasic (H-FIRE) pulses (Scuderi et al., 2019; Pirc et al., 2021) and nanosecond pulses (Silve et al., 2012; Novickij et al., 2020; Tunikowska et al., 2020; Rembiałkowska et al., 2022). Reports on the use of nanosecond pulses in electrochemotherapy are promising: a decrease of cell survival has been observed *in vitro* and tumor regression *in vivo*. Although (irreversible) electroporation with nanosecond pulses alone showed antitumor activity (Beebe et al., 2002; Nuccitelli et al., 2006), the combination of nanosecond pulses and a chemotherapeutic agent results in more significant cell death than exposure to electric pulses alone (Silve et al., 2012; Rembiałkowska et al., 2022). Because electrochemotherapy is based on reversible electroporation, lower electric field strengths are required than with irreversible electroporation. However, the previously mentioned studies that have used nanosecond pulses in electrochemotherapy have not adequately investigated the effects of different nanosecond pulse parameters on the efficacy of reversible electroporation in combination with bleomycin and cisplatin. Therefore, it is still unclear what are the optimal pulse parameters of the nanosecond pulses for use in electrochemotherapy. From the previous work it is also not clear if nanosecond pulses can be as effective as with the standard eight 100 μ s pulses in electrochemotherapy. Because the underlying mechanisms of action in electrochemotherapy with nanosecond pulses have not yet been investigated, it remains unknown whether the mechanisms are the same as in conventional electrochemotherapy with the eight 100 μ s pulses.

1.2 AIMS OF THE STUDY

This study was designed as a comprehensive *in vitro* research with the general objective of comparing eight 100 μ s pulses, which are standardly used in electroporation-based applications, with newer, more recently introduced pulse waveforms (namely nanosecond and short high-frequency biphasic (H-FIRE) pulses) at different levels important for electroporation-based applications.

The study also had the following specific objectives:

1. To determine the parameters of the electric field of nanosecond and H-FIRE pulses that have an equivalent biological effect as the standard eight 100 μ s pulses in terms of cell membrane permeabilization and cell survival after electroporation (i.e., equiefficient pulse parameters).
2. To compare the extent of electrochemical reactions occurring at the electrode-electrolyte interface after the application of standard eight 100 μ s pulses with equiefficient nanosecond and H-FIRE electric pulses by measuring the concentration of metal ions released from the electrodes.
3. To gain new insights into the effect of specific electric field parameters on metal release from electrodes, which will contribute to the optimization of pulse protocols in electroporation-based applications where it is of particular interest to minimize electrochemical reactions associated with the delivery of high-voltage pulses at minimum (e.g., applications in food technology).
4. To determine whether it is possible to reduce the extent of metal release from electrodes (and other electrochemical reactions) by using shorter duration and/or biphasic pulses with higher electric field strengths that have the same biological effect as the standardly used eight 100 μ s pulses.
5. To understand whether the role of membrane component oxidation of the (particularly lipid peroxidation) in cell membrane permeabilization after electroporation is maintained at different pulse waveforms and whether the extent of lipid peroxidation of the membrane can be correlated with the time required for cell membrane resealing after electroporation.
6. To comprehensively evaluate the possibility of using nanosecond pulses in electrochemotherapy *in vitro* and also in other electroporation-based applications with the aim of introducing small to medium sized molecules into cells by varying different parameters of the electric field and measuring the outcomes of electrochemotherapy and comparing the efficacy with the standard eight 100 μ s pulses.
7. To investigate the underlying mechanisms of electrochemotherapy with nanosecond pulses by measuring the intracellular uptake of the chemotherapeutic agent after electroporation and the effects of the high-voltage electric pulses on the molecular structure of the chemotherapeutic agent.

1.3 RESEARCH HYPOTHESES

The following hypotheses were tested in the study:

1. The application of monophasic nanosecond pulses or high-frequency biphasic electric pulses with a few microseconds pulse duration in electroporation-based technologies reduces electrochemical reactions, but cell membrane electroporation at equiefficient pulse parameters is equivalent to the classical eight 100 μ s electric pulses.
2. Electroporation of cells with pulses of different parameters that permeabilize the cell membrane causes comparable oxidation of cellular components.
3. The combination of electroporation with nanosecond pulses and an anticancer active ingredient enhances its effect due to increased intracellular accumulation of the active ingredient.

2 SCIENTIFIC WORKS

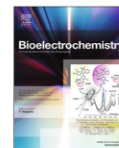
2.1 PUBLISHED SCIENTIFIC WORKS

2.1.1 Effect of interphase and interpulse delay in high-frequency irreversible electroporation pulses on cell survival, membrane permeabilization and electrode material release

Vižintin A., Vidmar J., Ščančar J., Miklavčič D. 2020. Effect of interphase and interpulse delay in high-frequency irreversible electroporation pulses on cell survival, membrane permeabilization and electrode material release. *Bioelectrochemistry*, 134: 107523, doi: 10.1016/j.bioelechem.2020.107523: 14 p.

To achieve high efficiency of electroporation and to minimize unwanted side effects, the electric field parameters must be optimized. Recently, it was suggested that biphasic high-frequency irreversible electroporation (H-FIRE) pulses reduce muscle contractions. However, it was also shown for sub-microsecond biphasic pulses that the opposite polarity phase of the pulse cancels the effect of the first phase if the interphase delay is short enough. We investigated the effect of interphase and interpulse delay (ranging from 0.5 to 10,000 μ s) of 1 μ s biphasic H-FIRE pulses on cell membrane permeabilization, on survival of four mammalian cell lines and determined metal release from aluminum, platinum and stainless steel electrodes. Biphasic H-FIRE pulses were compared to eight 100 μ s monophasic pulses. We show that a longer interphase and interpulse delay results in lower cell survival, while the effects on cell membrane permeabilization are ambiguous. The cancellation effect was observed only for the survival of one cell line. Application of biphasic H-FIRE pulses results in lower metal release from electrodes but the interphase and interpulse delay does not have a large effect. The electrode material, however, importantly influences metal release – the lowest release was measured from platinum and the highest from aluminum electrodes.

Supplementary data to this article can be found online at <https://doi.org/10.1016/j.bioelechem.2020.107523>.



Effect of interphase and interpulse delay in high-frequency irreversible electroporation pulses on cell survival, membrane permeabilization and electrode material release

Angelika Vižintin^a, Janja Vidmar^b, Janez Ščančar^b, Damijan Miklavčič^{a,*}

^a University of Ljubljana, Faculty of Electrical Engineering, Tržaška cesta 25, 1000 Ljubljana, Slovenia

^b Jožef Stefan Institute, Department of Environmental Sciences, Jamova cesta 39, 1000 Ljubljana, Slovenia

ARTICLE INFO

Article history:
Received 23 December 2019
Received in revised form 25 March 2020
Accepted 26 March 2020
Available online 30 March 2020

Keywords:
Electroporation
Cell survival
Membrane permeabilization
Metal release

ABSTRACT

To achieve high efficiency of electroporation and to minimize unwanted side effects, the electric field parameters must be optimized. Recently, it was suggested that biphasic high-frequency irreversible electroporation (H-FIRE) pulses reduce muscle contractions. However, it was also shown for sub-microsecond biphasic pulses that the opposite polarity phase of the pulse cancels the effect of the first phase if the interphase delay is short enough. We investigated the effect of interphase and interpulse delay (ranging from 0.5 to 10,000 μ s) of 1 μ s biphasic H-FIRE pulses on cell membrane permeabilization, on survival of four mammalian cell lines and determined metal release from aluminum, platinum and stainless steel electrodes. Biphasic H-FIRE pulses were compared to 8×100 μ s monophasic pulses. We show that a longer interphase and interpulse delay results in lower cell survival, while the effects on cell membrane permeabilization are ambiguous. The cancellation effect was observed only for the survival of one cell line. Application of biphasic H-FIRE pulses results in lower metal release from electrodes but the interphase and interpulse delay does not have a large effect. The electrode material, however, importantly influences metal release – the lowest release was measured from platinum and the highest from aluminum electrodes.

© 2020 Elsevier B.V. All rights reserved.

1. Introduction

Electroporation (also termed electropermeabilization or pulsed electric field treatment) is the phenomenon of increased cell membrane permeabilization due to exposure of cells/tissue to short electric pulses [1]. It is used in numerous applications including cell transfection/transformation, electrochemotherapy (ECT), tissue ablation, extraction of biomolecules from cells, inactivation of microorganisms in water and liquid foods [2–5]. Efficacy of electroporation depends on several physical and biological parameters. In electroporation-based applications, the electric field parameters like electric field strength, pulse shape, pulse duration, pulse polarity, delay between pulses and number of pulses must be adjusted to specific biomedical or biotechnological applications, i.e. to achieve specific electroporation objectives [6]. For example, in the case of cell transfection/transformation or ECT the aim is to achieve high cell permeabilization and high cell survival to allow the entry of the desired molecule (a plasmid or chemotherapeu-

tic agent) into the cells [7]. However, for tissue ablation or microbial inactivation, an efficient electroporation protocol results in low survival of the target cells (tumor or arrhythmogenic substrate) or microorganisms in food or water treatment [3,8,9].

In the past decade, irreversible electroporation (IRE) emerged as a new non-thermal ablation modality [10]. IRE is showing promising results in early clinical research of ablation of intra-abdominal tumors [11–13] and cardiac ablation [9,14–16]. During IRE treatment, electric pulses temporarily increase the semi-selective permeability of the cell membrane, thus allowing non-selective transport of molecules in and out of the targeted cells (through the compromised cell membrane). In IRE, different pulse parameters and delivery protocols are used in different studies. Most frequently, 70–100 pulses of 50–100 μ s duration and higher amplitude are used [8,17,18] compared to the standard eight 100 μ s pulses used in ECT [19]. In contrast to reversible electroporation, in IRE the membrane may reseal after the treatment, but the cell dies nevertheless. General anesthesia and the administration of neuromuscular blocking drugs are required in IRE to prevent pulse-induced muscle contractions [20] and pulse delivery must be synchronized with the electrocardiogram (ECG) to prevent the

* Corresponding author.
E-mail address: Damijan.Miklavcic@fe.uni-lj.si (D. Miklavčič).

induction of cardiac arrhythmias [21]. Recently, short biphasic pulses used for high-frequency irreversible electroporation (H-FIRE) have attracted considerable attention since they have shown reduced muscle contractions compared to treatments using monophasic pulses [22–26]. It also seems that H-FIRE limits the likelihood of cardiac interference [27]. In several studies, authors have shown that H-FIRE with short biphasic pulses necessitate higher amplitudes of pulses to be used, i.e. requiring higher electric field strengths compared to monophasic pulses to achieve the same biological effect—being it cell membrane permeabilization or cell kill [22,28–30]. At the same time, it was reported for nanosecond biphasic pulses that the opposite polarity phase of the pulse cancels the effect of the first phase if the interphase delay is short enough—a phenomenon called “cancellation effect”—which may explain why higher amplitudes are needed when using biphasic pulses. This cancellation effect was also observed in microsecond range of pulses, yet it is still not fully understood [31–35].

Another “side-effect” of electroporation are also electrochemical processes taking place at the electrode-electrolyte interface, such as electrolysis, generation of radicals and release of metal ions from the electrodes which results in electrode wear and fouling, sample contamination or/and chemical modification of the medium. Electrochemical processes occurring during the delivery of high-voltage electric pulses with an emphasis on food processing were described by Pataro et al. [36] and Saulis et al. [37]. These effects are often neglected although they change the composition of the electroporation medium, can affect cells or food that has been treated and even cause experimental errors [38–49]. On the other hand, the chemical interaction between the products of electrolysis and cells are exploited to cause cell death in electrolytic tissue ablation [50] and in the combination of electroporation and electrolysis (E2) [51].

Electrodes for electroporation procedures are most often made of aluminum, stainless steel or platinum [37]. Metal ions released from electrodes during electroporation can change the solution pH [43,49], precipitate proteins and nucleic acids [44,52], impact flavor and mouth feeling of treated food [47] and can be cytotoxic and/or affect the biochemistry of the exposed cells [42,45]. Released metal ions can also affect the methods we use to monitor electroporation, e.g. membrane permeabilization after electroporation with calcein since metal ions can form complexes with fluorescent dyes and quench their fluorescence [53]. Proposed strategies for reducing the intensity of electrochemical reactions include reduction of the voltage, shortening of the pulse duration, lowering of medium conductivity or the use of biphasic pulses [37]. It was confirmed experimentally that contamination with released metal ions can be largely reduced by using 100 μ s biphasic pulses instead of monophasic pulses [45] and that the shortening of the pulse limits electrochemical reactions and electrode corrosion [54]. However, when using shorter pulses, a stronger electric field (or higher number of pulses) must be applied to achieve the same electroporation efficiency [37,55]. It thus remains unclear whether shortening the pulse duration with concomitantly increased voltage reduces electrochemical reactions.

In this study, we investigated the effect of interphase delay and interpulse delay between biphasic pulses (i.e. pulse repetition rate) of 1 μ s symmetric rectangular biphasic H-FIRE pulses on cell membrane permeabilization and survival of CHO-K1 (Chinese hamster ovary), H9c2 (rat cardiomyoblast), C2C12 (mouse myoblast) and HT22 (mouse neuronal) cells. The interphase and interpulse delay ranged from 0.5 μ s to 10,000 μ s. We compared biphasic H-FIRE pulses to $8 \times 100 \mu$ s monophasic pulses widely used in ECT. For all pulses, the total energized time was 800 μ s. We show that not only longer interphase delay but also longer interpulse delay between biphasic pulses results in lower cell survival (i.e. in more

efficient cell kill) while the effects on cell membrane permeabilization are more ambiguous. The previously reported cancellation effect of the first phase of the pulse by the second was observed only for the survival of CHO cells. We also measured metal release from aluminum, platinum and stainless steel 304 wire electrodes. The electrode material has a big influence on the amount of released metal ions – we measured the lowest concentration of released ions from platinum electrodes and highest from aluminum electrodes. Our results suggest that contrary to cell survival and membrane permeabilization, the interphase and interpulse delay in the investigated range does not largely affect the concentration of released metal ions. We showed, however, that application of short biphasic H-FIRE pulses results in lower metal release from aluminum, platinum and stainless steel 304 electrodes compared to standard 100 μ s monophasic ECT and IRE pulses.

2. Materials and methods

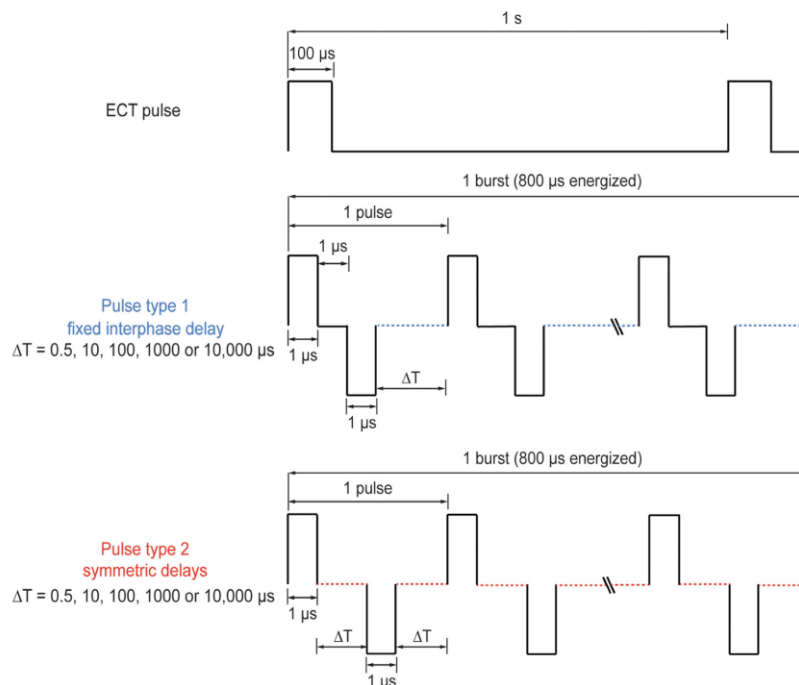
2.1. Electroporation set-up

We used a laboratory prototype pulse generator (University of Ljubljana), based on H-bridge digital amplifier with 1 kV MOSFETs (DE275-102N06A, IXYS, USA) [29], in the experiments. In cell membrane permeabilization, cell survival and metal release experiments, we applied 8 standard ECT rectangular pulses of 100 μ s duration with 1 Hz repetition rate or 1 burst of 400 biphasic H-FIRE rectangular pulses with the same amplitude (for all the total energized time was 800 μ s). 1 pulse in the case of H-FIRE pulses consists of the positive phase, negative phase and the interphase delay (see Schematic 1). The duration of the positive phase is 1 μ s and the duration of the negative phase is 1 μ s for all the H-FIRE pulses. For H-FIRE pulses, we varied the duration of the interphase delay and interpulse delay between pairs of biphasic pulses, and based on that named them as pulses of type 1 (fixed interphase delay) and type 2 (symmetric delays). For pulses of type 1 (fixed interphase delay), the interphase delay is fixed to 1 μ s, while the interpulse delay was set to 0.5, 10, 100, 1000 or 10,000 μ s. For pulses of type 2 (symmetric delays), the interphase and interpulse delay are of same duration: 0.5, 10, 100, 1000 or 10,000 μ s. The voltage and the electrical current were monitored in all experiments with the oscilloscope Wavesurfer 422 or Wavepro 7300A, differential voltage probe ADP305 and current probe CP030 or CP031A (all from Teledyne LeCroy, New York, USA). The voltage and current waveforms of some of the pulses are shown in Fig. 1. The measured voltage pulse shape looks very similar in the cell (1A, E) and metal release (cell-free) experiments (1B, F). However, the measured current pulse shape clearly looks different in the cell (1C, G) and the metal release experiments (1D, H).

Two different electrode configurations were used. For cell experiments, we used two parallel plate stainless steel 304 electrodes with distance between the inner edges of the electrodes set at 2 mm (Fig. 2A). In metal release experiments, we used two parallel rod-shaped wire electrodes with 1 mm diameter and distance between the inner edges of the electrodes set at 4 mm (Fig. 2B). The electrode materials were 99.999% aluminum (cat. no. AL005182, Goodfellow Cambridge, England, UK), 99.99% platinum (cat. no. PT005155, Goodfellow Cambridge) and stainless steel 304 (cat. no. FE225150, Goodfellow Cambridge) composed of 17–20% Cr, <2% Mn, 8–11% Ni, <800 ppm C and Fe balance.

2.2. Cell lines and cell culture

Chinese hamster ovary CHO-K1 cell line, obtained directly from the European Collection of Authenticated Cell Cultures (ECACC, cat. no. 85051005, mycoplasma free), was grown in 25 cm² culture



Schematic 1. Pulses used in the study. We applied 8 standard ECT pulses of 100 μs duration with 1 Hz repetition rate or 1 burst of 400 H-FIRE pulses (for all the total energized time was 800 μs). 1 pulse in the case of H-FIRE pulses consists of the positive phase, negative phase and the interphase delay. The duration of the positive phase is 1 μs and the duration of the negative phase is 1 μs for all H-FIRE pulses. For pulses of type 1 (fixed interphase delay) the interphase delay is 1 μs , while the interpulse delay between pairs of biphasic pulses is 0.5, 10, 100, 1000 or 10,000 μs . For pulses of type 2 (symmetric delays) the interphase delay and interpulse delay between pairs of biphasic pulses are of same duration: 0.5, 10, 100, 1000 or 10,000 μs .

flasks (TPP, Switzerland) in Nutrient Mixture F-12 Ham (cat. no. N6658, Sigma-Aldrich, Missouri, United States) for 2–4 days in an incubator (Kambič, Slovenia) at 37 °C and humidified atmosphere with 5% CO_2 . The growth medium (used in this composition through all experiments) was supplemented with 10% fetal bovine serum (FBS, cat. no. F9665, Sigma-Aldrich), 1.0 mM L-glutamine (cat. no. G7513, Sigma-Aldrich) and antibiotics: 1 U/ml penicillin/streptomycin (cat. no. P0781, Sigma-Aldrich) and 50 $\mu\text{g}/\text{ml}$ gentamycin (cat. no. G1397, Sigma-Aldrich). Rat cardiac myoblast cell line H9c2, obtained directly from ECACC (cat. no. 88092904, mycoplasma free), was grown in 75 cm^2 culture flasks (TPP) in Dulbecco's Modified Eagle Medium (DMEM, cat. no. D6546, Sigma-Aldrich) for 2–4 days in an incubator (Kambič) at 37 °C and humidified atmosphere with 10% CO_2 . The growth medium (used in this composition through all experiments) was supplemented with 10% FBS (cat. no. F2442, Sigma-Aldrich), 4.0 mM L-glutamine and antibiotics: 1 U/ml penicillin/streptomycin and 50 $\mu\text{g}/\text{ml}$ gentamycin. Mouse myoblast cell line C2C12, obtained directly from ECACC (cat. no. 91031101, mycoplasma free), was grown in 75 cm^2 culture flasks in Dulbecco's Modified Eagle Medium (DMEM, cat. no. D6546, Sigma-Aldrich) for 2–4 days in an incubator at 37 °C and humidified atmosphere with 10% CO_2 . The growth medium (used in this composition through all experiments) was supplemented with 10% FBS (cat. no. F9665, Sigma-Aldrich), 2.0 mM L-glutamine and antibiotics: 1 U/ml penicillin/streptomycin and 50 $\mu\text{g}/\text{ml}$ gentamycin. Mouse neuronal cell line

HT22, obtained directly from The Salk Institute for Biological Studies in California, USA, was grown in 25 cm^2 culture flasks in Dulbecco's Modified Eagle Medium (DMEM, cat. no. D5671, Sigma-Aldrich) for 2–3 days in an incubator at 37 °C and humidified atmosphere with 5% CO_2 . The growth medium (used in this composition through all experiments) was supplemented with 10% FBS (cat. no. F9665, Sigma-Aldrich), 2.0 mM L-glutamine and antibiotics: 1 U/ml penicillin/streptomycin and 50 $\mu\text{g}/\text{ml}$ gentamycin.

On the day of the experiment, cell suspension was prepared by detaching the cells with 1 \times trypsin-EDTA (cat. no. T4174, Sigma-Aldrich) diluted in 1 \times Hank's basal salt solution (cat. no. H4641, Sigma-Aldrich). Trypsin was inactivated by F-12 Ham (CHO) or DMEM (H9c2, C2C12 and HT22) complete growth medium. Cells were transferred to a 50 ml centrifuge tube (TPP) and centrifuged 5 min at 180 g and 23 °C. The supernatant was aspirated, and cells were re-suspended in the complete growth medium F-12 Ham (CHO) or DMEM (H9c2, C2C12 and HT22) which was used as electroporation buffer.

2.3. Cell survival

For cell survival experiments, cells were re-suspended at a cell density of 2×10^6 (CHO), 7.5×10^5 (H9c2), 1×10^6 (C2C12) or 9×10^5 (HT22) cells/ml. 50 μl of the cell suspension was transferred between plate stainless steel 304 electrodes, followed by pulse treatment (for the sham control no pulses were applied).

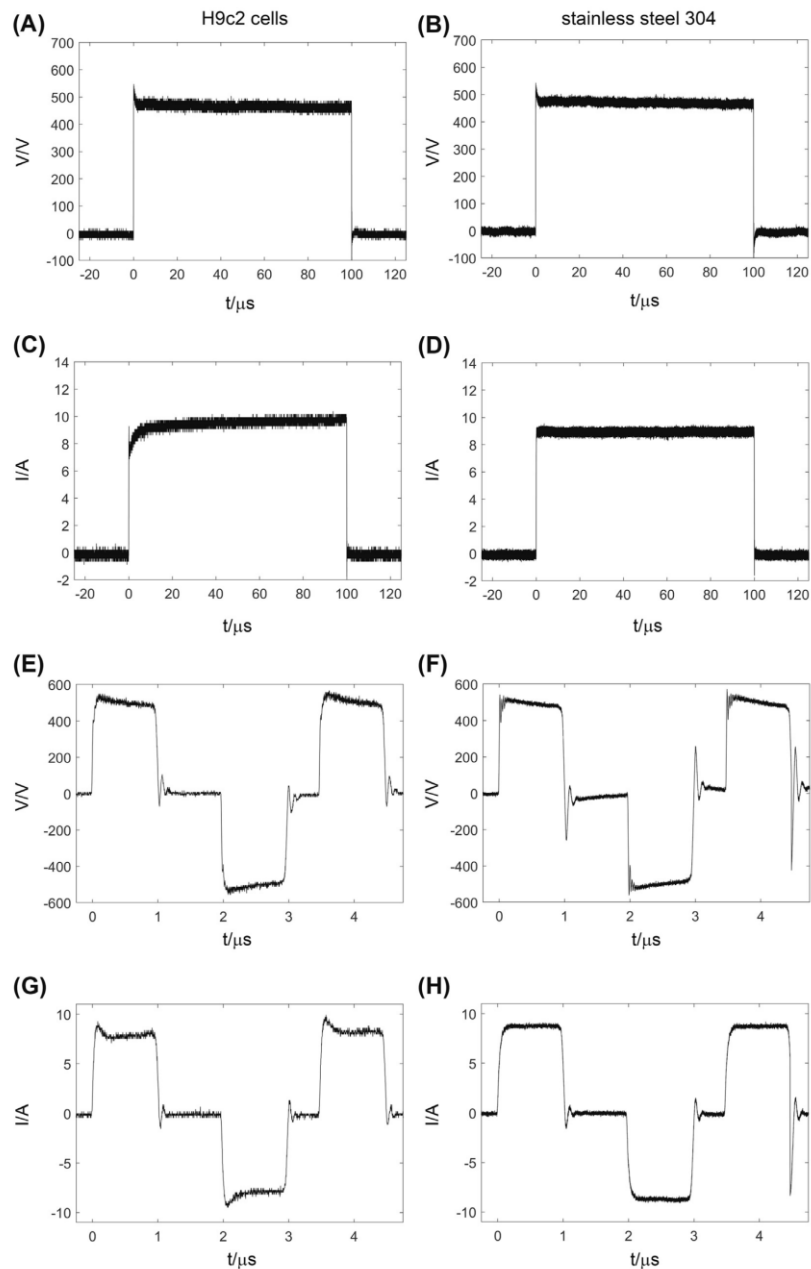
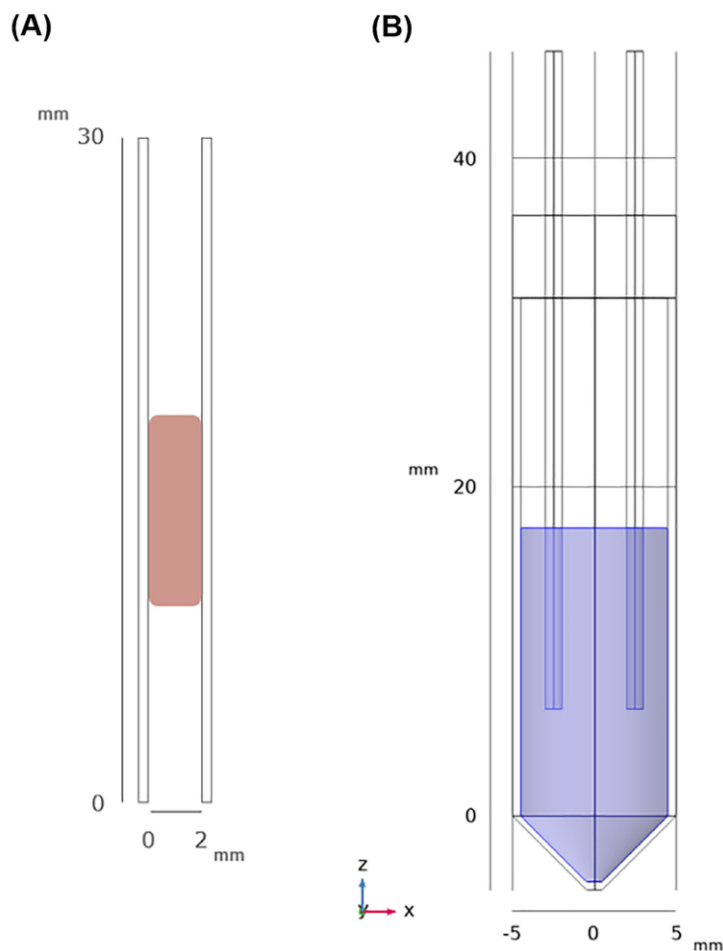


Fig. 1. Measured voltage and electrical current in (A, C, E, G) cell membrane permeabilization experiments with H9c2 cells and (B, D, F, H) metal release experiments with stainless steel 304 electrodes. (A, B, C, D) The first 100 μs pulse in the burst of $8 \times 100 \mu\text{s}$ monophasic pulses at 1 Hz repetition rate (ECT pulse, see Schematic 1) and (E, F, G, H) the first 4.75 μs of the burst of 1 μs biphasic pulses of type 1 (interphase delay = 1 μs) and interpulse delay of 0.5 μs . Note the different scales.



Schematic 2. Scheme of (A) plate electrodes used in cell experiments and (B) wire electrodes used in metal release experiments. (A) The electrodes are presented as white rectangles, the distance between the inner edges of the plate electrodes is 2 mm, the cell suspension between the electrodes is colored red. (B) The wire electrodes are shown as they were used in metal release experiments: immersed in a 2 ml microcentrifuge tube filled with 1.1 ml of 0.9% NaCl. The electrodes are presented as two rectangles and they are 4 mm (inner edge-inner edge) apart, the boundaries of the microcentrifuge tube are presented by a double grey line, the 0.9% NaCl solution is colored blue.

After pulse application, 40 μ l of the cell suspension was immediately transferred to a 1.5 ml microcentrifuge tube with 360 μ l of complete growth medium F-12 Ham (CHO) or DMEM (H9c2, C2C12 and HT22). The cell suspension was gently vortexed. Then, 100 μ l of the cell suspension was plated in a well of a flat bottom 96-well plate (TPP) in three technical repetitions. The plate was transferred to the incubator heated to 37 $^{\circ}$ C with 5% (CHO, HT22) or 10% (H9c2, C2C12) CO₂ for 24 h. Cell survival was assessed via the CellTiter 96[®] AQueous One Solution Cell Proliferation Assay (cat. no. G3580, Promega, Wisconsin, USA) which is a colorimetric method for determining the number of viable cells. The CellTiter 96[®] AQueous One Solution Cell Proliferation Assay contains the tetrazolium compound 3-(4,5-dimethylthiazol-2-yl)-5-(3-carboxymethoxyphenyl)-2-(4-sulfophenyl)-2H-tetrazolium (MTS) and the electron coupling reagent phenazine ethosulfate

(PES). The MTS is bioreduced by cells into a colored formazan product that is soluble in growth medium. The quantity of formazan product as measured by absorbance at 490 nm is directly proportional to the number of living cells in culture. 20 μ l of the CellTiter 96[®] AQueous One Solution Cell Proliferation Assay was added per well and after 2 h and 15 min incubation at 37 $^{\circ}$ C in incubator with 5% (CHO, HT22) or 10% (H9c2, C2C12) CO₂, the absorbance at 490 nm was measured with the spectrofluorometer Infinite[®] 200 (Tecan, Austria). The survival was calculated by first subtracting the absorbance of the blank (complete growth medium without cells) and then normalizing the average absorbance of the three technical repetitions of the sample to the absorbance of the sham controls. The experiments were repeated 3–5 times per each pulse treatment with different order of the pulse treatments.

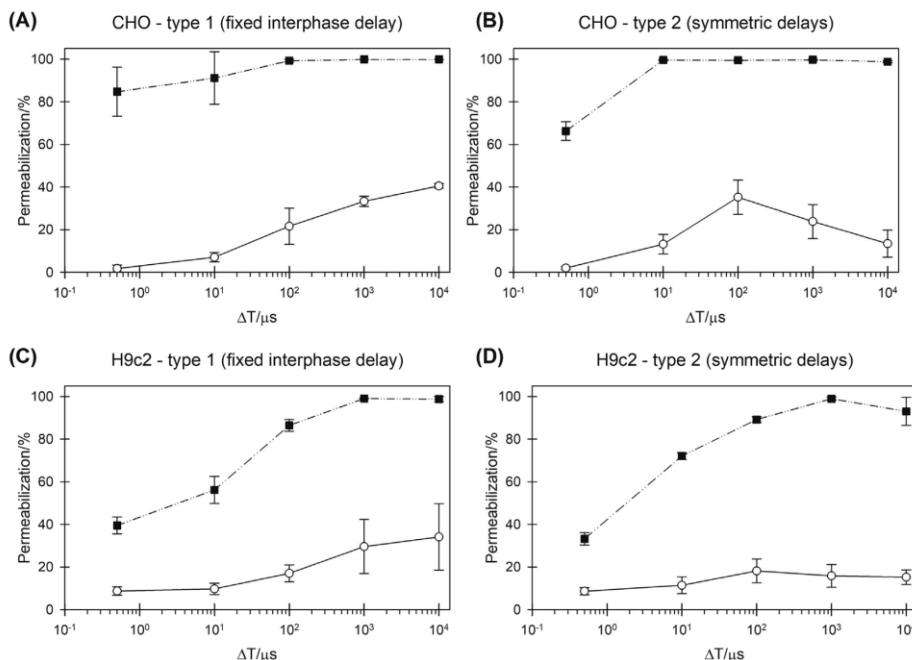


Fig. 2. Cell membrane permeabilization of CHO and H9c2 cells at different electric field strengths as a function of delay (ΔT) of biphasic H-FIRE pulses of (A, C) type 1 (fixed interphase delay) and (B, D) type 2 (symmetric interphase delay) (see Schematic 1). White circles and solid line represent the percentage of permeabilized cells at 1.5 kV/cm, black squares and dashed line represent the percentage of permeabilized cells at 2.5 kV/cm. Results are presented as an average of 3–5 repetitions. Bars represent standard deviation. Note the logarithmic scale on the horizontal axis.

2.4. Cell membrane permeabilization

For cell membrane permeabilization experiments, we used cells in suspension at a cell density of 2×10^6 (CHO) or 1×10^6 (H9c2, C2C12 and HT22) cells/ml. We wanted to use the same cell concentration as in cell survival experiments, however, we could not record 10,000 events on the flow cytometer if we used a concentration lower than 1×10^6 cells/ml. We thus decided to use 1×10^6 cells/ml for H9c2, C2C12 and HT22 cells. At this concentration, the cells should be sufficiently far apart from one another that they do not locally alter the electric field experienced by neighboring cells [56,57]. Right before application of electric pulses, the cell suspension was mixed with propidium iodide (PI, cat. no. P1304MP, Thermo Fisher Scientific, Massachusetts, USA) to final concentration of 136 μM . PI is a non-permeant fluorescent dye, which emits strong fluorescence after entering the cell and thus allows easy determination of cell electroporation and discrimination between electroporated and non-electroporated cells. 50 μl of the cells-PI mixture was transferred between plate stainless steel 304 electrodes, followed by pulse treatment. 40 μl of the treated cell suspension was transferred to a new 1.5 ml microcentrifuge tube. Three minutes after the last pulse, 150 μl of complete growth medium F-12 Ham (CHO) or DMEM (H9c2, C2C12 and HT22) was added to the cell suspension and the sample was gently vortexed and analyzed on the flow cytometer Attune NxT (Thermo Fisher Scientific). Cells were excited with blue-light laser at 488 nm, and the emitted fluorescence was detected through a 574/26 nm band-pass filter. The measurement was stopped when 10,000 events were acquired. The obtained data

was analyzed using the Attune NxT software (Thermo Fisher Scientific). Single cells were separated from all events by gating. The percentage of cells with permeabilized cell membrane was determined from the histogram of PI fluorescence. The experiments were repeated 3–5 times per each pulse treatment with different order of the pulse treatments. The sham control was handled in the same way as the samples with the exception that no pulses were delivered to the cell suspension.

2.5. Metal release

0.9% (w/v) NaCl in water solution was prepared from water for ultratrace analysis (cat. no. 14211, Sigma-Aldrich) and 99.999% pure NaCl (cat. no. 204439, Sigma-Aldrich). Before the application of each pulse treatment, aluminum, platinum or stainless steel 304 wire electrodes were cleaned with sonication in the ultrasonic bath Elmasonic P (Elma Schmidbauer, Germany) filled with 1% solution of the detergent Kemex A (Kemika, Croatia) in deionized water for 2 min at room temperature. After sonication, electrodes were first rinsed with deionized water and then with acetone (cat. no. 32201, Sigma-Aldrich) and let to dry in air. Electrodes were placed in a 2 ml microcentrifuge tube (ISOLAB, Germany) filled with 1.1 ml of 0.9% NaCl solution so that 11.5 mm of the electrodes was immersed in the 0.9% NaCl solution (see Schematic 2). After application of different H-FIRE biphasic or ECT monophasic pulses (see Schematic 1) with amplitude 500 V, 1 ml of the treated 0.9% NaCl solution was transferred to a new 15 ml centrifuge and 2.5 μl of 65% HNO_3 (Merck, Germany) was added. For the sham control, the electrodes were immersed in 0.9% NaCl solution for the

Table 1
 ICP-MS operating parameters for determination of elements.

Agilent 7700 ICP-MS		Agilent 8800 ICP-MS	
Parameter	Type/Value		
<i>Sample introduction</i>			
Nebulizer	Micromist		
Spray chamber	Scott		
Skimmer and sampler cone	Ni		
<i>Plasma condition</i>			
Forward power	1550 W		
Plasma gas flow	15.0 l min ⁻¹		
Carrier gas flow	0.95 l min ⁻¹	0.85 l min ⁻¹	0.95 l min ⁻¹
Dilution gas flow	0.15 l min ⁻¹	0.20 l min ⁻¹	0.10 l min ⁻¹
Sample depth	8.0 mm		
Cell gas flow	10 ml He min ⁻¹	/	10 ml He min ⁻¹
Energy discrimination	4.5 V	3.5 V	7.0 V
<i>Data acquisition parameters</i>			
Isotopes monitored	²⁷ Al	¹⁹⁵ Pt	⁵² Cr, ⁵⁵ Mn, ⁵⁶ Fe, ⁶⁰ Ni
Isotopes of internal standards	¹¹⁵ In	¹⁹³ Ir	¹⁰³ Rh

same duration as for other samples, but no pulses were applied. Experiments were performed in triplicates. For the 0.9% NaCl solution only, 5 µl of 65% HNO₃ was added to 2 ml of 0.9% NaCl solution in a 15 ml centrifuge. Samples were kept at 4 °C until analysis.

Total concentrations of Al, Pt, Fe, Ni, Cr and Mn in the analyzed samples were determined by inductively coupled plasma mass spectrometry (ICP-MS) against an external calibration curve. Concentrations of Al and Pt were determined on Agilent 7700 and those of Fe, Ni, Cr and Mn on Agilent 8800 ICP-MS instruments (Agilent Technologies, Tokyo, Japan). Optimized measurement parameters for the ICP-MS instruments are presented in Table 1. Calibration standard solutions of Al and Pt were prepared from Al stock solution (1000 µg Al ml⁻¹ in 2–3% HNO₃) and Pt stock solution (1000 µg Pt ml⁻¹ in 8% HCl), respectively, while calibration standard solutions of Fe, Ni, Cr and Mn were prepared from multi-element stock solution (containing 1000 µg/ml of each element in 6% HNO₃). All stock solutions were obtained from Merck (Germany). Calibration standards were prepared in 0.1% HNO₃ in the concentration range of 0.1–100 µg/l. The samples were, prior ICP-MS measurements, diluted 4-times with 0.1% HNO₃ for the determination of Fe, Ni, Cr and Mn and measured directly (without any dilution) for the determination of Al and Pt. All dilutions of the samples were made with ultrapure water (18.2 MΩ cm) obtained from a Direct-Q 5 Ultrapure water system (Millipore, Massachusetts, USA). To evaluate the accuracy of the ICP-MS analysis, the solution of 0.9% NaCl was spiked with standard solution containing all elements of interest to reach the final concentration of 10 µg/l in the spiked sample. Recoveries (the ratio between the measured and expected concentrations) were between 95% and 128% (N = 4) for all the elements – accuracy and precision of ICP-MS measurement for each element are listed in Table S1 in [Supplementary Material](#).

2.6. Statistical analysis

Levene's median test was used to assess equal variance and the Shapiro-Wilk test to test normality of data ($\alpha = 0.05$).

Analysis of cell survival and membrane permeabilization data was performed separately for all the cell lines. Cell membrane permeabilization data for C2C12 were, for statistical purposes, trans-

formed to a logarithmic scale to approximately conform to normality. Cell survival data for CHO and H9c2 and cell membrane permeabilization data for CHO and C2C12 were analyzed with analysis of variance (ANOVA). One factor was "pulse type" with two levels: type 1 (fixed interphase delay) and type 2 (symmetric delay), and the second factor was "delay" with five levels: 0.5, 10, 100, 1000 or 10,000 µs. Where statistically significant interaction or influence of one factor exists, Tukey's multiple comparison test was performed to test pairs of averages among treatments ($\alpha = 0.05$). Cell survival data for C2C12 and HT22 cells and cell membrane permeabilization data for H9c2 and HT22 cells were analyzed using the nonparametric Kruskal–Wallis test and p-values were adjusted with the post-hoc Holm method test ($\alpha = 0.05$) because the assumptions of the ANOVA were not met.

Metal release data were compared separately for Al, Pt, Fe, Mn, Cr and Ni. The concentration of released Al, Fe and Ni was, for statistical purposes, transformed to a logarithmic scale to approximately conform to normality and analyzed with one-way ANOVA. Tukey's multiple comparison test was performed to test pairs of averages among treatments ($\alpha = 0.05$). The concentration of released Pt, Cr and Mn was analyzed with the nonparametric Kruskal–Wallis test and p-values were adjusted with the post-hoc Holm method test ($\alpha = 0.05$) because the assumptions of the ANOVA were not met.

Data were processed and visualized using Microsoft Excel 2016, SigmaPlot 11.0 and R 3.5.2 [58].

3. Results

3.1. Membrane permeabilization and cell survival

First, we measured cell membrane permeabilization and cell survival of CHO and H9c2 cells after exposure to different pulses at two different electric field strengths (Fig. 2). In order to compare the effects of the delay, we opted for an electric field strength – where the differences between pulse treatments were most pronounced. In the case of membrane permeabilization, that value was determined to be 1.5 kV/cm – with increasing the electric field strength we achieved >90% membrane permeabilization with the majority of pulse treatments and thus the differences between pulses became less evident (or even undetectable). For cell survival, we chose to set the electric field strength at 2.5 kV/cm because at lower strengths we did not achieve a decrease in survival (data not shown).

Cell membrane permeabilization increased with increasing the delay of type 1 (fixed interphase delay) pulses, while for pulses of type 2 (symmetric delays) no increase or even a decrease was observed when pulses with delay of 1000 or 10,000 µs were used for all tested cell lines (Fig. 3). Because of the previously reported cancellation effect of the first phase by the second, we would expect that pulses of type 1 (which have a fixed interphase delay of 1 µs) are equivalent (i.e. permeabilize the same portion of the cells) as pulses of type 2 (symmetric delays) with short interphase delay. Prolonging the interphase delay in pulses of type 2, however, should abolish the "cancellation effect" making pulses of type 2 (symmetric delays) more efficient than pulses of type 1 (fixed interphase delay) [59]. For cell membrane permeabilization, we thus did not observe "cancellation effect" irrespective of the tested cell line. For all four cell lines, we measured lower permeabilization when cells were treated with pulses of type 2 (symmetric delays) of longer delays compared to type 1 (fixed interphase delay). Exposure to monophasic 8 × 100 µs pulses of the same electric field strength (1.5 kV/cm) resulted in > 99% permeabilized cells (data not shown), which indicates that biphasic H-FIRE pulses are less effective for membrane permeabilization (consistent with previous report by Sweeney et al. [29]).

The survival of all four cell lines decreased when increasing the interphase and/or interpulse delay (Fig. 4). When increasing the delay, the total duration of the burst is increased, while the pulse repetition rate is lowered. In other words, cell survival decreased at lower pulse repetition rates. Only for CHO cells, survival was significantly lower for pulses of type 2 (symmetric delays) with 1000 μ s interphase delay or longer compared to type 1 (fixed interphase delay). This is in agreement with the “cancellation effect” according to which pulses with longer interphase delay are expected to be more effective (i.e. result in lower cell survival). The lowest survival (6.0% for CHO, \sim 2.0% for H9c2, \sim 5.0% for C2C12 and 1.3% for HT22) was achieved with monophasic 8×100 μ s pulses of the same electric field strength (2.5 kV/cm) (data not shown) thus suggesting that 1 μ s biphasic H-FIRE of the same total duration (i.e. 800 μ s) are less effective also in terms of reducing cell survival, i.e. cell kill. In other words, higher electric field strengths are needed to achieve the same biological effect when using biphasic H-FIRE pulses compared to standard ECT/IRE monophasic pulses of the same cumulative duration.

The biphasic H-FIRE pulses that most effectively permeabilized the cell membrane at 1.5 kV/cm, however, were not the most effective ones in terms of decreasing the cell survival at 2.5 kV/cm. For example, for CHO cells statistically significant higher membrane permeabilization was achieved after treatment with type 1 (fixed interphase delay) pulse with 10,000 μ s delay (40.5%) than type 2 pulse (symmetric delays) with 10,000 μ s delay which permeabilized 13.5% of cells. Treatment with the respective type 2 (symmetric delays) pulse, however, resulted in significantly lower cell survival (19.2%) compared to the type 1 (fixed interphase delay) pulse (48.7%). Membrane permeabilization of CHO cells after

application of the type 2 (symmetric delays) pulse with 10,000 μ s delay was significantly lower even than with the type 2 (symmetric delays) pulse with 100 μ s delay (35.2%). However, the type 2 (symmetric delays) pulse with 100 μ s delay did not decrease the cell survival at all, while the application of type 2 (symmetric delays) pulse with 10,000 μ s delay resulted in 19.2% cell survival.

3.2. Metal release

We also measured the concentration of released Al ions from wire electrodes made from pure aluminum, concentration of released Pt from platinum wire electrodes and concentration of released Fe, Cr, Mn and Ni ions from stainless steel 304 wire electrodes in 0.9% (w/v) NaCl solution after delivery of different pulses (biphasic H-FIRE or monophasic ECT). As reported in Table S2 in the [Supplementary Material](#), the metal ions of interest were detected also in the sham control sample in which the electrodes were immersed in the 0.9% NaCl solution only for a few seconds and no pulses were applied. For all the different pulse treatments, the lowest concentration of all measured metal ions was measured from platinum electrodes followed by stainless steel 304 electrodes and aluminum electrodes (Table S2 in [Supplementary Material](#) and Fig. 5). Significantly higher concentration of released Al from aluminum electrodes and Fe and Ni from stainless steel 304 electrodes was detected after treatment with 8×100 μ s monophasic pulses than any of the biphasic H-FIRE pulses (Table S3, S5 and S8 in [Supplementary Material](#)). Although the measured Pt from platinum electrodes after treatment with ECT monophasic pulses was approximately 10 to 100 times higher than after the application of biphasic H-FIRE pulses, the differences are statistically sig-

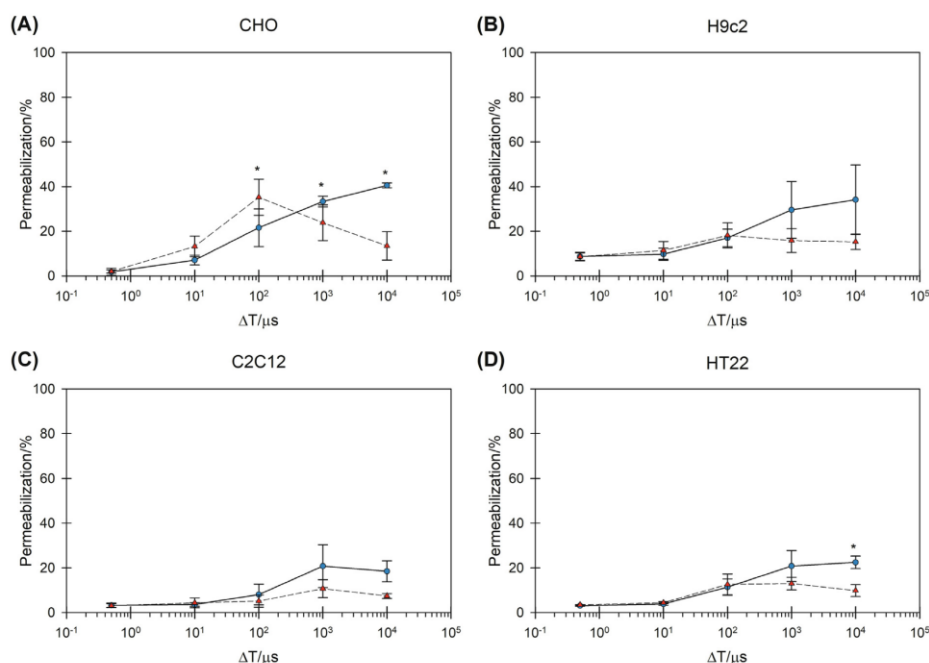


Fig. 3. Cell membrane permeabilization of (A) CHO, (B) H9c2, (C) C2C12 and (D) HT22 cells at 1.5 kV/cm as a function of delay (ΔT) of H-FIRE pulses. Blue circles and solid line represent pulses of type 1 (fixed interphase delay), red triangles and dashed line represent pulses of type 2 (symmetric delays) (see [Schematic 1](#)). Results are presented as an average of 3–5 repetitions. Bars represent standard deviation, asterisks (*) represent statistically significant ($p < 0.05$) difference between type 1 (fixed interphase delay) and type 2 (symmetric delays) pulses with the same delay. Note the logarithmic scale on the horizontal axis.

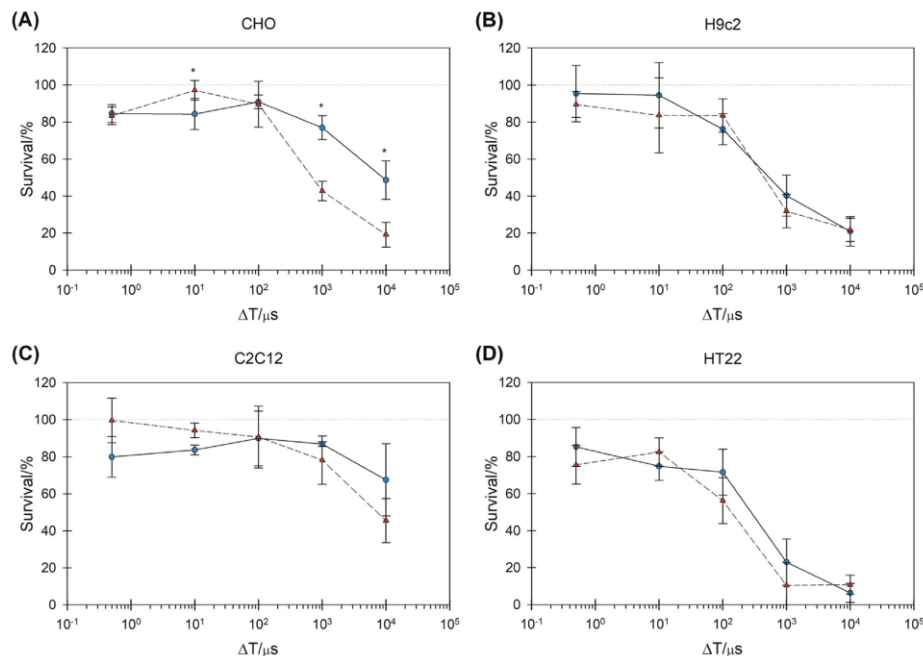


Fig. 4. Cell survival of (A) CHO, (B) H9c2, (C) C2C12 and (D) HT22 cells at 2.5 kV/cm as a function of delay (ΔT) of H-FIRE pulses. Blue circles and solid line represent pulses of type 1 (fixed interphase delay), red triangles and dashed line represent pulses of type 2 (symmetric delays) (see Schematic 1). Results are presented as an average of 3–5 repetitions. Bars represent standard deviation, asterisks (*) represent statistically significant ($p < 0.05$) difference between type 1 (fixed interphase delay) and type 2 (symmetric delays) pulses with the same delay. Note the logarithmic scale on the horizontal axis.

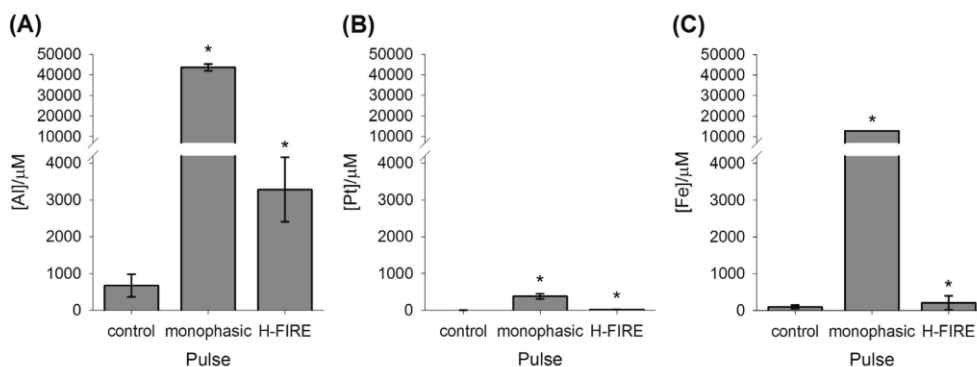


Fig. 5. Concentration of released (A) Al ions from aluminum wire electrodes, (B) Pt ions released from platinum wire electrodes and (C) Fe ions from stainless steel 304 wire electrodes in 0.9% NaCl solution determined by ICP-MS. The concentration of metal ions was measured after the electrodes were only immersed in the 0.9% NaCl solution (control), after delivery of $8 \times 100 \mu\text{s}$ monophasic pulses (monophasic) with 500 V amplitude and after the delivery of a burst of 400 type 1 (interphase delay fixed at $1 \mu\text{s}$) biphasic H-FIRE pulses with 10,000 μs interpulse delay with amplitude 500 V (H-FIRE). Results are presented as an average of 3 repetitions. Bars represent standard deviation, asterisks (*) represent statistically significant difference ($p < 0.05$) to control. Note the scale break.

nificant only between certain biphasic H-FIRE pulses and the ECT monophasic pulses (Table S2 and S4 in [Supplementary Material](#)). The interphase and interpulse delay did not have a significant effect on metal release from aluminum or from stainless steel 304 electrodes (Table S3, S5, S6, S7 and S8 in [Supplementary Material](#)). For platinum electrodes, however, significantly higher metal

release was measured after the application of biphasic H-FIRE pulses with longer interphase and interpulse delay compared to biphasic H-FIRE pulses with shorter delays. For pulses of type 1 (fixed interphase delay) with 1000 and 10,000 μs interpulse delay and type 2 (symmetric delays) pulse with 1000 μs interphase and interpulse delay, we measured more Pt than for other H-FIRE

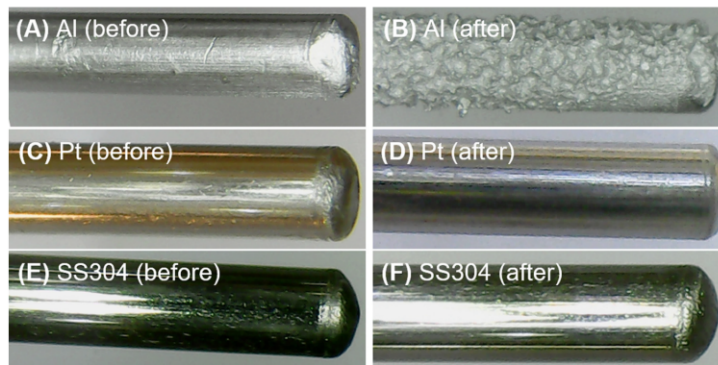


Fig. 6. Pictures of aluminum, platinum and stainless steel 304 wire electrodes (A, C, E) before and (B, D, F) after delivery of biphasic H-FIRE and monophasic ECT pulses in metal release experiments.

pulses (Table S2 and Table S4 in [Supplementary Material](#)). Electrode corrosion after pulse delivery was apparent for the aluminum electrodes (Fig. 6).

4. Discussion

The aim of this study was to investigate the effect of the interphase delay and interpulse delay between pairs of biphasic pulses (i.e. pulse repetition rate) of symmetric 1 μ s rectangular H-FIRE pulses on cell membrane permeabilization, cell survival/cell kill of four different cell lines—CHO (Chinese hamster ovary), H9c2 (rat cardiomyoblast), C2C12 (mouse myoblast) and HT22 (mouse neuronal)—and release of metal ions from aluminum, platinum, and stainless steel 304 electrodes.

4.1. Cell survival and membrane permeabilization

We showed on four cell lines that it is possible to increase the effectiveness (i.e. achieve lower cell survival) of short biphasic H-FIRE pulses by increasing the interphase and interpulse delay, i.e. reducing pulse repetition rate. This is in agreement with previous reports that lower pulse repetition rates are more effective [60–62] and also with the findings of Arena et al. [22] that the addition of a delay between the positive and negative phase in H-FIRE pulses results in more efficient cell kill. However, even biphasic H-FIRE pulses with longer delays were less effective than $8 \times 100 \mu$ s monophasic pulses, requiring the use of higher electric field strengths to achieve the same biological effect. For CHO cells, we showed that the previously reported cancellation effect of the positive phase by the negative phase [29,31,35,59] exists for cell survival for interphase delay of up to 100–1000 μ s. Pulses of type 2 with interphase delays of 0.5, 10 or 100 μ s were no more effective (i.e. they did not decrease the cell survival) than pulses of type 1 (with 1 μ s of interphase delay). However, when prolonging the interphase delay of pulses of type 2 (symmetric delays) to 1000 and 10,000 μ s and keeping the interphase delay of type 1 pulses at 1 μ s, the “cancellation effect” was abolished and pulses of type 2 became more effective than pulses of type 1. We did not observe the cancellation effect for cell survival with the three other tested cell lines (H9c2, C2C12 and HT22). However, knowing the composition of the electroporation medium can influence the response of the cells to the electric pulses [63–65], it is important to note that

the cells were electroporated in different media (CHO in F-12 Ham and the others in variations of the DMEM medium).

The effect of the interphase and interpulse delay on membrane permeabilization on the other hand seems to be more complex. The shape of the permeabilization curve (Fig. 3) is surprisingly different from the previously reported cancellation effect for biphasic nanosecond and microsecond pulses [31,34,35,59] since we observed lower membrane permeabilization with pulses of type 2 (symmetric delays) of longer interphase delays (1000 or 10,000 μ s) than pulses of type 1 with 1 μ s interphase delay. Our results also suggest that higher membrane permeabilization does not always result in lower cell survival and vice versa that low cell survival is not necessarily a consequence of high membrane permeabilization. This indicates a more complex interplay between membrane permeabilization and cell survival and suggests that cell survival is affected also by other factors besides membrane permeabilization.

The majority of previous studies has focused on the use of biphasic H-FIRE pulses for tissue ablation [22,23,25]. Tissue ablation is based on irreversible electroporation and thus an effective protocol must result in low cell survival. Recently, short biphasic H-FIRE pulses have also been explored for use in ECT [30]. ECT is based on reversible electroporation and the authors have shown *in vitro* that is possible to use also biphasic H-FIRE pulses (which they named high frequency electroporation (HF-EP) pulses) for cisplatin ECT—but again with higher electric field strengths than the commonly used $8 \times 100 \mu$ s monophasic pulses. Our results suggest that for ECT and other applications based on reversible electroporation also 1 μ s biphasic H-FIRE pulses with interphase delay of up to 100–1000 μ s can be used since we achieved high membrane permeabilization without decrease in cell survival with their application.

H-FIRE pulses have attracted attention because it has been shown that their application results in reduced pain and muscle contractions compared to monophasic pulses of the same amplitude. The results of a numerical model study [66] indicate that it is possible to avoid nerve stimulation with the use of bursts of short biphasic pulses which achieve the same IRE efficacy as conventional 100 μ s monophasic pulses because the stimulation thresholds raise faster than the irreversible electroporation thresholds. However, higher electric field strength is required to achieve the same effect as with monophasic pulses. It thus remains to be tested also experimentally if pain and muscle contractions remain reduced when using biphasic H-FIRE pulses at amplitudes that pro-

duce the same biological effect as monophasic pulses. Reduced muscle contraction was so far shown after the application of biphasic pulses of 1, 2, 5 or 10 μs duration of each phase and symmetric interphase delay and interpulse delay between biphasic pulses of 2 or 5 μs [22,23,25,26]. It would be thus necessary to test pulse-induced muscle contractions with the application of biphasic H-FIRE pulses of longer interphase and interpulse delays to see if such pulses do not cause more intense contractions.

4.2. Metal release

This is the first report of metal release from aluminum, platinum and stainless steel 304 wire electrodes after treatment with short biphasic H-FIRE pulses. We opted for electrodes made from pure aluminum in the absence of specification of material from which commercial aluminum cuvettes are made. The amount of metal release depends largely on the particular electrode material—the measured concentration of Al ions from aluminum electrodes was higher than the concentration of released Fe from stainless steel 304 and both were higher than the measured concentration of Pt from platinum electrodes. However, the application of some pulses resulted in higher concentration of released Pt from platinum electrodes than Cr and Mn from stainless steel 304 electrodes. The highest measured concentration of Pt ions from platinum electrodes (after the application of monophasic $8 \times 100 \mu\text{s}$ pulses) was lower than the lowest measured concentration of Al ions released from aluminum electrodes (in sham control samples in which the electrodes were only immersed in the 0.9% NaCl solution and no pulses were delivered). In agreement with previous reports [45], the application of biphasic H-FIRE pulses resulted in significantly lower metal dissolution compared to monophasic $8 \times 100 \mu\text{s}$ pulses for aluminum and stainless steel 304 electrodes, however, for platinum electrodes the metal release after application of biphasic H-FIRE pulses was not always statistically significant lower than for monophasic $8 \times 100 \mu\text{s}$ pulses. Different delays of the 1 μs biphasic H-FIRE pulses did not result in significant differences in concentrations of released metals from aluminum and stainless steel 304 electrodes in the range of pulse parameters tested. However, more Pt ions were detected after biphasic H-FIRE pulses of type 1 (fixed interphase delay) and type 2 (symmetric delays) pulses with longer delays were applied compared to biphasic H-FIRE pulses with shorter delays. Additional work is needed to explain how the delays affect the release of Pt.

We measured an increase (although not statistically significant for some of the tested metals) in concentration of metal ions also in sham control sample where electrodes were only immersed in 0.9% NaCl solution and no pulses were delivered. This metal release could be explained by the fact that when an electrode is placed into an electrolyte, a so-called double layer is formed immediately, even if no external voltage is applied. The double layer consists of a layer of charged particles and/or orientated dipoles that exist at the electrode-electrolyte interface. Chemical reactions occur immediately and electrons are transferred between the electrode and the electrolyte which results in formation of an electric field between the electrode and the layer of ions that influences further chemical reactions and promotes oxidation reactions [54].

The differences in concentrations of Fe, Cr, Mn and Ni determined after the delivery of the same pulse with the stainless steel 304 electrodes are probably related to different concentrations of elements in stainless steel 304 and differences in standard potentials of reduction half reactions. The stainless steel 304 wire from which our electrodes were made is, according to manufacturer's specification, composed of 18% Cr, 10% Ni, <2% Mn, <800 ppm C and the rest is Fe. We measured the concentration of Fe, Cr, Ni and Mn. After the delivery of $8 \times 100 \mu\text{s}$ monophasic pulses, the highest concentration of Fe ions was measured followed by Cr, Ni

and Mn (proportional to the stainless steel 304 composition). However, after the application of biphasic H-FIRE pulses, we detected a similar concentration of released Cr and Mn, slightly higher concentration of released Ni and the highest concentration of Fe, which is not proportional neither to the stainless steel 304 composition or to the standard potentials of the oxidation reactions. Further work would be needed in order to understand the effect of different pulses on the concentration of released metals.

The medium in which metal release experiments were performed was a pure 0.9% NaCl solution in water. We are aware that such solution does not mimic real-life electroporation media or tissue, however, it allowed us to detect very small amounts of metal ions. In preliminary metal release experiments, we used growth medium F-12 Ham (data not shown), however, this medium already contains some metals, especially Fe and Mn, in concentrations of several orders of magnitude higher than the concentrations of released metal ions from electrodes measured in our experiments.

A limitation in our study was that we used electrodes of different geometry for the cell experiments (plate electrodes) and metal release experiments (wire electrodes) resulting also in different contact surface and current densities. The contact surface for the plate electrodes is approximately 1.5 times smaller than for wire electrodes, resulting in an approximately 1.5 times larger current density for plate electrodes. While the plate electrodes provide a relatively homogeneous field in the suspension, the field is nonhomogeneous when wire electrodes are used. We still believe that the following conclusion based on our results is valid: for biphasic H-FIRE pulses of 1 μs duration, it is possible to increase the delay up to 10,000 μs and to improve the effectiveness by reducing the pulse repetition rate without drastically increasing metal release from electrodes. It is important to note also that the delivery of pulses, especially $8 \times 100 \mu\text{s}$ monophasic, caused visible corrosion of the aluminum electrodes that also changed the electrode geometry. No corrosion was observed for platinum and stainless steel 304 electrodes.

Aluminum, platinum and stainless steel are commonly used materials for electrode fabrication. It was shown previously that the use of aluminum, platinum and stainless steel electrodes results in release of the electrode material [41–43,45,47,48,54,67–69]. Pt metal is biologically inert [70], however, Al and Fe ions showed to be cytotoxic and to affect the biochemistry of electroporated cells [42,45,71]. The effects of other metals from which the stainless steel 304 electrodes are composed (Mn, Cr, Ni) on electroporated cells has not been studied yet to the best of our knowledge. However, these metals have been shown to be toxic and carcinogenic or to have reproductive and developmental toxicity [71–74]. In some *in vitro* cell studies, Mn in the concentration from 2 μM to a few hundred μM already affected cells [75–77]. The concentration of released Mn from stainless steel 304 electrodes in our experiments was also in this concentration range. Cr(VI) in submicromolar concentration has been shown to decrease the survival of cells *in vitro* [77,78], while in our experiments the concentration of released Cr was in the micro- and millimolar range (although we do not know the oxidation state of Cr). The concentration of different Ni compounds that reduced the cell survival/cloning efficiency and caused transformations in *in vitro* cell studies, was reported to be in the micro- and millimolar range [79–81], which is in the same range as the Ni released from stainless steel 304 electrodes in our experiments.

5. Conclusions

Short biphasic H-FIRE pulses with longer delays (i.e. lower pulse repetition rates) are more effective in terms of decreased survival

(achieving cell kill) and do not significantly increase electrolytic contamination with metal ions from the electrodes. Lower pulse repetition rates also reduce temperature increase [82], but prolong the treatment time. To achieve the same biological effect as with $8 \times 100 \mu\text{s}$ monophasic pulses, however, a higher electric field strength is needed. Higher cell membrane permeabilization does not always result in lower cell survival which indicates a more complex interplay between cell membrane permeabilization and cell survival. It still has to be determined if application of short biphasic H-FIRE pulses with higher voltage results in reduced muscle contractions and lower metal release from electrodes compared to commonly used $8 \times 100 \mu\text{s}$ monophasic pulses with equivalent biological effect.

Declaration of Competing Interest

The authors declare that they have no known competing financial interests or personal relationships that could have appeared to influence the work reported in this paper.

Acknowledgments

The study was funded by Medtronic and the Slovenian Research Agency (ARRS) (research core funding No. (P2-0249)). The work was partially performed within the network of research and infrastructural centres of University of Ljubljana, which is financially supported by Slovenian Research Agency through infrastructural grant IP-0510. Authors would like to thank T. Polajžer, L. Vukanović and D. Hodžić for their help in the cell culture laboratory, R. Šmerc and S. Mahnič-Kalamiza for their assistance with creating images and T. Jarm for his thoughtful comments.

Appendix A. Supplementary material

Supplementary data to this article can be found online at <https://doi.org/10.1016/j.bioelechem.2020.107523>.

References

- [1] T. Kotnik, L. Rems, M. Tarek, D. Miklavčič, Membrane Electroporation and electroporation: mechanisms and models, *Annu. Rev. Biophys.* 48 (2019) 63–91, <https://doi.org/10.1146/annurev-biophys-052118-115451>.
- [2] M.L. Yarmush, A. Golberg, G. Serša, T. Kotnik, D. Miklavčič, Electroporation-based technologies for medicine: principles, applications, and challenges, *Annu. Rev. Biomed. Eng.* 16 (2014) 295–320, <https://doi.org/10.1146/annurev-biomed-071813-104622>.
- [3] T. Kotnik, W. Frey, M. Sack, S. Haberl Meglič, M. Peterka, D. Miklavčič, Electroporation-based applications in biotechnology, *Trends Biotechnol.* 33 (2015) 480–488, <https://doi.org/10.1016/j.tibtech.2015.06.002>.
- [4] G. Saldaña, I. Álvarez, S. Condón, J. Raso, Microbiological aspects related to the feasibility of PEF technology for food pasteurization, *Crit. Rev. Food Sci. Nutr.* 54 (2014) 1415–1426, <https://doi.org/10.1080/10408398.2011.638995>.
- [5] S. Mahnič-Kalamiza, E. Vorobiev, D. Miklavčič, Electroporation in food processing and biorefinery, *J. Membr. Biol.* 247 (2014) 1279–1304, <https://doi.org/10.1007/s00232-014-9737-x>.
- [6] A. Županič, B. Kos, D. Miklavčič, Treatment planning of electroporation-based medical interventions: electrochemotherapy, gene electrotransfer and irreversible electroporation, *Phys. Med. Biol.* 57 (2012) 5425–5440, <https://doi.org/10.1088/0031-9155/57/17/5425>.
- [7] J. Gehl, Electroporation: theory and methods, perspectives for drug delivery, gene therapy and research, *Acta Physiol. Scand.* 177 (2003) 437–447, <https://doi.org/10.1046/j.1365-201X.2003.01093.x>.
- [8] C. Jiang, R.V. Davalos, J.C. Bischof, A review of basic to clinical studies of irreversible electroporation therapy, *IEEE Trans. Biomed. Eng.* 62 (2015) 4–20, <https://doi.org/10.1109/TBME.2014.2367543>.
- [9] A. Sugrue, V. Vaidya, C. Witt, C.V. DeSimone, O. Yasin, E. Maor, A.M. Killu, S. Kapa, C.J. McLeod, D. Miklavčič, S.J. Asirvatham, Irreversible electroporation for catheter-based cardiac ablation: a systematic review of the preclinical experience, *J. Interv. Card. Electrophysiol.* 55 (2019) 251–265, <https://doi.org/10.1007/s10840-019-00574-3>.
- [10] R.V. Davalos, L.M. Mir, B. Rubinsky, Tissue ablation with irreversible electroporation, *Ann. Biomed. Eng.* 33 (2005) 223–231, <https://doi.org/10.1007/s10439-005-8981-8>.
- [11] J. Moir, S.A. White, J.J. French, P. Littler, D.M. Manas, Systematic review of irreversible electroporation in the treatment of advanced pancreatic cancer, *Eur. J. Surg. Oncol.* 40 (2014) 1598–1604, <https://doi.org/10.1016/j.ejso.2014.08.480>.
- [12] M. Silk, D. Tahour, G. Srimathveeravalli, S.B. Solomon, R.H. Thornton, The state of irreversible electroporation in interventional oncology, *Semin. Intervent. Radiol.* 31 (2014) 111–117, <https://doi.org/10.1055/s-0034-1373785>.
- [13] M.J.V. Scheltema, W. van den Bos, D.M. de Bruin, H. Wijkstra, M.P. Laguna, T.M. de Reijke, J.J. de la Rosette, Focal vs extended ablation in localized prostate cancer with irreversible electroporation: a multi-center randomized controlled trial, *BMC Cancer.* 16 (2016) 299, <https://doi.org/10.1186/s12885-016-2332-z>.
- [14] E. Maor, A. Sugrue, C. Witt, V.R. Vaidya, C.V. DeSimone, S.J. Asirvatham, S. Kapa, Pulsed electric fields for cardiac ablation and beyond: A state-of-the-art review, *Hear. Rhythm.* 16 (2019) 1112–1120, <https://doi.org/10.1016/j.hrthm.2019.01.012>.
- [15] M.T. Stewart, D.E. Haines, A. Verma, N. Kirchhof, N. Barka, E. Grassl, B. Howard, Intracardiac pulsed field ablation: proof of feasibility in a chronic porcine model, *Hear. Rhythm.* 16 (2019) 754–764, <https://doi.org/10.1016/j.hrthm.2018.10.030>.
- [16] V.Y. Reddy, P. Neuzil, J.S. Koruth, J. Petru, M. Funosako, H. Cochet, L. Sediva, M. Chovanec, S.R. Dukkupati, P. Jais, Pulsed field ablation for pulmonary vein isolation in atrial fibrillation, *J. Am. Coll. Cardiol.* 74 (2019) 315–326, <https://doi.org/10.1016/j.jacc.2019.04.021>.
- [17] R.C.G. Martin II, A.N. Durham, M.G. Besselink, D. Iannitti, M.J. Weiss, C.L. Wolfgang, K.-W. Huang, Irreversible electroporation in locally advanced pancreatic cancer: a call for standardization of energy delivery, *J. Surg. Oncol.* 114 (2016) 865–871, <https://doi.org/10.1002/jso.24404>.
- [18] B. Kos, P. Voigt, D. Miklavčič, M. Moche, Careful treatment planning enables safe ablation of liver tumors adjacent to major blood vessels by percutaneous irreversible electroporation (IRE), *Radiol. Oncol.* 49 (2015) 234–241, <https://doi.org/10.1515/raon-2015-0031>.
- [19] M. Marty, G. Serša, J.R. Garbay, J. Gehl, C.G. Collins, M. Snoj, V. Billard, P.F. Geertsen, J.O. Larkin, D. Miklavčič, I. Pavlovic, S.M. Paulin-Košir, M. Čemažar, N. Morsli, D.M. Soden, Z. Rudolf, C. Robert, G.C. O'Sullivan, L.M. Mir, Electrochemotherapy – an easy, highly effective and safe treatment of cutaneous and subcutaneous metastases: results of ESOPE (European Standard Operating Procedures of Electrochemotherapy) study, *Eur. J. Cancer Suppl.* 4 (2006) 3–13, <https://doi.org/10.1016/j.ejcsup.2006.08.002>.
- [20] P.G. Wagstaff, M. Buijs, W. van den Bos, D.M. de Bruin, P.J. Zondervan, J.J. de la Rosette, M.P. Laguna, Irreversible electroporation: state of the art, *Oncotargets Ther.* 9 (2016) 2437–2446, <https://doi.org/10.2147/OTT.S88086>.
- [21] A. Deodhar, T. Dickfeld, G.W. Single, W.C.J. Hamilton, R.H. Thornton, C.T. Sofocleous, M. Maybody, M. Gonen, B. Rubinsky, S.B. Solomon, Irreversible electroporation near the heart: ventricular arrhythmias can be prevented with ECG synchronization, *AJR. Am. J. Roentgenol.* 196 (2011) W330–W335, <https://doi.org/10.2214/AJR.10.4490>.
- [22] C.B. Arena, M.B. Sano, J.H. Rossmeisl Jr, J.L. Caldwell, P.A. Garcia, M.N. Rylander, R.V. Davalos, High-frequency irreversible electroporation (H-FIRE) for non-thermal ablation without muscle contraction, *Biomed. Eng. Online.* 10 (2011) 102, <https://doi.org/10.1186/1475-2875-10-102>.
- [23] I.A. Siddiqui, E.L. Latouche, M.R. Dewitt, J.H. Swet, R.C. Kirks, E.H. Baker, D.A. Iannitti, D. Vrochides, R.V. Davalos, J.H. McKillop, Induction of rapid, reproducible hepatic ablations using next-generation, high frequency irreversible electroporation (H-FIRE) in vivo, *HPB (Oxford)* 18 (2016) 726–734, <https://doi.org/10.1016/j.hpb.2016.06.015>.
- [24] C. Yao, S. Dong, Y. Zhao, Y. Lv, H. Liu, L. Gong, J. Ma, H. Wang, Y. Sun, Bipolar microsecond pulses and insulated needle electrodes for reducing muscle contractions during irreversible electroporation, *IEEE Trans. Biomed. Eng.* 64 (2017) 2924–2937, <https://doi.org/10.1109/TBME.2017.2690624>.
- [25] S. Dong, C. Yao, Y. Zhao, Y. Lv, H. Liu, Parameters optimization of bipolar high frequency pulses on tissue ablation and inhibiting muscle contraction, *IEEE Trans. Dielectr. Electr. Insul.* 25 (2018) 207–216, <https://doi.org/10.1109/TDEL.2018.006303>.
- [26] V.M. Ringel-Scaia, N. Beitel-White, M.F. Lorenzo, R.M. Brock, K.E. Huie, S. Coutermarsh-Ott, K. Eden, D.K. Mcdaniel, S.S. Verbridge, J.H.J. Rossmeisl, K.J. Oestreich, R.V. Davalos, L.C. Allen, High-frequency irreversible electroporation is an effective tumor ablation strategy that induces immunologic cell death and promotes systemic anti-tumor immunity, *EBioMedicine.* 44 (2019) 112–125, <https://doi.org/10.1016/j.ebiom.2019.05.036>.
- [27] T.J. O'Brien, M. Passeri, M.F. Lorenzo, J.K. Sulzer, W.B. Lyman, J.H. Swet, D. Vrochides, E.H. Baker, D.A. Iannitti, R.V. Davalos, J.H. McKillop, Experimental high-frequency irreversible electroporation using a single-needle delivery approach for nonthermal pancreatic ablation in vivo, *J. Vasc. Interv. Radiol.* 30 (2019) 854–862.e7, <https://doi.org/10.1016/j.jvir.2019.01.032>.
- [28] M.B. Sano, C.B. Arena, M.R. DeWitt, D. Saur, R.V. Davalos, In-vitro bipolar nano- and microsecond electro-pulse bursts for irreversible electroporation therapies, *Bioelectrochemistry* 100 (2014) 69–79, <https://doi.org/10.1016/j.bioelechem.2014.07.010>.
- [29] D.C. Sweeney, M. Reberšek, J. Dermol, L. Rems, D. Miklavčič, R.V. Davalos, Quantification of cell membrane permeability induced by monopolar and high-frequency bipolar bursts of electrical pulses, *Biochim. Biophys. Acta - Biomembr.* 2016 (1858) 2689–2698, <https://doi.org/10.1016/j.bbamem.2016.06.024>.
- [30] M. Scuderi, M. Reberšek, D. Miklavčič, J. Dermol-Černe, The use of high-frequency short bipolar pulses in cisplatin electrochemotherapy in vitro, *Radiol. Oncol.* 53 (2019) 194–205, <https://doi.org/10.2478/raon-2019-0025>.

- [31] A.G. Pakhomov, I. Semenov, S. Xiao, O.N. Pakhomova, B. Gregory, K.H. Schoenbach, J.C. Ullery, H.T. Beier, S.R. Rajulapati, B.L. Ibey, Cancellation of cellular responses to nanosecond electroporation by reversing the stimulus polarity, *Cell. Mol. Life Sci.* 71 (2014) 4431–4441, <https://doi.org/10.1007/s00018-014-1626-z>.
- [32] B.L. Ibey, J.C. Ullery, O.N. Pakhomova, C.C. Roth, I. Semenov, H.T. Beier, M. Tarango, S. Xiao, K.H. Schoenbach, A.G. Pakhomov, Bipolar nanosecond electric pulses are less efficient at electroporation and killing cells than monopolar pulses, *Biochem. Biophys. Res. Commun.* 443 (2014) 568–573, <https://doi.org/10.1016/j.bbrc.2013.12.004>.
- [33] M.B. Sano, C.B. Arena, K.R. Bittleman, M.R. Dewitt, H.J. Cho, C.S. Szot, D. Saur, J. M. Cissell, J. Robertson, Y.W. Lee, R.V. Davalos, Bursts of bipolar microsecond pulses inhibit tumor growth, *Sci. Rep.* 5 (2015) 14999, <https://doi.org/10.1038/srep14999>.
- [34] A.G. Pakhomov, S. Grigoryev, I. Semenov, M. Casciola, C. Jiang, S. Xiao, The second phase of bipolar, nanosecond-range electric pulses determines the electroporation efficiency, *Bioelectrochemistry* 122 (2018) 123–133, <https://doi.org/10.1016/j.bioelechem.2018.03.014>.
- [35] E.C. Gianulis, M. Casciola, S. Xiao, O.N. Pakhomova, A.G. Pakhomov, Electroporation-mediated by uni- or bipolar nanosecond electric pulses: the impact of extracellular conductivity, *Bioelectrochemistry* 119 (2018) 10–19, <https://doi.org/10.1016/j.bioelechem.2017.08.005>.
- [36] G. Pataro, G.M.J. Barca, G. Donsi, G. Ferrari, On the modelling of the electrochemical phenomena at the electrode-solution interface of a PEF treatment chamber: effect of electrical parameters and chemical composition of model liquid food, *J. Food Eng.* 165 (2015) 45–51, <https://doi.org/10.1016/j.jfoodeng.2015.05.010>.
- [37] G. Saulis, R. Rodaitė, R. Rodaitė-Riševičienė, V.S. Dainauskaitė, R. Saulė, Electrochemical processes during high-voltage electric pulses and their importance in food processing technology, in: R. Rai V (Ed.), *Adv. Food Biotechnol.*, John Wiley & Sons Ltd, 2015, pp. 575–592, <https://doi.org/10.1002/9781118864463.ch35>.
- [38] H. Hulsheger, E.G. Niemann, Lethal effects of high-voltage pulses on *E. coli* K12, *Radiat. Environ. Biophys.* 18 (1980) 281–288.
- [39] Y. Tada, M. Sakamoto, T. Fujimura, Efficient gene introduction into rice by electroporation and analysis of transgenic plants: use of electroporation buffer lacking chloride ions, *Theor. Appl. Genet.* 80 (1990) 475–480, <https://doi.org/10.1007/BF00226748>.
- [40] N. Meneses, H. Jaeger, D. Knorr, pH-changes during pulsed electric field treatments – Numerical simulation and in situ impact on polyphenoloxidase inactivation, *Innov. Food Sci. Emerg. Technol.* 12 (2011) 499–504, <https://doi.org/10.1016/j.ifset.2011.07.001>.
- [41] A. Gad, S. Member, S.H. Jayaram, Effect of electric pulse parameters on releasing metallic particles from stainless steel electrodes during PEF processing of milk, *IEEE Trans. Ind. Appl.* 50 (2014) 1402–1409, <https://doi.org/10.1109/TIA.2013.2278424>.
- [42] J.W. Loomis-Hussell, P.J. Cullen, R.F. Irvine, A.P. Dawson, Electroporation can cause artefacts due to solubilization of cations from the electrode plates. aluminum ions enhance conversion of inositol 1,3,4,5-tetrakisphosphate into inositol 1,4,5-trisphosphate in electroporated L1210 cells, *Biochem. J.* 277 (Pt 3) (1991) 883–885.
- [43] U. Friedrich, N. Stachowicz, A. Simm, G. Fuhr, K. Lucas, U. Zimmermann, High efficiency electroporation with aluminum electrodes using microsecond controlled pulses, *Bioelectrochem. Bioenerg.* 47 (1998) 103–111, [https://doi.org/10.1016/S0302-4598\(98\)00163-9](https://doi.org/10.1016/S0302-4598(98)00163-9).
- [44] R. Stapulionis, Electric pulse-induced precipitation of biological macromolecules in electroporation, *Bioelectrochem. Bioenerg.* 48 (1999) 249–254, [https://doi.org/10.1016/S0302-4598\(98\)00206-2](https://doi.org/10.1016/S0302-4598(98)00206-2).
- [45] T. Kotnik, D. Miklavčič, L.M. Mir, Cell membrane electroporation by symmetrical bipolar rectangular pulses: Part. II Reduced electrolytic contamination, *Bioelectrochemistry* 54 (2001) 91–95, [https://doi.org/10.1016/S1567-5394\(01\)00115-3](https://doi.org/10.1016/S1567-5394(01)00115-3).
- [46] K.M.F.A. Reyns, A.M.J. Diels, C.W. Michiels, Generation of bactericidal and mutagenic components by pulsed electric field treatment, *Int. J. Food Microbiol.* 93 (2004) 165–173, <https://doi.org/10.1016/j.jfoodmicro.2003.10.014>.
- [47] G.A. Evrendilek, S. Li, W.R. Dantzer, Q.H. Zhang, Pulsed electric field processing of beer: microbial, sensory, and quality analyses, *J. Food Sci.* 69 (2004) M228–M232, <https://doi.org/10.1111/j.1365-2621.2004.tb09892.x>.
- [48] B. Roodenburg, J. Morren, H.E. Iekje I. Berg, S.W.H. De Haan, S.W.H. de Haan, Metal release in a stainless steel pulsed electric field (PEF) system: Part II, the treatment of orange juice; related to legislation and treatment chamber lifetime, *Innov. Food Sci. Emerg. Technol.* 6 (2005) 337–345, <https://doi.org/10.1016/j.ifset.2005.04.004>.
- [49] G. Saulis, R. Lape, R. Pranevičiūtė, D. Mickevičius, Changes of the solution pH due to exposure by high-voltage electric pulses, *Bioelectrochemistry*, 67 (2005) 101–108, <https://doi.org/10.1016/j.bioelechem.2005.03.001>.
- [50] E. Nilsson, H. von Euler, J. Berendson, A. Thörne, P. Wersäll, I. Näslund, A.-S. Lagerstedt, K. Narfström, J.M. Olsson, Electrochemical treatment of tumours, *Bioelectrochemistry* 51 (2000) 1–11, [https://doi.org/10.1016/S0302-4598\(99\)00073-2](https://doi.org/10.1016/S0302-4598(99)00073-2).
- [51] N. Klein, E. Guenther, P. Mikus, M.K. Stehling, B. Rubinsky, Single exponential decay waveform: a synergistic combination of electroporation and electrolysis (E2) for tissue ablation, *PeerJ*, 5 (2017), <https://doi.org/10.7717/peerj.3190> e3190.
- [52] S.A.A. Kooijmans, S. Stremersch, K. Braeckmans, S.C. de Smedt, A. Hendrix, M.J. A. Wood, R.M. Schiffelers, K. Raemdonck, P. Vader, Electroporation-induced siRNA precipitation obscures the efficiency of siRNA loading into extracellular vesicles, *J. Control. Release*, 172 (2013) 229–238, <https://doi.org/10.1016/j.jconrel.2013.08.014>.
- [53] U.F. Pliquet, C.A. Gusbeth, Overcoming electrically induced artifacts in penetration studies with fluorescent tracers, *Bioelectrochemistry* 51 (2000) 75–79, [https://doi.org/10.1016/S0302-4598\(99\)00068-9](https://doi.org/10.1016/S0302-4598(99)00068-9).
- [54] J. Morren, B. Roodenburg, S.W.H. de Haan, Electrochemical reactions and electrode corrosion in pulsed electric field (PEF) treatment chambers, *Innov. Food Sci. Emerg. Technol.* 4 (2003) 285–295, [https://doi.org/10.1016/S1466-8564\(03\)00041-9](https://doi.org/10.1016/S1466-8564(03)00041-9).
- [55] G. Pucihar, J. Krmelj, M. Reberšek, T. Batista Napotnik, D. Miklavčič, Equivalent pulse parameters for electroporation, *IEEE Trans. Biomed. Eng.* 58 (2011) 3279–3288, <https://doi.org/10.1109/TBME.2011.2167232>.
- [56] R. Susil, D. Semrov, D. Miklavčič, Electric field-induced transmembrane potential depends on cell density and organization, *Electro- Magneto Biol.* 17 (1998) 391–399, <https://doi.org/10.3109/15368379809030739>.
- [57] P.J. Canatella, J.F. Karr, J.A. Petros, M.R. Prausnitz, Quantitative study of electroporation-mediated molecular uptake and cell viability, *Biophys. Acta* 80 (2001) 755–764, [https://doi.org/10.1016/S0006-3495\(01\)76055-9](https://doi.org/10.1016/S0006-3495(01)76055-9).
- [58] R. Core Team, R: A Language and Environment for Statistical Computing, (2018), (accessed 12 November 2019), <https://www.r-project.org/>.
- [59] C.M. Valdez, R.B. Jr, C.C. Roth, E. Moen, B. Ibey, The interphase interval within a bipolar nanosecond electric pulse modulates bipolar cancellation, *Bioelectromagnetics* 39 (2018) 441–450, <https://doi.org/10.1002/bem.22134>.
- [60] G. Pucihar, L.M. Mir, D. Miklavčič, The effect of pulse repetition frequency on the uptake into electroporated cells in vitro with possible applications in electrochemotherapy, *Bioelectrochemistry* 57 (2002) 167–172, [https://doi.org/10.1016/S1567-5394\(02\)00116-0](https://doi.org/10.1016/S1567-5394(02)00116-0).
- [61] G. Serša, S. Kranjc, J. Ščančar, M. Kržan, M. Čemažar, Electrochemotherapy of mouse sarcoma tumors using electric pulse trains with repetition frequencies of 1 Hz and 5 kHz, *J. Membr. Biol.* 236 (2010) 155–162, <https://doi.org/10.1007/s00232-010-9268-z>.
- [62] O.N. Pakhomova, B.W. Gregory, V.A. Khorokhorina, A.M. Bowman, S. Xiao, A.G. Pakhomov, Electroporation-induced electrosensitization, *PLoS One* 6 (2011) 36–38, <https://doi.org/10.1371/journal.pone.0017100>.
- [63] C.S. Djuzenova, U. Zimmermann, H. Frank, V.L. Sukhorukov, E. Richter, G. Fuhr, Effect of medium conductivity and composition on the uptake of propidium iodide into electroporated myeloma cells, *Biochim. Biophys. Acta - Biomembr.* 1284 (1996) 143–152, [https://doi.org/10.1016/S0005-2736\(96\)00119-8](https://doi.org/10.1016/S0005-2736(96)00119-8).
- [64] J. Dermol, O.N. Pakhomova, A.G. Pakhomov, D. Miklavčič, Cell electrosensitization exists only in certain electroporation buffers, *PLoS One* 11 (2016) e0159434, <https://doi.org/10.1371/journal.pone.0159434>.
- [65] M.J. van den Hoff, A.F. Moorman, W.H. Lamers, Electroporation in “intracellular” buffer increases cell survival, *Nucleic Acids Res.* 20 (1992) 2902, <https://doi.org/10.1093/nar/20.11.2902>.
- [66] B. Mercadal, C.B. Arena, R.V. Davalos, A. Iovorra, Avoiding nerve stimulation in irreversible electroporation: a numerical modeling study, *Phys. Med. Biol.* 62 (2017) 8060–8079, <https://doi.org/10.1088/1361-6560/aa8c53>.
- [67] T. Tomov, I. Tsoneva, Are the stainless steel electrodes inert?, *Bioelectrochemistry*, 51 (2000) 207–209, [https://doi.org/10.1016/S0302-4598\(00\)00069-6](https://doi.org/10.1016/S0302-4598(00)00069-6).
- [68] B. Roodenburg, J. Morren, H.E. Iekje I. Berg, S.W.H. De Haan, S.W.H. de Haan, Metal release in a stainless steel Pulsed Electric Field (PEF) system: Part I, effect of different pulse shapes: theory and experimental method, *Innov. Food Sci. Emerg. Technol.* 6 (2005) 327–336, <https://doi.org/10.1016/j.ifset.2005.04.006>.
- [69] R.C. Black, P. Hannaker, Dissolution of smooth platinum electrodes in biological fluids, *Appl. Neurophysiol.* 42 (1980) 366–374, <https://doi.org/10.1159/000102382>.
- [70] J.B. Leikin, F.P. Paloucek, *Poisoning and toxicology handbook*, 4th Ed., CRC Press, Boca Raton, 2007, <https://doi.org/10.3109/9781420044805>.
- [71] P.D.L. Lima, M.C. Vasconcellos, R.C. Montenegro, M.O. Bahia, E.T. Costa, L.M.G. Antunes, R.R. Burbano, Genotoxic effects of aluminum, iron and manganese in human cells and experimental systems: a review of the literature, *Hum. Exp. Toxicol.* 30 (2011) 1435–1444, <https://doi.org/10.1177/0960327110396531>.
- [72] J. Crossgrove, W. Zheng, Manganese toxicity upon overexposure, *NMR Biomed.* 17 (2004) 544–553, <https://doi.org/10.1002/nbm.931>.
- [73] K.S. Kasprzak, F.W. Sunderman, K. Salnikow, Nickel carcinogenesis, *Mutat. Res.* 533 (2003) 67–97, <https://doi.org/10.1016/j.mrfmmm.2003.08.021>.
- [74] T.J. O'Brien, S. Ceryak, S.R. Patierno, Complexities of chromium carcinogenesis: role of cellular response, repair and recovery mechanisms, *Mutat. Res.* 533 (2003) 3–36, <https://doi.org/10.1016/j.mrfmmm.2003.09.006>.
- [75] D. Ding, J. Roth, R. Salvi, Manganese is toxic to spiral ganglion neurons and hair cells in vitro, *Neurotoxicology* 32 (2011) 233–241, <https://doi.org/10.1016/j.neuro.2010.12.003>.
- [76] F. Rovetta, S. Catalani, N. Steimberg, J. Boniotti, M.E. Gilberti, M.A. Mariggiò, G. Mazzoleni, Organ-specific manganese toxicity: a comparative in vitro study on five cellular models exposed to MnCl₂, *Toxicol. Vitro* 21 (2007) 284–292, <https://doi.org/10.1016/j.tiv.2006.08.010>.
- [77] L.E. Pascal, D.M. Tessier, Cytotoxicity of chromium and manganese to lung epithelial cells in vitro, *Toxicol. Lett.* 147 (2004) 143–151, <https://doi.org/10.1016/j.toxlet.2003.11.004>.

- [78] A.G. Levis, V. Bianchi, G. Tamino, B. Pegoraro, Cytotoxic effects of hexavalent and trivalent chromium on mammalian cells in vitro, *Br. J. Cancer*. 37 (1978) 386–396, <https://doi.org/10.1038/bjc.1978.58>.
- [79] H. Babich, C. Shopsis, E. Borenfreund, In vitro cytotoxicity testing of aquatic pollutants (cadmium, copper, zinc, nickel) using established fish cell lines, *Ecotoxicol. Environ. Saf.* 11 (1986) 91–99, [https://doi.org/10.1016/0147-6513\(86\)90030-8](https://doi.org/10.1016/0147-6513(86)90030-8).
- [80] M.W. Wlr, R.L. Schenley, E.-L. Tan, M.W. Williams, R.L. Schenley, S.W. Perdue, T. L. Hayden, J.E. Turner, A.W. Hsie, The toxicity of sixteen metallic compounds in Chinese hamster ovary cells, *Toxicol. Appl. Pharmacol.* 74 (1984) 330–336, [https://doi.org/10.1016/0041-008X\(84\)90286-2](https://doi.org/10.1016/0041-008X(84)90286-2).
- [81] K. Hansen, R.M. Stern, In vitro toxicity and transformation potency of nickel compounds, *Environ. Health Perspect.* 51 (1983) 223–226, <https://doi.org/10.1289/ehp.8351223>.
- [82] I. Lacković, R. Magjarević, D. Miklavčič, Three-dimensional finite-element analysis of joule heating in electrochemotherapy and in vivo gene electrotransfer, *IEEE Trans. Dielectr. Electr. Insul.* 16 (2009) 1338–1347, <https://doi.org/10.1109/TDEI.2009.5293947>.



Angelika Vižintin Angelika Vižintin obtained her BSc and MSc at the University of Ljubljana, Slovenia. Currently she is employed at the University of Ljubljana, Faculty of Electrical Engineering and is enrolled in the interdisciplinary doctoral program in Biosciences at the University of Ljubljana. Her main research interests lie in the field of electroporation based-technologies for biomedicine, including tissue ablation and electrochemotherapy.



Janja Vidmar Janja Vidmar obtained her PhD in Environmental Sciences at Jožef Stefan International Postgraduate School in Slovenia. She is currently Postdoctoral Researcher at the National Food Institute at the Technical University of Denmark. Her research work lies in the field of inorganic analytical chemistry of the environmental and biological systems. Janja has been mainly focused on detection and characterization of metal-based nanoparticles in environmental, biological and food samples, with the use of mass spectrometry with inductively coupled plasma in single particle mode (splCP-MS). She has worked on several European and national research projects (Globaqua, RusaLCA, CytoTreath).



Janez Ščančar He has been actively involved in the research for more than 25 years. Since 1997 he is employed at the Jožef Stefan Institute, Slovenia where currently is a Head of Research Group for Trace Elements Speciation. His main research interests are investigations on the role of metal ions in the environment and living organisms by applying methods of chemical speciation. As full professor he is engaged in lecturing at the Jožef Stefan International Postgraduate School and the University of Nova Gorica. Among others, he has written more than 145 original scientific articles papers in analytical, environmental and life science journals.



Damijan Miklavčič Damijan Miklavčič was born in Ljubljana, Slovenia, in 1963. He received his PhD degree in electrical engineering from the University of Ljubljana in 1993. He is currently a tenured Professor at the Faculty of Electrical Engineering of the University of Ljubljana. His current research interests include electroporation-based treatments and therapies, including cancer treatment by means of electrochemotherapy, cardiac tissue ablation by irreversible electroporation, and gene transfer for DNA vaccination. His research involves biological experimentation, numerical modeling of biological processes, and hardware development.

2.1.2 Electroporation with nanosecond pulses and bleomycin or cisplatin results in efficient cell kill and low metal release from electrodes

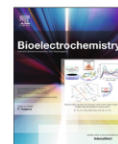
Vižintin A., Marković S., Ščančar J., Miklavčič D. 2021. Electroporation with nanosecond pulses and bleomycin or cisplatin results in efficient cell kill and low metal release from electrodes. *Bioelectrochemistry*, 140: 107798, doi: 10.1016/j.bioelechem.2021.107798: 12 p.

Nanosecond electric pulses have several potential advantages in electroporation-based procedures over the conventional micro- and millisecond pulses including low level of heating, reduced electrochemical reactions and reduced muscle contractions making them alluring for use in biomedicine and food industry. The aim of this study was to evaluate if nanosecond pulses can enhance the cytotoxicity of chemotherapeutics bleomycin and cisplatin *in vitro* and to quantify metal release from electrodes in comparison to 100 μ s pulses commonly used in electrochemotherapy. The effects of nanosecond pulse parameters (voltage, pulse duration, number of pulses) on cell membrane permeabilization, resealing and on cell survival after electroporation only and after electrochemotherapy with bleomycin and cisplatin were evaluated on Chinese hamster ovary cells. Application of permeabilizing nanosecond pulses in combination with chemotherapeutics resulted in successful cell kill. Higher extracellular concentrations of bleomycin – but not cisplatin – were needed to achieve the same decrease in cell survival with nanosecond pulses as with eight 100 μ s pulses, however, the tested bleomycin concentrations were still considerably lower compared to doses used in clinical practice. Decreasing the pulse duration from microseconds to nanoseconds and concomitantly increasing the amplitude to achieve the same biological effect resulted in reduced release of aluminum ions from electroporation cuvettes.

Supplementary data to this article can be found online at <https://doi.org/10.1016/j.bioelechem.2021.107798>.



This work is licensed under a [Creative Commons Attribution-NonCommercial-NoDerivatives 4.0 International License](https://creativecommons.org/licenses/by-nc-nd/4.0/).



Electroporation with nanosecond pulses and bleomycin or cisplatin results in efficient cell kill and low metal release from electrodes

Angelika Vižintin^a, Stefan Marković^b, Janez Ščančar^b, Damijan Miklavčič^{a,*}

^a University of Ljubljana, Faculty of Electrical Engineering, Tržaška cesta 25, 1000 Ljubljana, Slovenia

^b Jožef Stefan Institute, Department of Environmental Sciences, Jamova cesta 39, 1000 Ljubljana, Slovenia

ARTICLE INFO

Article history:

Received 20 November 2020
Received in revised form 19 February 2021
Accepted 1 March 2021
Available online 9 March 2021

Keywords:

Electroporation
Nanosecond pulses
Electrochemotherapy
Metal release

ABSTRACT

Nanosecond electric pulses have several potential advantages in electroporation-based procedures over the conventional micro- and millisecond pulses including low level of heating, reduced electrochemical reactions and reduced muscle contractions making them alluring for use in biomedicine and food industry. The aim of this study was to evaluate if nanosecond pulses can enhance the cytotoxicity of chemotherapeutics bleomycin and cisplatin *in vitro* and to quantify metal release from electrodes in comparison to 100 μ s pulses commonly used in electrochemotherapy. The effects of nanosecond pulse parameters (voltage, pulse duration, number of pulses) on cell membrane permeabilization, resealing and on cell survival after electroporation only and after electrochemotherapy with bleomycin and cisplatin were evaluated on Chinese hamster ovary cells. Application of permeabilizing nanosecond pulses in combination with chemotherapeutics resulted in successful cell kill. Higher extracellular concentrations of bleomycin – but not cisplatin – were needed to achieve the same decrease in cell survival with nanosecond pulses as with eight 100 μ s pulses, however, the tested bleomycin concentrations were still considerably lower compared to doses used in clinical practice. Decreasing the pulse duration from microseconds to nanoseconds and concomitantly increasing the amplitude to achieve the same biological effect resulted in reduced release of aluminum ions from electroporation cuvettes.

© 2021 The Author(s). Published by Elsevier B.V. This is an open access article under the CC BY-NC-ND license (<http://creativecommons.org/licenses/by-nc-nd/4.0/>).

1. Introduction

Exposure of cells/tissue to pulsed electric fields allows transmembrane transport of otherwise impermeant molecules. This phenomenon of increased cell membrane permeabilization due to exposure to short electric pulses is called electroporation, sometimes termed also electropermeabilization or pulsed electric field treatment. The underlying mechanisms of electroporation have been recently reviewed by Kotnik et al. [1]. Electroporation with nanosecond pulses alleviates multiple limitations existing in conventional micro- and millisecond range electroporation. Nanosecond pulses penetrate the cell interior, having more profound effects on the organelles [2–7]; however, as was first theoretically predicted and later confirmed experimentally, the plasma membrane is also affected [8–10]. Permeabilization of the cell membrane to medium sized molecules like bleomycin [11] and siRNA [12], and more recently even the delivery of plasmids [13] was reported using nanosecond pulses. Nanosecond pulses electroporate cells of different sizes and shapes at similar

thresholds [14,15]. Electroporation with nanosecond pulses showed induction of apoptosis and antitumor activity [16–23]. The use of pulses of high electric field strength but very short duration means that the energy transmitted by the pulses to the treated volume is very low and leads to a low level of heating, thus minimizing the possibility of thermal damage to tissue [2,24].

Electroporation with longer (i.e. in the micro- and millisecond range) pulses is used in various applications including transfection of cells/transformation of bacteria, extraction of biomolecules from cells, inactivation of microorganisms in water and liquid foods, tissue ablation and electrochemotherapy (ECT) [25–28]. ECT is a local treatment of cancer which combines the use of electric pulses delivered on the tumor area and some standard chemotherapeutic agents for which plasma membrane represents a barrier for reaching their intracellular target. ECT is being introduced into clinical practice based on extensive preclinical data, on its effectiveness on different tumors and on solid evidence of its mechanisms of action [29]. Several mechanisms of action have already been identified: increased membrane permeability and intracellular drug accumulation, vascular disruption, vascular lock and involvement of immune response; the dominant mechanisms being increased cellular uptake of non-permeant or low permeant anticancer drug with

* Corresponding author.

E-mail address: Damijan.Miklavcic@fe.uni-lj.si (D. Miklavčič).

<https://doi.org/10.1016/j.bioelechem.2021.107798>

1567-5394/© 2021 The Author(s). Published by Elsevier B.V.

This is an open access article under the CC BY-NC-ND license (<http://creativecommons.org/licenses/by-nc-nd/4.0/>).

a very high intrinsic cytotoxicity due to exposure of cells or tumors to cell membrane-permeabilizing electric pulses [30]. Increased cytotoxicity of bleomycin and *cis*-diaminedichloroplatinum (II) (cisplatin), two most often used chemotherapeutics in ECT, was demonstrated *in vitro*, with several-fold potentiation [31,32] and confirmed *in vivo* on different animal tumor models and patients [33–37]. Despite the success of the therapy, some side effects were reported. According to the patients, the most unpleasant or even painful side effects were the sensations during the pulse delivery, which were mainly attributed to peripheral nerve stimulation and muscle contractions [38–43]. The applied electric pulses in ECT are most commonly delivered in trains of eight monophasic pulses of 100 μ s duration with 1 Hz or 5 kHz pulse repetition rate. It seems that muscle contractions are significantly reduced when using nanosecond pulses compared to microsecond-long pulses [44,45], although more studies would be needed to further support this point, thus making the use of nanosecond pulses in electroporation-based applications in medicine like ECT compelling. The increased cytotoxicity of bleomycin after electroporation and consecutive cell death *in vitro* was already shown with 10 ns pulses [11] and Tunikowska et al. [46] have reported a case study of successful ECT in feline oral malignant melanoma using bleomycin and 15 ns pulses after CO₂ laser surgery. Novickij et al. [47] showed a comparable delay of tumor growth in mice treated with a combination of doxorubicin and eight 100 μ s pulses or 250 800 ns pulses. However, until now, there are no reports of comprehensive exploration of the effects of various nanosecond pulse parameters on effectiveness of reversible electroporation combined with bleomycin or cisplatin which could aid in developing effective ECT protocols for use in the clinic.

In electroporation procedures, the electric field in cell suspension or tissue is usually established by delivering electric pulses through metallic electrodes in contact with the treated medium/tissue. During delivery of high-voltage electric pulses to cells in suspension or in tissue, electrochemical processes occur at the electrode–electrolyte interface, such as electrolysis, generation of radicals and release of metal ions from the electrodes which results in corrosion and fouling of the electrodes, release of the electrode material or/and chemical modification of the medium [48,49]. For research purposes, the use of aluminum cuvettes is common, where delivery of electroporation pulses causes also release of aluminum ions from the electrodes [50–53]. The release of aluminum ions has been associated with a change of the solution pH [52,53]. The released aluminum ions can precipitate nucleic acids and proteins [54,55] and affect the biochemistry of the electroporated cells [51]. It was confirmed experimentally that shortening of the pulse and/or use of biphasic pulses reduces electrochemical reactions [50,56–58]. However, shorter pulses necessitate the use of higher electric field strengths and/or higher number of pulses to achieve

the same biological effect as with longer pulses [59]. It thus remains unclear whether shortening the pulse duration to nanoseconds with concomitantly increasing the voltage (and/or number of pulses used) still results in reduced electrochemical reactions.

The aim of our study was to evaluate *in vitro* if nanosecond electric pulses can enhance the cytotoxicity of bleomycin and cisplatin to a similar extent as eight 100 μ s pulses commonly used in electrochemotherapy and to quantify the release of aluminum ions from electroporation cuvettes in comparison to eight 100 μ s pulses.

2. Materials and methods

2.1. Electroporation set-up and pulse delivery

In cell experiments, a laboratory prototype pulse generator (University of Ljubljana), based on H-bridge digital amplifier with 1 kV MOSFETs (DE275-102N06A, IXYS, USA) [60] was used to deliver eight standard ECT monophasic rectangular pulses of 100 μ s duration with 1 Hz repetition rate. In metal release experiments, the Cliniporator Vitae (IGEA, Italy) was used to deliver the eight 100 μ s monophasic rectangular pulses with 1 Hz repetition rate. The CellFX System (Pulse Biosciences, California, USA) was used to deliver monophasic nanosecond rectangular pulses of 200, 400 or 550 ns duration (set duration on the pulse generator which fits well also with the full width at half maximum). We delivered 1, 25 or 100 nanopulses at repetition rate of 10 Hz. The voltage and the electrical current were monitored in all experiments. For microsecond pulses, the oscilloscope WaveSurfer 422, 200 MHz, high-voltage differential voltage probe ADP305 and current probe CP030, CP031A or CP150 (all from Teledyne LeCroy, New York, USA) was used. For nanosecond pulses, the current was measured by Pearson current monitor model 2878 (1 V/10 A, 70 MHz) and the voltage was measured by 1 k Ω resistor and Pearson current monitor model 2877 (1 V/1 A, 200 MHz) (all from Pearson Electronics, California, USA); the signals were monitored by the oscilloscope WaveSurfer 3024Z, 200 MHz (Teledyne LeCroy). The electric field strength (E) was calculated by dividing the measured voltage with the distance between the electrodes (i.e. the size of the gap of the electroporation cuvette). The waveforms of a 200 ns and 100 μ s pulse are shown in Fig. 1. The energy delivered by the electric pulses was estimated by multiplying the pulse duration and number of pulses with the measured amplitude of the voltage and measured amplitude of the electric current. The cell suspension in the electroporation cuvettes was at room temperature during pulse delivery. Temperature rise was measured by the fiber optic temperature sensor OTG-M170 and ProSens signal conditioner (both OpSens, Canada). The sensor was placed inside a 2 mm or 4 mm gap electroporation cuvette (VWR, Pennsylvania, USA) filled with

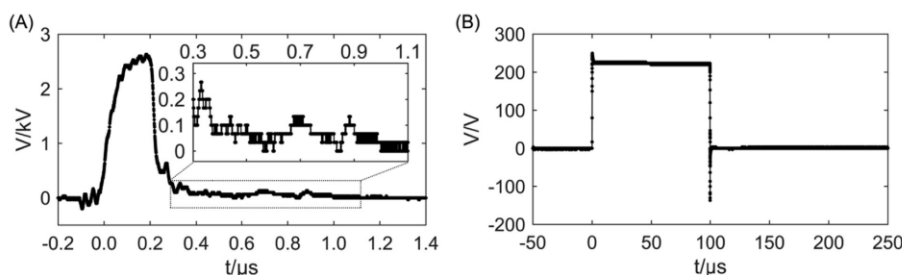


Fig. 1. Waveforms of pulses used in the study: (A) 200 ns, electric field strength of 6.1 kV/cm, and (B) 100 μ s, electric field strength of 1.1 kV/cm. (A) the amplitude of the 200 ns pulse from 0.3 to 1.1 μ s is zoomed in to show the reflected waves.

cell suspension and temperature was measured before, during and after delivery of electric pulses.

2.2. Cell culture

CHO-K1 Chinese hamster ovary cell line, obtained directly from the European Collection of Authenticated Cell Cultures (ECACC, cat. no. 85051005, mycoplasma free), was grown in Nutrient Mixture F-12 Ham (cat. no. N6658, Sigma-Aldrich, Missouri, United States) supplemented with 10% fetal bovine serum (FBS, cat. no. F9665, Sigma-Aldrich), 1.0 mM L-glutamine (cat. no. G7513, Sigma-Aldrich), 1 U/ml penicillin/streptomycin (cat. no. P0781, Sigma-Aldrich) and 50 µg/ml gentamycin (cat. no. G1397, Sigma-Aldrich) for 2–4 days at 37 °C in a humidified, 5% CO₂ atmosphere. On the day of the experiment, cells were detached with 1 × trypsin-EDTA (cat. no. T4174, Sigma-Aldrich) diluted in 1 × Hank's basal salt solution (cat. no. H4641, Sigma-Aldrich). Trypsin was inactivated by Dulbecco's Modified Eagle Medium (DMEM, cat. no. D5671, Sigma-Aldrich) supplemented with 10% FBS (cat. no. F9665, Sigma-Aldrich), 2.0 mM L-glutamine, 1 U/ml penicillin/streptomycin and 50 µg/ml gentamycin (used in this composition through all experiments). Cells were transferred to a 50 ml centrifuge tube and centrifuged 5 min at 180g and 23 °C. The supernatant was aspirated, and cells were re-suspended at a cell density of 4×10^6 (for cell survival and cell membrane permeabilization experiments after electroporation) or 4.2×10^6 (for ECT experiments) cells/ml in the complete growth medium DMEM which was used as electroporation medium. Conductivity of complete growth media F-12 Ham and DMEM were measured at room temperature with conductometer MA 5950 (Metrel, Slovenia).

2.3. Cell membrane permeabilization and resealing

To determine the percentage of permeabilized cells at different electric field strengths, the suspension of CHO cells was mixed with YO-PRO-1 iodide (cat. no. Y3603, Thermo Fisher Scientific, Massachusetts, USA) to final concentration of 1 µM right before application of electric pulses. 600 µl (for treatment with nanopulses) or 150 µl (for treatment with 8×100 µs pulses) of the cells-YO-PRO-1 mixture was transferred in an electroporation cuvette with 4 mm (nanopulses) or 2 mm (8×100 µs pulses) gap, followed by pulse application. 20 µl of the treated cell suspension was transferred to a new 1.5 ml microcentrifuge tube. Three minutes after the last pulse, 150 µl of complete growth medium DMEM was added. To determine the time needed for cell membrane resealing, 600 µl (for treatment with nanopulses) or 150 µl (for treatment with 8×100 µs pulses) of suspension of CHO cells was transferred in an electroporation cuvette with 4 mm (nanopulses) or 2 mm (8×100 µs pulses) gap, followed by pulse application. 10 µl of the treated cell suspension was transferred to 13 new 1.5 ml microcentrifuge tubes. Every 2 min after the last pulse (until 26 min after the last pulse), 1 µl of 0.01 mM YO-PRO-1 in complete growth medium DMEM was added to the cell suspension in one of the tubes and 3 min after addition of YO-PRO-1, 150 µl of complete growth medium DMEM was added to the cell suspension. Cell suspensions from both cell membrane permeabilization and resealing experiments were gently vortexed before analysis on the flow cytometer Attune NxT (Thermo Fisher Scientific). Cells were excited with a blue laser at 488 nm, and the emitted fluorescence was detected through a 530/30 nm band-pass filter. The measurement was stopped when 10,000 events were acquired. The obtained data were analyzed using the Attune NxT software (Thermo Fisher Scientific). Single cells were separated from all events by gating. The percentage of cells with permeabilized cell membrane and median YO-PRO-1 fluorescence was determined from the histogram of YO-PRO-1 fluorescence. The experiments

were repeated 3–4 times per each pulse protocol. The sham control was handled in the same way as the samples with the exception that no pulses were delivered.

2.4. Cell survival after electroporation

Just before pulse delivery, 600 µl (for treatment with nanopulses) or 150 µl (for treatment with 8×100 µs pulses) of suspension of CHO cells in complete growth medium DMEM was pipetted in an electroporation cuvette with 4 mm (nanopulses) or 2 mm (8×100 µs pulses) gap. The electroporation cuvettes were placed in the cuvette holder and electric pulses were applied (for the sham control no pulses were applied). Then, the cell suspension (20 µl) was transferred to a new 1.5 ml microcentrifuge tube and 25 min after the last pulse, complete growth medium F-12 Ham (380 µl) was added. The cell suspension was gently vortexed and plated (100 µl) in a well of a flat bottom 96-well plate in three technical replicates. Cells were kept at room temperature outside the incubator for the duration of the whole experiment (approximately one hour). The plate was incubated at 37 °C in a humidified, 5% CO₂ atmosphere. Cell survival was assessed by MTS assay. After 24 h of incubation, 20 µl of The CellTiter 96 AQueous One Solution Cell Proliferation Assay (cat. no. G3580, Promega, Wisconsin, USA) was added per well of the 96-well plate. After 2 h 35 min of incubation at 37 °C in a humidified, 5% CO₂ atmosphere, absorbance at 490 nm was measured with the spectrofluorometer Infinite 200 (Tecan, Austria). The survival was calculated by first subtracting the absorbance of the blank (5 µl of complete growth medium DMEM and 95 µl of complete growth medium F-12 Ham) and then normalizing the average absorbance of the three technical replicates of the sample to the absorbance of the sham controls. The experiments were repeated 3–5 times per each pulse protocol.

2.5. Cell survival after electrochemotherapy

Bleomycin sulphate (Medac, Germany) was diluted in water to concentration of 2 mM, aliquoted and stored at –20 °C. On the day of experiment, an aliquot was thawed and diluted in saline solution to prepare working solutions that after addition to the cell suspension resulted in final concentrations of 1 nM, 5 nM, 10 nM, 20 nM, 40 nM, 60 nM, 80 nM 100 nM, 140 nM, 200 nM, 300 nM, 400 nM or 500 nM bleomycin. Cisplatin (Cisplatin Kabi, 1 mg/mL, Fresenius Kabi, Germany) was diluted in saline solution on the day of the experiment to prepare working solutions that after addition to the cell suspension resulted in final concentrations of 10 µM, 30 µM or 50 µM cisplatin. 600 µl (nanopulses) or 165 µl (8×100 µs pulses) of the cell suspension was pipetted in 1.5 ml microcentrifuge tubes. Just before electroporation, 32 µl (nanopulses) or 8.8 µl (8×100 µs pulses) of appropriate dilution of the drug in saline solution (for control without drug: saline solution only) was added so that the final cell concentration was 4×10^6 cell/ml. Then, 600 µl (nanopulses) or 150 µl (8×100 µs pulses) of the cells–drug mixture was transferred in an electroporation cuvette with 4 mm (nanopulses) or 2 mm (8×100 µs pulses) gap. 7.5 µl (for MTS assay) or 5 µl (for clonogenic assay) from the remaining cells–drug mixture was transferred to a new 1.5 ml microcentrifuge tube for non-electroporated control. For clonogenic assay, the rest of the cells–drug mixture was mixed with trypan blue and counted with Countess Automated Cell Counter (Invitrogen, Thermo Fisher Scientific) following manufacturer's instructions. Electric pulses were applied to the electroporation cuvettes and 7.5 µl (for MTS assay) or 5 µl (for clonogenic assay) of the electroporated cells was pipetted into a new 1.5 ml microcentrifuge tube. Complete growth medium F-12 Ham (600 µl for MTS assay or 495 µl for clonogenic assay) was added to the electroporated cells and non-electroporated controls 25 min after pulse delivery. Cells were kept at room temperature

outside the incubator for the duration of the whole experiment (approximately one hour). For MTS assay, the cell suspension (110 μ l) was plated in a well of a flat bottom 96-well plate in three technical replicates. The plate was incubated at 37 °C in a humidified, 5% CO₂ atmosphere. After 72 h, CellTiter 96 Aqueous One Solution Cell Proliferation Assay (22 μ l) was added per well of the 96-well plate. The plate was incubated at 37 °C in a humidified, 5% CO₂ atmosphere and after 2 h 35 min, absorbance at 490 nm was measured with the spectrofluorometer Infinite 200. The survival was calculated by first subtracting the absorbance of the blank (110 μ l of complete growth medium F-12 Ham) and then normalizing the average absorbance of the three technical replicates of the sample to the absorbance of the non-electroporated controls without the drug. For clonogenic assay, the cell suspension was additionally diluted in growth medium Ham F12 to achieve the desired cell concentration and 2.5 ml was plated in a well of a 6-well plate in three technical replicates. The plates were incubated at 37 °C in a humidified, 5% CO₂ atmosphere. After 7 days of incubation, the growth medium was aspirated and 1 ml of 0.2% crystal violet in 80% methanol (both from Sigma-Aldrich, Merck, Germany) was added to fix and stain the colonies. After 10 min, the crystal violet-methanol mixture was removed and the plates were rinsed in water. Average plating efficiency from the 3 technical replicates was calculated by dividing the number of counted colonies (colonies containing < 50 cells were disregarded) with the number of plated cells. Surviving fraction was calculated by dividing the plating efficiency with the plating efficiency of the untreated control (non-electroporated cells without the drug). The experiments were repeated 3–6 times per pulse protocol. Integrated modulation contrast (IMC) micrographs of cells were taken 72 h after exposure to the electric pulses and/or drug with DM IL LED (Leica, Germany) inverted microscope using 10 \times objective.

2.6. Metal release

In contrast to cell experiments where DMEM growth medium was used as electroporation medium, pure NaCl solution was used in metal release experiments because it allowed us to detect very low concentrations of aluminum ions. Electroporation cuvettes with 4 mm gap were filled with 600 μ l of 0.9% (w/v) NaCl in water solution, prepared from water for ultratrace analysis (cat. no. 14211, Sigma-Aldrich) and 99.999% pure NaCl (cat. no. 204439, Sigma-Aldrich). After application of electric pulses (no pulses were applied for the sham control), the treated 0.9% NaCl solution (0.5 ml) was transferred to a new 15 ml centrifuge tube and 1.25 μ l of 65% HNO₃ (Merck) was added. Experiments were performed in four replicates. For reagent blanks, 65% HNO₃ (5 μ l) was added to 2 ml of 0.9% NaCl solution in a 15 ml centrifuge tube. Samples were kept at 4 °C until analysis. Al content in samples was determined by inductively coupled plasma mass spectrometry (ICP-MS). Prior to ICP-MS analysis, the samples were diluted with MilliQ water (18.2 M Ω cm obtained from a Direct-Q 5 Ultrapure water system, Merck Millipore, Massachusetts, USA). Quantification of Al by ICP-MS was performed based on external calibration by measuring Al standards in the concentration range of 0.1 – 1000 μ g/l with online internal standardization (25 μ g/l solution of Sc, Ge, Y, Rh, In, Ir and Bi). Calibration standard solutions were prepared from Al stock solution (1000 mg/l in 5% HNO₃ obtained from Merck). Surface (SPS-SW1) water reference materials, supplied by Spectrapure Standards AS (Norway), were used to assess the accuracy of determinations. For ICP-MS analysis, an Agilent 7900 ICP-MS (Agilent Technologies, California, USA) equipped with an auto sampler (SPS4, Agilent Technologies) was used. Optimization of instrumental parameters (summarized in Table S1 in [Supplementary Material](#)) was performed on daily basis in order

to achieve satisfactory sensitivity and low levels of oxides and doubly charged ions.

2.7. Statistical analysis

Membrane resealing data were analyzed with the nonparametric Kruskal–Wallis test because the assumption of equal variances (tested by Levene's median test at $\alpha = 0.05$) was not met. P-values were adjusted with the post-hoc Holm method test ($\alpha = 0.05$). The normalized survival after ECT measured by MTS was compared to the untreated control with one sample *t*-test ($\alpha = 0.05$), survival after ECT measured by the clonogenic assay was compared to the untreated control with Welch's *t*-test ($\alpha = 0.05$). The concentration of released Al after delivery of each pulse protocol was compared to the sham control or to the measured concentration after delivery of $8 \times 100 \mu$ s pulses with Welch's *t*-test because of unequal variances (tested by F-test). The relative standard deviation was obtained by multiplying the standard deviation by 100% and dividing this product by the average. Data were processed and visualized using Microsoft Excel (Microsoft, Washington, USA), MATLAB R2020a (MathWorks, Massachusetts, USA) and R 3.5.2 [61].

3. Results and discussion

3.1. Cell membrane permeabilization and cell survival after electroporation

To determine the optimal parameters for electrochemotherapy (i.e. highest cell survival and highest cell membrane permeabilization in terms of fraction of permeabilized cells), cell membrane permeabilization and cell survival of CHO cells was measured after exposure to classical $8 \times 100 \mu$ s pulses and nanospikes at different electric field strengths ([Fig. 2](#) and [Fig. S1 in Supplementary Material](#)). Growth medium was not added to cells right after the electroporation but after an incubation period of 25 min at room temperature to allow cell membrane resealing before plating/analyzing the electroporated cells. For delivery of nanospikes, electroporation cuvettes with 4 mm gap filled with 600 μ l of sample at room temperature were used to match the CellFX generator and the load in terms of reflections [23]. Delivery of $8 \times 100 \mu$ s pulses to electroporation cuvettes with 4 mm gap filled with 600 μ l of sample would have resulted in an electric current out of the safe operation area of the microsecond pulse generator at amplitudes required for electroporation. Therefore electroporation cuvettes with 2 mm gap filled with 150 μ l of sample were used with the microsecond pulse generator.

CHO cells were cultivated in the Ham F-12 growth medium (which is the recommended culture medium for this cell line), however, delivering pulses of higher amplitudes to electroporation cuvettes filled with Ham F-12 medium resulted in arcing. Arcing was not detected when DMEM growth medium was used to deliver pulses of same amplitudes and was thus selected as electroporation medium for cell experiments. Although both media are highly conductive (the conductivity at room temperature was 13.8 mS/cm for Ham F-12 and 14.2 mS/cm for DMEM), resulting in electric currents in the range of tens and even hundreds of amperes, the measured temperature increase after pulse delivery was very small, < 3 °C. Cell death due to thermal damage or effect of temperature increase on membrane permeabilization is thus highly unlikely.

The proportion of cells with permeabilized cell membrane increased with increasing the electric field strength and for shorter pulses, higher electric field strengths were needed to reach the same level of cell membrane permeabilization as with longer pulses; and with increasing the number of pulses, lower electric

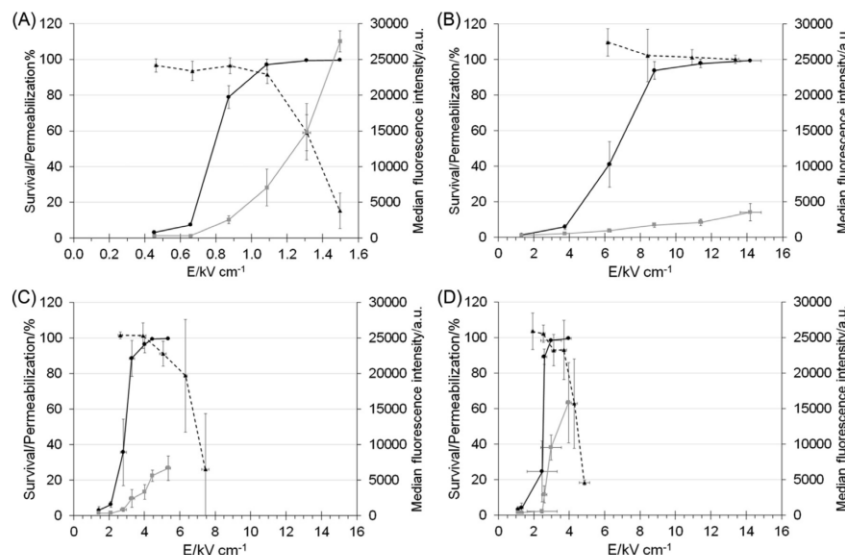


Fig. 2. Cell survival (triangles, dashed black line), cell membrane permeabilization rate (circles, solid black line) and median fluorescence intensity of YO-PRO-1 (squares, solid grey line) at different electric field strengths (E) after delivery of (A) $8 \times 100 \mu\text{s}$ pulses, 1 Hz repetition rate, (B) 1 $\times 400 \text{ ns}$ pulse, (C) $25 \times 400 \text{ ns}$ pulses, 10 Hz repetition rate, (D) $100 \times 400 \text{ ns}$ pulses, 10 Hz repetition rate. Note the different scale for (A) $8 \times 100 \mu\text{s}$ pulses. Bars represent standard deviation. Survival and permeabilization curves for other pulse parameters are on Fig. S1 in Supplementary Material.

field strengths were required to achieve the same effect – in accordance with expectations [59].

The optimal values of the electric field strength for the $8 \times 100 \mu\text{s}$ pulses, 1 Hz repetition rate, was determined to be 1.1 kV/cm, which is comparable to previous studies [62,63]. The optimal electric field strengths for the nanopulse treatments were higher and are given in Table 1. We noticed a sample to sample variation in the measured amplitude and electric current on the load when delivering nanopulses with the same amplitude set – the variations were larger at higher voltages. When setting the voltage, which was determined to be the maximal voltage in the safe operation of the CellFX generator, the average calculated electric field strength resulted to be 12.6 kV/cm for 200 ns pulses but 13.2 kV/cm for 400 and 500 ns pulses (Table 1). These differences in the voltage on the load, along with some other possible variations e.g. in the geometry of the electroporation cuvettes, are a source of variation between samples because when a certain voltage was set, the cells were not always exposed to exactly the same electric field.

Table 1
Experimentally determined optimal values of the electric field strength (E) for electroporation.

Pulse parameters	Optimal value of E (kV/cm)
8 pulses of $100 \mu\text{s}$, 1 Hz repetition rate	1.1
1 pulse of 200 ns	12.6
1 pulse of 400 ns	13.2
1 pulse of 500 ns	13.2
25 pulses of 200 ns, 10 Hz repetition rate	6.1
25 pulses of 400 ns, 10 Hz repetition rate	3.9
25 pulses of 500 ns, 10 Hz repetition rate	3.1
100 pulses of 200 ns, 10 Hz repetition rate	4.3
100 pulses of 400 ns, 10 Hz repetition rate	2.5
100 pulses of 500 ns, 10 Hz repetition rate	2.5

With increasing the electric field strength, high (i.e. > 99%) cell membrane permeabilization was achieved for all pulse treatments except for 1 pulse of 200 ns; this pulse treatment resulted in 85% cell membrane permeabilization at 12.6 kV/cm (which was previously determined to be the highest electric field strength within the safe operation range of the CellFX pulse generator). For 1 pulse of 200, 400 or 500 ns we did not observe a decrease in cell survival compared to the sham control even at the highest electric field strength, but when using 25 or 100 pulses, the survival decreased at higher electric field strengths. When increasing the number of pulses, the survival started decreasing before the cell membrane permeabilization reached its maximum. For applications based on irreversible electroporation (e.g. tissue ablation), using more pulses of lower electric field strengths might thus be more adequate. However, if the goal is to achieve reversible electroporation (like in ECT), the use of fewer pulses at higher electric fields strengths gives a wider window in which cells are reversibly electroporated.

Increasing the electric field strength above the value that permeabilized > 99% of cell resulted in increased median fluorescence of YO-PRO-1, indicating that at higher electric field strengths, more molecules of the dye entered the cells. As can be seen from Fig. 2 and Fig. S1 in Supplementary Material, the lowest fluorescence intensity was measured with nanosecond pulse protocols with only one pulse – the median fluorescence intensity did not exceed 5 000 a.u. even when applying the maximum voltage; in case of one 200 ns pulse, the maximum measured fluorescence intensity was even below 1 500 a.u. At the electric field strength determined to be optimal for ECT, the highest YO-PRO-1 fluorescence intensity was measured for the $8 \times 100 \mu\text{s}$ pulse protocol.

3.2. Cell membrane resealing

Cell membrane resealing was determined by measuring the percentage of permeabilized cells every 2 min from 2 min to

26 min after electroporation with pulses at the optimal electric field strength for ECT, as determined in previous cell survival and cell membrane permeabilization experiments (Table 1). For nanosecond pulse treatments, the time needed for membrane resealing was similar or longer as for the $8 \times 100 \mu\text{s}$ pulses (for which the membrane reseals in < 5 min). After electroporation with twenty-five 200 ns, 400 ns or 550 ns pulses, one 400 ns or 550 ns pulse or one hundred 550 ns pulses, the membrane needed a significantly longer time (> 10 min) to reseal (Fig. 3). Electroporation with nanosecond pulses has been shown to degrade the microtubule network structure and attenuate lysosome movement in calcium-containing and calcium-free solution [64,65]. Since lysosomes are involved in some of the key cell membrane repair mechanism (membrane patching and endocytosis-mediated pore removal) [66,67], modulation of lysosome transport or even direct damage to the lysosomes caused by nanosecond pulses could interfere with the cell membrane repair resulting in longer membrane resealing time.

3.3. Electrochemotherapy with bleomycin and cisplatin

Cytotoxicity of bleomycin and cisplatin was assessed using the MTS assay and for selected parameters also using clonogenic assay. Our results demonstrate that pulses in the nanosecond range are suitable for use in ECT because they increase the bleomycin and cisplatin cytotoxicity severalfold (Figs. 4 and 5). No decrease in cell survival was detected for non-electroporated cells incubated with bleomycin in the range of concentrations used, however, a decrease in survival was observed for non-electroporated cells incubated for 25 min with $50 \mu\text{M}$ of cisplatin. Higher extracellular concentrations of bleomycin were needed to reduce the cell survival to the same extent as with the standard $8 \times 100 \mu\text{s}$ pulses. The tested extracellular bleomycin concentrations are, however, still considerably lower compared to the therapeutic doses used in clinical practice. Kosjek et al. [68] measured the concentration of bleomycin in the serum of patients with a head and neck cancer who were treated with electrochemotherapy. The determined concentration of bleomycin in the serum was around 2000 nM at 5 min and 900 nM at 40 min after systemic injection of the therapeutic dose ($15,000 \text{ IU m}^{-2}$). On the other hand, pulse duration did not have a significant effect on the potentiation of cytotoxicity of cisplatin. The differences between the measured cell survival after electrochemotherapy with bleomycin and cisplatin might be a consequence differences in size, cellular uptake and mechanisms of action of the two drugs. In previous reports, the cytotoxicity of bleomycin is potentiated several hundred-fold or even thousand-fold by ECT, while that of cisplatin up to ten-fold [30]. The plasma membrane dramatically limits the number of bleomycin molecules reaching the cell interior. In the absence of electric pulses, bleomycin molecules penetrate the cells by a receptor-mediated endocytosis [69], while cisplatin enters mainly by passive diffusion through the cell membrane [70]. Bleomycin (ca. 1500 Da) is bigger than cisplatin (ca. 300 Da) and pores produced by nanosecond pulses are believed to be smaller compared to pores produced by longer electroporation pulses [9,71,72] – thus at the same extracellular bleomycin concentration, more bleomycin molecules might have entered into cells through the pores produced by the $8 \times 100 \mu\text{s}$ pulses than through nanopulse-induced pores because the microsecond pulses produced more pores through which bleomycin could enter.

The survival of cells exposed to $8 \times 100 \mu\text{s}$ pulses, 1 Hz repetition rate at 1.1 kV/cm and 25×400 ns pulses, 10 Hz at 3.9 kV/cm at different bleomycin concentrations was also determined with the clonogenic assay. For cells electroporated with the micro- or nanosecond pulse protocol in the presence of bleomycin or cisplatin, lower survival was determined by the

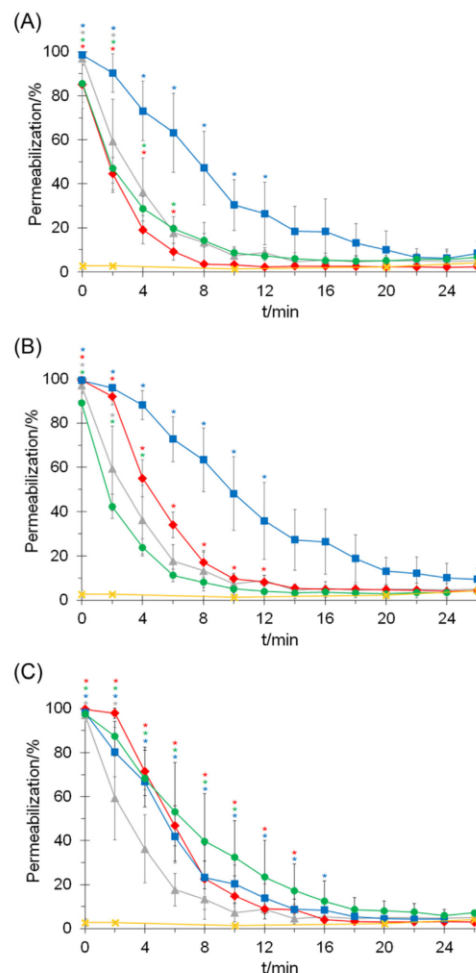


Fig. 3. Cell membrane permeabilization after different time of YO-PRO-1 addition after electroporation with (A) 200 ns pulses, (B) 400 ns pulses, (C) 550 ns pulses, (A, B, C) $8 \times 100 \mu\text{s}$ pulses delivered at 1.1 kV/cm and 1 Hz repetition rate (triangle, grey) and sham control (cross, amber). (A): 1×200 ns pulse at 12.9 kV/cm (diamond, red), 25×200 ns pulses at 6.3 kV/cm, 10 Hz repetition rate (square, blue), 100×200 ns pulses at 4.3 kV/cm, 10 Hz repetition rate (circle, green). (B): 1×400 ns pulse at 13.2 kV/cm (diamond, red), 25×400 ns pulses at 3.9 kV/cm, 10 Hz repetition rate (square, blue), 100×400 ns pulses at 3.0 kV/cm, 10 Hz repetition rate (circle, green). (C): 1×550 ns pulse at 13.2 kV/cm (diamond, red), 25×550 ns pulses at 3.2 kV/cm, 10 Hz repetition rate (square, blue), 100×550 ns pulses at 2.5 kV/cm, 10 Hz repetition rate (circle, green). Bars represent standard deviation, asterisks (*) represent statistically significant ($P < 0.05$) difference from baseline (i.e. the lowest measured permeabilization) determined by the Kruskal-Wallis test with post-hoc Holm method.

clonogenic assay as with MTS assay which is in agreement with Jakšys et al. [73] who used among others the MTT assay (a colorimetric assay in principle similar to the MTS assay) and the clonogenic assay. In our study, the survival determined by the clonogenic assay decreased to around 1% when cells were

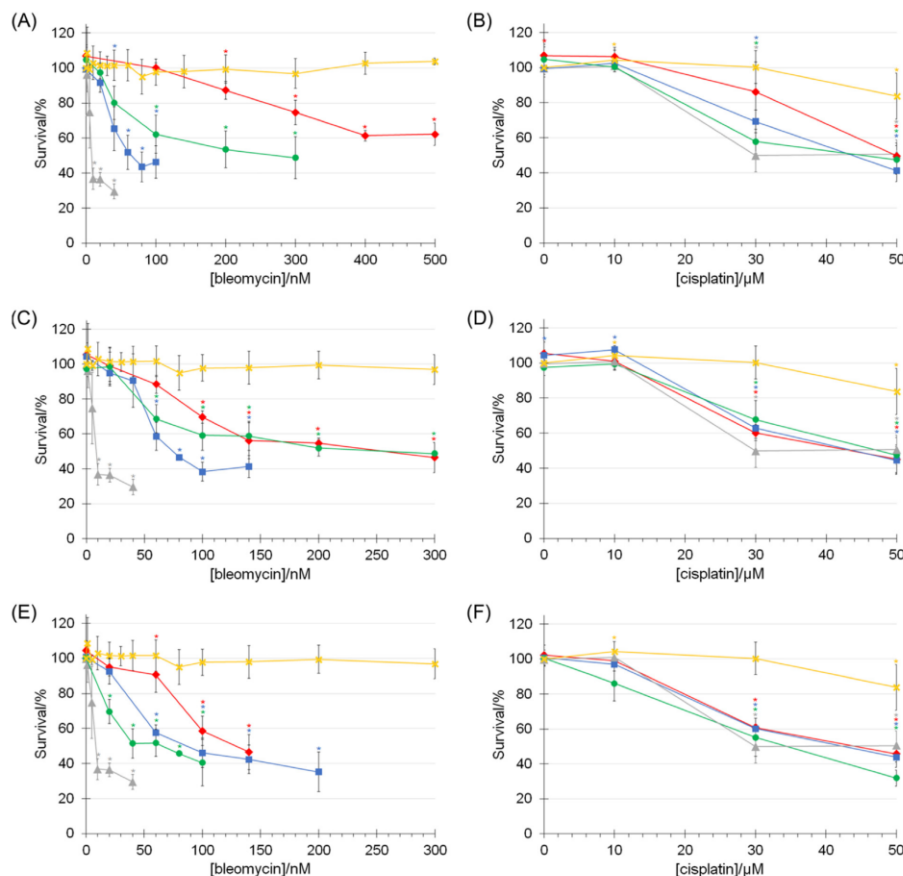


Fig. 4. Cell survival determined by the MTS assay at different (A, C, E) bleomycin and (B, D, F) cisplatin concentrations for non-electroporated CHO cells (cross, amber) and cells electroporated with different nanosecond pulses and $8 \times 100 \mu\text{s}$ pulses delivered at 1.1 kV/cm and 1 Hz repetition rate (triangle, grey). (A, B): $1 \times 200 \text{ ns}$ pulse at 12.9 kV/cm (diamond, red), $25 \times 200 \text{ ns}$ pulses at 6.3 kV/cm , 10 Hz repetition rate (square, blue), $100 \times 200 \text{ ns}$ pulses at 4.3 kV/cm , 10 Hz repetition rate (circle, green). (C, D): $1 \times 400 \text{ ns}$ pulse at 13.2 kV/cm (diamond, red), $25 \times 400 \text{ ns}$ pulses at 3.9 kV/cm , 10 Hz repetition rate (square, blue), $100 \times 400 \text{ ns}$ pulses at 3.0 kV/cm , 10 Hz repetition rate (circle, green). (E, F): $1 \times 550 \text{ ns}$ pulse at 8.5 kV/cm (diamond, red), $25 \times 550 \text{ ns}$ pulses at 3.2 kV/cm , 10 Hz repetition rate (square, blue), $100 \times 550 \text{ ns}$ pulses at 2.5 kV/cm , 10 Hz repetition rate (circle, green). Bars represent standard deviation, asterisks (*) represent statistically significant ($P < 0.05$) difference from untreated control (t -test). (For interpretation of the references to colour in this figure legend, the reader is referred to the web version of this article.)

exposed to 40 nM bleomycin and $8 \times 100 \mu\text{s}$ pulses, to 140 nM bleomycin and $25 \times 400 \text{ ns}$ pulses or to $50 \mu\text{M}$ cisplatin and $8 \times 100 \mu\text{s}$ or 400 ns pulses, while with the MTS assay, the survival was determined to be around $30 - 50\%$ at these conditions. Since the two assays used to determine cytotoxicity differ in their principles, they give different results. The MTS assay, a colorimetric method for determining the number of viable cells, is based on the bioreduction of the tetrazolium compound 3-(4,5-dimethylthiazol-2-yl)-5-(3-carboxymethoxyphenyl)-2-(4-sulfophenyl)-2H-tetrazolium (MTS). It is easy to use and rapid and thus it allows screening many different treatments [74]. The disadvantage of the method is its dependence on the metabolic state of the cell population that can significantly differ from the actual percentage of viable cells – since cells are being stressed by electroporation,

their metabolic activity might increase [75]. Clonogenic assay is based on the assumption that each remaining viable cell after exposure will form a colony after sufficient time. For cell lines that do form colonies, clonogenic assay is the best option for assessment of exact number of viable, proliferating cells after treatment [76]. However, the assay is time consuming. The type of cell death caused by bleomycin depends on the number of molecules internalized into the cells. It was reported that bleomycin caused an arrest in the G2-M phase of the cell cycle in electroporated cells at extracellular concentrations in the nanomolar range similar to the present study [77]. The toxic effects of cisplatin are believed to be primarily a consequence of covalent adducts formation between cisplatin and DNA which inhibits DNA replication and cell division [70]. The cells treated with electric pulses and bleomycin

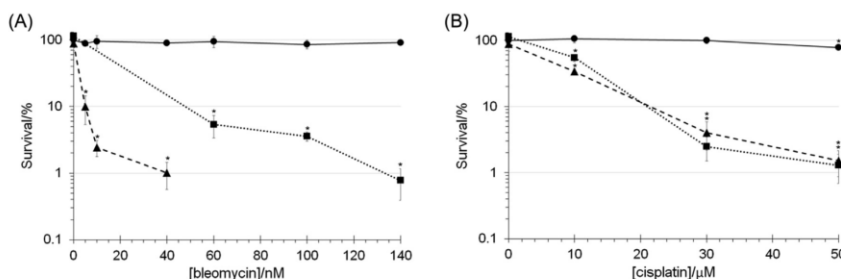


Fig. 5. Cell survival at different (A) bleomycin and (B) cisplatin concentrations determined by the clonogenic assay for non-electroporated cells (circles, solid line), cells electroporated with $8 \times 100 \mu\text{s}$ pulses delivered at 1.1 kV/cm and 1 Hz repetition rate (triangles, dashed line) and cells electroporated with $25 \times 400 \text{ ns}$ pulses at 3.9 kV/cm, 10 Hz repetition rate (squares, dotted line). Bars represent standard deviation, asterisks (*) represent statistically significant ($P < 0.05$) difference from untreated control (Welch's *t*-test).

or cisplatin could thus still be metabolically active and produce a signal in the MTS assay, however, they are unable to form colonies in the clonogenic assay.

The lowest decrease in cell metabolic activity was observed for both bleomycin and cisplatin when cells were electroporated with one 200 pulses at 12.6 kV/cm, which is not surprising since this pulse protocol permeabilized the cell membrane of only 85% of the cells. When MTS assay was used to assess cytotoxicity, we observed that the combination of $8 \times 100 \mu\text{s}$ pulses, 1 Hz repetition rate at 1.1 kV/cm and bleomycin resulted in a significant loss of metabolic activity of the cells (to around 40% of the untreated control) when increasing the extracellular concentration of bleomycin up to 10 nM. Higher bleomycin concentration did not further decrease the cells' metabolic activity measured by the MTS assay. The measured cell activity after ECT reached a plateau, i.e. with further increasing the bleomycin concentration, the metabolic activity decreased only slightly. Such a plateau was observed also for cells electroporated with nanosecond pulses, only at higher concentrations of bleomycin compared to the $8 \times 100 \mu\text{s}$ pulses. When using the clonogenic assay, however, this plateau was not observed – cell survival was decreasing with increasing the bleomycin extracellular concentration. For cisplatin, concentrations above $50 \mu\text{M}$ were not tested because a decrease of survival was observed also for non-electroporated cells incubated for 25 min with $50 \mu\text{M}$ cisplatin.

Interestingly, when using specific nanopulse electroporation protocols, lower concentrations of bleomycin were needed to achieve a cytotoxic effect – these pulse protocols ($25 \times 200 \text{ ns}$ pulses, 10 Hz at 6.1 kV/cm; $25 \times 400 \text{ ns}$ pulses, 10 Hz at 3.9 kV/cm; $100 \times 550 \text{ ns}$ pulses, 10 Hz at 3.1 kV/cm) are also the ones with the longest cell membrane resealing time. The time required for membrane resealing might be affected also by the size of pores that form on the membrane because different repair mechanisms may be activated depending on the pore size. For laser-induced pores it was shown that for smaller pores, longer time is required for membrane resealing than for larger pores [78]. The cell is probably more tolerant to small wounds, but larger pores in the membrane need to be repaired faster for the cell to survive the injury [67]. Since the transmembrane transport is an integral of flux over time, a longer resealing time results in higher intracellular accumulation and consequently higher cytotoxicity of bleomycin. In future studies, measurements of the intracellular bleomycin concentration is required to determine how many bleomycin molecules are being internalized after electroporation with different pulse protocols.

As can be seen from micrographs taken 72 h after ECT experiments (Fig. 6), the combination of electric pulses and bleomycin or cisplatin at concentrations that decreased the cell

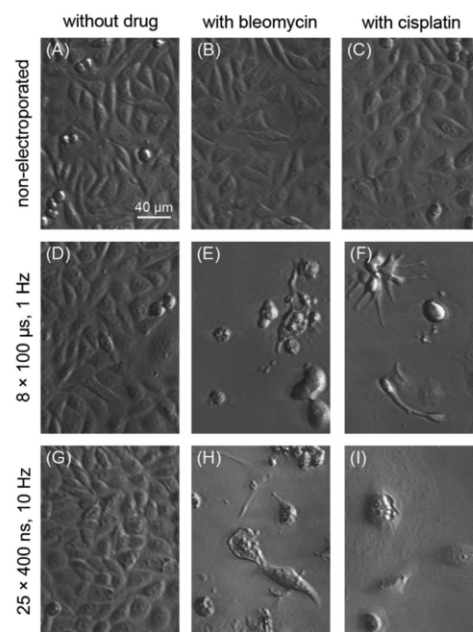


Fig. 6. IMC images of CHO cells 72 h after ECT experiments: (A) control that was exposed neither to electric pulses nor to any drug, (B) non-electroporated cells exposed to 140 nM bleomycin, (C) non-electroporated cells exposed to $50 \mu\text{M}$ cisplatin, (D) cells exposed to eight $100 \mu\text{s}$ pulses, 1 Hz, 1.1 kV/cm, (E) cells exposed to eight $100 \mu\text{s}$ pulses, 1 Hz, 1.1 kV/cm and 40 nM bleomycin, (F) cells exposed to eight $100 \mu\text{s}$ pulses, 1 Hz, 1.1 kV/cm and $50 \mu\text{M}$ cisplatin, (G) cells exposed to $25 \times 400 \text{ ns}$ pulses, 10 Hz, 3.9 kV/cm, (H) cells exposed to $25 \times 400 \text{ ns}$ pulses, 10 Hz, 3.9 kV/cm and 140 nM bleomycin, (I) cells exposed to $25 \times 400 \text{ ns}$ pulses, 10 Hz, 3.9 kV/cm and $50 \mu\text{M}$ cisplatin.

survival to around 1% according to the clonogenic assay, caused significant morphological changes – the cells were enlarged, of irregular morphologies and also blebbing occurred. On the other hand, no differences were observed in cells that were exposed only to the electric pulses or only to the drug.

In our study we show that combination of nanosecond pulses and bleomycin or cisplatin, two most commonly used chemother-

apeutic drugs in ECT, causes successful cell kill. In case of contraindications for one drug (e.g. due to allergic reaction or exceeding the cumulative dose), the other could be used. Antitumor effects of ECT with nanosecond pulses and bleomycin/doxorubicin have already been reported *in vivo* on a feline oral malignant melanoma [46] and on myeloma tumor models in mice [47], however, it is not clear from these reports how the nanosecond pulses, bleomycin/doxorubicin and/or CO₂ laser surgery contributed to the overall success of the therapy because of lack of controls treated with electric pulses, the drugs and CO₂ laser only. Our study is, therefore, providing evidence of effectiveness for ECT with nanosecond pulses and contributes to the optimization of such procedures by elucidating the most effective pulse protocols. Since bleomycin is a medium-sized molecule, our findings can be extended also to other nanosecond electroporation-based applications with the aim to introduce medium sized molecules (like siRNA) into cells.

3.4. Metal release

The concentration of released aluminum ions from electroporation cuvettes was measured after delivery of $8 \times 100 \mu\text{s}$ pulses and nanopulses at previously determined optimal voltages in 0.9% (w/v) NaCl solution. We are aware that the NaCl solution is not usually used as electroporation medium, however, we chose pure NaCl solution for this set of experiments because the growth medium contains aluminum in trace amounts; the pure NaCl solution allowed us to detect even very small amounts of aluminum ions. A new electroporation cuvette from the same manufacturer was used for each sample. Significantly higher concentration of released aluminum from electroporation cuvettes was detected after delivery of $8 \times 100 \mu\text{s}$ pulses than any of the nanosecond pulses (Table 2). Since aluminum alloy and not pure aluminum is used for manufacturing electroporation cuvettes, also other metal ions might be released.

The results of metal release from electrodes after application of electroporation pulses in the nanosecond range thus confirm the theoretical predictions that shorter pulse duration results in less electrochemical reactions [56]. We proved that shorter pulse duration decreases the amount of metal release from electrodes – even if the voltage and/or number of pulses is increased (compared to longer electroporation pulses) to achieve the same biological effect.

Table 2

Concentration of released Al ions from electroporation cuvettes (N = 4) after delivery of different pulses and estimated energies for the $8 \times 100 \mu\text{s}$ and nanosecond pulses, the relative standard deviation (RSD) and estimated energy delivered by the electric pulses. Asterisk (*) represents statistically significant difference ($P < 0.05$) to the concentration of released Al after delivery of $8 \times 100 \mu\text{s}$ pulses, hash (#) represents statistically significant difference ($P < 0.05$) to sham control (no pulses delivered) determined by Welch's t-test.

Pulse protocol	Energy (J)	[Al] (ng/ml)	
		Average	RSD
blank		6.3*#	3.0
sham control		56.5*	52
8 pulses of 100 μs , 1 Hz frequency 0.9 kV/cm	4.7	2660#	5.2
1 pulse of 200 ns 14.7 kV/cm	0.3	519*	69
1 pulse of 400 ns 15.3 kV/cm	0.7	184*	54
1 pulse of 550 ns 15.3 kV/cm	1.0	427*	75
25 pulses of 200 ns, 10 Hz frequency 6.9 kV/cm	1.8	148*#	12
25 pulses of 400 ns, 10 Hz frequency 4.2 kV/cm	1.4	153*#	7.1
25 pulses of 550 ns, 10 Hz frequency 3.4 kV/cm	1.3	170*#	6.3
100 pulses of 200 ns, 10 Hz frequency 4.2 kV/cm	2.6	414*#	49
100 pulses of 400 ns, 10 Hz frequency 2.8 kV/cm	2.4	411*#	5.9
100 pulses of 550 ns, 10 Hz frequency 2.8 kV/cm	3.3	521*#	13

Electrode material release, corrosion and fouling of the electrodes, products of electrolysis and chemical changes to the treated medium (all consequences of electrochemical reactions at the electrode–electrolyte interface) are limiting factors for application of electroporation-based technologies in the food industry [48]. Uptake of electrolysis species in permeabilized cells induces cell death [79] and metal ions, released from the electrodes during electroporation, are cytotoxic and affect the biochemistry of electroporated cells [50,51,80]. Development of methods for reducing these unwanted electrochemical effects is thus of interest for a wider spread of electroporation-based applications in research, food processing, biotechnology and medical applications of electroporation such as ECT, tissue ablation and gene electrotransfer.

When comparing different nanopulse protocols, the concentration of released metal ions does not seem to correlate with the estimated energy: the lowest energy was estimated for 1 pulse of 200 ns at 14.7 kV/cm, however, for this pulse protocol, we measured one of the highest concentrations of released aluminum ions. This indicates that the amount of released metal ions from electrodes does not solely depend on the applied energy but is affected also by other pulse parameters including pulse duration, voltage, and number of pulses. Perhaps the most unexpected were the concentrations of released aluminum measured after delivery of single nanopulses at the same voltage (which, however, resulted in a slightly different electric field strength: 14.7 kV/cm for 200 ns and 15.3 for 400 and 500 ns). Contrary to expectations that at the same voltage and number of pulses the lowest concentration of released aluminum will be measured for the shortest pulse duration, the highest average concentration of aluminum ion was measured after delivery of one 200 ns (i.e. the shortest) nanopulse. If excluding an outlying measurement (which is probably an experimental error because the measured aluminum concentration was even lower than in sham controls), the mean value for one 200 ns pulse at 14.7 kV/cm increases even more, to 680 ng/ml of aluminum.

Electroporation cuvettes with 4 mm gap filled with 600 μl of the NaCl solution were used in metal release experiments for delivery of all pulses to ensure the same geometry/contact surface of the electrode and electrolyte. This is contrary to cell experiments in which we used electroporation cuvettes with 2 mm gap for delivering the $8 \times 100 \mu\text{s}$ pulses because of the limitations of the microsecond pulse generator, while 4 mm cuvettes were used to deliver nanopulses. To be able to deliver $8 \times 100 \mu\text{s}$ pulses to electroporation cuvettes with 4 mm gap filled with 600 μl of NaCl solution, we needed to use a different pulse generator: the Cliniporator Vitae. In cell experiments, the microsecond pulse generator was set to deliver $8 \times 100 \mu\text{s}$ pulses at 250 V which resulted in an electric field strength of 1.1 kV/cm considering the distance between electrodes to be 2 mm. For metal release experiments, the distance between electrodes was 4 mm, thus, to achieve the same electric field strength, we set the voltage at 500 V on the Cliniporator Vitae. However, 500 V is the minimum voltage for this device and for every successive 100 μs pulse in the train, we observed a drop in the voltage and electric current, resulting in the measured electric field strength of 0.9 kV/cm. Nonetheless, the measured concentration of released aluminum ions after the delivery of $8 \times 100 \mu\text{s}$ pulses was significantly (at least five times) higher than after any of the nanopulse protocols, thus proving our point that metal release from electrodes is significantly reduced if using nanopulses compared to the classical $8 \times 100 \mu\text{s}$. If the electric field strength of 1.1 kV had been achieved for the $8 \times 100 \mu\text{s}$, the concentration of the released aluminum ion would most probably be even higher.

Even though the same pulse generator was used to deliver nanopulses, discrepancies in the calculated electric field strength from cell and metal release experiments were observed for some of the pulse protocols (Tables 1 and 2). The source of the

discrepancies might be the use of different medium (DMEM growth medium in cell experiments vs. NaCl solution in metal release experiments) resulting in a different voltage on the load, possible variations in the cuvette's geometry since a new electroporation cuvette was used for every sample, and also the already mentioned differences in the delivered voltage that were observed from sample to sample, especially at very high voltages.

Compared to the reagent blanks (0.9% NaCl solution with addition of HNO_3), significant increase in the concentration of aluminum ions was detected also in sham control samples for which the 0.9% NaCl solution was added to the electroporation cuvette and no pulses were applied. The addition of the NaCl solution caused the development of the double layer, a layer of charged particles and/or orientated dipoles at each electrode-electrolyte interface. Even if no external voltage is applied, chemical reactions occur immediately, and electrons are transferred between the electrode and the electrolyte. The electron transfer results in an electric field between the electrode and the layer of ions/dipoles which influences further chemical reactions, accelerating the oxidation reaction (and consequently metal release from electrodes), while inhibiting the reverse reduction reaction; if no voltage is applied, the competing oxidation and reduction reactions reach an equilibrium [56].

The use of nanosecond pulses has several advantages over conventional micro- and millisecond electroporation pulses: low level of heating, reduced muscle contractions [2,24,44,45] and, as we show in this study, reduced contamination with metal ions released from the electrodes, making nanosecond pulses alluring for use in clinical practice and electroporation-based applications in which electrochemical reactions should be kept at minimum, e.g. food technology.

4. Conclusions

The aim of this *in vitro* study on CHO cells was to evaluate the effects of nanosecond pulse parameters (voltage, pulse duration, number of pulses) on cell membrane permeabilization and resealing and on cell survival after electroporation only and after electrochemotherapy with bleomycin and cisplatin, and compare them to the $8 \times 100 \mu\text{s}$ pulses commonly used in ECT. Cell survival after electroporation decreased and cell membrane permeabilization increased with increasing electric field strength and number of nanosecond pulses. As expected, for shorter pulses, higher electric field strengths were needed to reach the same effect as with longer pulses. We show that the application of permeabilizing nanosecond pulses in combination with bleomycin or cisplatin results in successful cell kill. The pulse duration did not considerably affect the decrease of survival caused by ECT with cisplatin. On the other hand, higher bleomycin concentrations were needed to achieve the same effect with nanosecond pulses compared to the standard $8 \times 100 \mu\text{s}$ pulses, however, the bleomycin concentration was still considerably lower than concentrations used in clinical practice. Nanosecond pulses with parameters that caused the longest cell membrane resealing times were also the ones that decreased cell survival most effectively in ECT experiments with bleomycin. We also show that decreasing the pulse duration from microseconds to nanoseconds with concomitantly increasing the amplitude to achieve the same biological effect results in reduced electrochemical reactions, which in our study was monitored by quantifying the release of aluminum ions from electrodes.

Declaration of Competing Interest

Damijan Miklavčič holds patents on electrochemotherapy that have been licensed to IGEA S.p.A (Carpì, Italy) and is also a

consultant to various companies with an interest in electroporation-based technologies and treatments. The other authors have no competing interests.

Acknowledgments

The study was funded by Pulse Biosciences and the Slovenian Research Agency (ARRS) (research core funding No. (P2-0249)). The work was partially performed within the network of research and infrastructural centres of University of Ljubljana, which is financially supported by Slovenian Research Agency through infrastructural grant IP-0510. A.V. was granted a scholarship from the University Foundation of ing. Lenarčič Milan. A.V. would like to thank D. Hodžič and L. Vukanović for their help in the cell culture laboratory and M. Reberšek for his assistance with the electroporation set-up.

Appendix A. Supplementary material

Supplementary data to this article can be found online at <https://doi.org/10.1016/j.bioelechem.2021.107798>.

References

- [1] T. Kotnik, L. Rems, M. Tarek, D. Miklavčič, Membrane Electroporation and Electroporation: Mechanisms and Models, *Annu. Rev. Biophys.* 48 (2019) 63–91, <https://doi.org/10.1146/annurev-biophys-052118-115451>.
- [2] K.H. Schoenbach, S.J. Beebe, E.S. Buescher, Intracellular effect of ultrashort electrical pulses, *Bioelectromagnetics*. 22 (2001) 440–448, <https://doi.org/10.1002/bem.71>.
- [3] K.H. Schoenbach, A. Abou-Ghazala, T. Vithoulkas, R.W. Alden, R. Turner, S. Beebe, The effect of pulsed electrical fields on biological cells, in: *Dig. Tech. Pap. 11th IEEE Int. Pulsed Power Conf.* (Cat. No.97CH36127), 1 (1997) 73–78, <https://doi.org/10.1109/PPC.1997.679279>.
- [4] E. Tekle, H. Oubrahim, S.M. Dzekunov, J.F. Kolb, P.B. Chock, Selective Field Effects on Intracellular Vacuoles and Vesicle Membranes with Nanosecond Electric Pulses, *Biophys. J.* 89 (2005) 274–284, <https://doi.org/10.1529/biophysj.104.054494>.
- [5] J.A. White, P.F. Blackmore, K.H. Schoenbach, S.J. Beebe, Stimulation of capacitative calcium entry in HL-60 cells by nanosecond pulsed electric fields, *J. Biol. Chem.* 279 (2004) 22964–22972, <https://doi.org/10.1074/jbc.M311135200>.
- [6] T. Batista Napotnik, Y.-H. Wu, M.A. Gundersen, D. Miklavčič, P.T. Vernier, Nanosecond electric pulses cause mitochondrial membrane permeabilization in Jurkat cells, *Bioelectromagnetics*. 33 (2012) 257–264, <https://doi.org/10.1002/bem.20707>.
- [7] R. Nuccitelli, A. McDaniel, R. Connolly, B. Zelikson, H. Hartman, Nano-Pulse Stimulation Induces Changes in the Intracellular Organelles in Rat Liver Tumors Treated In Situ, *Lasers Surg. Med.* (2020) 1–8, <https://doi.org/10.1002/lsm.23239>.
- [8] T. Kotnik, D. Miklavčič, Theoretical evaluation of voltage induction on internal membranes of biological cells exposed to electric fields, *Biophys. J.* 90 (2006) 480–491, <https://doi.org/10.1529/biophysj.105.070771>.
- [9] P.T. Vernier, Y. Sun, M.A. Gundersen, Nanosecond-pulse-driven membrane perturbation and small molecule permeabilization, *BMC Cell Biol.* 7 (2006) 1–16, <https://doi.org/10.1186/1471-2121-7-37>.
- [10] T.B. Napotnik, M. Reberšek, T. Kotnik, E. Lebrasseur, G. Cabodevila, D. Miklavčič, Electroporation of endocytotic vesicles in B16 F1 mouse melanoma cells, *Med. Biol. Eng. Comput.* 48 (2010) 407–413, <https://doi.org/10.1007/s11517-010-0599-9>.
- [11] A. Silve, I. Leray, L.M. Mir, Demonstration of cell membrane permeabilization to medium-sized molecules caused by a single 10 ns electric pulse, *Bioelectrochemistry*. 87 (2012) 260–264, <https://doi.org/10.1016/j.bioelechem.2011.10.002>.
- [12] M. Breton, L. Delemotte, A. Silve, L.M. Mir, M. Tarek, Transport of siRNA through Lipid Membranes Driven by Nanosecond Electric Pulses: An Experimental and Computational Study, *J. Am. Chem. Soc.* 134 (2012) 13938–13941, <https://doi.org/10.1021/ja3052365>.
- [13] P. Ruzgys, V. Novickij, J. Novickij, S. Šatkauskas, Nanosecond range electric pulse application as a non-viral gene delivery method: proof of concept, *Sci. Rep.* 8 (2018) 15502, <https://doi.org/10.1038/s41598-018-33912-y>.
- [14] L. Rems, M. Ušaj, M. Kandušer, M. Reberšek, D. Miklavčič, G. Puchar, Cell electrofusion using nanosecond electric pulses, *Sci. Rep.* 3 (2013) 3382, <https://doi.org/10.1038/srep03382>.
- [15] A.M. Bowman, O.M. Nesin, O.N. Pakhomova, A.G. Pakhomov, Analysis of plasma membrane integrity by fluorescent detection of $\text{Ti}^{(+)}$ uptake, *J. Membr. Biol.* 236 (2010) 15–26, <https://doi.org/10.1007/s00232-010-9269-y>.

- [16] S.J. Beebe, P.M. Fox, L.J. Rec, E.L.K. Willis, K.H. Schoenbach, Nanosecond, high-intensity pulsed electric fields induce apoptosis in human cells, *FASEB J.* 17 (2003) 1493–1495, <https://doi.org/10.1096/fj.02-0859fje>.
- [17] W.E. Ford, W. Ren, P.F. Blackmore, K.H. Schoenbach, S.J. Beebe, Nanosecond pulsed electric fields stimulate apoptosis without release of pro-apoptotic factors from mitochondria in B16F10 melanoma, *Arch. Biochem. Biophys.* 497 (2010) 82–89, <https://doi.org/10.1016/j.abb.2010.03.008>.
- [18] S.J. Beebe, P.M. Fox, L.J. Rec, K. Somers, R.H. Stark, K.H. Schoenbach, Nanosecond pulsed electric field (nsPEF) effects on cells and tissues: apoptosis induction and tumor growth inhibition, *IEEE Trans. Plasma Sci.* 30 (2002) 286–292, <https://doi.org/10.1109/TPS.2002.1003872>.
- [19] R. Nuccitelli, U. Pliquet, X. Chen, W. Ford, R. James Swanson, S.J. Beebe, J.F. Kolb, K.H. Schoenbach, Nanosecond pulsed electric fields cause melanomas to self-destruct, *Biochem. Biophys. Res. Commun.* 343 (2006) 351–360.
- [20] S. Guo, Y. Jing, N.I. Burcus, B.P. Lassiter, R. Tanaz, R. Heller, S.J. Beebe, Nanopulse stimulation induces potent immune responses, eradicating local breast cancer while reducing distant metastases, *Int. J. Cancer.* 142 (2018) 629–640, <https://doi.org/10.1002/ijc.31071>.
- [21] S.J. Beebe, J. White, P.F. Blackmore, Y. Deng, K. Somers, K.H. Schoenbach, Diverse Effects of Nanosecond Pulsed Electric Fields on Cells and Tissues, *DNA Cell Biol.* 22 (2003) 785–796, <https://doi.org/10.1089/104454903322624993>.
- [22] R. Nuccitelli, J. Huynh, K. Lui, R. Wood, M. Kreis, B. Athos, P. Nuccitelli, Nanoelectroablation of human pancreatic carcinoma in a murine xenograft model without recurrence, *Int. J. Cancer.* 132 (2013) 1933–1939, <https://doi.org/10.1002/ijc.27860>.
- [23] T. Batista Napotnik, M. Reberšek, P.T. Vernier, B. Mali, D. Miklavčič, Effects of high voltage nanosecond electric pulses on eucaryotic cells (in vitro): A systematic review, *Bioelectrochemistry.* 110 (2016) 1–12, <https://doi.org/10.1016/j.bioelechem.2016.02.011>.
- [24] U. Pliquet, R. Nuccitelli, Measurement and simulation of Joule heating during treatment of B-16 melanoma tumors in mice with nanosecond pulsed electric fields, *Bioelectrochemistry.* 100 (2014) 62–68, <https://doi.org/10.1016/j.bioelechem.2014.03.001>.
- [25] T. Kotnik, W. Frey, M. Sack, S. Haberl Meglič, M. Peterka, D. Miklavčič, Electroporation-based applications in biotechnology, *Trends Biotechnol.* 33 (2015) 480–488, <https://doi.org/10.1016/j.tibtech.2015.06.002>.
- [26] G. Saldaña, I. Alvarez, S. Condón, J. Raso, Microbiological aspects related to the feasibility of PEF technology for food pasteurization, *Crit. Rev. Food Sci. Nutr.* 54 (2014) 1415–1426, <https://doi.org/10.1080/10408398.2011.638995>.
- [27] S. Mahnič-Kalamiza, E. Vorobiev, D. Miklavčič, Electroporation in Food Processing and BioRefinery, *J. Membr. Biol.* 247 (2014) 1279–1304, <https://doi.org/10.1007/s00232-014-9737-x>.
- [28] B. Geboers, H.J. Scheffer, P.M. Graybill, A.H. Ruars, S. Nieuwenhuizen, R.S. Puijk, P.M. van den Tol, R.V. Dávalos, B. Rubinsky, T.D. de Grijl, D. Miklavčič, M.R. Meijerink, High-Voltage Electrical Pulses in Oncology: Irreversible Electroporation, Electrochemotherapy, Gene Electroransfer, Electrofusion, and Electroimmunotherapy, *Radiology.* 295 (2020) 254–272, <https://doi.org/10.1148/radiol.2020192190>.
- [29] L.G. Campana, D. Miklavčič, G. Bertino, R. Marconato, S. Valpione, I. Imarisio, M. V. Dieci, E. Granziera, M. Cemazar, M. Alaibac, G. Sersa, Electrochemotherapy of superficial tumors – Current status: Basic principles, operating procedures, shared indications, and emerging applications, *Semin. Oncol.* 46 (2019) 173–191, <https://doi.org/10.1053/j.seminoncol.2019.04.002>.
- [30] D. Miklavčič, B. Mali, B. Kos, R. Heller, G. Sersa, Electrochemotherapy: From the drawing board to medical practice, *Biomed. Eng. Online.* 13 (2014) 1–20, <https://doi.org/10.1186/1475-2875-13-29>.
- [31] L.M. Mir, S. Orlowski, J.J. Belehradek, C. Paoletti, Electrochemotherapy potentiation of antitumor effect of bleomycin by local electric pulses, *Eur. J. Cancer.* 27 (1991) 68–72.
- [32] M.J. Jaroszeski, V. Dang, C. Pottinger, J. Hickey, R. Gilbert, R. Heller, Toxicity of anticancer agents mediated by electroporation in vitro, *Anticancer. Drugs.* 11 (2000) 201–208.
- [33] R. Heller, M. Jaroszeski, J. Leo-Messina, R. Perrot, N. Van Voorhis, D. Reintgen, R. Gilbert, Treatment of B16 mouse melanoma with the combination of electropermeabilization and chemotherapy, *Bioelectrochem. Bioenerg.* 36 (1995) 83–87, [https://doi.org/10.1016/0302-4598\(94\)05013-K](https://doi.org/10.1016/0302-4598(94)05013-K).
- [34] M. Hyacinthe, M.J. Jaroszeski, V.V. Dang, D. Coppola, R.C. Karl, R.A. Gilbert, R. Heller, Electrically enhanced drug delivery for the treatment of soft tissue sarcoma, *Cancer.* 85 (1999) 409–417.
- [35] M.J. Jaroszeski, R.A. Gilbert, R. Heller, In vivo antitumor effects of electrochemotherapy in a hepatoma model, *Biochim. Biophys. Acta.* 1334 (1997) 15–18.
- [36] G. Sersa, M. Čemažar, D. Miklavčič, Antitumor effectiveness of electrochemotherapy with cis-diamminedichloroplatinum(II) in mice, *Cancer Res.* 55 (1995) 3450–3455.
- [37] G. Sersa, B. Štabuc, M. Čemažar, B. Jančar, D. Miklavčič, Z. Rudolf, Electrochemotherapy with cisplatin: Potentiation of local cisplatin antitumor effectiveness by application of electric pulses in cancer patients, *Eur. J. Cancer.* 34 (1998) 1213–1218, [https://doi.org/10.1016/S0959-8049\(98\)00025-2](https://doi.org/10.1016/S0959-8049(98)00025-2).
- [38] D. Miklavčič, G. Pucihar, M. Pavlovac, S. Ribarič, M. Mali, A. Maček-Lebar, M. Petkovšek, J. Nastran, S. Kranjc, M. Čemažar, G. Sersa, The effect of high frequency electric pulses on muscle contractions and antitumor efficiency in vivo for a potential use in clinical electrochemotherapy, *Bioelectrochemistry.* 65 (2005) 121–128, <https://doi.org/10.1016/j.bioelechem.2004.07.004>.
- [39] A. Županič, S. Ribarič, D. Miklavčič, Increasing the repetition frequency of electric pulse delivery reduces unpleasant sensations that occur in electrochemotherapy, *Neoplasma.* 54 (2007) 246–250.
- [40] M. Kendler, M. Micheluzzi, T. Wetzig, J.C. Simon, Electrochemotherapy under tumescent local anesthesia for the treatment of cutaneous metastases, *Dermatologic Surg.* 39 (2013) 1023–1032, <https://doi.org/10.1111/dsu.12190>.
- [41] Z. Rudolf, B. Štabuc, M. Cemazar, D. Miklavčič, L. Vodovnik, G. Sersa, Electrochemotherapy with bleomycin. The first clinical experience in malignant melanoma patients, *Radiol. Oncol.* 29 (1995) 229–235.
- [42] G. Sersa, M. Čemažar, R. Zvonimir, Electrochemotherapy: advantages and drawbacks in treatment of cancer patients, *Cancer Ther.* 1 (2003) 133–142.
- [43] M. Marty, G. Sersa, J.R. Garbay, J. Gehl, C.G. Collins, M. Snoj, V. Billard, P.F. Geertsens, J.O. Larkin, D. Miklavčič, I. Pavlovic, S.M. Paulin-Košir, M. Čemažar, N. Morsli, D.M. Soden, Z. Rudolf, C. Robert, G.C. O'Sullivan, L.M. Mir, Electrochemotherapy – An easy, highly effective and safe treatment of cutaneous and subcutaneous metastases: Results of ESOPE (European Standard Operating Procedures of Electrochemotherapy) study, *Eur. J. Cancer Suppl.* 4 (2006) 3–13, <https://doi.org/10.1016/j.ejcsup.2006.08.002>.
- [44] G. Long, P.K. Shires, D. Plescia, S.J. Beebe, J.F. Kolb, K.H. Schoenbach, Targeted tissue ablation with nanosecond pulses, *IEEE Trans. Biomed. Eng.* 58 (2011) 2161–2167, <https://doi.org/10.1109/TBME.2011.2113183>.
- [45] W.R. Rogers, J.H. Merritt, J.A. Comeaux, C.T. Kuhnel, D.F. Moreland, D.G. Teltchick, J.H. Lucas, M.R. Murphy, Strength-duration curve an electrically excitable tissue extended down to near 1 nanosecond, *IEEE Trans. Plasma Sci.* 32 (2004) 1587–1599, <https://doi.org/10.1109/TPS.2004.831758>.
- [46] J. Tunikowska, A. Antończyk, N. Rembiałkowska, Ł. Jóźwiak, V. Novickij, I. Kulbacka, The first application of nanoelectrochemotherapy in feline oral malignant melanoma treatment – case study, *Animals.* 10 (2020) 556, <https://doi.org/10.3390/ani10040556>.
- [47] V. Novickij, V. Malýško, A. Želvys, A. Balevičiute, A. Zinkevičienė, J. Novickij, I. Girkontaite, Electrochemotherapy using doxorubicin and nanosecond electric field pulses: A pilot in vivo study, *Molecules.* 25 (2020), <https://doi.org/10.3390/molecules25204601>.
- [48] G. Pataro, G. Ferrari, Limitations of pulsed electric field utilization in food industry, in: v. F.J. Barba, O. Pamiakov, A. Wiktor (Ur.), *Pulsed Electr. Fields to Obtain Heal. Sustain. Food Tomorrow*, Academic Press, 2020: str. 283–310, <https://doi.org/https://doi.org/10.1016/B978-0-12-816402-0.00013-6>.
- [49] G. Saulis, R. Rodaite, R. Rodaite-Riševienė, V. S. Dainauskaitė, R. Saulė, Electrochemical processes during high-voltage electric pulses and their importance in food processing technology, in: R. Rai V (Ur.), *Adv. Food Biotechnol.*, John Wiley & Sons Ltd str (2015) 575–592.
- [50] T. Kotnik, D. Miklavčič, L.M. Mir, Cell membrane electropermeabilization by symmetrical bipolar rectangular pulses: Part II. Reduced electrolytic contamination, *Bioelectrochemistry.* 54 (2001) 91–95, [https://doi.org/10.1016/S1567-5394\(01\)00115-3](https://doi.org/10.1016/S1567-5394(01)00115-3).
- [51] J.W. Loomis-Hussellbee, P.J. Cullen, R.F. Irvine, A.P. Dawson, Electroporation can cause artefacts due to solubilization of cations from the electrode plates. Aluminum ions enhance conversion of inositol 1,3,4,5-tetrakisphosphate into inositol 1,4,5-trisphosphate in electroporated L1210 cells, *Biochem. J.* 277 (Pt 3) (1991) 883–885.
- [52] U. Friedrich, N. Stachowicz, A. Simm, G. Fuhr, K. Lucas, U. Zimmermann, High efficiency electrotransfection with aluminum electrodes using microsecond controlled pulses, *Bioelectrochem. Bioenerg.* 47 (1998) 103–111, [https://doi.org/10.1016/S0302-4598\(98\)00163-9](https://doi.org/10.1016/S0302-4598(98)00163-9).
- [53] G. Saulis, R. Lape, R. Pranevičiute, D. Mickevičius, Changes of the solution pH due to exposure by high-voltage electric pulses, *Bioelectrochemistry.* 67 (2005) 101–108, <https://doi.org/10.1016/j.bioelechem.2005.03.001>.
- [54] S.A.A. Kooijmans, S. Stremersch, K. Braeckmans, S.C. de Smedt, A. Hendrix, M.J. A. Wood, R.M. Schiffer, K. Raemdonck, P. Vader, Electroporation-induced siRNA precipitation obscures the efficiency of siRNA loading into extracellular vesicles, *J. Control. Release.* 172 (2013) 229–238, <https://doi.org/10.1016/j.jconrel.2013.08.014>.
- [55] R. Stapulionis, Electric pulse-induced precipitation of biological macromolecules in electroporation, *Bioelectrochem. Bioenerg.* 48 (1999) 249–254, [https://doi.org/10.1016/S0302-4598\(98\)00206-2](https://doi.org/10.1016/S0302-4598(98)00206-2).
- [56] J. Morren, B. Roodenburg, S.W.H. de Haan, Electrochemical reactions and electrode corrosion in pulsed electric field (PEF) treatment chambers, *Innov. Food Sci. Emerg. Technol.* 4 (2003) 285–295, [https://doi.org/10.1016/S1466-8564\(03\)00041-9](https://doi.org/10.1016/S1466-8564(03)00041-9).
- [57] A. Vižintin, J. Vidmar, J. Ščančar, D. Miklavčič, Effect of interphase and interpulse delay in high-frequency irreversible electroporation pulses on cell survival, membrane permeabilization and electrode material release, *Bioelectrochemistry.* 134 (2020), <https://doi.org/10.1016/j.bioelechem.2020.107523>.
- [58] S. Mahnič-Kalamiza, D. Miklavčič, Scratching the electrode surface: Insights into a high-voltage pulsed-field application from in vitro & in silico studies in indifferent fluid, *Electrochim. Acta.* 363 (2020), <https://doi.org/10.1016/j.electacta.2020.137187>.
- [59] G. Pucihar, J. Krmelj, M. Reberšek, T. Batista Napotnik, D. Miklavčič, Equivalent Pulse Parameters for Electroporation, *IEEE Trans. Biomed. Eng.* 58 (2011) 3279–3288, <https://doi.org/10.1109/TBME.2011.2167232>.
- [60] D.C. Sweeney, M. Reberšek, J. Dermol, L. Rems, D. Miklavčič, R.V. Dávalos, Quantification of cell membrane permeability induced by monopolar and high-frequency bipolar bursts of electrical pulses, *Biochim. Biophys. Acta - Biomembr.* 2016 (1858) 2689–2698, <https://doi.org/10.1016/j.bbmem.2016.06.024>.
- [61] R Core Team, R: A Language and Environment for Statistical Computing, (2018), <https://www.r-project.org/>.

- [62] M. Ušaj, K. Trontelj, D. Miklavčič, M. Kanduđer, Cell-Cell Electrofusion: Optimization of Electric Field Amplitude and Hypotonic Treatment for Mouse Melanoma (B16-F1) and Chinese Hamster Ovary (CHO) Cells, *J. Membr. Biol.* 236 (2010) 107–116, <https://doi.org/10.1007/s00232-010-9272-3>.
- [63] M.-P. Rols, J. Teissié, Electroporation of Mammalian Cells to Macromolecules: Control by Pulse Duration, *Biophys. J.* 75 (1998) 1415–1423, [10.1016/S0006-3495\(98\)74060-3](https://doi.org/10.1016/S0006-3495(98)74060-3).
- [64] G.L. Thompson, C.C. Roth, D.R. Dalzell, M.A. Kuipers, B.L. Ivey, Calcium influx affects intracellular transport and membrane repair following nanosecond pulsed electric field exposure, *J. Biomed. Opt.* 19 (2014) 1, <https://doi.org/10.1117/1.jbo.19.5.055005>.
- [65] G.L. Thompson, H.T. Beier, B.L. Ivey, Tracking lysosome migration within Chinese Hamster Ovary (CHO) cells following exposure to nanosecond pulsed electric fields, *Bioengineering*, 5 (2018), <https://doi.org/10.3390/BIOENGINEERING5040103>.
- [66] A. Draeger, R. Schoenauer, A.P. Atanasoff, H. Wolfmeier, E.B. Babychuk, Dealing with damage: Plasma membrane repair mechanisms, *Biochimie*, 107 (2014) 66–72, <https://doi.org/10.1016/j.biochi.2014.08.008>.
- [67] A.J. Jimenez, F. Perez, Physico-chemical and biological considerations for membrane wound evolution and repair in animal cells, *Semin. Cell Dev. Biol.* 45 (2015) 2–9, <https://doi.org/10.1016/j.semcdb.2015.09.023>.
- [68] T. Kosjek, A. Krajnc, T. Gornik, D. Žigon, A. Grošelj, G. Serša, M. Čemazar, Identification and quantification of bleomycin in serum and tumor tissue by liquid chromatography coupled to high resolution mass spectrometry, *Talanta*, 160 (2016) 164–171, <https://doi.org/10.1016/j.talanta.2016.06.062>.
- [69] G. Pron, N. Mahrour, S. Orłowski, O. Tounekti, B. Poddevin, J. Belehradek, L.M. Mir, Internalisation of the bleomycin molecules responsible for bleomycin toxicity: A receptor-mediated endocytosis mechanism, *Biochem. Pharmacol.* 57 (1999) 45–56, [https://doi.org/10.1016/S0006-2952\(98\)00282-2](https://doi.org/10.1016/S0006-2952(98)00282-2).
- [70] T. Makovec, Cisplatin and beyond: Molecular mechanisms of action and drug resistance development in cancer chemotherapy, *Radiol. Oncol.* 53 (2019) 148–158, <https://doi.org/10.2478/raon-2019-0018>.
- [71] A.G. Pakhomov, J.F. Kolb, J.A. White, R.P. Joshi, S. Xiao, K.H. Schoenbach, Long-lasting plasma membrane permeabilization in mammalian cells by nanosecond Pulsed Electric Field (nsPEF), *Bioelectromagnetics*, 28 (2007) 655–663, <https://doi.org/10.1002/bem.200354>.
- [72] A.G. Pakhomov, A.M. Bowman, B.L. Ivey, F.M. Andre, O.N. Pakhomova, K.H. Schoenbach, Lipid nanopores can form a stable, ion channel-like conduction pathway in cell membrane, *Biochem. Biophys. Res. Commun.* 385 (2009) 181–186, <https://doi.org/10.1016/j.bbrc.2009.05.035>.
- [73] B. Jakštyš, P. Ruzgys, M. Tamošiūnas, S. Šatkauskas, Different Cell Viability Assays Reveal Inconsistent Results After Bleomycin Electroporation In Vitro, *J. Membr. Biol.* 248 (2015) 857–863, <https://doi.org/10.1007/s00232-015-9813-x>.
- [74] J. Gehl, T. Skovsgaard, L.M. Mir, Enhancement of cytotoxicity by electroporation: an improved method for screening drugs, *Anticancer. Drugs*, 9 (1998), https://journals.lww.com/anti-cancerdrugs/Fulltext/1998/04000/Enhancement_of_cytotoxicity_by_5.aspx.
- [75] T. Forjanic, B. Markelc, M. Marcan, E. Bellard, F. Couillaud, M. Golzio, D. Miklavcic, Electroporation-Induced Stress Response and Its Effect on Gene Electroporation Efficacy. In *Vivo Imaging and Numerical Modeling*, IEEE Trans. Biomed. Eng., 66 (2019) 2671–2683, <https://doi.org/10.1109/TBME.2019.2894659>.
- [76] S. Šatkauskas, B. Jakštyš, P. Ruzgys, M. Jakutavičiūtė, Different Cell Viability Assays Following Electroporation In Vitro, v: D. Miklavčič (Ur.), *Handb. Electroporation*, Springer International Publishing, Cham, 2017: str. 1411–1424, https://doi.org/10.1007/978-3-319-32886-7_140.
- [77] O. Tounekti, G. Pron, J. Belehradek, L.M. Mir, Bleomycin, an Apoptosis-mimetic Drug That Induces Two Types of Cell Death Depending on the Number of Molecules Internalized, *Cancer Res.* 53 (1993) 5462–5469.
- [78] A.J. Jimenez, P. Maiuri, J. Lafaurie-Janvore, S. Divoux, M. Piel, F. Perez, ESCRT machinery is required for plasma membrane repair, *Science* (80-.) (2014) 343, <https://doi.org/10.1126/science.1247136>.
- [79] N. Klein, B. Mercadal, M. Stehling, A. Ivorra, In vitro study on the mechanisms of action of electrolytic electroporation (E2), *Bioelectrochemistry*, 133 (2020), <https://doi.org/10.1016/j.bioelechem.2020.107482>.
- [80] P.D.L. Lima, M.C. Vasconcellos, R.C. Montenegro, M.O. Bahia, E.T. Costa, L.M.G. Antunes, R.R. Burbano, Genotoxic effects of aluminum, iron and manganese in

human cells and experimental systems: a review of the literature, *Hum. Exp. Toxicol.* 30 (2011) 1435–1444, <https://doi.org/10.1177/0960327110396531>.



Angelika Vižintin obtained her BSc and MSc at the University of Ljubljana, Slovenia. Currently she is employed at the University of Ljubljana, Faculty of Electrical Engineering and is enrolled in the interdisciplinary doctoral program in Biosciences at the University of Ljubljana. Her main research interests lie in the field of electroporation based-technologies for biomedicine, including tissue ablation and electrochemotherapy.



Stefan Marković is a PhD student at the Jožef Stefan International Postgraduate, Ljubljana, Slovenia school since 2017, after he obtained a MSc in environmental chemistry from University of Belgrade, Serbia. His main research is focused on elemental bioimaging by laser ablation inductively coupled plasma mass spectrometry, and trace element analysis in the environment and living organisms.



Janez Ščančar has been actively involved in the research for more than 25 years. Since 1997 he is employed at the Jožef Stefan Institute, Slovenia where currently is a Head of Research Group for Trace Elements Speciation. His main research interests are investigations on the role of metal ions in the environment and living organisms by applying methods of chemical speciation. As full professor he is engaged in lecturing at the Jožef Stefan International Postgraduate School and the University of Nova Gorica. Among others, he has written more than 150 original scientific articles papers in analytical, environmental and life science journals.



Damijan Miklavčič was born in Ljubljana, Slovenia, in 1963. He received his PhD degree in electrical engineering from the University of Ljubljana in 1993. He is currently a tenured Professor at the Faculty of Electrical Engineering of the University of Ljubljana. His current research interests include electroporation-based treatments and therapies, including cancer treatment by means of electrochemotherapy, cardiac tissue ablation by irreversible electroporation, and gene transfer for DNA vaccination. His research involves biological experimentation, numerical modeling of biological processes, and hardware development.

2.1.3 Nanosecond electric pulses are equally effective in electrochemotherapy with cisplatin as microsecond pulses

Vižintin A., Marković S., Ščančar J., Kladnik J., Turel I., Miklavčič D. 2022. Nanosecond electric pulses are equally effective in electrochemotherapy with cisplatin as microsecond pulses. *Radiology and Oncology*, 56, 3: 326–335

Nanosecond electric pulses showed promising results in electrochemotherapy, but the underlying mechanisms of action are still unexplored. The aim of this work was to correlate cellular cisplatin amount with cell survival of cells electroporated with nanosecond or standardly used $8 \times 100 \mu\text{s}$ pulses and to investigate the effects of electric pulses on cisplatin structure. Chinese hamster ovary CHO and mouse melanoma B16F1 cells were exposed to $1 \times 200 \text{ ns}$ pulse at 12.6 kV/cm or $25 \times 400 \text{ ns}$ pulses at 3.9 kV/cm , 10 Hz repetition rate or $8 \times 100 \mu\text{s}$ pulses at 1.1 (CHO) or $0.9 \text{ (B16F1)} \text{ kV/cm}$, 1 Hz repetition rate at three cisplatin concentrations. Cell survival was determined by the clonogenic assay, cellular platinum was measured by inductively coupled plasma mass spectrometry. Effects on the structure of cisplatin were investigated by nuclear magnetic resonance spectroscopy and high-resolution mass spectrometry. Nanosecond pulses equivalent to $8 \times 100 \mu\text{s}$ pulses were established *in vitro* based on membrane permeabilization and cell survival. Equivalent nanosecond pulses were equally efficient in decreasing the cell survival and accumulating cisplatin intracellularly as $8 \times 100 \mu\text{s}$ pulses after electrochemotherapy. The number of intracellular cisplatin molecules strongly correlates with cell survival for B16F1 cells, but less for CHO cells, implying the possible involvement of other mechanisms in electrochemotherapy. The high-voltage electric pulses did not alter the structure of cisplatin. Equivalent nanosecond pulses are equally effective in electrochemotherapy as standardly used $8 \times 100 \mu\text{s}$ pulses.

Supplementary data to this article can be found online at https://sciendo-parsed-data-feed.s3.eu-central-1.amazonaws.com/62f7aaf9c7121310277c85cb/raon-2022-0028_sm.pdf.



This work is licensed under a [Creative Commons Attribution-NonCommercial-NoDerivatives 4.0 International License](https://creativecommons.org/licenses/by-nc-nd/4.0/).

Nanosecond electric pulses are equally effective in electrochemotherapy with cisplatin as microsecond pulses

Angelika Vizintin¹, Stefan Markovic², Janez Scancar², Jerneja Kladnik³, Iztok Turel³, Damijan Miklavcic¹

¹ Faculty of Electrical Engineering, University of Ljubljana, Ljubljana, Slovenia

² Department of Environmental Sciences, Jožef Stefan Institute, Ljubljana, Slovenia

³ Faculty of Chemistry and Chemical Technology, University of Ljubljana, Ljubljana, Slovenia

Radiol Oncol 2022; 56(3): 326-335.

Received 7 June 2022
Accepted 19 June 2022

Correspondence to: Prof. Damijan Miklavcic, Ph.D., Faculty of Electrical Engineering, University of Ljubljana, Tržaška cesta 25, SI-1000 Ljubljana, Slovenia. E-mail: Damijan.Miklavcic@fe.uni-lj.si

Disclosure: No potential conflicts of interest were disclosed.

This is an open access article under the CC BY-NC-ND license (<http://creativecommons.org/licenses/by-nc-nd/4.0/>).

Background. Nanosecond electric pulses showed promising results in electrochemotherapy, but the underlying mechanisms of action are still unexplored. The aim of this work was to correlate cellular cisplatin amount with cell survival of cells electroporated with nanosecond or standardly used $8 \times 100 \mu\text{s}$ pulses and to investigate the effects of electric pulses on cisplatin structure.

Materials and methods. Chinese hamster ovary CHO and mouse melanoma B16F1 cells were exposed to $1 \times 200 \text{ ns}$ pulse at 12.6 kV/cm or $25 \times 400 \text{ ns}$ pulses at 3.9 kV/cm , 10 Hz repetition rate or $8 \times 100 \mu\text{s}$ pulses at 1.1 (CHO) or 0.9 (B16F1) kV/cm , 1 Hz repetition rate at three cisplatin concentrations. Cell survival was determined by the clonogenic assay, cellular platinum was measured by inductively coupled plasma mass spectrometry. Effects on the structure of cisplatin were investigated by nuclear magnetic resonance spectroscopy and high-resolution mass spectrometry.

Results. Nanosecond pulses equivalent to $8 \times 100 \mu\text{s}$ pulses were established *in vitro* based on membrane permeabilization and cell survival. Equivalent nanosecond pulses were equally efficient in decreasing the cell survival and accumulating cisplatin intracellularly as $8 \times 100 \mu\text{s}$ pulses after electrochemotherapy. The number of intracellular cisplatin molecules strongly correlates with cell survival for B16F1 cells, but less for CHO cells, implying the possible involvement of other mechanisms in electrochemotherapy. The high-voltage electric pulses did not alter the structure of cisplatin.

Conclusions. Equivalent nanosecond pulses are equally effective in electrochemotherapy as standardly used $8 \times 100 \mu\text{s}$ pulses.

Key words: electroporation; electrochemotherapy; nanosecond pulses; cisplatin

Introduction

Electrochemotherapy (ECT) is a local cancer treatment. The dominant mechanism of ECT is increased cellular uptake of impermeant or low permeant anticancer drugs with high intrinsic cytotoxicity - most commonly bleomycin and *cis*-diaminedichloroplatinum(II) (cisplatin) - due to transiently increased membrane permeability of

cells/tumors after exposure to short high-voltage electric pulses.¹

Over the past ten years, the number of ECT treatments performed for superficial tumors has increased dramatically and new indications have been added, such as treatment of skin metastases from visceral or hematological malignancies, vulvar cancer, deep-seated malignancies, and some noncancerous skin lesions.² ECT has become

broadly accepted mainly because of its simplicity (it is easy to master) and versatility (it allows treating a variety of cancers). Its efficacy, tolerability, and high patient satisfaction have been demonstrated in several studies, but also some side effects have been reported. According to the reports, the main side effects are unpleasant sensations, which can be painful, and muscle contractions triggered by applied high voltage electric pulses.^{3,4} Most commonly, electric pulses are administrated as trains of eight monophasic pulses with a duration of 100 μ s at 1 Hz or 5 kHz pulse repetition rate.

Nanosecond pulses have shown potential advantages over micro- and millisecond pulses in electroporation-based applications. The use of pulses with high electric field strength, but very short duration (i.e., in the nanosecond range) results in low energy transfer by the pulses to the treated volume, resulting in a low heating^{5,6} and thereby minimizing the possibility of thermal damage to the tissue, which is very important for sparing delicate structures in and around the treated area.⁷ In addition, nanosecond pulses limit electrochemical reactions at the electrode-electrolyte interface⁸ which may affect the treated medium or cells/tissues.⁹⁻¹¹ Although a much higher electric field strength is required to achieve a comparable biological effect, excitation thresholds appear to be higher than the electroporation thresholds with nanosecond pulses¹²⁻¹⁶, implying that shortening the pulse duration to nanosecond pulses could also reduce neuromuscular stimulation in electroporation-based applications.

Recently, nanosecond pulses have been explored in ECT and calcium electroporation and have shown promising results – either tumor regression *in vivo* or a decrease in cell survival *in vitro*.^{8,17-21} We have previously reported that nanosecond pulses of an appropriately chosen amplitude in combination with cisplatin decreased cell survival in *in vitro* assays to the same extent as standard $8 \times 100 \mu$ s pulses.⁸ The aim of our present work was to investigate the underlying mechanisms of ECT with nanosecond pulses and cisplatin *in vitro* on Chinese hamster ovary CHO and mouse skin melanoma B16F1 cells. Two nanosecond pulse protocols (1×200 ns pulse at 12.6 kV/cm and 25×400 ns pulses at 3.9 kV/cm, 10 Hz repetition rate) were compared with $8 \times 100 \mu$ s pulses at 1.1 (CHO) or 0.9 (B16F1) kV/cm, 1 Hz repetition rate standardly used in ECT. Accumulation of cisplatin and cell survival after *in vitro* ECT were measured and effects of high voltage electric pulses on the cisplatin molecular structure were investigated by nu-

clear magnetic resonance (NMR) spectroscopy and high-resolution mass spectrometry (HRMS).

Materials and methods

Cell culture of Chinese hamster ovary (CHO) cells and *in vitro* cell survival after ECT experiment protocols were described previously.⁸ Mouse skin melanoma cell line B16F1 (European Collection of Authenticated Cell Cultures, cat. no. 92101203, Sigma Aldrich, Germany, mycoplasma free) was cultured in the same way as CHO cells except that Dulbecco's Modified Eagle Medium (DMEM, cat. no. D5671, Sigma-Aldrich, Missouri, United States) supplemented with 10% FBS (cat. no. F9665, Sigma-Aldrich), 2.0 mM L-glutamine, 1 U/ml penicillin/streptomycin and 50 μ g/ml gentamycin was used instead of Nutrient Mixture F-12 Ham. Briefly, cisplatin (Cisplatin Kabi, 1 mg/mL, Fresenius Kabi, Germany or Cisplatin Accord, 1 mg/mL, Accord, UK) diluted in saline was added to cells suspended in complete growth medium DMEM just before electroporation so that the final concentration was 4×10^6 cell/mL and 0, 10, 30 or 50 μ M cisplatin. The cell suspension was exposed to monophasic rectangular pulses (1×200 ns pulse at 12.6 kV/cm or 25×400 ns at 3.9 kV/cm, 10 Hz repetition rate or $8 \times 100 \mu$ s at 1.1 (CHO) or 0.9 (B16F1) kV/cm, 1 Hz pulse repetition rate) or no pulses (non-electroporated controls). Cell survival was determined by the clonogenic assay.

For determination of cellular cisplatin, 125 μ L of the treated cell suspension was diluted 40–100 times in complete growth medium Ham F-12 (CHO) or complete growth medium DMEM (B16F1) 25 min after electroporation (or addition of cisplatin/saline for non-electroporated controls) and centrifuged at 900 g for 5 min at 23°C in 15 ml centrifuge tubes. The supernatant was separated from the cell pellet and the pellet was washed with 2 ml saline and centrifuged again. After centrifugation, saline was discarded, and the cell pellet was kept at –20°C until digestion. For digestion, 0.1 ml H₂O₂ and 0.1 ml HNO₃ (both from Merck, Germany) were added to the cell pellets, and the tubes were closed and sealed with Teflon tape and left overnight at 80°C. After digestion, 1.8 ml of Milli-Q water (18.2 M Ω obtained from a Direct-Q 5 Ultrapure water system, Merck Millipore, Massachusetts, USA) was added and samples were measured by inductively coupled plasma mass spectrometry (7900 ICP-MS Agilent Technologies, Japan) with ¹⁹³Ir used as an inter-

nal standard during the measurement. The experiments were repeated 4–7 times. The number of cisplatin molecules per cell was calculated by first dividing the measured total mass of Pt in the cell pellet by the number of cells in the pellet, then subtracting the average mass of Pt per cell of non-electroporated cell pellets that were not incubated with cisplatin, and finally calculating the number of cisplatin molecules per cell from the difference of the mass of Pt per cell in samples (assuming 1 mol of Pt is equivalent to 1 mol of cisplatin).

Cell survival and amount of Pt data (after outliers, defined using the interquartile range method, were removed) were analyzed using the Kruskal–Wallis test and p-values were adjusted with the post-hoc Holm method test ($\alpha = 0.05$) because the Shapiro–Wilk normality test failed ($\alpha = 0.05$). The Spearman correlation coefficient was calculated to test the correlation between the number of cisplatin molecules per cell and cell survival. The data were processed and visualized using Microsoft Excel 2016 and R 3.6.1.²²

Potential structural changes of cisplatin in the solution treated with high voltage electric pulses were investigated by NMR spectroscopy and HRMS. For practical reasons, both microsecond and nanosecond pulses were delivered to electroporation cuvettes with 2 mm gap with the laboratory prototype pulse generator based on an H-bridge digital amplifier for this set of experiments. For microsecond pulses, $8 \times 100 \mu\text{s}$ at 1.1 kV/cm at 1 Hz pulse repetition rate were delivered (same pulse protocol as in cellular electrochemotherapy experiments). For nanosecond pulses, $25 \times 400 \text{ ns}$ at 2.2 kV/cm at 10 Hz repetition rate were delivered – the electric field strength for this pulse protocol was lower than in cellular electrochemotherapy experiments because of the technical limitations of the prototype pulse generator. $1 \times 200 \text{ ns}$ pulse was not applied because the pulse generator used is not capable of generating such short pulses. ^1H NMR spectra were obtained on NMR Bruker Ascend™ 600 MHz spectrometer at room temperature at 600 MHz. Chemical shifts, reported in ppm, are referenced to residual peaks of D_2O at 4.79 ppm. Spectra were recorded in D_2O (with and without NaCl) as well as in 90% $\text{H}_2\text{O}/10\% \text{D}_2\text{O}$ (with or without NaCl) using water suppression (WATERGATE) method. NMR data were processed with MestReNova 11.0.4. To approximately 1–2 mg of cisplatin (Sigma Aldrich) 1 mL of a) D_2O , b) D_2O containing 154 mM NaCl, c) 90% $\text{H}_2\text{O}/10\% \text{D}_2\text{O}$ or d) 90% $\text{H}_2\text{O}/10\% \text{D}_2\text{O}$ containing 154 mM NaCl was added. The obtained suspension was filtered through Minisart NML

Cellulose Acetate Syringe Filter (28 mm, 0.2 μL). ^1H NMR spectra were recorded immediately after the filtration when not treated with any pulse protocol or directly after microsecond or nanosecond pulse application. HRMS spectra were recorded on Agilent 6224 Accurate Mass Time of Flight (TOF) Liquid Chromatography–Mass Spectrometry (LC–MS) instrument using water–acetonitrile solution (80:20, v/v) as the mobile phase. Fragmentor voltage was set to 150.0 V. To approximately 1–2 mg of cisplatin (Sigma Aldrich) 1 mL of distilled water or saline was added and obtained suspension was filtered through Minisart NML Cellulose Acetate Syringe Filter (28 mm, 0.2 μL). Filtered solutions underwent a) no pulses, b) microsecond pulses, or c) nanosecond pulses application as mentioned above, followed by immediate injection of such solutions into the LC–MS.

Results

CHO and B16F1 cells were electroporated in presence of 10, 30 and 50 μM cisplatin with: $1 \times 200 \text{ ns}$ pulse at 12.6 kV/cm; $25 \times 400 \text{ ns}$ pulses at 3.9 kV/cm, 10 Hz pulse repetition rate; or $8 \times 100 \mu\text{s}$ pulses at 1.1 (CHO) or 0.9 (B16F1) kV/cm, 1 Hz pulse repetition rate. The electric field strengths for specific pulse parameters were selected based on survival–permeabilization curves (refer to Vižintin *et al.*⁸ for graphs for CHO cells and to Figure S1 in the Supplementary material for graphs for B16F1 cells).

Cell survival results after ECT determined by the clonogenic assay are shown in Figure 1. Survival data of CHO cells were combined from the previous⁸ (for non-electroporated cells and cells electroporated with $25 \times 400 \text{ ns}$ and $8 \times 100 \mu\text{s}$ pulses) and the present study (additional non-electroporated cells and cells electroporated with $1 \times 200 \text{ ns}$ pulse). As intended, electroporation alone (i.e., in the absence of cisplatin) did not decrease cell survival in both cell lines compared with the non-electroporated control for any of the pulse protocols tested. For the non-electroporated cells treated with cisplatin, a statistically significant decrease in cell survival was observed only for CHO cells at the highest (50 μM) cisplatin concentration tested. On the other hand, electroporation in the presence of cisplatin decreased cell survival except for B16F1 cells treated with $1 \times 200 \text{ ns}$ pulse. For CHO cells, $1 \times 200 \text{ ns}$, $25 \times 400 \text{ ns}$, and $8 \times 100 \mu\text{s}$ pulse protocols were all equally effective at decreasing cell survival at all the three tested cisplatin concentrations (Figure 1A). In B16F1 cells, $25 \times 400 \text{ ns}$ and 8

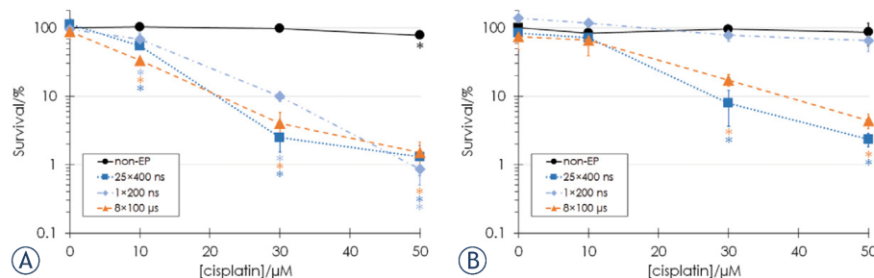


FIGURE 1. Cell survival of (A) CHO and (B) B16F1 cells at different cisplatin concentrations determined by the clonogenic assay for non-electroporated (non-EP) cells (black circles) and cells electroporated with 25 × 400 ns pulses at 3.9 kV/cm, 10 Hz repetition rate (dark blue squares), 1 × 200 ns pulse at 12.6 kV/cm (light blue diamonds) or 8 × 100 μs pulses at 1.1 (CHO) or 0.9 (B16F1) kV/cm, 1 Hz pulse repetition rate (orange triangles). Bars represent standard deviation, asterisks (*) show statistically significant differences ($p < 0.05$) to the survival of non-electroporated cells without cisplatin. Survival data were combined from the previous⁸ (for non-electroporated cells and cells electroporated with 25 × 400 ns and 8 × 100 μs pulses) and the present study (for B16F1 cells, additional non-electroporated CHO cells and CHO cells electroporated with 1 × 200 ns pulse).

× 100 μs pulses were equally effective, whereas 1 × 200 ns pulse protocol was less effective (Figure 1B).

The amount of Pt in the cells was determined by measuring the total mass of Pt in the cell pellets by ICP-MS. Electroporation increased the cellular Pt amount. For both cell lines, there were no statistically significant differences in the measured Pt amount in cells electroporated with 25 × 400 ns or 8 × 100 μs pulses at the same cisplatin concentration. For CHO cells, the amount of Pt in cells electroporated with 1 × 200 ns pulse was statistically significantly lower compared to the amount of Pt in cells electroporated with 25 × 400 ns and 8 × 100 μs pulse incubated only at 50 μM cisplatin (Figure 2A). For B16F1 cells, lower cellular Pt was measured after application of 1 × 200 ns pulse compared to 25 ×

400 ns and 8 × 100 μs pulses at all tested cisplatin concentrations (Figure 2B).

From the measured Pt content, the number of cisplatin molecules per cell was calculated and plotted against the cell survival data. The number of cisplatin molecules per cell and cell survival were more strongly correlated for B16F1 cells (Spearman's correlation coefficient: $\rho = -0.85$, $p < 0.001$ for CHO and $\rho = -0.92$, $p < 0.01$ for B16F1). In the case of CHO cells, at the same number of cisplatin molecules per cell, notably lower cell survival was measured for electroporated cells compared to non-electroporated cells (Figure 3A). For example, cell survival of 98% was achieved for non-electroporated cells with 9.4×10^6 cisplatin molecules per cell, whereas cell survival of 68.5%

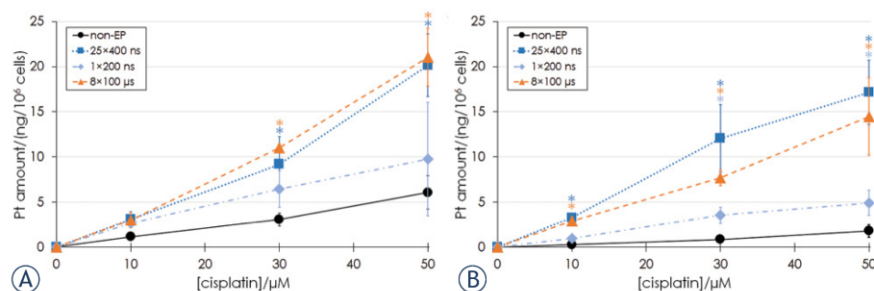


FIGURE 2. Pt amount in cell pellets of (A) CHO and (B) B16F1 cells after 25 min incubation at different extracellular cisplatin concentrations in non-electroporated (non-EP) cells (black circles) and cells electroporated with 25 × 400 ns pulses at 3.9 kV/cm, 10 Hz repetition rate (dark blue squares), 1 × 200 ns pulse at 12.6 kV/cm (light blue diamonds) or 8 × 100 μs pulses at 1.1 (CHO) or 0.9 (B16F1) kV/cm, 1 Hz pulse repetition rate (orange triangles). Bars represent standard deviation, asterisks (*) show statistically significant differences ($p < 0.05$) to the measured number of cisplatin molecules in non-electroporated cells at the same extracellular cisplatin concentration.

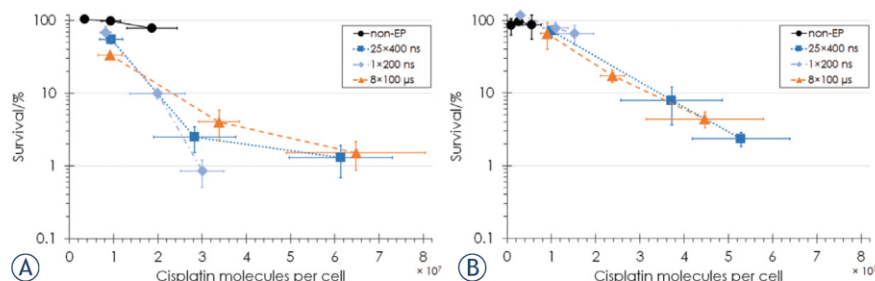


FIGURE 3. Cell survival as a function of the number of cisplatin molecules per cell for (A) CHO cells and (B) B16F1 cells in non-electroporated (non-EP) cells (black circles) and cells electroporated with 25 × 400 ns pulses at 3.9 kV/cm, 10 Hz repetition rate (dark blue squares), 1 × 200 ns pulse at 12.6 kV/cm (light blue diamonds) or 8 × 100 μs pulses at 1.1 (CHO) or 0.9 (B16F1) kV/cm, 1 Hz pulse repetition rate (orange triangles). Bars represent standard deviation. Survival data were combined from the previous⁹ (for non-electroporated CHO cells and CHO cells electroporated with 25 × 400 ns and 8 × 100 μs pulses) and the present study (for B16F1 cells, additional non-electroporated CHO cells and CHO cells electroporated with 1 × 200 ns pulse).

was measured for cells electroporated with 1 × 200 ns pulse with 8.2×10^6 cisplatin molecules per cell, cell survival of 54.8% was measured for cells electroporated with 25 × 400 ns pulses with 9.5×10^6 cisplatin molecules per cell, and cell survival of 33.7% was measured for cells electroporated with 8 × 100 μs pulses with 9.2×10^6 cisplatin molecules per cell. From the data acquired, it could not be concluded if also in B16F1 cells a lower number of cisplatin molecules per cell causes a larger decrease in cell survival because the range of the number of cisplatin molecules in electroporated and non-electroporated cells did not overlap and thus survival could not be compared at approximately the same number of cisplatin molecules per cells (Figure 3B).

Cisplatin has been widely investigated for its biospeciation in aqueous solutions due to its diverse stepwise ligand displacement reactions.²³ Therefore, ¹H NMR spectroscopy was applied to investigate potential structural changes of cisplatin due to high voltage electric pulses. First, spectra of cisplatin in D₂O and D₂O with 154 mM NaCl (corresponding to physiological saline 0.9% NaCl) not exposed to electric pulses were recorded (Figure 4A–B). Weak broadened peaks for hydrogen atoms of amino ligands (NH₃) were found at approximately 4.08 ppm. Similarly, also representative peaks of cisplatin after treatment with 8 × 100 μs pulses at 1.1 kV/cm at 1 Hz pulse repetition rate or 25 × 400 ns pulses at 2.2 kV/cm at 10 Hz repetition rate remained at the same shift. The only major difference was observed in the spectrum of cisplatin recorded in D₂O with 154 mM NaCl after treatment with microsecond pulses (Figure 4B),

where the broad peak for hydrogens of cisplatin disappeared. This can be attributed to the fast hydrogen-deuterium (H/D) exchange of deuterium from D₂O with hydrogen atoms of NH₃ ligands.²⁴ However, when spectra of cisplatin were recorded in 90% H₂O/10% D₂O solution containing 154 mM NaCl acquiring water suppression (to minimize the intensity of water signal to obtain a stronger signal of the NH₃ ligand) no such disappearance of the peak was observed (Figure 4D). Comparable spectra with peaks at 4.08 ppm were obtained also when no electric pulses or nanosecond pulses were applied. Similarly, the hydrogen peak of NH₃ was observed in the samples recorded in a 90% H₂O/10% D₂O solution without NaCl (Figure 4C). It is also important to note that no new peaks appeared in other regions of the NMR spectra.

High-resolution mass spectrometry (HRMS), which can also provide abundant information on molecular structure, was also performed to investigate possible newly formed cisplatin species. In some reports, authors detected hydrolysis products corresponding to mono-, di- and trimeric species, by mass spectrometry.^{25–28} Therefore, HRMS was used in our structural investigation of cisplatin in water and saline (0.9% NaCl) exposed to micro- and nanosecond pulses.

First, cisplatin in H₂O was investigated and on the full-scan positive-ion mass spectrum (mass range of *m/z* 100–1100) presented in Figure S2 in Supplementary Material. It can be observed that the most abundant peaks occur in the mass range of *m/z* 280–330, where the following fragments were observed: [Pt(NH₃)₂(N₂)

$\text{Cl}]^+$ (m/z 292.9909), $[\text{M}+\text{NH}_4]^+$ (M – indicates molecular formula for cisplatin, i.e. $[\text{Pt}(\text{NH}_3)_2\text{Cl}_2]$) (m/z 317.9872) (both Figure S3), $[\text{M}+\text{H}]^+$ (m/z 300.9601) (Figure S4), $[\text{Pt}(\text{NH}_3)_2(\text{CH}_3\text{CN})\text{Cl}]^+$ (m/z 306.0101) (Figure S5) and $[\text{M}+\text{Na}]^+$ (m/z 322.9425) (Figure S6). Additionally, three lower abundant clusters can be found in the mass range of m/z 540–590. Two of them were identified as $[\text{Pt}(\text{NH}_3)_2\text{Cl}_2\text{Pt}(\text{NH}_3)\text{Cl}]^+$ (m/z 547.9121) and $[\text{Pt}(\text{NH}_3)_2\text{Cl}_2\text{Pt}(\text{NH}_3)_2\text{Cl}]^+$ (m/z 564.9378) (Figure S7). Additionally, one cluster at m/z 610–630 with the main ion fragment at m/z 617.9408 belongs to $[\text{2M}+\text{NH}_4]^+$ (Figure S8). Similar fragments have been observed when the samples were treated with micro- and nanosecond pulses (Figure S9–10 and Figure S11–12). The species observed are in agreement with those reported in the literature.²⁶ Figure S19 represents the spectrum of water from the electroporation cuvette without the application of electric pulses. No differences were observed between the solutions treated with either nanosecond or microsecond pulses or untreated control.

HRMS experiments have been further performed in saline, where more extensive fragmentation was observed throughout the mass range of m/z 100–1100 (Figure S13). However, these peaks are comparable to the ones in the spectrum of saline from electroporation cuvette without the application of electric pulses (Figure S20). Similarly to spectra without NaCl, peaks of $[\text{Pt}(\text{NH}_3)_2(\text{N}_3)\text{Cl}]^+$ fragment and sodium $[\text{M}+\text{Na}]^+$ adduct were identified on zoom-scan spectrum (Figure S14). Again, spectra recorded in saline that was not treated with electric pulses are comparable with the spectra where cisplatin in saline solutions were treated with micro- and nanosecond pulses (Figures S15–16 and Figures S17–18, respectively).

Overall, NMR, as well as HRMS investigations, point to cisplatin remaining structurally comparable after the exposure to high voltage electric pulses similar to those used in *in vitro* ECT experiments with respect to its aqueous solutions without electric pulses.

Discussion

ECT has been shown to be a safe and effective cancer treatment, requiring much lower doses of the chemotherapeutic agent than conventional chemotherapy. However, pain and muscle contractions were reported as a drawback. Nanosecond pulses and high-frequency biphasic pulses of a few microsecond duration (H-FIRE)^{29–31} were suggested

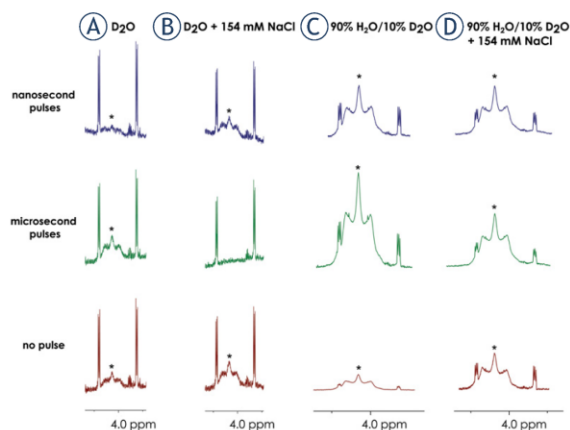


FIGURE 4. ^1H NMR spectra of cisplatin, showing the signals for hydrogens of NH_3 ligands labeled with asterisks (*). Spectra were recorded in a) D_2O , b) D_2O containing 154 mM NaCl, c) 90% $\text{H}_2\text{O}/10\%$ D_2O and d) 90% $\text{H}_2\text{O}/10\%$ D_2O containing 154 mM NaCl treated with 25×400 ns pulses (blue), 8×100 μs pulses (green) or no pulses (red).

to limit neuromuscular stimulation and contractions.^{15,16} Additionally, with nanosecond pulses, the possibility of thermal damage to the tissue is minimized^{5,6} due to low energy being transferred to the treated area and electrochemical reactions are reduced.⁸ ECT with nanosecond pulses has shown promising results^{8,17–19}, but the underlying mechanisms of the observed decrease in cell survival and tumor regression remain to be explained.

In this study, we measured cell survival and cisplatin accumulation after *in vitro* ECT with 8×100 μs pulses, which are standardly used in ECT procedures, and equivalent nanosecond pulses, i.e. pulse protocols that have an equivalent biological effect on cell survival and cell membrane permeabilization. The electric field strength was chosen for each pulse protocol at a value that resulted in the highest permeabilization (determined as the percentage YO-PRO1 fluorescing cells) of the cell membrane without a decrease in cell survival (measured by the metabolic MTS assay). In the case of 8×100 μs pulses, 1.1 kV/cm was selected for CHO cells, but the survival for B16F1 cells was around 55% at this electric field strength, thus a lower (i.e. 0.9 kV/cm) electric field strength was used for electroporating B16F1 cells with this pulse protocol. For 25×400 ns pulses, the same electric field strength (3.9 kV/cm) was determined to be optimal for both cell lines. For 1×200 ns pulse, we used the highest experimentally achievable electric field

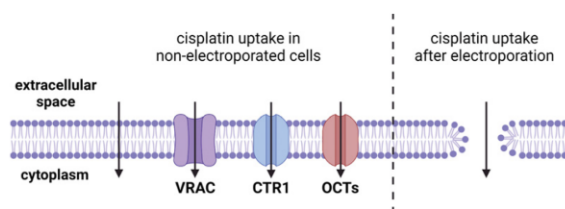


FIGURE 5. The mechanism of cisplatin uptake into cells is not completely elucidated. In non-electroporated cells, cisplatin enters partially through passive diffusion and facilitated diffusion through ion channels including LRRC8 volume-regulated anion channels (VRAC) and membrane transporters like copper transporter 1 (CTR1) and organic cation transporters (OCTs). In electroporated cells, more cisplatin can enter through the permeabilized cell membrane (pore is a symbolic presentation of increased membrane permeability even though the mechanisms behind electroporation are more complex – refer to³⁴).

strength (i.e. 12.6 kV/cm), which did not decrease the cell survival in either cell line. Electroporating both cell lines with $8 \times 100 \mu\text{s}$ or $25 \times 400 \text{ ns}$ pulses at the selected electric field strengths resulted in $> 95\%$ permeabilization (optimal for ECT), while for the $1 \times 200 \text{ ns}$ pulse at 12.6 kV/cm the permeabilization was 85% for CHO and only 42% for B16F1 cells (suboptimal for ECT). However, $1 \times 200 \text{ ns}$ pulse protocol was also included in the study based on results of cell survival of CHO cells after ECT determined by the metabolic MTS assay that showed that this pulse protocol was as effective in decreasing cell survival in ECT with cisplatin as the $25 \times 400 \text{ ns}$ protocol at all cisplatin concentrations.⁸

The aim was to test whether the combination of permeabilizing electric pulses (that alone do not cause a decrease in cell survival) and cisplatin results in increased cellular cisplatin accumulation (compared to non-electroporated cells) and whether the amount of cellular cisplatin is correlated to cell survival due to the increase of intracellular accumulation of the chemotherapeutic agent being one of the main mechanisms of action of ECT. To exert its cytotoxic effect, cisplatin must enter the cell. The exact mechanisms of cisplatin uptake have not been fully elucidated. Cisplatin is only slightly permeant; thus, it only partially enters the cell through passive diffusion across the cell membrane. Recent studies pointed out active transport mechanisms such as facilitated diffusion involved in cisplatin uptake - and LRRC8 volume-regulated anion channels (VRAC), copper transporter 1 (CTR1), and organic cation transporters (OCTs) were shown to be involved in cisplatin uptake.^{32,33} Electroporation makes the cell membrane non-se-

lectively permeable, allowing a larger quantity of cisplatin to enter the cell (Figure 5).

As expected, the measured amount of Pt was higher in electroporated cells when compared to non-electroporated cells incubated at the same cisplatin concentration, although the differences were not always statistically significant (Figure 2). These results indicate that the application of electric pulses indeed increases the intracellular accumulation of cisplatin. Overall, the amount of Pt in B16F1 was lower than in CHO cells exposed to the same cisplatin concentration, with or without electroporation, which also correlates with the higher cell survival of B16F1 cells (Figure 1). A comparison of cell survival of CHO and B16F1 cells with a similar number of cisplatin molecules per cell (Figure 3) reveals that a higher number of cisplatin molecules is needed to decrease the cell survival of B16F1 cells compared to CHO.

There were no statistically significant differences in the cell survival and amount of cellular Pt obtained in cells electroporated with $25 \times 400 \text{ ns}$ and $8 \times 100 \mu\text{s}$ pulses at the same cisplatin concentration when comparing within the same cell line. Thus, it can be assumed that by using equivalent nanosecond pulses, it is possible to achieve the same decrease in cell survival and same cisplatin accumulation in cells and the as with the standard $8 \times 100 \mu\text{s}$ pulses; in other words, equivalent nanosecond pulses are equally effective in ECT as $8 \times 100 \mu\text{s}$ pulses.

The $1 \times 200 \text{ ns}$ pulse in combination with cisplatin did not decrease cell survival in B16F1 cells. This could be explained by the fact that $1 \times 200 \text{ ns}$ pulse permeabilizes less than half of the cell population of B16F1 and is also consistent with the measured Pt amount which was not significantly higher as in non-electroporated cells (Figure 2B). Application of $1 \times 200 \text{ ns}$ pulse alone (i.e., in the absence of cisplatin) seemed to even slightly promote cell growth (although the cell survival was not statistically significantly higher compared to the non-electroporated control). More interestingly, however, is that application of $1 \times 200 \text{ ns}$ pulse to CHO cells resulted in a lower amount of Pt in cells electroporated with $1 \times 200 \text{ ns}$ pulse as with $25 \times 400 \text{ ns}$ or $8 \times 100 \mu\text{s}$ pulses, but the same decrease in cell survival was achieved with the $1 \times 200 \text{ ns}$ pulse as with $25 \times 400 \text{ ns}$ or $8 \times 100 \mu\text{s}$ pulses. The lower amount of cisplatin in CHO cells electroporated with $1 \times 200 \text{ ns}$ could be explained *per se* by the fact that this pulse protocol achieved suboptimal cell membrane permeabilization compared to the $25 \times 400 \text{ ns}$ and $8 \times 100 \mu\text{s}$ pulse protocols.

Nevertheless, a comparable decrease in cell survival was achieved, suggesting that increased accumulation of cisplatin into cells may not be the only cause of cell death in ECT. Figure 2A indicates that in electroporated CHO cells, a lower number of cisplatin molecules per cell is required to decrease cell survival to the same extent as in non-electroporated cells. Similar results have been reported previously in the literature^{35,36}, but not discussed. There may be a synergistic effect of cisplatin and electroporation, i.e., the observed decrease in cell survival in ECT is not the sum of the decrease in cell survival caused by electric pulses and cisplatin alone, but electroporation appears to make cells more susceptible to cisplatin.

The results of survival and number of internalized cisplatin molecules for B16F1 cells, however, do not show a similar synergistic effect of cisplatin and electroporation. Contrary to CHO cells, the number of cisplatin molecules per cell seems to linearly correlate with the logarithm of cell survival for B16F1 cells (Figure 3). Nonetheless, as mentioned above, lower cellular cisplatin was consistently measured for the B16F1 cell line and there is only one experimental point from the electroporated cells (cells electroporated with 1×200 ns pulse at $10 \mu\text{M}$ cisplatin) that falls in the range of the number of molecules of the non-electroporated cells. A similar number of internalized cisplatin molecules was measured for non-electroporated cells at $30 \mu\text{M}$ cisplatin and for cells electroporated with 1×200 ns pulse at $10 \mu\text{M}$ cisplatin, but the cell survival was even slightly higher for the latter. As discussed above, however, the 1×200 ns pulse protocol did not effectively permeabilize B16F1 cells. More data (from non-electroporated cells incubated at higher cisplatin concentrations) would thus be needed to determine if also in the case of B16F1 cells a lower number of internalized cisplatin molecules is needed to decrease cell survival in electroporated cells.

To test whether electric pulses could affect cisplatin by modifying the structure of the molecule as proposed in theoretical studies³⁷, we used NMR spectroscopy and HRMS spectrometry and found that the structure of cisplatin remains comparable after the application of electric pulses to either its saline or water solution (representing a simplified extra- and intracellular environment, respectively). Thus, high voltage electric pulses did not affect the structure of the studied complex under the conditions used in our experiments. Therefore, the reason for the observed increased susceptibility of the electroporated CHO cells to cisplatin is probably a consequence of the effect of electroporation on the

cells. The cytotoxicity of cisplatin is thought to be mediated primarily by the formation of DNA adducts and the resulting impairment of transcriptional and/or DNA replication mechanisms. It was shown that electroporation increases the amount of cisplatin bound to the DNA, which could increase cisplatin cytotoxicity in electroporated cells.^{35,38} However, additional mechanisms play an important role in exerting the toxic effects of cisplatin, including generation of ROS, mitochondrial dysfunction, increase in intracellular Ca^{2+} concentration, and activation of signal transduction pathways.³⁹ Electric pulses can also lead to generation of intracellular reactive oxygen species (ROS)^{40,41}, damage mitochondria^{42,43}, and disrupt calcium homeostasis through the entry of Ca^{2+} from the extracellular space or intracellular stores.^{44,45} It has been shown that an increase in ROS enhances the efficacy of cisplatin and vice versa.^{46,47} Moreover, an increase in intracellular Ca^{2+} concentration enhances cisplatin-mediated ROS production and increases cisplatin cytotoxicity.⁴⁸⁻⁵⁰ This type of potentiation of cisplatin cytotoxicity may be responsible for the enhanced cisplatin cytotoxicity in electroporated cells, but it yet needs to be elucidated. Michel *et al.*⁵¹ observed an increased immunoreactivity with SOD-2 (an enzyme that clears mitochondrial ROS) in cells subjected to ECT with cisplatin. To the best of our knowledge, this is the only report that measured ROS after ECT with cisplatin.

Our study also has limitations. Two different pulse generators and electrode geometries (i.e., electroporation cuvettes with 2 or 4 mm gap) were used in the cell experiments because of the technical limitations of the pulse generators used. Also in cell experiments, we did not directly measure the amount of cisplatin in cell pellets, but Pt was measured instead and assumed that cisplatin most likely accounts for the majority of the measured amount of Pt in cells incubated with cisplatin. This assumption is supported by the fact that the amount of Pt in non-electroporated cells that were not incubated with cisplatin was 2–3 orders of magnitude lower than in samples incubated with cisplatin or even below the detection limit. We also do not know whether the measured Pt was located inside the cells or was e.g. bound to the surface of the cell membrane. However, the formation of reactive hydrolyzed cisplatin products that would bind immediately and irreversibly to cell membrane phospholipids is not expected because the electroporation medium used has a high concentration of chloride ions so cisplatin should be stable in it and the measured Pt most probably

comes from intracellular cisplatin.⁵² Additionally, in experiments investigating the effects of electric pulses on cisplatin structure, the conditions before the measurements by NMR spectroscopy and HRMS spectrometry could not be fully matched with the conditions in the cell experiments due to several reasons. First, it was namely not possible to record spectra of cisplatin in growth media due to many species present in the growth medium which interfere with cisplatin signals; thus, pulses were delivered to cisplatin dissolved in water or saline for NMR spectroscopy and HRMS spectrometry. Second, because of the limitations of the pulse generator used for NMR spectroscopy and HRMS spectrometry experiments, 25×400 ns pulses were delivered at lower amplitudes than in the cell experiments. Third, because of the difference in conductivity, electric pulses delivered to H_2O and D_2O had a notably different shape than pulses delivered to saline or cells in growth medium; due to the low conductivity of the load, they resembled an exponentially decaying rather than a rectangular pulse shape.

In conclusion, we have shown that by using equivalent nanosecond pulses in ECT, the same decrease in cell survival is achieved and the same amount of cisplatin accumulates in the cells as with the standard $8 \times 100 \mu s$ pulses, i.e., that in ECT, equivalent nanosecond pulses are equally efficient as $8 \times 100 \mu s$ pulses. By investigating the underlying mechanisms in nanosecond pulse ECT, we discovered that electroporated CHO cells are more susceptible to cisplatin than non-electroporated cells (regardless of the pulse protocol). The electric pulses used for electroporation do not appear to alter the structure of the cisplatin molecule, so the observed increased susceptibility is likely a consequence of the effect of electroporation on the cells. The use of nanosecond pulses in ECT is promising as it was demonstrated to be effective with the potential to mitigate muscle contractions. Because extensive preclinical data and solid evidence of mechanisms of action have been the basis for introducing ECT into clinical practice, further studies of nanosecond pulse ECT *in vivo* are necessary to enable translation into clinical trials.

Acknowledgements

The study was funded by Pulse Biosciences and the Slovenian Research Agency (ARRS) (research core funding No. P2-0249 and P1-0175). The work was partially performed within the network of

research and infrastructural centres of University of Ljubljana, which is financially supported by Slovenian Research Agency through infrastructural grant IP-0510. A.V. was granted a scholarship from the University Foundation of ing. Lenarčič Milan. We would like to acknowledge dr. Damijana Urankar for HRMS analyses.

References

1. Miklavčič D, Mali B, Kos B, Heller R, Serša G. Electrochemotherapy: from the drawing board into medical practice. *BioMed Eng Online* 2014; **13**: 1-20. doi: 10.1186/1475-925X-13-29
2. Campana LG, Miklavčič D, Bertino G, Marconato R, Valpione S, Imarisio I, M, et al. Electrochemotherapy of superficial tumors – Current status: basic principles, operating procedures, shared indications, and emerging applications. *Semin Oncol* 2019; **46**: 173-91. doi: 10.1053/j.seminoncol.2019.04.002
3. Gehl J, Sersa G, Matthiessen LW, Muir T, Soden D, Occhini A, Quagliaro P, et al. Updated standard operating procedures for electrochemotherapy of cutaneous tumours and skin metastases. *Acta Oncol* 2018; **57**: 874-82. doi: 10.1080/0284186X.2018.1454602
4. Kendler M, Micheluzzi M, Wetzig T, Simon JC. Electrochemotherapy under tumescent local anesthesia for the treatment of cutaneous metastases. *Dermatologic Surg* 2013; **39**: 1023-32. doi: 10.1111/dsu.12190
5. Schoenbach KH, Beebe SJ, Buescher ES. Intracellular effect of ultrashort electrical pulses. *Bioelectromagnetics* 2001; **22**: 440-8. doi: 10.1002/bem.71
6. Pliquett U, Nuccitelli R. Measurement and simulation of Joule heating during treatment of B-16 melanoma tumors in mice with nanosecond pulsed electric fields. *Bioelectrochemistry* 2014; **100**: 62-8. doi: 10.1016/j.bioelechem.2014.03.001
7. Cornelis FH, Cindrić H, Kos B, Fujimori M, Petre EN, Miklavčič D, et al. Peritumoral metallic implants reduce the efficacy of irreversible electroporation for the ablation of colorectal liver metastases. *Cardiovas Intervent Radiol* 2020; **43**: 84-93. doi: 10.1007/s00270-019-02300-y
8. Vižintin A, Marković S, Ščančar J, Miklavčič D. Electroporation with nanosecond pulses and bleomycin or cisplatin results in efficient cell kill and low metal release from electrodes. *Bioelectrochemistry* 2021; **140**: 107898. doi: 10.1016/j.bioelechem.2021.107798
9. Saulis G, Rodaite R, Rodaitė-Riševičienė R, Dainauskaitė VS, Saulė R. Electrochemical processes during high-voltage electric pulses and their importance in food processing technology. In: Rai VR, editor. *Advances in food biotechnology*. First Edition. Wiley Online Books, John Wiley & Sons Ltd; 2016. p. 575-92.
10. Kotnik T, Miklavčič D, Mir LM. Cell membrane electroporation by symmetrical bipolar rectangular pulses: Part II. Reduced electrolytic contamination. *Bioelectrochemistry* 2001; **54**: 91-5. doi: 10.1016/S1567-5394(01)00115-3
11. Loomis-Husselbee JW, Cullen PJ, Irvine RF, Dawson AP. Electroporation can cause artefacts due to solubilization of cations from the electrode plates. Aluminum ions enhance conversion of inositol 1,3,4,5-tetrakisphosphate into inositol 1,4,5-trisphosphate in electroporated L1210 cells. *Biochem J* 1991; **277**(Pt 3): 883-5. doi: 10.1042/bj2770883
12. Long G, Shires PK, Plescia D, Beebe SJ, Kolb JF, Schoenbach KH. Targeted tissue ablation with nanosecond pulses. *IEEE Trans Biomed Eng* 2011; **58**: 2161-7. doi: 10.1109/TBME.2011.2113183
13. Rogers WR, Merritt JH, Comeaux JA, Kuhnel CT, Moreland DF, Teltschik DG, et al. Strength-duration curve of an electrically excitable tissue extended down to near 1 nanosecond. *IEEE Trans on Plasma Sci* 2004; **32**: 1587-99. doi: 10.1109/TPS.2004.831758
14. Pakhomov AG, Pakhomova ON. The interplay of excitation and electroporation in nanosecond pulse stimulation. *Bioelectrochemistry* 2020; **136**: 107598. doi: 10.1016/j.bioelechem.2020.107598

15. Gudvangen EK, Kondratiev O, Redondo L, Xiao S, Pakhomov AG. Peculiarities of neurostimulation by intense nanosecond pulsed electric fields: how to avoid firing in peripheral nerve fibers. *Int J Mol Sci* 2021; **22**: 1763. doi: 10.3390/ijms22137051
16. Gudvangen EK, Novickij V, Battista F, Pakhomov AG. Electroporation and cell killing by milli-to nanosecond pulses and avoiding neuromuscular stimulation in cancer ablation. *Sci Rep* 2022; **12**: 1-15. doi: 10.1038/s41598-022-04868-x
17. Silve A, Leray I, Mir LM. Demonstration of cell membrane permeabilization to medium-sized molecules caused by a single 10 ns electric pulse. *Bioelectrochemistry* 2012; **87**: 260-4. doi: <https://doi.org/10.1016/j.bioelechem.2011.10.002>
18. Tunikowska J, Antorczyk A, Rembiałkowska N, Jóźwiak Ł, Novickij V, Kulbacka J. The first application of nanoelectrochemotherapy in feline oral malignant melanoma treatment – case study. *Animals* 2020; **10**: 556. doi: 10.3390/ani10040556
19. Novickij V, Malysko V, Želvyas A, Balevičiūtė A, Zinkevičiūnė A, Novickij J, et al. Electrochemotherapy using doxorubicin and nanosecond electric field pulses: a pilot in vivo study. *Molecules* 2020; **25**: 4601. doi: 10.3390/molecules25204601
20. Kielbik A, Szlasa W, Novickij V, Szewczyk A, Maciejewska M, Sączko J, et al. Effects of high-frequency nanosecond pulses on prostate cancer cells. *Sci Rep* 2021; **11**: 1-10. doi: 10.1038/s41598-021-95180-7
21. Kulbacka J, Rembiałkowska N, Szewczyk A, Moreira H, Szyjka A, Girkontaitė I, et al. The impact of extracellular Ca²⁺ and nanosecond electric pulses on sensitive and drug-resistant human breast and colon cancer cells. *Cancers* 2021; **13**: 3216. doi: 10.3390/cancers13133216
22. R Core Team R. A language and environment for statistical computing. [Internet]. 2018. Available at: <https://www.r-project.org/>
23. Berners-Price SJ, Appleton TG. The chemistry of cisplatin in aqueous solution. In: Kelland LR, Farrell NP, editors. *Platinum-based drugs in cancer therapy*. Cancer drug discovery and development. Totowa, NJ: Humana Press; 2000. p. 3-35. doi: 10.1007/978-1-59259-012-4_1
24. Chen Y, Guo Z, Sadler PJ. 195Pt- and 15N-NMR spectroscopic studies of cisplatin reactions with biomolecules. In: Lippert B, editor. *Cisplatin. Chemistry and biochemistry of a leading anticancer drug*. Wiley Online Library; p. 293-318. doi: 10.1002/9783906390420.ch11
25. Cui M, Mester Z. Electrospray ionization mass spectrometry coupled to liquid chromatography for detection of cisplatin and its hydrated complexes. *Rapid Commun Mass Spectrom* 2003; **17**: 1517-27. doi: 10.1002/rcm.1030
26. Feifan X, Pieter C, Jan VB. Electrospray ionization mass spectrometry for the hydrolysis complexes of cisplatin: implications for the hydrolysis process of platinum complexes. *J Mass Spectrom* 2017; **52**: 434-41. doi: <https://doi.org/10.1002/jms.3940>
27. Du Y, Zhang N, Cui M, Liu Z, Liu S. Investigation on the hydrolysis of the anticancer drug cisplatin by Fourier transform ion cyclotron resonance mass spectrometry. *Rapid Commun Mass Spectrom* 2012; **26**: 2832-6. doi: <https://doi.org/10.1002/rcm.6408>
28. Cui M, Ding L, Mester Z. Separation of cisplatin and its hydrolysis products using electrospray ionization high-field asymmetric waveform ion mobility spectrometry coupled with ion trap mass spectrometry. *Anal Chem* 2003; **75**: 5847-53. doi: 10.1021/ac0344182
29. Arena CB, Sano MB, Rossmel Jr JH, Caldwell JL, Garcia PA, Rylander MN, et al. High-frequency irreversible electroporation (H-FIRE) for non-thermal ablation without muscle contraction. *BioMed Eng Online* 2011; **10**: 102. doi: 10.1186/1475-925X-10-102
30. Scuderi M, Reberšek M, Miklavčič D, Dermol-Cerne J. The use of high-frequency short bipolar pulses in cisplatin electrochemotherapy in vitro. *Radiol Oncol* 2019; **53**: 194-205. doi: 10.2478/raon-2019-0025
31. Pirč E, Miklavčič D, Uršič K, Serša G, Reberšek M. High-frequency and high-voltage asymmetric bipolar pulse generator for electroporation based technologies and therapies. *Electronics* 2021; **10**: doi: 10.3390/electronics10101203
32. Makovec T. Cisplatin and beyond: molecular mechanisms of action and drug resistance development in cancer chemotherapy. *Radiol Oncol* 2019; **53**: 148-58. doi: 10.2478/raon-2019-0018
33. Hucce A, Ciarrimboli G. The role of transporters in the toxicity of chemotherapeutic drugs: focus on transporters for organic cations. *J Clin Pharmacol* 2016; **56**(Suppl 7): S157-72. doi: 10.1002/jcph.706
34. Kotnik T, Rems L, Tarek M, Miklavčič D. Membrane electroporation and electroporation: mechanisms and models. *Annu Rev Biophys* 2019; **48**: 63-91. doi: 10.1146/annurev-biophys-052118-115451
35. Ursic K, Kos S, Kamensek U, Cemazar M, Scancar J, Bucek S, Kranjc S, Staresinic B, Sersa G. Comparable effectiveness and immunomodulatory actions of oxaliplatin and cisplatin in electrochemotherapy of murine melanoma. *Bioelectrochemistry* 2018; **119**: 161-71. doi: 10.1016/j.bioelechem.2017.09.009
36. Zakelj MN, Prevc A, Kranjc S, Cemazar M, Todorovic V, Savarin M, et al. Electrochemotherapy of radioresistant head and neck squamous cell carcinoma cells and tumor xenografts. *Oncol Rep* 2019; **41**: 1658-68. doi: 10.3892/or.2019.6960
37. Zhang L, Ye Y, Zhang X, Li X, Chen Q, Sun JCW. Cisplatin under oriented external electric fields: a deeper insight into electrochemotherapy at the molecular level. *Int J Quantum Chem* 2020; **121**: e26578. doi: 10.1002/qua.26578
38. Cemažar M, Miklavčič D, Ščančar J, Dolžan V, Golouh R, Serša G. Increased platinum accumulation in SA-1 tumour cells after in vivo electrochemotherapy with cisplatin. *Br J Cancer* 1999; **79**: 1386-91. doi: 10.1038/sj.bjc.690222
39. Florea AM, Büsnelberg D. Cisplatin as an anti-tumor drug: cellular mechanisms of activity, drug resistance and induced side effects. *Cancers* 2011; **3**: 1351-71. doi: 10.3390/cancers3011351
40. Pakhomova ON, Khorokhorina VA, Bowman AM, Rodaite-Riševičienė R, Saulis G, Xiao S, et al. Oxidative effects of nanosecond pulsed electric field exposure in cells and cell-free media. *Arch Biochem Biophys* 2012; **527**: 55-64. doi: 10.1016/j.abb.2012.08.004
41. Szlasa W, Kielbik A, Szewczyk A, Rembiałkowska N, Novickij V, Tarek M, et al. Oxidative effects during irreversible electroporation of melanoma cells – in vitro study. *Molecules* 2021; **26**: doi: 10.3390/molecules26010154
42. Batista Napotnik T, Wu Y-H, Gundersen MA, Miklavčič D, Vernier PT. Nanosecond electric pulses cause mitochondrial membrane permeabilization in Jurkat cells. *Bioelectromagnetics* 2012; **33**: 257-64. doi: 10.1002/bem.20707
43. Nuccitelli R, McDaniel A, Connolly R, Zelickson B, Hartman H. Nano-pulse stimulation induces changes in the intracellular organelles in rat liver tumors treated in situ. *Lasers Surg Med* 2020; **52**: 882-9. doi: 10.1002/lsm.23239
44. Semenov I, Xiao S, Pakhomov AG. Primary pathways of intracellular Ca²⁺ mobilization by nanosecond pulsed electric field. *Biochim Biophys Acta - Biomembr* 2013; **1828**: 981-9. doi: 10.1016/j.bbame.2012.11.032
45. Frandsen SK, Gissel H, Hojman P, Tramm T, Eriksen J, Gehl J. Direct therapeutic applications of calcium electroporation to effectively induce tumor necrosis. *Cancer Res* 2012; **72**: 1336-41. doi: 10.1158/0008-5472.CAN-11-3782
46. Marullo R, Werner E, Degtyareva N, Moore B, Altavilla G, Ramalingam SS, et al. Cisplatin induces a mitochondrial-ROS response that contributes to cytotoxicity depending on mitochondrial redox status and bioenergetic functions. *PLoS ONE* 2013; **8**: 1-15. doi: 10.1371/journal.pone.0081162
47. Kleih M, Böpple K, Dong M, Gaißler A, Heine S, Olayoye MA, et al. Direct impact of cisplatin on mitochondria induces ROS production that dictates cell fate of ovarian cancer cells. *Cell Death Dis* 2019; **10**: 31-59. doi: 10.1038/s41419-019-2081-4
48. Kawai Y, Nakao T, Kunimura N, Kohda Y, Gemba M. Relationship of intracellular calcium and oxygen radicals to cisplatin-related renal cell injury. *J Pharmacol Sci* 2006; **100**: 65-72. doi: 10.1254/jphs.FP0050661
49. Al-Taweel N, Varghese E, Florea A-M, Büsnelberg D. Cisplatin (CDDP) triggers cell death of MCF-7 cells following disruption of intracellular calcium ([Ca²⁺]_i) homeostasis. *J Toxicol Sci* 2014; **39**: 765-74. doi: 10.2131/jts.39.765
50. Galdani R, de Clippele M, Ratbi I, Gailly P, Tajeddine N. Store-operated calcium entry contributes to cisplatin-induced cell death in non-small cell lung carcinoma. *Cancers* 2019; **11**: 2023. doi: 10.3390/cancers11030430
51. Michel O, Kulbacka J, Sączko J, Mączyska J, Błasiak P, Rossowska J, et al. Electrochemotherapy with cisplatin against metastatic pancreatic cancer: in vitro study on human primary cell culture. *Biomed Res Int* 2018; **2018**: 7364539. doi: 10.1155/2018/7364539
52. Speelmans G, Sips WHM, Grisel RHJ, Staffhorst RWHM, Fichtinger-Schepman AMJ, Reedijk J, et al. The interaction of the anti-cancer drug cisplatin with phospholipids is specific for negatively charged phospholipids and takes place at low chloride ion concentration. *Biochim Biophys Acta - Biomembr* 1996; **1283**: 60-6. doi: 10.1016/0005-2736(96)00080-6

2.2 REMAINING LINKING SCIENTIFIC WORK

2.2.1 Survival-permeabilization curves of B16F1 cells

To determine the optimal electric field strength for electrochemotherapy (i.e., the electric field strength that results in the highest cell membrane permeabilization without a decrease in cell survival) for each pulse protocol, cell membrane permeabilization (expressed as the percentage of cells that fluoresce YO-PRO-1) and cell survival (determined by the metabolic assay containing the tetrazolium salt 3-(4,5-dimethylthiazol-2-yl)-5-(3-carboxymethoxyphenyl)-2-(4-sulfophenyl)-2H-tetrazolium (MTS)) after electroporation of mouse skin melanoma B16F1 cells were measured at electric field strengths for nanosecond pulses with different parameters (pulse duration: 200, 400 or 550 ns, number of pulses: 1, 25 or 100 pulses, 10 Hz pulse repetition rate). The rectangular monophasic nanosecond pulses were delivered with the CellFX System (Pulse Biosciences, California, USA). Signals were monitored with a WaveSurfer 3024Z, 200 MHz oscilloscope (Teledyne LeCroy, New York, USA), voltage was measured with a 1 k Ω resistor and a Pearson model 2877 (1 V/1 A, 200 MHz) current monitor; and electric current was measured with a Pearson model 2878 (1 V/10 A, 70 MHz) current monitor (all from Pearson Electronics, California, USA). Electric field strength was calculated by dividing the measured voltage by the electroporation cuvette gap (i.e., the distance between parallel plate electrodes).

B16F1 cells, obtained directly from the European Collection of Authenticated Cell Cultures (cat. no. 92101203, Sigma Aldrich, Germany) were grown for 2–4 days at 37 °C in a humidified, 5 % CO₂ atmosphere in Dulbecco's Modified Eagle Medium (DMEM, catalog number D5671, Sigma-Aldrich) supplemented with 10 % fetal bovine serum (catalog number F9665, Sigma-Aldrich), 2.0 mM L-glutamine, 50 μ g/ml gentamycin and 1 U/ml penicillin/streptomycin – referred to as complete growth medium DMEM and used in this composition through all experiment. On the day of the experiment, cells were detached with 1 \times trypsin-ethylenediaminetetraacetic acid (EDTA, cat. no T4174, Sigma-Aldrich) diluted in 1 \times Hank's basal salt solution (catalog number H4641, Sigma-Aldrich). Trypsin was inactivated by complete growth medium DMEM. Cells were transferred to a 50 ml centrifuge tube and centrifuged at 180 g for 5 min at room temperature (centrifuge 3-16PK, Sigma-Aldrich). The supernatant was discarded, and the cells were resuspended at a cell density of 4 \times 10⁶ cells/ml in complete growth medium DMEM, which was used as electroporation medium.

To determine the percentage of permeabilized cells at different electric field strengths, the cell suspension was mixed with YO-PRO-1 iodide (cat. no. Y3603, Thermo Fisher Scientific, Massachusetts, USA) at a final concentration of 1 μ M immediately before the

application of electric pulses. The cells mixed with YO-PRO-1 (600 μ l) were transferred to an electroporation cuvette with 4 mm gap (VWR, Pennsylvania, USA) and then the pulses were applied. The treated cell suspension (20 μ l) was transferred to a new 1.5 ml microcentrifuge tube. Three minutes after the last pulse, 150 μ l of complete growth medium DMEM was added. The cell suspension was gently vortexed and analyzed using the Attune NxT flow cytometer (Thermo Fisher Scientific). A blue laser at 488 nm was used for excitation and a 530/30 nm bandpass filter was used to detect emitted fluorescence from YO-PRO-1. Single cells were separated from all events by gating. The measurement was stopped when 10,000 cells had been recorded. The data obtained were analyzed using Attune NxT software (Thermo Fisher Scientific). The percentage of cells with permeabilized cell membrane was determined from the histogram of YO-PRO-1 fluorescence. Experiments were repeated 3–4 times for each pulse protocol. The sham control was treated in the same manner as the samples, except that no pulses were delivered.

For measurements of cell survival, the cell suspension (600 μ l) was pipetted into an electroporation cuvette with 4 mm gap (VWR). The electroporation cuvette was placed in the cuvette holder and electric pulses were delivered (no pulses were delivered for sham control). Then, the cell suspension (20 μ l) was transferred to a new 1.5 ml microcentrifuge tube and 25 min after the last pulse, the complete growth medium DMEM (380 μ l) was added. The cell suspension was gently vortexed and plated (100 μ l) in three technical replicates into a well of a flat bottom 96-well plate. The plate was then placed in an incubator at 37 °C in a humidified, 5 % CO₂ atmosphere. After 24 h, 20 μ l of the CellTiter 96 AQueous One Solution Cell Proliferation Assay (cat. no. G3580, Promega, Wisconsin, USA) was added to each well of the 96-well plate. After 2 h 35 min of incubation at 37 °C in a humidified atmosphere containing 5 % CO₂, absorbance was measured at 490 nm using an Infinite 200 (Tecan, Austria) spectrofluorometer. Cell survival was calculated by first subtracting the absorbance of the blank (complete growth medium DMEM) and then normalizing the average absorbance of the three technical replicates of the sample to the absorbance of the sham controls. Experiments were repeated 3–5 times for each pulse protocol.

The curves for cell membrane permeabilization and cell survival are shown in Figure 2.

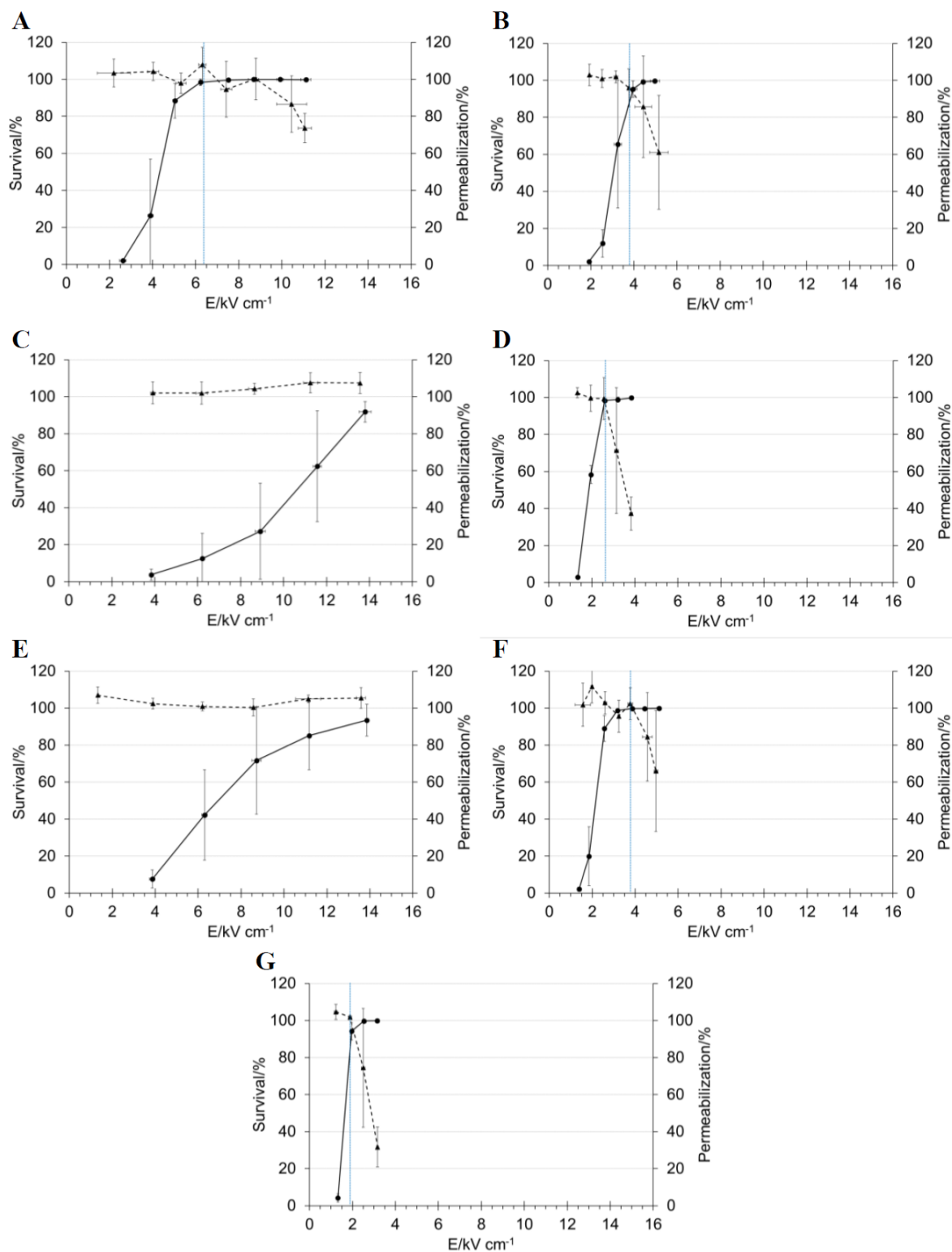


Figure 2: Cell survival (triangles, dashed line) and cell membrane permeabilization (circles, solid line) of B16F1 cells after electroporation with (A) twenty-five 200 ns pulses at 10 Hz repetition rate, (B) one hundred 200 ns pulses at 10 Hz repetition rate, (C) one 400 ns pulse, (D) one hundred 400 ns pulses at 10 Hz repetition rate, (E) one 550 ns pulse, (F) twenty-five 550 ns pulses at 10 Hz repetition rate, (G) one hundred 550 ns pulses at 10 Hz repetition rate at different electric field strengths (E). The bars represent the standard

deviation, and the blue vertical line marks the determined optimal electric field strength for electrochemotherapy.

The percentage of cells with permeabilized cell membrane increased with increasing electric field strength. With shorter pulses, higher electric field strengths were required to reach the same degree of cell membrane permeabilization as with longer pulses; and with increasing the number of pulses, lower electric field strengths were required to achieve the same effect. We were unable to achieve > 99 % cell membrane permeabilization of B16F1 cells when using one nanosecond pulse (of 200, 400 or 550 ns duration) at the highest voltage in safe operation of the CellFX pulse generator. High (i.e., > 99 %) cell membrane permeabilization was achieved with all other nanosecond pulse protocols.

Cell survival decreased with increasing electric field strength, with the exception of a one pulse of 200, 400, or 550 ns, for which we observed no decrease in cell survival compared with sham control, even at the highest electric field strength. For longer pulse durations and for a larger number of pulses, the cell survival started decreasing at lower electric field strengths compared to pulse protocols with shorter pulse durations and fewer pulses. When delivering one hundred nanosecond pulses of all the three pulse durations tested, cell survival started decreasing before the cell membrane permeabilization reached its maximum.

2.2.2 Lipid peroxidation after electroporation

To measure lipid peroxidation in Chinese hamster ovary cells (CHO) after electroporation with twenty-five 400 ns and eight 100 μ s pulses, the Click-iT Lipid Peroxidation Imaging Kit - Alexa Fluor 488 (catalog number C10446 Invitrogen, Thermo Fisher Scientific) was used, with some modification of the manufacturer's protocol to adapt to the CHO cell line.

CHO-K1 cells, obtained from the European Collection of Authenticated Cell Cultures (catalog number 85051005, mycoplasma free), were grown in Nutrient Mixture F-12 Ham (catalog number N6658, Sigma-Aldrich, Massachusetts, United States) supplemented with 10 % fetal bovine serum (catalog number F9665, Sigma-Aldrich), 1.0 mM L-glutamine (catalog number G7513, Sigma-Aldrich), 50 μ g/ml gentamycin (catalog number G1397, Sigma-Aldrich) and 1 U/ml penicillin/streptomycin (catalog number P0781, Sigma-Aldrich) for 2–4 days at 37 °C in a humidified, 5 % CO₂ atmosphere. On the day of the experiment, cells were detached with 1 \times trypsin-EDTA (cat. no T4174, Sigma-Aldrich) diluted in 1 \times Hank's basal salt solution (catalog number H4641, Sigma-Aldrich). Trypsin was inactivated by DMEM (catalog number D5671, Sigma-Aldrich) supplemented with 10 % fetal bovine serum (catalog number F9665, Sigma-Aldrich), 2.0 mM L-glutamine, 50 μ g/ml gentamycin

and 1 U/ml penicillin/streptomycin – referred to as complete growth medium DMEM and used in this composition through all experiment. Cells were transferred to a 50 ml centrifuge tube and centrifuged at 180 g for 5 min (centrifuge 3-16PK, Sigma-Aldrich) at room temperature. The supernatant was discarded, and the cells were resuspended at a cell density of 4×10^6 cells/ml in complete growth medium DMEM, which was used as electroporation medium. Linoleamide alkyne was added to the cell suspension at a final concentration of 200 μ M. 600 μ l of the cell suspension was transferred to multiple electroporation cuvettes with 4 mm gap (VWR). 150 μ l of the cell suspension was transferred to multiple 1.5 ml centrifuge tubes for unstained and positive controls and to several electroporation cuvettes with 2 mm gap (VWR). To the positive controls, 1.5 μ l of cumene hydroperoxide 10 mM working solution in complete growth medium DMEM was added. 15 min after the addition of linoleamide alkyne, the cell suspension was electroporated in electroporation cuvettes at room temperature. Using the CellFX System (Pulse Biosciences), 400 ns monophasic rectangular pulses with 10 Hz repetition rate at 3.9 kV/cm were delivered to the cell suspension in electroporation cuvettes with 4 mm gap. Signals were monitored with a WaveSurfer 3024Z, 200 MHz oscilloscope (Teledyne LeCroy), voltage was measured with a 1 k Ω resistor and a Pearson model 2877 (1 V/1 A, 200 MHz) current monitor; and electric current was measured with a Pearson model 2878 (1 V/10 A, 70 MHz) current monitor (all from Pearson Electronics). A laboratory prototype pulse generator (University of Ljubljana) based on an H-bridge digital amplifier with 1 kV MOSFETs (DE275-102N06A, IXYS, USA) (Sweeney et al., 2016) was used to deliver eight 100 μ s monophasic rectangular pulses with 1 Hz pulse repetition rate at 1.1 kV/cm to the cell suspension in electroporation cuvettes with 2 mm gap. Voltage and electric current were monitored using WaveSurfer 422, 200 MHz oscilloscope, CP030 current probe, and ADP305 high-voltage differential voltage probe (all from Teledyne LeCroy). Electric field strength was calculated by dividing the measured voltage by the electroporation cuvette gap (i.e., the distance between parallel plate electrodes). For the negative (sham) controls, the electroporation cuvettes were placed on the cuvette holders connected to the pulse generators, but no electric pulses were delivered. After electroporation, 150 μ l of the cell suspension from the electroporation cuvette was transferred to a 1.5 ml centrifuge tube and incubated at 37 °C in a humidified 5 % CO₂ atmosphere and vortexed from time to time to prevent cells from sticking to the bottom of the tube. At 2 h after the addition of linoleamide alkyne, the cells were centrifuged at 300 g for 5 min at room temperature. The supernatant was discarded, and the cells were washed with 200 μ l of phosphate buffered saline (PBS). Centrifugation and washing were repeated two more times. Then, the cell pellet was resuspended in 300 μ l of PBS and transferred to a well of a 24-well cell culture plate. The cells were left at room temperature for 30 min to attach to the bottom of the well. The PBS was then removed and 300 μ l of 3.7 % formaldehyde in PBS was added to each well. The cells were incubated with formaldehyde for 15 min at room temperature, then the formaldehyde was removed and cells were washed

three times with 400 μ l of PBS. After the last wash, PBS was removed and 300 μ l of 0.25 % Triton X-100 in PBS was added to each well. After 10 min of incubation at room temperature, Triton X-100 was removed and 300 μ l of 1 % BSA in PBS was added to each well. After 30 min, the BSA solution was removed and 250 μ l of the Click-iT reaction cocktail (prepared according to the manufacturer's protocol) was added to each well, except for the wells containing the unstained controls (the unstained controls were kept in PBS instead). The plate was incubated for 1 h 30 min at room temperature protected from light. After incubation, the Click-iT reaction cocktail was removed, and the cells were washed twice with 300 μ l of 1 % BSA in PBS and then two times with 300 μ l of PBS. After the last wash, PBS was removed and 250 μ l of pre-warmed trypsin-EDTA in 1 \times Hank's basal salt solution was added to the cells. After 1.5 min, trypsin was inactivated by adding 250 μ l of complete growth medium DMEM. Cell suspensions were analyzed using the Attune NxT flow cytometer (Thermo Fisher Scientific). A blue laser at 488 nm was used for excitation and a 530/30 nm bandpass filter was used to detect the emitted fluorescence of Alexa Fluor 488. Individual cells were separated from all events by gating. The measurement was stopped when 10,000 single cells were recorded. The data obtained were analyzed using Attune NxT software (Thermo Fisher Scientific). The median fluorescence of the cells was determined from the Alexa Fluor 488 fluorescence histogram. Experiments were performed in duplicate for each treatment and repeated on 4 different days. Data were analyzed by the one-way analysis of variance (ANOVA) and post hoc Tukey test ($\alpha = 0.05$). The average median fluorescence for each group is shown on Figure 3.

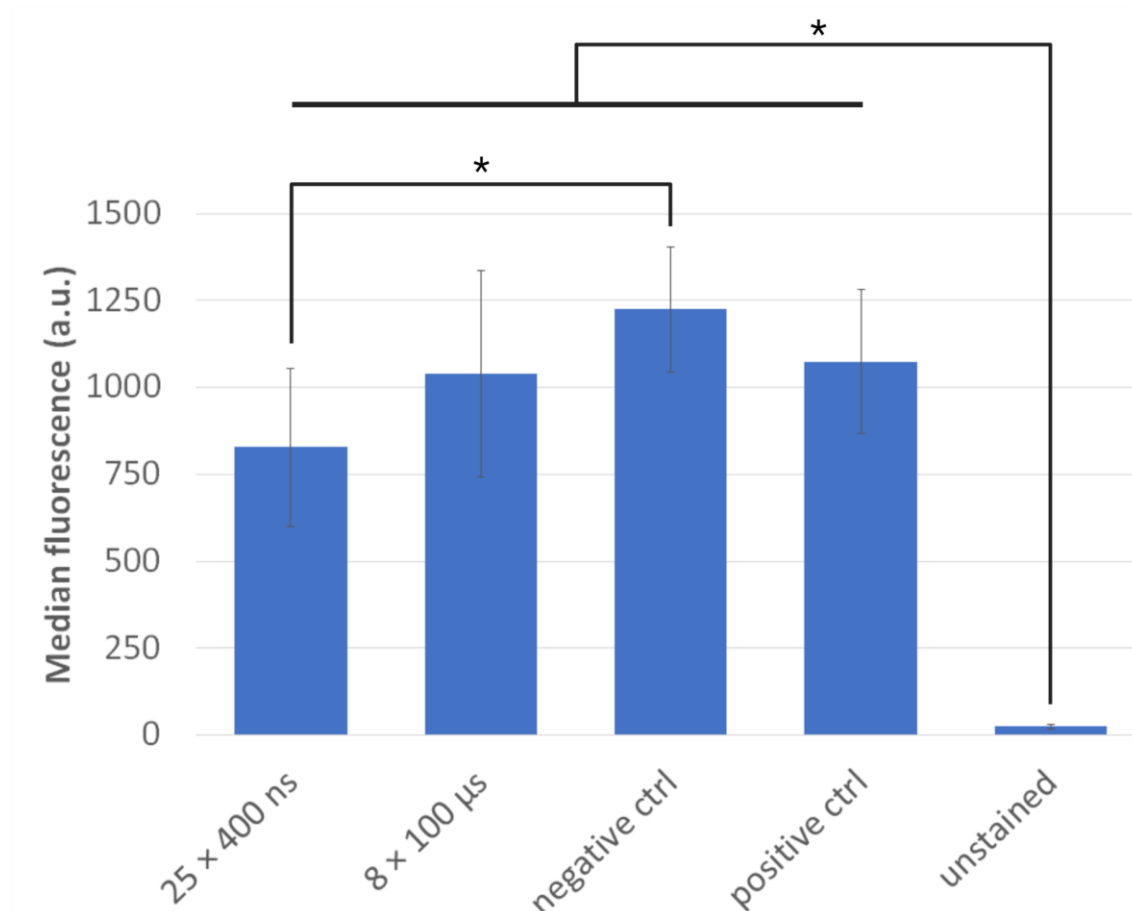


Figure 3: Lipid peroxidation of CHO cells measured with the Click-iT Lipid Peroxidation Imaging Kit - Alexa Fluor 488. Cells were electroporated with twenty-five 400 ns pulses at 3.9 kV/cm with a pulse repetition rate of 10 Hz (25×400 ns) or eight 100 μ s pulses at 1.1 kV/cm with a pulse repetition rate of 1 Hz (8×100 μ s). The negative control (negative ctrl) was treated in the same manner as the electroporated cells, except that no electric pulses were delivered to the electroporation cuvette. Cumene hydroperoxide was added to the positive control (positive ctrl) to induce lipid peroxidation. An asterisk (*) indicates statistically significant differences ($p < 0.05$) between groups.

As can be observed in Figure 3, the signal from the negative control, positive control, and all electroporated cells was statistically significantly higher than that from the unstained cells, and the signal from the cells electroporated with twenty-five 400 ns pulses was statistically significantly lower than that from the negative control. Contrary to expectations, the average value of the positive control was even slightly lower than that of the negative control, although the differences between the two were not statistically significant. These results suggest that the Click-iT Lipid Peroxidation Imaging Kit - Alexa Fluor 488 is not a suitable method for detecting lipid peroxidation of CHO cells at least within the first hours after electroporation.

3 DISCUSSION AND CONCLUSIONS

3.1 DISCUSSION

3.1.1 Determination of equiefficient pulses

In our study, we first measured cell survival and cell membrane permeabilization of different cell lines after electroporation to empirically determine the pulse parameters of H-FIRE (Vižintin et al., 2020) and nanosecond pulses (Vižintin et al., 2021, 2022) that are equiefficient to the standard eight 100 μ s pulses with 1 Hz repetition rate.

For H-FIRE pulses, we delivered a burst of 400 biphasic rectangular pulses. One pulse was defined as consisting of the positive phase, the interphase delay, and the negative phase. The duration of the positive phase was 1 μ s and the duration of the negative phase was 1 μ s for all H-FIRE pulses, while the duration of the interphase delay (i.e., the delay between the positive phase and the negative phase) and the interpulse delay (i.e., the delay between pairs of biphasic pulses) were varied from 0.5 to 10,000 μ s. All H-FIRE pulse protocols and the eight 100 μ s pulses had the same amplitude – to be able to determine the effects of delay, we chose an amplitude at which the differences between the different pulse protocols were most pronounced. For membrane permeabilization (measured by uptake of propidium iodide), an amplitude of 300 V (corresponding to an electric field strength of 1.5 kV/cm) was chosen. For cell survival, measured by the metabolic MTS assay, a pulse amplitude of 500 V (resulting in an electric field strength of 2.5 kV/cm) was chosen. Four different cell lines were tested: Chinese hamster ovary CHO-K1, rat cardiac myoblast H9c2, mouse myoblast C2C12, and mouse neuronal cell line HT22.

We have shown in all four cell lines tested that by extending the interphase and interpulse delay (or in other words, reducing the pulse repetition rate) of the H-FIRE pulses, lower cell survival can be achieved while maintaining the same pulse amplitude and duration of positive and negative phase. This is consistent with previous studies reporting that pulses with lower pulse repetition rates are more effective for electroporation (Pucihar et al., 2002; Serša et al., 2010; Arena et al., 2011; Pakhomova et al., 2011). However, only the H-FIRE pulse protocol with an interphase and interpulse delay of 10,000 μ s decreased the cell survival as effectively as the standard eight 100 μ s pulses for the CHO and HT22 cell lines.

The duration of the interphase and interpulse delay had a more complex effect on membrane permeabilization. When the interphase delay was kept at 1 μ s, the rate of cell membrane permeabilization increased with the extension of the interpulse delay, which is consistent with the cell survival results. However, when the interphase and interpulse delays were of

the same duration, no increase or even a decrease in cell membrane permeabilization was measured for pulses with a delay of 1000 or 10,000 μ s, in contrast to what was observed for cell survival. All H-FIRE pulse protocols tested were less effective than the standard eight 100 μ s pulses in terms of cell membrane permeabilization in all four tested cell lines tested, which is consistent with previous reports (Sweeney et al., 2016). The discrepancy between cell survival and membrane permeabilization results underscores the importance of clearly defining the goal of electroporation when establishing equiefficient pulse protocols.

H-FIRE pulses have attracted attention because their application has been shown to result in reduced muscle contractions (the main drawback of medical and veterinary electroporation-based applications) compared with monophasic pulses of equal amplitude. However, higher electric field strengths are generally required to achieve the same effect with H-FIRE as with monophasic pulses. Until recently, it was not clear whether H-FIRE pulses with higher amplitudes would still reduce muscle contractions and pain sensation compared with equally effective monophasic pulses with lower amplitudes, because as pulse amplitude increases, muscle contractions increase as well. Our results indicate that the efficiency of H-FIRE pulses could be improved by extending the delays instead of increasing the pulse amplitude, but we did not investigate the effects of the delays on muscle contractions and pain sensations. A theoretical study (Aycock et al., 2021) suggested that shortening the interphase delay and extending the interpulse delay in H-FIRE pulses, both the ablation volume (the goal of tissue ablation with irreversible electroporation) and the thresholds for nerve excitation increase, implying that higher pulse amplitudes are required to excite the nerves as are needed to achieve the desired ablation volume. Their results were partially confirmed in a recent human study – Cvetkoska et al. (2022) confirmed that pulses with short interphase delays and longer interpulse delays reduced muscle contractions but not painful sensations. On the other hand, they showed that a simultaneous increase in interphase and interpulse duration in H-FIRE pulses up to 10 μ s increased the muscle contractions but did not elicit strong painful sensations and muscle contractions were still significantly lower compared with the standard eight 100 μ s pulses. When the interpulse delay was extended beyond 10 μ s, they observed a decrease in muscle contractions but also an increase in pain perception. Overall, their results suggest that pulse-induced muscle contractions do not necessarily correlate with pain sensations and vice versa. This could be a consequence of the different response of the different types of nerve fibers involved in signal transmission to electric pulses with different parameters, and that the interphase and interpulse delays indeed play an important role in muscle contractions and/or pain sensations induced by H-FIRE pulses.

To elucidate nanosecond pulse protocols which are equiefficient to eight 100 μ s pulses, cell membrane permeabilization (defined as the percentage of YO-PRO-1-stained cells) and cell survival (determined by the metabolic MTS assay) of CHO and mouse melanoma B16F1

cells were measured after electroporation with the standard 100 μ s pulses lines at a pulse repetition rate of 1 Hz and nanosecond pulse protocols with different pulse parameters at different electric field strengths. Nanosecond pulses with three different pulse durations (200, 400, or 550 ns), three different numbers of pulses (1, 25, or 100 pulses), and one pulse repetition rate (10 Hz) were studied on CHO cells, while only selected nanosecond pulse protocols (namely one 200 pulse and twenty-five 400 ns pulses at a pulse repetition rate of 10 Hz) were tested on B16F1 cells. From the survival-permeabilization curves, the electric field strength that caused the highest cell membrane permeabilization without decreasing cell survival was selected for each pulse protocol. These conditions (i.e., high cell survival and high cell membrane permeabilization) were selected because they were optimal for electrochemotherapy and the pulse protocols were next to be tested in *in vitro* electrochemotherapy experiments. As expected, higher electric field strengths were required to achieve high membrane permeabilization with shorter pulses. The optimal electric field strength value for the eight 100 μ s pulses was determined to be 1.1 kV/cm for CHO and 0.9 kV/cm for B16F1 cells, whereas all optimal electric field strengths for the nanosecond pulse protocols were higher. When comparing nanosecond pulses of the same duration, lower electric field strengths were required to achieve high membrane permeabilization when a larger number of pulses was used, as expected. For CHO cells, all pulse protocols tested permeabilized more than 99 % of the cells at the selected optimal electric field strength, with the exception of one 200 ns pulse which permeabilized around 85 % of the cell population at the highest electric field strength within the safe operating range of the pulse generator used. In the case of the B16F1 cell line, cell membrane permeabilization of less than 99 % was achieved with one nanosecond pulse of 200, 400 and also 550 ns pulse duration at the highest electric field strength, suggesting that higher electric field strengths are required for permeabilization of B16F1 cells compared with CHO cells when only one nanosecond pulse is used. This is in contrast to what was observed with the eight 100 μ s pulses – lower electric field strength was required for these pulses to permeabilize B16F1 cells than CHO cells.

In addition to the percentage of YO-PRO-1-stained cells, the median fluorescence intensity of YO-PRO-1 was also measured for CHO cells, which provides information on how many molecules of YO-PRO-1 entered the permeabilized cells. At the determined optimal electric field strength, the highest fluorescence intensity was measured for the eight 100 μ s pulses, while the lowest intensities were measured for pulse protocols with only one nanosecond pulse. Increasing the electric field strength above the optimal value also increased the fluorescence intensity for all pulses, suggesting that although virtually the entire population is already permeabilized at lower electric field strengths, more molecules of YO-PRO-1 enter the cells at higher electric field strengths. We have also found that for applications based on reversible electroporation (such as electrochemotherapy or gene electrotransfer), the use of a lower number of pulses at a higher electric field strength may be more

appropriate than the use of a higher number of pulses at a lower electric field strength, because with fewer pulses there is a wider range of electric field strengths at which a very high cell membrane permeabilization is achieved without a noticeable decrease in cell survival.

3.1.2 Release of metal from electrodes

Our study was the first report of metal release of from electrodes after application of H-FIRE and nanosecond pulses.

The concentration of metal ions in saline was measured by inductively coupled plasma mass spectrometry after delivery of H-FIRE pulses (as in the cell experiments) and the standard eight 100 μ s pulses to wire electrode of aluminum, stainless steel and platinum. All of the H-FIRE pulses tested caused significantly less metal release from aluminum and stainless steel electrodes compared to the eight 100 μ s pulses with the same pulse amplitude, which is consistent with previous reports that biphasic pulses cause a less metal release than monophasic pulses (Kotnik and others, 2001a). However, in the case of platinum electrodes, metal release was not significantly lower for all H-FIRE pulses – for some H-FIRE pulse protocols, there were no statistically significant differences in the concentration of released platinum ions as with the eight 100 μ s pulses, although 1-2 orders of magnitude lower concentration of released platinum was measured after application of H-FIRE pulses. With the exception of platinum, it could be concluded from our study that it is possible to extend the delays in the H-FIRE pulses to achieve an equivalent biological effect as with the standard eight 100 μ s pulses with still lower metal release from the electrodes. H-FIRE pulses appear to be superior to the standard eight 100 μ s in terms of limiting electrochemical reactions, which was confirmed in another experimental and numerical *in vitro* study (Mahnič-Kalamiza and Miklavčič, 2020).

Different interphase and interpulse delays in the H-FIRE pulse protocol resulted in significant differences in the concentration of released metals from aluminum and stainless steel electrodes. However, more platinum ions were measured after application of H-FIRE pulses with 1 μ s interphase delay and various other durations of interpulse delay than with H-FIRE pulses that had interphase and interpulse delays of the same duration. Our study could not explain why this was observed. Further work would be needed to understand the effects of the pulse delays in H-FIRE pulses on metal release from platinum electrodes. It is also interesting to note that after eight 100 μ s pulses were delivered to the stainless steel electrodes, the highest concentration of iron ions was measured, followed by chromium, nickel, and manganese ions, which is proportional to the composition of the stainless steel wire used to fabricate the electrodes. However, delivery of H-FIRE pulses to the stainless

steel electrodes resulted in a similar concentration of released chromium and manganese ions, a slightly higher concentration of nickel ions, and the highest concentration of iron ions, which is not proportional to either the composition of the stainless steel or to the standard potentials of the oxidation half-reactions. Future work would be needed to understand how different pulse waveforms affect metal release from the electrodes.

Aluminum, stainless steel, and platinum are commonly used as electrode materials. Metal release from all three materials has been previously reported (Black and Hannaker, 1980; Loomis-Husselbee et al., 1991; Friedrich et al., 1998; Tomov and Tsoneva, 2000; Kotnik et al., 2001; Morren et al., 2003; Evrendilek et al., 2004; Roodenburg et al., 2005a, 2005b; Gad et al., 2014). However, it is difficult to compare the results of different studies because there are large differences in the set-up, electrode geometry, electrolyte composition, and the various parameters of the electric pulses used. On the other hand, in our study the conditions were the same for all electrodes and pulse protocols and, so amounts of released metals can be compared. The amount of metal ions released from the electrodes varied greatly between the three electrode materials tested – the absolute highest amount of released metal ions was measured for aluminum electrodes and the lowest for platinum electrodes. It was also found that the delivery of electric pulses, particularly the eight 100 μ s pulses, caused visible corrosion of the aluminum electrodes, while no corrosion was observed for stainless steel or platinum electrodes.

The amount of aluminum ions released from the electroporation cuvettes after delivery of nanosecond pulses was measured by inductively coupled plasma mass spectrometry. Nanosecond pulses protocols and the standard eight 100 μ s pulses with electric field strengths determined to be optimal for electrochemotherapy of CHO cells were delivered to electroporation cuvettes (made of an aluminum alloy of unknown composition) filled with saline. A significantly lower concentration of released aluminum ions was measured when any of the nanosecond pulse protocols was delivered to the electroporation cuvettes compared to the eight 100 μ s pulses. We demonstrated that shortening the pulse duration to a few hundred nanosecond pulses reduced the amount of metal released from the electrodes, even when the voltage and number of pulses were increased to achieve a comparable biological effect as with longer duration pulses. Because metal release from electrodes is a subgroup of the electrochemical reactions at the electrode-electrolyte interface, this argues for the use of nanosecond pulses over microsecond pulses if the electrochemical reactions are to be kept to a minimum. However, the metal release does not seem to depend only on the pulse duration – comparison of individual nanosecond pulses with the same set amplitude and different pulse durations (200, 400 and 500 ns) shows that, contrary to expectations, the highest concentration of aluminum ions was measured after delivery of the shortest (i.e. 200 ns) pulse. The amount of metal ions released also does not appear to correlate well with

the energy delivered to the cuvette (estimated by multiplying the pulse duration and the number of pulses by the measured amplitude of the voltage and the measured amplitude of the electric current) – for example, the estimated energy for one 200 ns pulse was the lowest, but the measured amount of metal ions released was one of the highest.

We confirmed our first hypothesis that H-FIRE and nanosecond pulses limit electrochemical reactions also when the pulse parameters are adjusted to achieve the same biological effect as with longer monophasic pulses. As presented in the Chapter 1 Presentation of the problem and hypotheses, electrochemical reactions at the electrode-electrolyte interface during the delivery of high-voltage electric pulses cause a number of effects, including (but not limited to) electrode fouling and corrosion, bubble formation, and release of the electrode material, limiting the prevalence of electroporation-based applications in food processing, biotechnology, medicine, and other fields. Electrodes in electroporation-based applications are most commonly made of metal. The metal ions released from the electrodes can affect the treated cells or media in a variety of ways, from cytotoxic effects to chemical alteration of the medium. Since the metal ions released pose a major health risk of foods treated with electric pulses, it is of utmost importance that the metal ion concentrations are within health safety standards. It is therefore important to limit electrochemical reactions when they are undesirable, and one of the strategies to achieve this is to optimize pulse parameters (Saulis et al., 2015; Pataro and Ferrari, 2020). However, a direct comparison between the H-FIRE and nanosecond pulses from is not possible based on the results of our study because different electrode materials (pure aluminum for H-FIRE vs. aluminum alloy in the case of nanosecond pulses) and different electrode geometries (wire electrodes in microcentrifuge tubes for H-FIRE vs. electroporation cuvettes in the case of nanosecond pulses) were used, resulting in different contact areas and current densities. The electric field distribution is inhomogeneous when wire electrodes are used, while the electrodes in the electroporation cuvettes are essentially plate electrodes that are parallel to each other and give relatively homogeneous field distribution (Reberšek et al., 2014).

In both sets of experiments, some metal ions were released from the electrodes into the solution, even in the sham controls where the solution was in contact with the electrodes for only a few seconds and no pulses were delivered. This was probably the result of the formation of the so-called double layer of charged particles and/or oriented dipoles at the electrode-electrolyte interface, which forms immediately after the electrodes are immersed in the electrolyte. Due to the formation of an electric field between the electrode and the layer of ions in the double layer, electrons are transferred between the electrode and the electrolyte and chemical reactions are initiated, even when no external voltage is applied. This accelerates the oxidation reactions, and consequently causes the release of metal ions from these electrodes (Morren et al., 2003).

A very pure saline (i.e., 0.9 % NaCl solution in water) was used for metal release experiments. Although the saline does not mimic the real electroporation media or tissue well, it was chosen because it contains only minimal amounts of the metal ions of interest, allowing us to detect very small amounts of metal ions released. In contrast, the growth medium used in the cell experiments contains several orders of magnitude higher amounts of some of the metal ions of interest, as released from the electrodes, and for this reason was unsuitable for this set of experiments.

3.1.3 Cell membrane resealing and lipid peroxidation

Our aim was to compare the extent of lipid peroxidation after electroporation with electric pulses of different waveforms and to correlate lipid peroxidation with cell membrane resealing. Cell membrane resealing was measured for different nanosecond pulse protocols and the eight 100 μ s pulses at the electric field strength determined to be optimal for electrochemotherapy in survival and permeabilization experiments by adding YO-PRO-1 to CHO cells every 2 min from 2 to 26 min after electroporation and measuring the percentage of YO-PRO-1-fluorescent cells (Vižintin et al., 2021). The Click-iT Lipid Peroxidation Imaging Kit - Alexa Fluor 488 was used to measure lipid peroxidation in CHO cells electroporated with twenty-five 400 ns pulses or eight 100 μ s pulses at the electric field strength determined to be optimal for electrochemotherapy.

The cell membrane resealed in less than 5 min after application of eight 100 μ s pulses. For some of the nanosecond pulse protocols, the time required to reseal the cell membrane was not significantly longer, but for the twenty-five 200 ns, twenty-five 400 ns, twenty-five 550 ns, one hundred 550 ns pulses and one 400 ns and one 550 ns pulse, the membrane required a significantly longer time (more than 10 min) to reseal.

Some reports suggest that electroporation with nanosecond pulses forms smaller pores in the cell membrane than to pores formed by longer pulses (Vernier et al., 2006; Pakhomov et al., 2007a, 2009). For laser-induced pores, it has been shown that a longer time is required for resealing the membrane with smaller pores than with larger pores (Jimenez et al., 2014). This is consistent with the assumption that cells are more tolerant of small wounds, whereas larger pores in the membrane must be repaired more quickly for the cell to survive the injury (Jimenez and Perez, 2015), suggestive of different mechanisms being activated depending on pore size. The size of the pores could thus affect the time it takes for the cell membrane to reseal.

Electroporation with nanosecond pulses also degrades the microtubule network structure and dampens lysosome movement (Thompson et al., 2014, 2018). Modulation of microtubule-mediated lysosome transport or even direct damage to lysosomes could affect cell membrane repair and lead to in longer membrane resealing time because lysosomes are involved in key cell membrane repair mechanisms, including membrane patching and endocytosis-mediated pore removal (Draeger et al., 2014; Jimenez and Perez, 2015).

It remains unclear whether lipid peroxidation of cell membrane lipids contributes equally to the observed increased cell membrane permeability after electroporation with different pulse waveforms. Using eight 100 μ s pulses, Michel et al. (2020) observed oxidation of C-11 BODIPY (probe for detection of lipid peroxidation) after electroporation at similar electric field strengths that permeabilized the cell membrane to YO-PRO-1. In contrast, when cells were electroporated with a single 300 ns pulse, higher electric field strengths were required to observe oxidation of C-11 BODIPY than for cell membrane permeabilization. Szlasa et al. (2021) used the Click-iT Lipid Peroxidation Imaging Kit - Alexa Fluor 488 to measure lipid peroxidation in melanotic melanoma A375 cells 36 h after electroporation with eight 100 μ s and eight 10 ms pulses at different electric field strengths. When comparing eight 100 μ s and eight 10 ms pulses at an electric field strength of 200 V/cm, statistically significant higher lipid peroxidation was measured with the former, although application of these two pulse protocols resulted in similar cell membrane permeabilization and cell survival. However, because lipid peroxidation was measured only after 36 h, it could also be a consequence of the oxidative stress induced by electroporation rather than a direct effect of the electric pulses on membrane lipids (Borza et al., 2013).

In our study, the same method as in Szlasa et al. (2021) was chosen to measure lipid peroxidation after electroporation of CHO cells, i.e., the Click-iT Lipid Peroxidation Imaging Kit - Alexa Fluor 488, but our aim was to measure lipid peroxidation earlier after electroporation. We decided to fix the electroporated cells 2 h and 30 min after electroporation – this decision was made on the bases of on preliminary experiments in which fixation of cells was performed between 40 min and 3 h after electroporation to deduce how much time is needed for sufficient signal development in the assay. However, the statistically significant differences were measured only between the unstained cells and all other samples and between the negative control and the cells electroporated with twenty-five 400 ns pulses, and contrary to expectations, the measured signal was lower in the latter. Not even the signal of the positive control was statistically significantly different from the negative control, and, contrary to expectations, the average value of the positive control was even slightly lower than that of the negative control. There was also a large variance between duplicates performed on the same day and also between samples from different days. These results suggest that the Click-iT Lipid Peroxidation Imaging Kit - Alexa Fluor 488 is not a

suitable method for detecting lipid peroxidation of CHO cells at least within the first hours after electroporation. Therefore, we could neither confirm nor refute our second hypothesis that electroporation of cells with membrane-permeabilizing pulses of different parameters causes comparable oxidation of cellular components. Other methods should be tried to assess lipid peroxidation after electroporation, such as mass spectrometry-based shotgun lipidomics (Hu et al., 2017).

3.1.4 Electrochemotherapy with nanosecond pulses

First, cell survival of CHO cells after *in vitro* electrochemotherapy with bleomycin or cisplatin was measured using the metabolic MTS assay 72 hours after treatment (Vižintin et al., 2021). This method is fast and easy to use and allowed us to test many nanosecond pulse protocols using different pulse parameters. We used nanosecond pulses of three different pulse durations (200, 400, or 550 ns) and three different numbers of pulses (1, 25, or 100 pulses) at a pulse repetition rate of 10 Hz and the standard eight 100 μ s pulses at a pulse repetition rate of 1 Hz at the electric field strength previously determined to be optimal for each parameter or, in the case of one 200 pulse, at the highest experimentally achievable electric field strength. For selected pulse protocols (namely, one 200 ns pulse, twenty-five 400 ns pulses, and the eight 100 μ s pulses), cell survival after electrochemotherapy was also measured by the clonogenic assay (Vižintin et al., 2021, 2022). Cell survival after electrochemotherapy with cisplatin was also measured for the B16F1 cell line by the clonogenic assay for the one 200 ns pulse at the highest experimentally achievable electric field strength and for twenty-five 400 ns pulses and the eight 100 μ s pulses at the electric field strength previously determined to be optimal for this cell line (Vižintin et al., 2022). For the one 200 ns pulse and the twenty-five 400 ns pulses, the same electric field strengths were used as for CHO (i.e., 12.6 kV/cm and 3.9 kV/cm, respectively), whereas for the eight 100 μ s pulses, an electric field strength of 1.1 kV/cm was used for CHO, but 0.9 kV/cm for B16F1 cells. Since the increase of intracellular accumulation of the chemotherapeutic agent has been identified as one of the main mechanisms of action of electrochemotherapy, and the mechanisms of action of electrochemotherapy with nanosecond pulses have not yet been explored, we tested, whether the combination of permeabilizing electric pulses (which alone do not decrease cell survival) and cisplatin leads to increased cellular cisplatin accumulation (compared with non-electroporated cells) and whether the amount of cellular cisplatin correlates with cell survival after electrochemotherapy. In addition, the effects of the high-voltage electric pulses on the structure of cisplatin were investigated by nuclear magnetic resonance spectroscopy and high-resolution mass spectrometry.

Electroporation alone (i.e., without bleomycin or cisplatin) did not decrease cell survival. Within the range of bleomycin and cisplatin concentrations tested, a decrease in cell survival

of non-electroporated cells was observed only in CHO cells incubated with 50 μ M cisplatin. The combination of electroporation and bleomycin or cisplatin resulted in a decrease in cell survival of both cell lines for all pulse protocols the tested, with the sole exception of the one 200 ns pulse in B16F1 cells.

The smallest decrease in cell survival was measured with the MTS assay for CHO cells electroporated with one 200 ns pulse at 12.6 kV/cm and bleomycin, and with the clonogenic assay for B16F1 cells electroporated with the same pulse protocol and cisplatin. This is not surprising because this pulse protocol permeabilized the cell membrane of only 85 % of CHO cells and less than 50 % of B16F1 cells, which is suboptimal for electrochemotherapy. More interestingly, however, despite the suboptimal cell membrane permeabilization, one 200 ns pulse was as effective in decreasing cell survival of CHO cells in electrochemotherapy with cisplatin as the twenty-five 400 ns and eight 100 μ s pulses.

In cells subjected to the same treatment (i.e., same pulse protocol and same concentration of bleomycin/cisplatin), considerably lower cell survival was measured by the clonogenic assay than the MTS assay. This is in agreement with Jakštys et al. (2015), who compared the results of various cell viability assays after *in vitro* electrochemotherapy with bleomycin, including the MTT assay, a colorimetric metabolic assay in principle similar to the MTS assay, and the clonogenic assay. In our study, the clonogenic assay measured a decrease in cell survival to about 1 % after CHO cells were exposed to 40 nM bleomycin and eight 100 μ s pulses, 140 nM bleomycin and twenty-five 400 ns pulses, or 50 μ M cisplatin and eight 100 μ s or twenty-five 400 ns pulses, whereas the MTS assay measured the cell survival to be about 30 – 50 % under these conditions. Cell survival measured with the MTS assay also reached a plateau at a certain bleomycin concentration, i.e., with further increasing bleomycin concentration, the measured signal only slightly decreased. In contrast, when cell survival after electrochemotherapy with bleomycin was measured by the clonogenic assay, no such plateau was not observed— cell survival decreased with increasing bleomycin concentration. The different results of the two assays are a consequence of differences in their principles. The MTS assay is based on bioreduction of the tetrazolium salt MTS. It is a simple and rapid colorimetric method for determining the number of viable cells and thus allows screening of many different treatments (Gehl et al., 1998). However, the disadvantage of this assay is its dependence on the metabolic state of the cells, i.e., cells that are metabolically more active produce a stronger signal and vice versa, resulting in discrepancies between the measured signal and the actual number of viable cells. It is known that cells are stressed by electroporation, so their metabolic activity increases after the treatment and influence the results of the test (Forjanic et al., 2019; Dovgan et al., 2021). The clonogenic assay, on the other hand, is based on the assumption that after treatment any remaining viable cell will form a colony after a sufficient time. For cell lines that form colonies, the clonogenic assay

is the best way to determine the number of viable proliferating cells after treatment (Šatkauskas et al., 2017). However, the clonogenic assay is time consuming and therefore rapid screening with the MTS assay is often preferred by researchers. The reason for the discrepancies between the survival measured with the MTS and the clonogenic assay could be that some cells treated with electric pulses and bleomycin or cisplatin are still metabolically active and generate a signal in the MTS assay, but because of the chemotherapeutic-induced reproductive cell death (i.e., loss of replicative capacity) (Tounekti et al., 2001) cannot divide and therefore do not form colonies in the clonogenic assay.

In electrochemotherapy with bleomycin, the nanosecond pulses required the use of higher extracellular concentrations of bleomycin to reduce the survival of CHO cells to the same extent as the eight 100 μ s pulses, but even the highest bleomycin concentration used was still significantly lower than the therapeutic doses used in electrochemotherapy treatments in clinical practice. Among the different nanosecond pulse protocols tested, three protocols (namely, twenty-five 200 ns pulses, twenty-five 400 ns pulses and one hundred 550 ns pulses) decreased cell survival of electroporated CHO cells at lower bleomycin concentrations than other nanosecond pulse protocols tested. For these three pulse protocols also the longest cell membrane resealing time after electroporation was observed. The electroporated cells were diluted 25 min after electroporation. This is more than the longest measured time for cell membrane resealing, allowing sufficient time for bleomycin to penetrate through the permeabilized cell membrane. Because transmembrane transport is an integral of flux (i.e., the number of molecules passing through the membrane per unit time) over time, we can assume that a longer resealing time leads to a higher intracellular accumulation of bleomycin and consequently a greater decrease in cell survival. However, to confirm this assumption, intracellular bleomycin concentration should be measured. Since bleomycin is a medium-sized molecule, our findings could be applied to other applications based on reversible electroporation with nanosecond pulses aimed at introducing medium-sized molecules (e.g., siRNA) into cells.

On the other hand, for electrochemotherapy with cisplatin, there were no differences in measured cell survival between nanosecond and eight 100 μ s pulses at the same cisplatin concentration, again with the sole exception of the one 200 ns pulse in B16F1 cells, which did not decrease the cell survival even at the highest cisplatin concentration tested. The observed differences in measured cell survival after electrochemotherapy with nanosecond pulses between bleomycin and cisplatin could be a consequence of the different molecular size, and mechanisms of action of the two drugs. Bleomycin (about 1500 Da) is larger than cisplatin (about 300 Da). The eight 100 μ s may have created more pores large enough to allow the passage of bleomycin than nanosecond pulses. The type of cell death caused by

bleomycin depends on how many molecules are taken up into the cells. Bleomycin has been reported to arrest cells in the G2-M phase of the cell cycle when cells are electroporated at extracellular bleomycin concentrations in the nanomolar range (the range used in our study). In contrast, when several million bleomycin molecules are internalized, apoptosis-like cell death and DNA fragmentation are observed (Tounekti et al., 1993). The toxic effect of cisplatin is thought to be primarily due to the formation of covalent DNA adducts and the resulting impairment of transcription and/or DNA replication mechanisms (Makovec, 2019).

Total platinum was measured in cell pellets after electrochemotherapy by inductively coupled plasma mass spectrometry, not specifically cisplatin, with the assumption that cisplatin most likely accounted for most of the total platinum measured. This assumption is supported by the fact that the amount of platinum measured in samples to which cisplatin was not added was 2 – 3 orders of magnitude lower than in samples with cisplatin, or was even below the detection limit. A limitation of our study was that we did not know whether the measured platinum was inside the cells or bound to the cell surface, for example. However, the medium in which the experiments were performed has a high concentration of chloride ions, so cisplatin should be stable and the formation of reactive hydrolyzed cisplatin products that would irreversibly bind to phospholipids in the cell membrane is not expected (Speelmans et al., 1996). Thus, the measured platinum most likely originates from within the cells.

In cells exposed to the same pulse protocol and cisplatin concentration, a higher amount of platinum was measured in CHO than in B16F1 cells. As expected, a higher total amount of platinum was measured in electroporated cells compared with non-electroporated cells incubated with the same concentration of cisplatin, except for the one 200 ns pulse in the CHO cell line, which did not cause a statistically significant higher accumulation of platinum. These results suggest that intracellular accumulation of cisplatin is also increased when nanosecond pulses are used for electrochemotherapy. We thus confirmed our third hypothesis that electroporation with nanosecond pulses increases the amount of cellular cisplatin and consequently enhances its cytotoxic effect. There were no statistically significant differences in cell survival and the amount of cellular platinum in cells electroporated with twenty-five 400 ns and eight 100 μ s pulses at the same cisplatin concentration within the same cell line. Interestingly, although a lower amount of platinum was measured in CHO cells electroporated with one 200 ns pulse than with twenty-five 400 ns and eight 100 μ s pulses, the same decrease in cell survival was obtained with all three pulse protocols.

The number of cisplatin molecules per cell was calculated from the measured platinum content and correlated with cell survival after electrochemotherapy for each cell line. Cell

survival was measured to be lower for electroporated CHO cells than for non-electroporated CHO cells at approximately the same number of cisplatin molecules per cell. Similar results have been previously reported in the literature but not discussed (Ursic et al., 2018; Zakelj et al., 2019). This suggests a possible synergistic effect of electroporation and cisplatin, because the observed decrease in cell survival in electrochemotherapy is not just the sum of the decrease in cell survival due to electric pulses and cisplatin alone, but electroporation appears to make cells more susceptible to cisplatin. However, the results of cell survival and the number of cisplatin molecules per cell for B16F1 do not indicate a synergistic effect of electroporation and cisplatin. In B16F1 cells, the number of cisplatin molecules per cell appears to correlate linearly with the logarithm of cell survival. However, there is only one experimental point of the electroporated B16F1 cells (i.e., cells electroporated with one 200 ns pulse at 10 μ M cisplatin) that falls within the range of the number of molecules of the non-electroporated cells. As mentioned earlier, the one 200 ns pulse did not effectively permeabilize nor decrease the cell survival after electrochemotherapy in B16F1 cells. More data (e.g., from non-electroporated cells incubated with higher concentrations of cisplatin for which the measured number of cisplatin molecules per cell would fall within the range of the electroporated cells) would therefore be required to determine whether a lower number of internalized cisplatin molecules is also required in the case of B16F1 cells to decrease cell survival in electroporated cells compared to non-electroporated cells.

There are several ways in which electroporation could affect cell susceptibility to cisplatin. Although formation of DNA adducts and impairment of DNA replication and transcription are thought to be the major mechanism behind the cytotoxic effects of cisplatin, generation of ROS, mitochondrial dysfunction, disruption of intracellular Ca^{2+} homeostasis, and activation of signal transduction pathways also play important roles (Florea and Büsselberg, 2011). An increase in ROS enhances the efficacy of cisplatin and vice versa (Marullo et al., 2013; Kleih et al., 2019). Moreover, an increase in intracellular Ca^{2+} concentration enhances cisplatin-mediated ROS production and increases cisplatin cytotoxicity (Kawai et al., 2006; Al-Taweel et al., 2014; Gualdani et al., 2019). Generation of intracellular ROS (Pakhomova et al., 2012; Szlasa et al., 2021), damage to mitochondria (Batista Napotnik et al., 2012; Nuccitelli et al., 2020), and disruption of calcium homeostasis by entry of Ca^{2+} from the extracellular space or from intracellular stores (Frandsen et al., 2012; Semenov et al., 2013) are also known effects of electroporation on cells. In addition, electroporation has been reported to induce DNA damage (Meaking et al., 1995; Stacey et al., 2003; Zou et al., 2013) and increase the amount of cisplatin bound to DNA (Cemažar et al., 1999; Ursic et al., 2018); after electroporation with nanosecond pulses, nuclear envelope disintegration has also been reported, which may facilitate cisplatin access to the DNA (Chen et al., 2004; Stacey et al., 2011; Ren et al., 2013). Density functional theory calculations indicated that electric pulses could alter the structure of cisplatin and thus enhance its anticancer properties (Zhang et al.,

2020). However, it remains to be determined whether there is an interplay between the aforementioned effects of electroporation and cisplatin that could be responsible for the enhanced cytotoxicity of cisplatin in electroporated cells. One study points to the importance of the increase in ROS after electrochemotherapy – Michel et al. (2018) observed an increase in of the mitochondrial enzyme superoxide dismutase 2 (SOD2), which clears ROS in cells subjected to electrochemotherapy with cisplatin.

Among the mentioned possible effects of electroporation that could increase the cytotoxicity of cisplatin, only the influence of the high-voltage electric pulses on the structure of cisplatin was investigated in our study. Spectra of cisplatin in deuterium oxide, 90% water and 10% deuterium oxide solution, solution of deuterium oxide with 154 mM NaCl (corresponding to saline) and 90% water and 10% deuterium oxide solution with 154 mM NaCl were recorded by ^1H nuclear magnetic resonance spectroscopy. Weak broadened peaks for hydrogen atoms of amino ligands (NH_3) were found at approximately 4.08 ppm in spectra and no new peaks appeared in other regions of the spectra of cisplatin that was or was not exposed to high-voltage twenty-five 400 ns pulses or eight 100 μs pulses. The only major difference was observed in the spectrum of cisplatin recorded in deuterium oxide with 154 mM NaCl after treatment with eight 100 μs pulses, where the broad peak for hydrogens of cisplatin disappeared, probably due to the fast hydrogen-deuterium exchange of deuterium with hydrogen atoms of NH_3 ligands (Chen et al., 1999). However, when spectra of cisplatin were recorded in 90% water and 10% deuterium oxide solution containing 154 mM NaCl (to minimize the intensity of water signal to obtain a stronger signal of the NH_3 ligand), no such disappearance of the peak was observed. With high-resolution mass spectrometry, similar fragments have been observed in cisplatin in water or saline that was or was not exposed to high-voltage electric pulses. Overall, nuclear magnetic resonance spectroscopy and high-resolution mass spectrometry showed that the structure of cisplatin remains comparable after the application of electric pulses to its saline or water solution under the conditions used in our experiments. Saline and water represented a simplified extracellular and intracellular environment, respectively, because it was not possible to record spectra of cisplatin in the growth medium DMEM in which the cell experiments were performed due to the presence of many species that interfere with the signals of cisplatin. Other limitations of the study were that, because of the limitations of the pulse generator used in this series of experiments, the twenty-five 400 ns pulses were delivered at lower amplitudes than in the cell experiments and that, because of the low conductivity of the load, the electric pulses delivered to water had a significantly different shape than those delivered to saline or cells in growth medium DMEM; they resembled an exponentially decaying rather than a rectangular pulse shape. Nevertheless, we concluded that the observed increased susceptibility of electroporated CHO cells to cisplatin was more probably a consequence of the effect of electroporation on the cells rather than structural changes in cisplatin caused by high-voltage electric pulses.

Overall, our results show that nanosecond pulses with properly chosen parameters are suitable for use in electrochemotherapy. The use of equiefficient nanosecond pulses results in the same decrease in cell survival and the same accumulation of cisplatin in the cells as with the standard eight 100 μ s pulses. We showed that electroporation with nanosecond pulses increases the amount of cellular cisplatin and consequently enhances its cytotoxic effect. However, the results in CHO cells suggest that other mechanisms besides the increased intracellular accumulation of cisplatin are involved in the cell death induced by electrochemotherapy with nanosecond pulses. The high-voltage electric pulses did not alter the structure of cisplatin under the conditions tested.

3.2 CONCLUSIONS

In this *in vitro* study, we compared the eight 100 μ s monophasic pulses standardly used in electroporation-based applications with nanosecond and H-FIRE pulses, which have some potential advantages over the standard pulses. After determining equiefficient pulses, the different pulse waveforms were compared on several levels that are important for electroporation-based applications: Extent of electrochemical reactions, time required for cell membrane resealing after electroporation, decrease of cell survival, and intracellular accumulation of chemotherapeutic agent after electrochemotherapy.

The main conclusions from our work can be summarized as follows:

1. We have shown in four different cell lines that the efficiency of H-FIRE pulses in decreasing cell survival can be improved by extending the interphase and interpulse delay of H-FIRE pulses while maintaining the same pulse amplitude and duration of positive and negative phase. However, only one H-FIRE pulse protocol with the longest interphase and interpulse delay tested decreased cell survival as effectively as the standard eight 100 μ s pulses in two cell lines.
2. To achieve high (i.e., > 99 %) cell membrane permeabilization with nanosecond pulses, higher electric field strengths were required than for the eight 100 μ s pulses. For the nanosecond pulse protocols with the same number of pulses, higher electric field strengths were required for shorter pulse durations to achieve high membrane permeabilization. When comparing nanosecond pulses of the same duration, lower electric field strengths were required to achieve high membrane permeabilization when a greater number of pulses were used.
3. The amount of metal ions released from the electrodes varied greatly between the aluminum, stainless steel and platinum electrodes – the absolute highest amount of released metal ions was measured for the aluminum electrodes and the lowest for the platinum electrodes.

4. All H-FIRE pulses tested caused significantly lower metal release from aluminum and stainless steel electrodes compared to the eight 100 μ s pulses with the same pulse amplitude. However, for platinum electrodes, a statistically non-significantly lower concentration of released platinum ions was measured for some H-FIRE pulse protocols than for the eight 100 μ s pulses. Different durations of interphase and interpulse delays in the H-FIRE pulse protocol resulted in significant differences in the concentration of released metals from aluminum and stainless steel electrodes. However, more platinum ions were measured after application of H-FIRE pulses with 1 μ s interphase delay and various other durations of interpulse delay than H-FIRE pulses with interphase and interpulse delays of the same duration.
5. A significantly lower concentration of released aluminum ions was measured when one of the nanosecond pulse protocols was delivered to the electroporation cuvettes compared with the eight 100 μ s pulses. However, the metal release does not appear to depend solely on the pulse duration, nor does the amount of metal ions released appear to correlate well with the energy delivered to the cuvette.
6. We proved the hypothesis that equiefficient H-FIRE or nanosecond pulses reduce electrochemical reactions compared to the standard eight 100 μ s pulses.
7. After electroporation with some of the nanosecond pulse protocols, the cell membrane required a significantly longer time to reseal than after electroporation with the eight 100 μ s pulses.
8. The Click-iT Lipid Peroxidation Imaging Kit - Alexa Fluor 488 is not a suitable method for detecting lipid peroxidation of CHO cells in the first hours after electroporation. Therefore, we could neither confirm nor refute the hypothesis that electroporation of cells with membrane-permeabilizing pulses of different parameters causes comparable oxidation of cell components.
9. The use of equiefficient nanosecond pulses achieves the same decrease in cell survival and the same cisplatin accumulation in cells as with the standard eight 100 μ s pulses.
10. In electrochemotherapy with bleomycin, the nanosecond pulses required the use of higher extracellular concentrations of bleomycin to reduce survival of CHO cells to the same extent as the eight 100 μ s pulses. In electrochemotherapy with cisplatin, there were no differences in measured cell survival between nanosecond and eight 100 μ s pulses at the same cisplatin concentration, with the sole exception of the one 200 ns pulse in B16F1 cells.
11. A higher total amount of platinum was measured in electroporated cells compared with non-electroporated cells incubated with the same cisplatin concentration, with the exception of the one 200 ns pulse in the CHO cell line, confirming the hypothesis that intracellular accumulation of the chemotherapeutic drug caused by electroporation enhances its cytotoxicity.

12. A lower number of internalized cisplatin molecules per cell was required to decrease the cell survival of electroporated CHO cells to the same extent as non-electroporated CHO cells.
13. The structure of cisplatin remains comparable after the application of high-voltage electric pulses to its water or saline solution under the conditions tested.

4 SUMMARY (POVZETEK)

4.1 SUMMARY

Electroporation is the phenomenon of increased cell membrane permeabilization due to exposure of cells/tissues to short high-voltage electric pulses which allows transmembrane transport of otherwise impermeant molecules. Formation of pores in the lipid part of the membrane, chemical changes in membrane lipids and modulation of protein structure and function are all generally recognized as underlying mechanisms of this transient increase in membrane permeability observed during electroporation.

The efficacy of electroporation depends on several biophysical parameters: cell parameters defining cell geometry (cell shape and size) and their environment (osmotic pressure, temperature, conductivity of the medium, ...), and electric field parameters (pulse shape, electric field strength and direction, pulse/phase duration, interphase and interpulse delay, number of pulses/bursts, pulse/burst repetition frequency, ...). In most cases, the efficacy of electroporation can be controlled only by the parameters of the electric field and by the geometry and placement of the electrodes. Similar electroporation outcomes can be obtained using pulses of different parameters, i.e., equiefficient pulses. For example, using multiple shorter pulses at higher electric field strengths gives the same outcome as measured after electroporation with a longer pulse at a lower electric field strength.

The pulses used in electroporation have a wide range of parameters. Nanosecond and recently also high-frequency biphasic pulses with a pulse duration of only a few microseconds have attracted a great deal of research interest because they mitigate several limitations that exist in conventional micro-millisecond range electroporation. Nanosecond pulses have more profound effects on organelles than longer pulses of micro- and millisecond duration, minimize the possibility of thermal damage, can induce apoptosis and antitumor activity and their excitation thresholds appear to be higher than the electroporation thresholds implying that their use could reduce pulse-induced neuromuscular stimulation, which is an undesirable side effect in medical electroporation-based applications. High-frequency biphasic pulses with pulse durations in the range of a few microseconds, known by the acronym H-FIRE, have shown reduced muscle contractions and also appear to limit the likelihood of interference with cardiac rhythm.

The electric field in electroporation procedures is established by delivering electric pulses through electrodes in contact with the medium/tissue. Electrodes for electroporation procedures are most often made of metal. When high-voltage electric pulses are delivered to cells in suspension, tissue or other medium, electrochemical reactions occur at the electrode-electrolyte interface. These electrochemical reactions lead to electrolysis of water, corrosion

and fouling of the electrodes, generation of radicals, changes of pH, chemical changes in the treated product, evolution of gas bubbles and release of metal ions from the electrodes. The metal ions released from the electrodes during electroporation have various effects on the treated cells and products: they can precipitate nucleic acids and proteins in solutions, affect the taste of the treated food and affect the viability of the cells, to mention only few.

Electroporation is used in various applications including cell transfection/transformation, extraction of biomolecules and juices, inactivation of microorganisms, biomass drying, cryopreservation, cell fusion, tissue ablation and electrochemotherapy. Electrochemotherapy is a local treatment of cancer that combines the use of membrane-permeabilizing high-voltage electric pulses delivered to the tumor with some standard chemotherapeutic agents with high intrinsic cytotoxicity for which the plasma membrane is a barrier to reach their intracellular target. The electric pulses are according to standard operating procedures delivered in trains of eight monophasic pulses of 100 μ s duration with 1 Hz or 5 kHz pulse repetition rate. The two most commonly used chemotherapeutic agents in electrochemotherapy are bleomycin and *cis*-diamminedichloroplatinum (II) (cisplatin). Several mechanisms of action have been identified; the dominant one is believed to be the increased intracellular accumulation of the chemotherapeutic agent due to increased permeability of the cell membrane caused by electroporation.

Numerous studies have demonstrated the efficacy, tolerability, and high patient satisfaction with electrochemotherapy. However, some side effects have also been reported - the most commonly reported are muscle contractions and unpleasant sensations (which can even be painful), mainly attributed the stimulation of peripheral nerves by the electric pulses. To overcome this limitation, new pulse protocols are being explored in electrochemotherapy, including nanosecond pulses. Reports on the use of nanosecond pulses in electrochemotherapy are promising: a decrease of cell survival has been observed *in vitro* and tumor regression *in vivo*. However, from the previous studies it is not clear if nanosecond pulses can be as effective as with the standard eight 100 μ s pulses in electrochemotherapy and they did not explore the underlying mechanisms of action in electrochemotherapy with nanosecond pulses.

This study was designed as a comprehensive *in vitro* research with the general aim of comparing the standard eight 100 μ s pulses with recently introduced pulse waveforms, namely nanosecond and short high-frequency biphasic (H-FIRE) pulses.

The following hypotheses were tested in the study:

1. The application of monophasic nanosecond pulses or high-frequency biphasic electric pulses with a few microseconds pulse duration in electroporation-based technologies reduces electrochemical reactions, but cell membrane electroporation

at equiefficient pulse parameters is equivalent to the classical eight 100 μ s electric pulses.

2. Electroporation of cells with pulses of different parameters that permeabilize the cell membrane causes comparable oxidation of cellular components.
3. The combination of electroporation with nanosecond pulses and an anticancer active ingredient enhances its effect due to increased intracellular accumulation of the active ingredient.

In our study, we first measured cell membrane permeabilization and cell survival of different cell lines after electroporation to empirically determine the pulse parameters of high-frequency biphasic (H-FIRE) and nanosecond pulses that are equiefficient to the standard eight 100 μ s pulses with 1 Hz repetition rate. For H-FIRE pulses, we delivered a burst of 400 biphasic rectangular pulses. One pulse was defined as consisting of the positive phase, the interphase delay, and the negative phase. The duration of the positive phase was 1 μ s and the duration of the negative phase was 1 μ s for all H-FIRE pulses, while the duration of the interphase delay (i.e., the delay between the positive phase and the negative phase) and the interpulse delay (i.e., the delay between pairs of biphasic pulses) were varied from 0.5 to 10,000 μ s. All H-FIRE pulse protocols and the eight 100 μ s pulses had the same amplitude – to be able to determine the effects of delay, we chose an amplitude at which the differences between the different pulse protocols were most pronounced. For membrane permeabilization (measured by uptake of propidium iodide), an amplitude of 300 V (corresponding to an electric field strength of 1.5 kV/cm) was chosen. For cell survival, measured by metabolic MTS assay, a pulse amplitude of 500 V (resulting in an electric field strength of 2.5 kV/cm) was chosen. Four different cell lines were tested: Chinese hamster ovary CHO-K1, rat cardiac myoblast H9c2, mouse myoblast C2C12, and mouse neuronal cell line HT22. To elucidate nanosecond pulse protocols which are equiefficient to eight 100 μ s pulses, cell membrane permeabilization (defined as the percentage of YO-PRO-1-stained cells) and cell survival (determined by the metabolic MTS assay) of CHO and mouse melanoma B16F1 cells were measured after electroporation with the standard 100 μ s pulses lines at a pulse repetition rate of 1 Hz and nanosecond pulse protocols with different pulse parameters at different electric field strengths. Nanosecond pulses with three different pulse durations (200, 400, or 550 ns), three different numbers of pulses (1, 25, or 100 pulses), and one pulse repetition rate (10 Hz) were studied on CHO cells, while only selected nanosecond pulse protocols (namely one 200 pulse and twenty-five 400 ns pulses at a pulse repetition rate of 10 Hz) were tested on B16F1 cells. From the survival-permeabilization curves, the electric field strength that caused the highest cell membrane permeabilization without decreasing cell survival was selected for each pulse protocol. These conditions (i.e., high cell survival and high cell membrane permeabilization) were selected because they were

optimal for electrochemotherapy and the pulse protocols were next to be tested in *in vitro* electrochemotherapy experiments.

For H-FIRE pulses, we have shown in all four cell lines tested that by extending the interphase and interpulse delay, lower cell survival can be achieved while maintaining the same pulse amplitude and duration of positive and negative phase. Our results indicate that the efficiency of H-FIRE pulses could be improved by extending the delays instead of increasing the pulse amplitude. However, only the H-FIRE pulse protocol with an interphase and interpulse delay of 10,000 μ s decreased the cell survival as effectively as the standard eight 100 μ s pulses for the CHO and HT22 cell lines. The duration of the interphase and interpulse delay had a more complex effect on membrane permeabilization, but all the H-FIRE pulse protocols tested were less effective than the standard eight 100 μ s pulses in terms of cell membrane permeabilization in all four tested cell lines tested.

As expected, higher electric field strengths were required to achieve as high (i.e., > 99 %) cell membrane permeabilization with nanosecond pulses than the eight 100 μ s pulses. Among nanosecond pulse protocols with the same number of pulses, shorter duration pulses required higher electric field strengths to achieve high membrane permeabilization. When comparing nanosecond pulses of the same duration, lower electric field strengths were required to achieve high membrane permeabilization when a larger number of pulses was used. For CHO cells, all pulse protocols tested permeabilized more than 99 % of the cells at the selected optimal electric field strength, with the exception of one 200 ns pulse which permeabilized around 85 % of the cell population at the highest electric field strength within the safe operating range of the pulse generator used. In the case of the B16F1 cell line, cell membrane permeabilization of less than 99 % was achieved with one nanosecond pulse of 200, 400 and also 550 ns pulse duration at the highest electric field strength, suggesting that higher electric field strengths are required for permeabilization of B16F1 cells compared to CHO cells when only one nanosecond pulse is used. This is contrary to what was observed with the eight 100 μ s pulses – lower electric field strength was required for these pulses to permeabilize B16F1 cells than CHO cells.

Our study was the first to report metal release from electrodes after application of H-FIRE and nanosecond pulses. The concentration of metal ions in saline was measured by inductively coupled plasma mass spectrometry after delivery of H-FIRE pulses (as in the cell experiments) and the standard eight 100 μ s pulses of the same amplitude to wire electrodes of aluminum, stainless steel and platinum. Nanosecond pulses protocols and the standard eight 100 μ s pulses with electric field strengths determined to be optimal for electrochemotherapy of CHO cells were delivered to electroporation cuvettes (with electrodes made of an aluminum alloy) filled with saline.

The amount of metal ions released from the electrodes varied greatly between the three electrode materials tested – the absolute highest amount of released metal ions was measured for aluminum electrodes and the lowest for platinum electrodes. All of the H-FIRE pulses tested caused significantly less metal release from aluminum and stainless steel electrodes compared to the eight 100 μ s pulses with the same pulse amplitude. However, in the case of platinum electrodes, not statistically significant lower concentration of released platinum ions was measured for some H-FIRE pulse protocols than for the eight 100 μ s pulses. With the exception of platinum, it could be concluded that it is possible to extend the delays in the H-FIRE pulses to achieve an equivalent biological effect as with the standard eight 100 μ s pulses with still lowering the metal release from the electrodes. H-FIRE pulses appear to be superior to the standard eight 100 μ s in terms of limiting electrochemical reactions. Different interphase and interpulse delays in the H-FIRE pulse protocol resulted in significant differences in the concentration of released metals from aluminum and stainless steel electrodes.

A significantly lower concentration of released aluminum ions was measured with any of the nanosecond pulse protocols delivered to the electroporation cuvettes compared to the eight 100 μ s pulses. We demonstrated that shortening the pulse duration to a few hundred nanosecond pulses reduced the amount of metal released from the electrodes, even when the voltage and number of pulses were increased to achieve a comparable biological effect as with longer duration pulses. Because metal release from electrodes is a subgroup of the electrochemical reactions at the electrode-electrolyte interface, this argues for the use of nanosecond pulses over microsecond pulses if the electrochemical reactions are to be kept to a minimum. However, the metal release does not seem to depend only on the pulse duration or the amount of energy delivered to the cuvette (estimated by multiplying the pulse duration and the number of pulses by the measured amplitude of the voltage and the measured amplitude of the electric current). Comparison of individual nanosecond pulses with the same set amplitude and different pulse durations (200, 400 and 500 ns) shows that, contrary to expectations, the highest concentration of aluminum ions was measured after delivery of the shortest (i.e. 200 ns) pulse.

Chemical changes in membrane lipids, especially lipid peroxidation, could explain the longer-lasting (compared to the pulse duration) increased permeability of cell membranes after electroporation. In our study, cell membrane resealing in lipid peroxidation after electroporation was measured to compare the time needed for cell membrane resealing with the extent of lipid peroxidation and to determine if different pulse waveforms that permeabilize the cell membrane to the same degree also result in a comparable extent of lipid peroxidation of cell membrane lipids. Cell membrane resealing was measured for

different nanosecond pulse protocols and the eight 100 μ s pulses at the electric field strength determined to be optimal for electrochemotherapy in survival and permeabilization experiments by adding YO-PRO-1 to CHO cells every 2 min from 2 to 26 min after electroporation and measuring the percentage of YO-PRO-1-fluorescent cells (Vižintin et al., 2021). The Click-iT Lipid Peroxidation Imaging Kit - Alexa Fluor 488 was used to measure lipid peroxidation in CHO cells electroporated with twenty-five 400 ns pulses or eight 100 μ s pulses at the electric field strength determined to be optimal for electrochemotherapy.

The cell membrane resealed in less than 5 min after the application of eight 100 μ s pulses. For some of the nanosecond pulse protocols, the time required for resealing of the cell membrane was not significantly longer, but for the twenty-five 200 ns, twenty-five 400 ns, twenty-five 550 ns, one hundred 550 ns pulses and one 400 ns and one 550 ns pulse, the membrane required a significantly longer time (more than 10 min) for resealing. For lipid peroxidation, statistically significant differences were measured only between the unstained cells and all other samples and between the negative control and cells electroporated with twenty-five 400 ns pulses, and contrary to expectations, the measured signal was lower for the later. There was also a large variance between duplicates performed on the same day and also between samples from different days. These results suggest that the Click-iT Lipid Peroxidation Imaging Kit - Alexa Fluor 488 is not a suitable method for detecting lipid peroxidation of CHO cells, at least in the first hours after electroporation. Therefore, we could neither confirm nor refute the hypothesis that electroporation of cells with membrane-permeabilizing pulses of different parameters causes comparable oxidation of cellular components.

To evaluate nanosecond pulses for use in electrochemotherapy, many nanosecond pulse protocols with different pulse parameters and the standard eight 100 μ s pulses were screened by measuring survival of CHO cells after *in vitro* electrochemotherapy with bleomycin or cisplatin was measured using the metabolic MTS assay 72 hours after treatment. We used nanosecond pulses with three different pulse durations (200, 400, or 550 ns) and three different numbers of pulses (1, 25, or 100 pulses) at a pulse repetition rate of 10 Hz. at the electric field strength previously determined to be optimal for each parameter or, in the case of one 200 pulse, at the highest experimentally achievable electric field strength. For selected pulse protocols (namely, one 200 ns pulse, twenty-five 400 ns pulses, and the eight 100 μ s pulses), cell survival after *in vitro* electrochemotherapy was also measured by the clonogenic assay. Cell survival after *in vitro* electrochemotherapy with cisplatin was also measured for the B16F1 cell line by the clonogenic assay for the one 200 ns pulse at the highest experimentally achievable electric field strength and for twenty-five 400 ns pulses and the eight 100 μ s pulses at the electric field strength previously determined to be optimal for this

cell line. Since the increase of intracellular accumulation of the chemotherapeutic agent has been identified as one of the main mechanisms of action of electrochemotherapy, and the mechanisms of action of electrochemotherapy with nanosecond pulses have not yet been explored, we tested in this study, whether the combination of permeabilizing electric pulses (which alone do not decrease cell survival) and cisplatin leads to increased cellular cisplatin accumulation (compared with non-electroporated cells) and whether the amount of cellular cisplatin correlates with cell survival after electrochemotherapy. In addition, the effects of the high-voltage electric pulses on the structure of cisplatin were investigated by nuclear magnetic resonance spectroscopy and high-resolution mass spectrometry.

Electroporation alone (i.e., without bleomycin or cisplatin) did not decrease cell survival. Within the range of bleomycin and cisplatin concentrations tested, a decrease in cell survival of non-electroporated cells was observed only in CHO cells incubated with 50 μM cisplatin. The combination of electroporation and bleomycin or cisplatin resulted in a decrease in cell survival of both cell lines for all pulse protocols the tested, with the sole exception of the one 200 ns pulse in B16F1 cells.

The smallest decrease in cell survival was measured with the MTS assay for CHO cells electroporated with one 200 ns pulse at 12.6 kV/cm and bleomycin, and with the clonogenic assay for B16F1 cells electroporated with the same pulse protocol and cisplatin. This is not surprising because this pulse protocol permeabilized the cell membrane of only 85 % of CHO cells and less than 50 % of B16F1 cells, which is suboptimal for electrochemotherapy. More interestingly, however, despite the suboptimal cell membrane permeabilization, one 200 ns pulse was as effective in decreasing cell survival of CHO cells in electrochemotherapy with cisplatin as the twenty-five 400 ns and eight 100 μs pulses.

In cells subjected to the same treatment (i.e., same pulse protocol and same concentration of bleomycin/cisplatin), the clonogenic assay measured lower cell survival than the MTS assay. Cell survival measured with the MTS assay also reached a plateau at a certain bleomycin concentration, i.e., with further increasing bleomycin concentration, the measured signal only slightly decreased. In contrast, when cell survival after electrochemotherapy with bleomycin was measured by the clonogenic assay, no such plateau was observed— cell survival decreased with increasing bleomycin concentration. The different results of the two assays are a consequence of differences in their underlying detection mechanisms.

In electrochemotherapy with bleomycin, the nanosecond pulses required the use of higher extracellular concentrations of bleomycin to reduce the survival of CHO cells to the same extent as the eight 100 μs pulses, but even the highest bleomycin concentration used was still significantly lower than the therapeutic doses used in electrochemotherapy treatments in

clinical practice. Among the different nanosecond pulse protocols tested, three protocols (namely, twenty-five 200 ns pulses, twenty-five 400 ns pulses and one hundred 550 ns pulses) decreased cell survival of electroporated CHO cells at lower bleomycin concentrations than other nanosecond pulse protocols tested. For these three pulse protocols also the longest cell membrane resealing time after electroporation was observed. Since bleomycin is a medium-sized molecule, our findings could be applied to other applications based on reversible electroporation with nanosecond pulses aimed at introducing medium-sized molecules (e.g., siRNA) into cells.

On the other hand, for electrochemotherapy with cisplatin, there were no differences in measured cell survival between nanosecond and eight 100 μ s pulses at the same cisplatin concentration, again with the sole exception of the one 200 ns pulse in B16F1 cells, which did not decrease the cell survival even at the highest cisplatin concentration tested. The observed differences in measured cell survival after electrochemotherapy with nanosecond pulses between bleomycin and cisplatin could be a consequence of the different molecular size and mechanisms of action of the two drugs.

Total platinum was measured in cell pellets after electrochemotherapy by inductively coupled plasma mass spectrometry, with the assumption that cisplatin most likely accounted for most of the total platinum measured. This assumption is supported by the fact that the amount of platinum measured in samples to which cisplatin was not added was 2 – 3 orders of magnitude lower than in samples with cisplatin, or was even below the detection limit. In cells exposed to the same pulse protocol and cisplatin concentration, a higher amount of platinum was measured in CHO than in B16F1 cells. As expected, a higher total amount of platinum was measured in electroporated cells compared with non-electroporated cells incubated with the same concentration of cisplatin, except for the one 200 ns pulse in the CHO cell line. These results suggest that intracellular accumulation of cisplatin is also increased when nanosecond pulses are used for electrochemotherapy. There were no statistically significant differences in cell survival and the amount of cellular platinum in cells electroporated with twenty-five 400 ns and eight 100 μ s pulses at the same cisplatin concentration within the same cell line. Interestingly, although a lower amount of platinum was measured in CHO cells electroporated with one 200 ns pulse than with twenty-five 400 ns and eight 100 μ s pulses, the same decrease in cell survival was obtained with all three pulse protocols.

The number of cisplatin molecules per cell was calculated from the measured platinum content and correlated with cell survival after electrochemotherapy for each cell line. Cell survival was measured to be lower for electroporated CHO cells than for non-electroporated CHO cells at approximately the same number of cisplatin molecules per cell. This suggests

a possible synergistic effect of electroporation and cisplatin in addition to the increased cisplatin uptake due to pulse-induced membrane permeabilization. However, in B16F1 cells, the number of cisplatin molecules per cell appears to correlate linearly with the logarithm of cell survival – electroporation causes an increase in cisplatin uptake, but the results of cell survival and the number of cisplatin molecules per cell for B16F1 do not indicate a synergistic effect of electroporation and cisplatin. However, there is only one experimental point of the electroporated B16F1 cells that falls within the range of the number of molecules of the non-electroporated cells. More data would therefore be required to determine whether a lower number of internalized cisplatin molecules is also required in the case of B16F1 cells to decrease cell survival in electroporated cells compared to non-electroporated cells.

Electroporation could affect the susceptibility of cells to cisplatin in several ways, e.g. by generation of ROS, disruption of intracellular Ca^{2+} homeostasis or by improving the anticancer properties of cisplatin by modifying the structure of the molecule. Of the possible effects of electroporation on the increase of cytotoxicity of cisplatin, only the impact of the high-voltage electric pulses on the structure of cisplatin was investigated in our study. Nuclear magnetic resonance spectroscopy and high-resolution mass spectrometry revealed that the structure of cisplatin remains comparable after the application of electric pulses in either saline or water under the conditions used in our experiments.

Overall, our results demonstrate that nanosecond pulses with properly selected parameters are suitable for use in electrochemotherapy. The use of equiefficient nanosecond pulses results in the same cisplatin decrease in cell survival and the same accumulation of cisplatin in the cells as with the standard eight 100 μs pulses. We thus confirmed the hypothesis that electroporation with nanosecond pulses increases the amount of cellular cisplatin and consequently enhances its cytotoxic effect. However, the results in CHO cells suggest that other mechanisms beside the increased intracellular accumulation of cisplatin are involved in the cell death induced by electrochemotherapy with nanosecond pulses.

To summarize, we confirmed our first hypothesis that H-FIRE and nanosecond pulses limit electrochemical reactions also when the pulse parameters are adjusted to achieve the same biological effect as with longer monophasic pulses. We could neither confirm nor refute our second hypothesis that electroporation of cells with membrane-permeabilizing pulses of different parameters causes comparable oxidation of cellular components because the Click-iT Lipid Peroxidation Imaging Kit - Alexa Fluor 488 proved to not be a suitable method for detecting lipid peroxidation within the first hours after electroporation. We confirmed our third hypothesis that electroporation with nanosecond pulses increases the amount of the chemotherapeutic agent inside cell and consequently enhances its cytotoxic effect.

4.2 POVZETEK

Elektroporacija je pojav povečanja prepustnosti celične membrane zaradi izpostavitve celice/telesa električnemu polju, kar omogoči transport molekul preko membrane, tudi tistih za katere je celična membrana običajno neprepustna. Splošno sprejeta razlaga pojava elektroporacije temelji na nastanku vodnih por v lipidnem dvosloju kot glavnemu mehanizmu. Vendar se v simulacijah molekularne dinamike vodne pore zaprejo v nekaj deset do nekaj sto nanosekundah po prenehanju delovanja zunanega električnega polja, v poskusih pa je povečana prepustnost celične membrane opažena še nekaj minut in celo ur po tem, ko električno polje ni več prisotno. Vse več dokazov kaže na pomembno vlogo oksidacije membranskih lipidov in modulacijo strukture in funkcije proteinov zaradi vpliva električnih pulzov pri elektroporaciji.

Elektroporacija povzroči vdor Ca^{2+} v citoplazmo iz zunajceličnega prostora in iz notranjih zalog, odtekanje ATP in K^+ iz celice, depolarizacijo, osmotsko neravnovesje in nabrekanje celice, sproščanje s poškodbami povezanih molekularnih vzorcev (angl. damage-associated molecular pattern, DAMP), aktivacijo različnih signalnih poti, spremembe v izražanju genov in sintezi proteinov, aktivacijo različnih popravljenih mehanizmov in lahko vodi v celično smrt. Vse spremembe v celici in celični membrani kot tudi vse poznejše procese, povezane z elektroporacijo, ki so aktivni tudi, ko povečane prepustnosti celične membrane ni več opaziti, imenujemo elektropermeom.

V študijah *in vitro* je učinkovitost elektroporacije običajno izražena bodisi z odstotkom elektroporiranih celic, s privzemom določene molekule v elektroporirane celice ali s preživetjem celic. Na učinkovitost elektroporacije vpliva več biofizikalnih parametrov: geometrija celice (oblika in velikost celice), okoljski parametri (osmotski tlak, temperatura, prevodnost medija, ...) in parametri električnega polja (oblika pulza, električna poljska jakost in smer, čas trajanja pulza/faze, pavza med pulzi, število pulzov, ponavljalna frekvenca, ...). V večini primerov lahko na učinkovitost elektroporacije vplivamo le s parametri električnega polja ter z geometrijo in postavitvijo elektrod. Podobne rezultate elektroporacije je mogoče doseči z uporabo pulzov različnih parametrov, t.i. enako učinkovitimi pulzi. Na primer, z uporabo več krajših pulzov pri višji električni poljski jakosti lahko dosežemo enak rezultat kot z enim daljšim pulzom pri nižji električni poljski jakosti. Vendar iskanje kombinacije pulznih parametrov, ki vodijo v enako učinkovite pulze, ni enostavno – zanašanje na preproste povezave med pulznimi parametri, kot je npr. uporaba pulzov z enako energijo ali skupnim časom trajanja, se je izkazalo za neustrezno.

Pulzi, ki se uporabljajo pri elektroporaciji, imajo širok razpon parametrov. V zadnjem času so nanosekundni in visokofrekvenčni bipolarni pulzi s časom trajanja pulza le nekaj

mikrosekund pritegnili veliko raziskovalnega zanimanja, ker omogočajo premostitev določenih omejitev, ki se pojavljajo pri običajni elektroporaciji s pulzi s časi trajanja v območju mikro- in milisekund. Vpliv nanosekundnih pulzov prodre globlje v celično notranjost, saj imajo za razliko od mikro- in milisekundnih pulzov neposredne učinke tudi na organele, ne le na celično membrano. Poleg tega so prednosti nanosekundnih pulzov tudi zmanjšanje možnosti pojava toplotnih poškodb, zmožnost sprožitve apoptoze in protitumorska aktivnost, njihovi pragovi vzbujanja nevronov pa naj bi bili višji od pragov elektroporacije, kar pomeni, da njihova uporaba lahko zmanjša živčno-mišično vzdraženje, ki je neželen stranski učinek na elektroporaciji temelječih medicinskih aplikacij. Za visokofrekvenčne bipolarne pulze s trajanjem pulza v območju nekaj mikrosekund, znanimi pod akronimom H-FIRE, pa so pokazali, da zmanjšujejo mišično krčenje ter verjetno tudi zmanjšujejo verjetnost pojava motenj v delovanju srca ob dovajanju pulzov.

Električno polje se pri postopkih elektroporacije vzpostavi z dovajanjem električnih pulzov prek elektrod, ki so v stiku z medijem/tkivom. Elektrode so najpogosteje kovinske. Ob dovajanju visokonapetostnih električnih pulzov pa prihaja do elektrokemijskih reakcij na stiku elektrode in elektrolita. Te elektrokemijske reakcije med drugim vodijo do elektrolize vode in nastajanja plinskih mehurčkov, korozije elektrod, nastanka radikalov, sprememb pH in sproščanja kovinskih ionov z elektrod. Kovinski ioni, ki se sproščajo z elektrod med elektroporacijo, lahko med drugim oborijo nukleinske kisline in proteine v raztopinah, spremenijo okus hrane in vplivajo na preživetje celic. Eksperimenti nakazujejo, da je mogoče zmanjšati elektrokemijske reakcije z uporabo pulzov s krajšim časom trajanja in/ali bipolarnih pulzov.

Elektroporacija se uporablja na številnih področjih vključno s transfekcijo celic in transformacijo bakterij, ekstrakcijo biomolekul in sokov, inaktivacijo mikroorganizmov, sušenjem biomase, krioprezervacijo, fuzijo celic, ablacijo tkiv in elektrokemoterapijo. Elektrokemoterapija je lokalno zdravljenje raka, ki združuje uporabo visokonapetostnih električnih pulzov, ki začasno povečajo prepustnost celične membrane, s standardnim kemoterapevtikom z visoko intrinzično citotoksičnostjo, za katerega celična membrana sicer predstavlja oviro za vstop v celice. Električni pulzi se običajno dovajajo v nizu osmih monopolarnih pulzov s časom trajanja 100 μ s in s ponavljalno frekvenco 1 Hz ali 5 kHz. Dva najpogostejša kemoterapevtika v elektrokemoterapiji sta bleomicin in cisplatin. Prepoznanih je bilo več mehanizmov delovanja elektrokemoterapije, prevladujoči pa je povečano znotrajcelično kopičenje kemoterapevtika kot posledica povečane prepustnosti celične membrane zaradi elektroporacije.

V številnih študijah so pokazali učinkovitost, dobro sprejemljivost in veliko zadovoljstvo bolnikov z elektrokemoterapijo. Omenjeni pa so bili tudi neželeni učinki – najpogosteje

mišične kontrakcije in neprijetni (lahko celo boleči) občutki, ki so posledica vzdraženja perifernih živcev z električnimi pulzi. Za premagovanje te omejitve raziskujejo možnost uporabe drugačnih pulzov v elektrokemoterapiji, vključno z H-FIRE in nanosekundnimi pulzi. Poročila o uporabi nanosekundnih pulzov v elektrokemoterapiji so obetavna: *in vitro* so raziskovalci in raziskovalke opazili zmanjšanje preživetja celic, *in vivo* pa regresijo tumorja. Vendar pa v teh študijah niso celovito raziskali učinkov različnih parametrov nanosekundnih pulzov, zato ni jasno, kateri so optimalni parametri nanosekundnih pulzov za uporabo v elektrokemoterapiji. Iz predhodnih raziskav tudi ni jasno, ali so nanosekundni pulzi enako učinkoviti kot standardni osem 100 μ s pulzov v elektrokemoterapiji in ali so mehanizmi delovanja v elektrokemoterapiji z nanosekundnimi pulzi enaki kot pri konvencionalni elektrokemoterapiji z osmimi 100 μ s pulzi.

V okviru doktorske disertacije smo zasnovali obsežno *in vitro* raziskavo s splošnim ciljem primerjave osmih 100 μ s pulzov, ki se standardno uporabljajo v aplikacijah, ki temeljijo na elektroporaciji, z novejšimi oblikami pulzov (in sicer z nanosekundnimi in kratkimi visokofrekvenčnimi bipolarnimi (H-FIRE) pulzi) na različnih ravneh, pomembnih za aplikacije, ki temeljijo na elektroporaciji.

V študiji smo preizkušali sledeče hipoteze:

1. Pri uporabi monopolarnih nanosekundnih ali bipolarnih visokofrekvenčnih električnih pulzov s časom trajanja nekaj mikrosekund v elektroporacijskih postopkih so spremljajoče elektrokemijske reakcije zmanjšane, elektroporacija celične membrane pa je enakovredna klasičnim osmim 100 μ s pulzom.
2. Elektroporacija celic z električnimi pulzi z različnimi parametri, ki povečajo prepustnost celične membrane, povzroči primerljivo oksidacijo celičnih komponent.
3. Elektroporacija z nanosekundnimi pulzi v kombinaciji s protirakavo zdravilno učinkovino vodi do njene povečane učinkovitosti zaradi povečanega znotrajceličnega kopičenja zdravilne učinkovine.

Na štirih celičnih linijah, ki smo jih uporabljali v študiji (ovarijske celice kitajskega hrčka CHO, podganji kardiomioblasti H9c2, mišji mioblasti C2C12 in mišji nevroni HT22), smo pokazali, da je mogoče pri enaki amplitudi in času trajanja pozitivne in negativne faze pulzov H-FIRE s podaljšanjem pavze med fazami in/ali podaljšanjem pavze med pari bipolarnih pulzov doseči manjše preživetje celic. Naši rezultati kažejo, da bi lahko učinkovitost pulzov H-FIRE izboljšali s podaljšanjem pavze namesto povečanjem amplitude pulza. Vendar pa je le pulzni protokol s pavzo med pozitivno in negativno fazo ter pavzo med pari bipolarnih pulzov v času trajanja 10.000 μ s zmanjšal celično preživetje enako učinkovito kot standardnih osem 100 μ s pulzov na celičnih linijah CHO in HT22. Učinek časa trajanja pavze med pozitivno in negativno fazo ter pavze med pari bipolarnih pulzov na

permeabilizacijo membrane je bil bolj kompleksen kot na preživetje, vendar je bilo skupno vsem preizkušenim pulznim protokolom H-FIRE to, da so bili manj učinkoviti od standardnih osmih 100 μ s pulzov v smislu permeabilizacije celične membrane v vseh štirih testiranih celičnih linijah.

Za dosego visoke (tj. > 99 %) permeabilizacije celične membrane z nanosekundnimi pulzi so bile potrebne višje električne poljske jakosti kot z osmimi 100 μ s pulzi. Med protokoli nanosekundnih pulzov z enakim številom pulzov smo morali za krajše pulze uporabiti višje električne poljske jakosti, da smo dosegli visoko permeabilizacijo membrane. Primerjava nanosekundnih pulzov z enakim časom trajanja je pokazala, da so protokoli z večjim številom pulzov dosegli visoko permeabilizacijo membrane pri nižjih električnih poljskih jakosti kot protokoli z manjšim številom pulzov. Na celicah CHO smo z vsemi preizkušenimi pulznimi protokoli dosegli več kot 99 % permeabilizacijo celic, z izjemo enega 200 ns pulza, ki je permeabiliziral približno 85 % celične populacije pri najvišji električni poljski jakosti znotraj varnega območja delovanja uporabljenega pulznega generatorja. Za celično linijo mišjega melanoma B16F1 nismo dosegli več kot 99 % permeabilizacije celične membrane kadar smo uporabili en nanosekundni pulz s časom trajanja 200, 400 ali 550 ns, tudi pri najvišji uporabljeni električni poljski jakosti. To nakazuje, da so pri uporabi enega samega nanosekundnega pulza potrebne višje električne poljske jakosti za doseganje istega odstotka permeabilizacije celic B16F1 v primerjavi s celicami CHO. To pa je v nasprotju s tem, kar smo opazili pri osmih 100 μ s pulzih – pri teh je bila potrebna nižja električna poljska jakost za permeabilizacijo enakega odstotka celic B16F1 kot CHO.

Naša študija je bila prva v kateri smo določili sproščanje kovin z elektrod po uporabi H-FIRE in nanosekundnih pulzov. Koncentracijo kovinskih ionov v fiziološki raztopini smo izmerili z masno spektrometrijo z induktivno sklopljeno plazmo po dovajanju pulzov H-FIRE (s parametri kot v celičnih poskusih) in standardnih osmih 100 μ s pulzov enake amplitude na žičnate elektrode iz aluminija, nerjavečega jekla in platine potopljene v fiziološko raztopino. Nanosekundne pulze in standardnih osem 100 μ s pulzov z jakostmi električnega polja, ki smo jih določili kot optimalne za elektrokemoterapijo celic CHO, pa smo dovajali v kivete za elektroporacijo (z elektrodami iz aluminijeve zlitine), v katerih je bila fiziološka raztopina.

Količina kovinskih ionov, sproščenih z elektrod, se je močno razlikovala med tremi testiranimi materiali elektrod – absolutno največjo količino sproščenih kovinskih ionov smo izmerili za aluminijaste elektrode, najmanjšo pa za platinaste elektrode. Vsi preizkušeni pulzi H-FIRE so povzročili bistveno manj sproščanja kovin z elektrod iz aluminija in nerjavečega jekla v primerjavi z osmimi 100 μ s pulzi z enako amplitudo. Vendar pa je bila

v primeru platinastih elektrod za nekatere protokole pulzov H-FIRE izmerjena statistično ne značilno nižja koncentracija sproščenih ionov platine kot za osem 100 μ s pulzov. Z izjemo platine lahko zaključimo, da je s podaljšanjem časa trajanja pavz pulzov H-FIRE mogoče doseči enakovredni biološki učinek kot s standardnimi osmimi 100 μ s pulzi ob nižji količini sproščanja kovinskih ionov z elektrod. To nakazuje, da so pulzi H-FIRE boljši od standardnih osmih 100 μ s pulzov v smislu omejevanja elektrokemijskih reakcij. Različni časi trajanja pavze med pozitivno in negativno fazo ter pavze med pari bipolarnih pulzov v pulzih H-FIRE so povzročili statistično značilne razlike v koncentraciji sproščenih kovinskih ionov z elektrod iz aluminija in nerjavečega jekla. Vendar je bilo po uporabi pulzov H-FIRE z 1 μ s pavzo med pozitivno in negativno fazo in različnimi časi trajanja pavze med pari bipolarnih pulzov izmerjenih več ionov platine kot pri pulzih H-FIRE, ki so imeli pavzo med pozitivno in negativno fazo ter pavzo med pari bipolarnih pulzov z enakim časom trajanja. Naša študija ni mogla pojasniti teh razlik. Za razumevanje učinkov časa trajanja pavze v pulzih H-FIRE na sproščanje kovin iz platinastih elektrod bi bile potrebne nadaljnje raziskave.

Po dovajanju nanosekundnih pulzov v kivete za elektroporacijo smo izmerili znatno nižjo koncentracijo sproščenih aluminijevih ionov kot po dovajanju osmih 100 μ s pulzov. Dokazali smo, da skrajšanje časa trajanja pulza na nekaj sto nanosekund zmanjša količino kovinskih ionov, ki se sprostijo z elektrod ob elektroporaciji, tudi ob povečanju amplitude in/ali števila pulzov za doseg ekvivalentnega biološkega učinka kot pri daljših pulzih. Ker je sproščanje kovin z elektrod podskupina elektrokemijskih reakcij, ki se dogajajo na elektrodi, ti izsledki govorijo v prid uporabi nanosekundnih namesto mikrosekundnih pulzov, kadar je cilj ohraniti intenzivnost elektrokemijskih reakcij na minimumu. Vendar se zdi, da sproščanje kovinskih ionov ni odvisno le od časa trajanja pulza ali energije, ki je bila z električnimi pulzi dovedena v kiveto (ocenjeno kot zmnožek časa trajanja pulza, števila pulzov, izmerjene napetosti in izmerjenega električnega toka) – primerjava posameznih nanosekundnih pulzov z enako amplitudo in različnimi časi trajanja pulza (200, 400 ali 500 ns) pokaže, da smo v nasprotju s pričakovanji največjo koncentracijo aluminijevih ionov izmerili po dovajanju najkrajšega (tj. 200 ns) pulza.

Kemijske spremembe membranskih lipidov, zlasti lipidna peroksidacija, bi lahko pojasnile dolgotrajnejšo (v primerjavi s trajanjem pulza) povečano prepustnost celičnih membran izmerjeno po elektroporaciji. V naši študiji smo izmerili čas potreben za zaceljenje membrane in peroksidacijo lipidov po elektroporaciji, da bi primerjali čas, potreben za zaceljenje, z obsegom peroksidacije lipidov in ugotovili, ali različne oblike pulzov, ki enako učinkovito permeabilizirajo celično membrano, povzročijo tudi primerljivo peroksidacijo lipidov celične membrane.

Čas za zaceljenje celične membrane celic CHO smo izmerili po dovajanju različnih nanosekundnih pulznih protokolov in osmih 100 μ s pulzov pri električni poljski jakosti, ki je bila določena za optimalno za elektrokemoterapijo, z dodajanjem YO-PRO-1 celicam CHO vsaki 2 minuti od 2 do 26 minut po elektroporaciji in merjenjem odstotka celic, ki fluorescirajo YO-PRO-1. Celična membrana se je zacelila v manj kot 5 min, kadar so bile celice elektroporirane z osmimi 100 μ s pulzi. Za večino nanosekundnih pulznih protokolov izmerjeni čas, potreben za zaceljenje celične membrane, ni bil bistveno daljši. Toda v primeru elektroporacije s petindvajsetimi 200 ns pulzi, petindvajsetimi 400 ns pulzi, petindvajsetimi 550 ns pulzi, stotimi 550 ns pulzi, enem 400 ns pulzu in enem 550 ns pulzu pa je membrana za zaceljenje potrebovala bistveno daljši čas (več kot 10 min).

Lipidno peroksidacijo v celicah CHO, elektroporiranih s petindvajsetimi 400 ns pulzi ali osmimi 100 μ s pulzi pri električni poljski jakosti, ki je bila določena kot optimalna za elektrokemoterapijo, smo izmerili s kitom Click-iT Lipid Peroxidation Imaging Kit - Alexa Fluor 488. Statistično značilne razlike smo izmerili le med neobarvanimi celicami in vsemi ostalimi vzorci ter med negativno kontrolo in celicami, elektroporiranimi s petindvajsetimi 400 ns pulzi, pri čemer je bil v nasprotju s pričakovanji izmerjeni signal pri slednjih nižji. Opazili smo tudi velike razlike v izmerjenih signalih med duplikati, izvedenimi istega dne, in tudi med vzorci iz različnih dni. Ti rezultati kažejo, da Click-iT Lipid Peroxidation Imaging Kit - Alexa Fluor 488 ni primerna metoda za merjenje lipidne peroksidacije celic CHO, vsaj ne v prvih urah po elektroporaciji. Zato nismo mogli niti potrditi niti ovreči hipoteze, da elektroporacija celic z različnimi pulzi, ki približno enako učinkovito permeabilizirajo celično membrano, povzroči primerljivo oksidacijo celičnih komponent.

Za ovrednotenje učinkovitosti nanosekundnih pulzov v elektrokemoterapiji smo izmerili preživetje celic CHO s presnovnim testom MTS po *in vitro* elektrokemoterapiji z bleomicinom ali cisplatinom 72 ur po eksperimentu. Preizkusili smo več nanosekundnih pulznih protokolov – spreminjali smo čas trajanja pulzov (200, 400 ali 550 ns) in število pulzov (1, 25 ali 100 pulzov), ponavljalna frekvenca pa je bila 10 Hz – in standardnih osem 100 μ s pulzov pri električni poljski jakosti, ki je bila predhodno določena kot optimalna za vsak pulzni protokol oz. v primeru enega 200 pulza pri najvišji eksperimentalno dosegljivi električni poljski jakosti. Za izbrane pulzne protokole (in sicer en 200 ns pulz, petindvajset 400 ns pulzov in osem 100 μ s pulzov) smo celično preživetje po *in vitro* elektrokemoterapiji izmerili tudi s testom klonogenosti. Preživetje celic po *in vitro* elektrokemoterapiji s cisplatinom je bilo izmerjeno tudi za celično linijo B16F1 s testom klonogenosti za en 200 ns pulz pri najvišji eksperimentalno dosegljivi električni poljski jakosti ter za petindvajset 400 ns pulzov in osem 100 μ s pulzov pri električni poljski jakosti, za katero je bilo predhodno ugotovljeno, da je optimalna za posamezni pulzni protokol za to celično linijo. Ker mehanizmi delovanja elektrokemoterapije z nanosekundnimi pulzi še niso raziskani,

povečanje znotrajceličnega kopičenja kemoterapevtika pa v splošnem velja za enega glavnih mehanizmov delovanja konvencionalne elektrokemoterapije z mikrosekundnimi pulzi, smo v tej študiji preizkusili, ali kombinacija permeabilizirajočih električnih pulzov (ki sami ne zmanjšajo celičnega preživetja) in cisplatina vodi do povečanega kopičenja cisplatina v celicah (v primerjavi z neelektroporiranimi celicami) in ali količina celičnega cisplatina korelira s celičnim preživetjem po elektrokemoterapiji.

Sama elektroporacija (tj. v odsotnosti bleomicina ali cisplatina) ni zmanjšala celičnega preživetja. Znotraj razpona preizkušenih koncentracij bleomicina in cisplatina smo opazili zmanjšanje celičnega preživetja neelektroporiranih celic samo pri celicah CHO inkubiranih s 50 μ M cisplatinom. Kombinacija elektroporacije in bleomicina ali cisplatina je povzročila zmanjšanje celičnega preživetja obeh celičnih linij za vse preizkušene pulzne protokole, z edino izjemo enega 200 ns pulza v celicah B16F1.

Najmanjše zmanjšanje preživetja celic je bilo izmerjeno s testom MTS za celice CHO, elektroporirane z enim 200 ns pulzom pri 12,6 kV/cm in bleomicinom, ter s testom klonogenosti za celice B16F1, elektroporirane z istim pulznim protokolom in cisplatinom. To ni presenetljivo, saj je ta pulzni protokol permeabiliziral celično membrano le 85 % celic CHO in manj kot 50 % celic B16F1, kar je suboptimalno za elektrokemoterapijo. Še bolj zanimivo pa je, da je bil kljub suboptimalni permeabilizaciji celične membrane en 200 ns pulz enako učinkovit pri zmanjševanju celičnega preživetja celic CHO v elektrokemoterapiji s cisplatinom kot petindvajset 400 ns in osem 100 μ s pulzov.

Pri celicah, ki so bile podvržene enakim pogojem (tj. enakemu pulznemu protokolu in enaki koncentraciji bleomicina/cisplatina), smo s testom klonogenosti izmerili nižje celično preživetje kot s testom MTS. Celično preživetje, izmerjeno s testom MTS, je pri določeni koncentraciji bleomicina doseglo plato, tj. z nadaljnjim naraščanjem koncentracije bleomicina se je izmerjeno preživetje le rahlo (če sploh) zmanjševalo. Pri celičnem preživetju, izmerjenem s testom klonogenosti, pa takega platoja nismo opazili – preživetje celic se je z naraščajočo koncentracijo bleomicina zmanjševalo. Različni rezultati obeh testov so posledica razlik v njunem načinu delovanja.

Pri elektrokemoterapiji z bleomicinom smo morali z nanosekundnimi pulzi uporabiti višjo zunajceličnih koncentracijo bleomicina za zmanjšanje preživetja celic CHO v enakem obsegu kot z osmimi 100 μ s pulzi, vendar je bila tudi najvišja uporabljena koncentracija bleomicina še vedno znatno nižja od terapevtskega odmerka, ki se uporablja pri elektrokemoterapiji v klinični praksi. Med različnimi preizkušenimi nanosekundnimi pulznimi protokoli so trije protokoli (in sicer petindvajset 200 ns pulzov, petindvajset 400 ns pulzov in sto 550 ns pulzov) zmanjšali celično preživetje elektroporiranih celic CHO pri

občutno nižjih koncentracijah bleomicina kot drugi nanosekundni pulzni protokoli. Zanimivo je, da smo pri teh treh pulznih protokolih izmerili tudi najdaljši čas zaceljenja celične membrane po elektroporaciji. Ker je bleomicin srednje velika molekula, bi naše ugotovitve lahko bile uporabne tudi za druge aplikacije, ki temeljijo na reverzibilni elektroporaciji z nanosekundnimi pulzi, s ciljem privzema srednje velikih molekul (npr. siRNA) v celice.

Po drugi strani pa pri elektrokemoterapiji s cisplatinom nismo izmerili razlik v celičnem preživetju po elektroporaciji z nanosekundnimi ali osmimi 100 μ s pulzi pri isti koncentraciji cisplatina, spet z edino izjemo enega 200 ns pulza pri celicah B16F1, ki ni zmanjšal preživetja celic tudi pri najvišji preizkušeni koncentraciji cisplatina. Opažene razlike v izmerjenem celičnem preživetju po elektrokemoterapiji z nanosekundnimi pulzi med bleomicinom in cisplatinom bi lahko bile posledica različne velikosti molekul in mehanizmov delovanja obeh kemoterapevtikov.

Z masno spektrometrijo z induktivno sklopljeno plazmo smo izmerili celokupno količino platine v celičnih peletih po elektrokemoterapiji s predpostavko, da cisplatin najverjetneje predstavlja večino izmerjene platine. To predpostavko podpira dejstvo, da je bila količina platine, izmerjena v vzorcih, ki jim cisplatin ni bil dodan, za 2 – 3 velikostne rede nižja kot v vzorcih s cisplatinom ali celo pod mejo detekcije. V celicah, ki so bile izpostavljene enakemu pulznemu protokolu in enaki koncentraciji cisplatina, smo za celično linijo CHO izmerili večjo količino platine kot v celicah B16F1. V elektroporiranih celicah smo izmerili večjo celokupno količino platine v primerjavi z neelektroporiranimi celicami, ki so bile inkubirane z enako koncentracijo cisplatina, razen v primeru enega 200 ns pulza za celično linijo CHO. Ti rezultati kažejo, da se znotrajcelično kopičenje cisplatina poveča tudi, ko se za elektrokemoterapijo uporabljajo nanosekundni pulzi. V celicah elektroporiranih s petindvajsetimi 400 ns in osmimi 100 μ s pulzi pri isti koncentraciji cisplatina znotraj iste celične linije ni bilo statistično značilnih razlik v preživetju celic in količini platine v celicah. Zanimivo pa je, da čeprav je bila v celicah CHO, elektroporiranih z enim 200 ns pulzom, izmerjena manjša količina platine kot s petindvajsetimi 400 ns pulzi in osmimi 100 μ s pulzi, je bila z vsemi tremi pulznimi protokoli dosežena enaka stopnja zmanjšanja celičnega preživetja.

Iz izmerjene količine platine smo izračunali število molekul cisplatina na celico in te podatke korelirali s preživetjem celic po elektrokemoterapiji za vsako celično linijo posebej. Pri približno enakem številu molekul cisplatina na celico je bilo celično preživetje nižje pri elektroporiranih celicah CHO kot pri neelektroporiranih celicah CHO. To kaže na možen sinergistični učinek elektroporacije in cisplatina. Vendar pa rezultati celičnega preživetja in števila molekul cisplatina na celico za B16F1 ne nakazujejo na sinergistični učinek

elektroporacije in cisplatina. Za celice B16F1 je število molekul cisplatina linearno koreliralo z logaritmom celičnega preživetja. Vendar pa smo imeli pri celicah B16F1 le eno eksperimentalno točko, pri kateri je bilo število molekul cisplatina na celico znotraj intervala števila molekul v neelektroporiranih celicah, zato bi potrebovali še več podatkov, kjer bi bilo število molekul cisplatina na celico pri elektroporiranih in neelektroporiranih celicah znotraj istega intervala, da bi lahko ugotovili ali je tudi v primeru celic B16F1 potrebno manjše število molekul cisplatina na celico v elektroporiranih celicah v primerjavi z neelektroporiranimi za doseganje isti ravni zmanjšanja celičnega preživetja.

Elektroporacija lahko na več načinov vpliva na občutljivost celic za cisplatin, npr. preko nastanka reaktivnih kisikovih zvrsti, motnjami znotrajcelične homeostaze Ca^{2+} ali z izboljšanjem protirakavih lastnosti cisplatina zaradi spremembe strukture molekule. Od možnih učinkov elektroporacije na povečanje citotoksičnosti cisplatina smo v naši raziskavi raziskovali le vpliv visokonapetostnih električnih pulzov na strukturo cisplatina. Z ^1H jedrsko magnetno resonančno spektroskopijo smo posneli spektre cisplatina v devterijevelem oksidu, raztopini iz 90 % vode in 10 % devterijevega oksida, raztopini devterijevega oksida s 154 mM NaCl ter raztopini iz 90 % vode in 10 % devterijevega oksida s 154 mM NaCl. V spektru cisplatina, ki je bil izpostavljen petindvajsetim 400 ns ali osmim 100 μs pulzom nismo opazili premikov vrhov, ki ustrezajo cisplatinu, niti novih vrhov, v primerjavi s spektrom cisplatina, ki ni bil izpostavljen električnim pulzom. Z masno spektrometrijo visoke ločljivosti smo opazili podobne fragmente v spektru cisplatina v vodi ali fiziološki raztopini, ki je bil ali ni bil izpostavljen visokonapetostnim električnim pulzom. Jedrska magnetna resonanca in masna spektrometrija visoke ločljivosti sta torej pokazali, da je struktura cisplatina ostala primerljiva pred in po izpostavitvi električnim pulzom pod pogoji, uporabljenimi v naših poskusih.

V splošnem naši rezultati kažejo, da so nanosekundni pulzi s primerno izbranimi parametri primerni za uporabo v elektrokemoterapiji. Uporaba enako učinkovitih nanosekundnih pulzov povzroči enako zmanjšanje preživetja celic zaradi cisplatina in enako kopičenje cisplatina v celicah kot pri standardnih osmih 100 μs pulzih. Tako smo potrdili hipotezo, da elektroporacija z nanosekundnimi pulzi poveča količino cisplatina v celicah in posledično poveča njegov citotoksični učinek. Vendar pa rezultati v celicah CHO kažejo, da so v celično smrt po elektrokemoterapiji z nanosekundnimi pulzi vpleteni še drugi mehanizmi poleg povečanega znotrajceličnega kopičenja cisplatina.

Če povzamemo, potrdili smo našo prvo hipotezo, da uporaba H-FIRE in nanosekundnih pulzov zmanjšuje elektrokemijske reakcije tudi, ko so parametri električnega polja (amplituda, pavza med pulzi, ...) prilagojeni tako, da imajo enak biološki učinek kot daljši monopolarni pulzi. Naše druge hipoteze, da elektroporacija celic z različnimi oblikami

pulzov, ki vodijo v primerljivo permeabilizacijo celične membrane, povzroči primerljivo oksidacijo celičnih komponent, nismo mogli niti potrditi niti ovreči, ker se je izkazalo, da Click-iT Lipid Peroxidation Imaging Kit - Alexa Fluor 488 ni ustrezna metoda za merjenje lipidne peroksidacije v prvih urah po elektroporaciji. Potrdili smo našo tretjo hipotezo, da elektroporacija z nanosekundnimi pulzi poveča količino kemoterapevtika v celici in posledično poveča tudi njegov citotoksični učinek.

5 REFERENCES

- Al-Taweel N., Varghese E., Florea A.-M., Büsselberg D. 2014. Cisplatin (CDDP) triggers cell death of MCF-7 cells following disruption of intracellular calcium ($[Ca^{2+}]_i$) homeostasis. *The Journal of Toxicological Sciences*, 39, 5: 765–774
- Arena C.B., Sano M.B., Rossmeisl Jr J.H., Caldwell J.L., Garcia P.A., Rylander M.N., Davalos R. V. 2011. High-frequency irreversible electroporation (H-FIRE) for non-thermal ablation without muscle contraction. *BioMedical Engineering OnLine*, 10: 102, doi: 10.1186/1475-925X-10-102: 20 p.
- Aycock K.N., Zhao Y., Lorenzo M.F., Davalos R. V. 2021. A Theoretical Argument for Extended Interpulse Delays in Therapeutic High-Frequency Irreversible Electroporation Treatments. *IEEE Transactions on Biomedical Engineering*, 68, 6: 1999–2010
- Batista Napotnik T., Wu Y.-H., Gundersen M.A., Miklavčič D., Vernier P.T. 2012. Nanosecond electric pulses cause mitochondrial membrane permeabilization in Jurkat cells. *Bioelectromagnetics*, 33, 3: 257–264
- Beebe S.J., Fox P.M., Rec L.J., Somers K., Stark R.H., Schoenbach K.H. 2002. Nanosecond pulsed electric field (nsPEF) effects on cells and tissues: apoptosis induction and tumor growth inhibition. *IEEE Transactions on Plasma Science*, 30, 1: 286–292
- Bendix M.B., Houston A., Forde P.F., Brint E. 2022. Electrochemotherapy and immune interactions; A boost to the system? *European Journal of Surgical Oncology*, 48, 9: 1895–1900
- Bennett W.F.D., Sapay N., Tieleman D.P. 2014. Atomistic simulations of pore formation and closure in lipid bilayers. *Biophysical Journal*, 106, 1: 210–219
- Benov L.C., Antonov P.A., Ribarov S.R. 1994. Oxidative damage of the membrane lipids after electroporation. *General physiology and biophysics*, 13, 2: 85–97
- Black R.C., Hannaker P. 1980. Dissolution of smooth platinum electrodes in biological fluids. *Applied neurophysiology*, 42, 6: 366–374
- Boonnoy P., Jarerattanachai V., Karttunen M., Wong-Ekkabut J. 2015. Bilayer Deformation, Pores, and Micellation Induced by Oxidized Lipids. *Journal of Physical Chemistry Letters*, 6, 24: 4884–4888
- Borza C., Muntean D., Dehelean C., Săvoiu G., Șerban C., Simu G., Andoni M., Butur M., Drăgan S. 2013. Oxidative Stress and Lipid Peroxidation – A Lipid Metabolism Dysfunction. In: *Lipid Metabolism*. Baez R.V. (ed.), Rijeka, IntechOpen: 23–38
- Breton M., Mir L.M. 2012. Microsecond and nanosecond electric pulses in cancer treatments. *Bioelectromagnetics*, 33, 2: 106–123
- Breton M., Mir L.M. 2018. Investigation of the chemical mechanisms involved in the electropulsation of membranes at the molecular level. *Bioelectrochemistry*, 119: 76–83
- Burke R.C., Bardet S.M., Carr L., Romanenko S., Arnaud-Cormos D., Leveque P., O'Connor R.P. 2017. Nanosecond pulsed electric fields depolarize transmembrane potential via voltage-gated K^+ , Ca^{2+} and TRPM8 channels in U87 glioblastoma cells. *Biochimica et Biophysica Acta - Biomembranes*, 1859, 10: 2040–2050

- Campana L.G., Miklavčič D., Bertino G., Marconato R., Valpione S., Imarisio I., Dieci M.V., Granziera E., Čemazar M., Alaibac M., Serša G. 2019. Electrochemotherapy of superficial tumors – Current status:: Basic principles, operating procedures, shared indications, and emerging applications. *Seminars in Oncology*, 46, 2: 173–191
- Canatella P.J., Karr J.F., Petros J.A., Prausnitz M.R. 2001. Quantitative study of electroporation-mediated molecular uptake and cell viability. *Biophysical Journal*, 80, 2: 755–764
- Cemazar M., Miklavčič D., Ščančar J., Dolžan V., Golouh R., Serša G. 1999. Increased platinum accumulation in SA-1 tumour cells after in vivo electrochemotherapy with cisplatin. *British Journal of Cancer*, 79, 9: 1386–1391
- Chen N., Schoenbach K.H., Kolb J.F., Swanson R.J., Garner A.L., Yang J., Joshi R.P., Beebe S.J. 2004. Leukemic cell intracellular responses to nanosecond electric fields. *Biochemical and Biophysical Research Communications*, 317, 2: 421–427
- Chen Y., Guo Z., Sadler P.J. 1999. 195Pt- and 15N-NMR Spectroscopic Studies of Cisplatin Reactions with Biomolecules. In: *Cisplatin*. Lippert B. (ed.). Weinheim, John Wiley & Sons, 293–318
- Cornelis F.H., Cindrič H., Kos B., Fujimori M., Petre E.N., Miklavčič D., Solomon S.B., Srimathveeravalli G. 2020. Peri-tumoral Metallic Implants Reduce the Efficacy of Irreversible Electroporation for the Ablation of Colorectal Liver Metastases. *CardioVascular and Interventional Radiology*, 43, 1: 84–93
- Craviso G.L., Choe S., Chatterjee P., Chatterjee I., Vernier P.T. 2010. Nanosecond Electric Pulses: A Novel Stimulus for Triggering Ca²⁺ Influx into Chromaffin Cells Via Voltage-Gated Ca²⁺ Channels. *Cellular and Molecular Neurobiology*, 30, 8: 1259–1265
- Cvetkoska A., Maček-Lebar A., Trdina P., Miklavčič D., Reberšek M. 2022. Muscle contractions and pain sensation accompanying high-frequency electroporation pulses. *Scientific Reports*, 12, 1: 1–15
- Cwiklik L., Jungwirth P. 2010. Massive oxidation of phospholipid membranes leads to pore creation and bilayer disintegration. *Chemical Physics Letters*, 486, 4–6: 99–103
- Dong S., Yao C., Zhao Y., Lv Y., Liu H. 2018. Parameters optimization of bipolar high frequency pulses on tissue ablation and inhibiting muscle contraction. *IEEE Transactions on Dielectrics and Electrical Insulation*, 25, 1: 207–216
- Dovgan B., Miklavčič D., Knežević M., Zupan J., Barlič A. 2021. Intracellular delivery of trehalose renders mesenchymal stromal cells viable and immunomodulatory competent after cryopreservation. *Cytotechnology*, 73, 3: 391–411
- Draeger A., Schoenauer R., Atanassoff A.P., Wolfmeier H., Babiychuk E.B. 2014. Dealing with damage: Plasma membrane repair mechanisms. *Biochimie*, 107, Part A: 66–72
- Evrendilek G.A., Li S., Dantzer W.R., Zhang Q.H. 2004. Pulsed electric field processing of beer: microbial, sensory, and quality analyses. *Journal of Food Science*, 69, 8: M228–M232
- Florea A.M., Büsselberg D. 2011. Cisplatin as an anti-tumor drug: Cellular mechanisms of activity, drug resistance and induced side effects. *Cancers*, 3, 1: 1351–1371
- Forjanic T., Markelc B., Marcan M., Bellard E., Couillaud F., Golzio M., Miklavcic D. 2019. Electroporation-Induced Stress Response and Its Effect on Gene Electrotransfer Efficacy: In Vivo Imaging and Numerical Modeling. *IEEE transactions on bio-medical engineering*, 66, 9: 2671–2683

- Frandsen S.K., Gissel H., Hojman P., Tramm T., Eriksen J., Gehl J. 2012. Direct therapeutic applications of calcium electroporation to effectively induce tumor necrosis. *Cancer Research*, 72, 6: 1336–1341
- Friedrich U., Stachowicz N., Simm A., Fuhr G., Lucas K., Zimmermann U. 1998. High efficiency electrotransfection with aluminum electrodes using microsecond controlled pulses. *Bioelectrochemistry and Bioenergetics*, 47, 1: 103–111
- Gabriel B., Teissié J. 1994. Generation of reactive-oxygen species induced by electroporation of Chinese hamster ovary cells and their consequence on cell viability. *European Journal of Biochemistry*, 223, 1: 25–33
- Gabriel B., Teissié J. 1995. Spatial compartmentation and time resolution of photooxidation of a cell membrane probe in electroporated Chinese hamster ovary cells. *European Journal of Biochemistry*, 228, 3: 710–718
- Gad A., Member S., Jayaram S.H. 2014. Effect of Electric Pulse Parameters on Releasing Metallic Particles From Stainless Steel Electrodes During PEF Processing of Milk. *IEEE Transactions on Industry Applications*, 50, 2: 1402–1409
- Geboers B., Scheffer H.J., Graybill P.M., Ruars A.H., Nieuwenhuizen S., Puijk R.S., van den Tol P.M., Davalos R. V., Rubinsky B., de Gruijl T.D., Miklavčič D., Meijerink M.R. 2020. High-Voltage Electrical Pulses in Oncology: Irreversible Electroporation, Electrochemotherapy, Gene Electrotransfer, Electrofusion, and Electroimmunotherapy. *Radiology*, 295, 2: 254–272
- Gehl J. 2003. Electroporation: theory and methods, perspectives for drug delivery, gene therapy and research. *Acta physiologica Scandinavica*, 177, 4: 437–447
- Gehl J., Serša G., Matthiessen L.W., Muir T., Soden D., Occhini A., Quagliano P., Curatolo P., Campana L.G., Kunte C., Clover A.J.P., Bertino G., Farricha V., Odili J., Dahlstrom K., Benazzo M., Mir L.M. 2018. Updated standard operating procedures for electrochemotherapy of cutaneous tumours and skin metastases. *Acta Oncologica*, 57, 7: 874–882
- Gehl J., Skovsgaard T., Mir L.M. 1998. Enhancement of cytotoxicity by electroporation: an improved method for screening drugs. *Anti-Cancer Drugs*, 9, 4: 319–25
- Gerlach D., Alleborn N., Baars A., Delgado A., Moritz J., Knorr D. 2008. Numerical simulations of pulsed electric fields for food preservation: A review. *Innovative Food Science and Emerging Technologies*, 9, 4: 408–417
- Graybill P.M., Davalos R. V. 2020. Cytoskeletal Disruption after Electroporation and Its Significance to Pulsed Electric Field Therapies. *Cancers*, 12, 5: 29–32
- Gualdani R., de Clippele M., Ratbi I., Gailly P., Tajeddine N. 2019. Store-operated calcium entry contributes to cisplatin-induced cell death in non-small cell lung carcinoma. *Cancers*, 11, 3: 430, doi: 10.3390/cancers11030430: 12 p.
- Gudvangen E., Kim V., Novickij V., Battista F., Pakhomov A.G. 2022. Electroporation and cell killing by milli- to nanosecond pulses and avoiding neuromuscular stimulation in cancer ablation. *Scientific Reports*, 12, 1: 1–15
- Heller R., Jaroszeski M., Leo-Messina J., Perrot R., Van Voorhis N., Reintgen D., Gilbert R. 1995. Treatment of B16 mouse melanoma with the combination of electroporation and chemotherapy. *Bioelectrochemistry and Bioenergetics*, 36, 1: 83–87
- Hu C., Wang M., Han X. 2017. Shotgun lipidomics in substantiating lipid peroxidation in redox biology: Methods and applications. *Redox Biology*, 12: 946–955

- Hyacinthe M., Jaroszeski M.J., Dang V. V, Coppola D., Karl R.C., Gilbert R.A., Heller R. 1999. Electrically enhanced drug delivery for the treatment of soft tissue sarcoma. *Cancer*, 85, 2: 409–417
- Jakštys B., Ruzgys P., Tamošiūnas M., Šatkauskas S. 2015. Different Cell Viability Assays Reveal Inconsistent Results After Bleomycin Electrotransfer In Vitro. *The Journal of Membrane Biology*, 248, 5: 857–863
- Jaroszeski M.J., Dang V., Pottinger C., Hickey J., Gilbert R., Heller R. 2000. Toxicity of anticancer agents mediated by electroporation in vitro. *Anti-cancer drugs*, 11, 3: 201–208
- Jaroszeski M.J., Gilbert R.A., Heller R. 1997. In vivo antitumor effects of electrochemotherapy in a hepatoma model. *Biochimica et biophysica acta*, 1334, 1: 15–18
- Jiang C., Davalos R. V, Bischof J.C. 2015. A Review of basic to clinical studies of irreversible electroporation therapy. *IEEE Transactions on Biomedical Engineering*, 62, 1: 4–20
- Jimenez A.J., Maiuri P., Lafaurie-Janvore J., Divoux S., Piel M., Perez F. 2014. ESCRT machinery is required for plasma membrane repair. *Science*, 343, 6174: 1247136, doi: 10.1126/science.1247136: 7 p.
- Jimenez A.J., Perez F. 2015. Physico-chemical and biological considerations for membrane wound evolution and repair in animal cells. *Seminars in Cell and Developmental Biology*, 45: 2–9
- Kawai Y., Nakao T., Kunimura N., Kohda Y., Gemba M. 2006. Relationship of intracellular calcium and oxygen radicals to cisplatin-related renal cell injury. *Journal of Pharmacological Sciences*, 100, 1: 65–72
- Kendler M., Micheluzzi M., Wetzig T., Simon J.C. 2013. Electrochemotherapy under tumescent local anesthesia for the treatment of cutaneous metastases. *Dermatologic Surgery*, 39, 7: 1023–1032
- Kim V., Gudvangen E., Kondratiev O., Redondo L., Xiao S., Pakhomov A.G. 2021. Peculiarities of Neurostimulation by Intense Nanosecond Pulsed Electric Fields: How to Avoid Firing in Peripheral Nerve Fibers. *International Journal of Molecular Sciences*, 22, 13: 7051, doi: 10.3390/ijms22137051: 18 p.
- Kleih M., Böpple K., Dong M., Gaißler A., Heine S., Olayioye M.A., Aulitzky W.E., Essmann F. 2019. Direct impact of cisplatin on mitochondria induces ROS production that dictates cell fate of ovarian cancer cells. *Cell Death and Disease*, 10: 851, doi: 10.1038/s41419-019-2081-4: 12 p.
- Kooijmans S.A.A., Stremersch S., Braeckmans K., de Smedt S.C., Hendrix A., Wood M.J.A., Schiffelers R.M., Raemdonck K., Vader P. 2013. Electroporation-induced siRNA precipitation obscures the efficiency of siRNA loading into extracellular vesicles. *Journal of Controlled Release*, 172, 1: 229–238
- Košir S., Vižintin A., Miklavčič D. 2021. Decreases in Cell Viability Resulting from Metal Ions Present in Stainless Steel in Electroporated and Nonelectroporated Cells. In: *Proceedings of the 30th International Electrotechnical and Computer Science Conference ERK 2021, Portorož, 20 - 21 September 2021*. Žemva A., Trost A. (eds.). Ljubljana, Slovenska sekcija IEEE: 399–402
- Kotnik T., Frey W., Sack M., Haberl Meglič S., Peterka M., Miklavčič D. 2015. Electroporation-based applications in biotechnology. *Trends in Biotechnology*, 33, 8: 480–488

- Kotnik T., Miklavčič D., Mir L.M. 2001. Cell membrane electropermeabilization by symmetrical bipolar rectangular pulses: Part II. Reduced electrolytic contamination. *Bioelectrochemistry*, 54, 1: 91–95
- Kotnik T., Rems L., Tarek M., Miklavčič D. 2019. Membrane Electroporation and Electropermeabilization: Mechanisms and Models. *Annual Review of Biophysics*, 48, 1: 63–91
- Levine Z.A., Vernier P.T. 2010. Life Cycle of an Electropore: Field-Dependent and Field-Independent Steps in Pore Creation and Annihilation. *The Journal of Membrane Biology*, 236, 1: 27–36
- Lis M., Wizert A., Przybylo M., Langner M., Swiatek J., Jungwirth P., Cwiklik L. 2011. The effect of lipid oxidation on the water permeability of phospholipids bilayers. *Physical Chemistry Chemical Physics*, 13, 39: 17555–17563
- Long G., Shires P.K., Plescia D., Beebe S.J., Kolb J.F., Schoenbach K.H. 2011. Targeted tissue ablation with nanosecond pulses. *IEEE Transactions on Biomedical Engineering*, 58, 8: 2161–2167
- Loomis-Husselbee J.W., Cullen P.J., Irvine R.F., Dawson A.P. 1991. Electroporation can cause artefacts due to solubilization of cations from the electrode plates. Aluminum ions enhance conversion of inositol 1,3,4,5-tetrakisphosphate into inositol 1,4,5-trisphosphate in electroporated L1210 cells. *The Biochemical journal*, 277, 3: 883–885
- Lopez A., Rols M.P., Teissie J. 1988. Phosphorus-31 NMR analysis of membrane phospholipid organization in viable, reversibly electropermeabilized Chinese hamster ovary cells. *Biochemistry*, 27, 4: 1222–1228
- Maccarrone M., Bladergroen M.R., Rosato N., Agrò A.F. 1995a. Role of lipid peroxidation in electroporation-induced cell permeability. *Biochemical and Biophysical Research Communications*, 209, 2: 417–425
- Maccarrone M., Rosato N., Agrò A.F. 1995b. Electroporation enhances cell membrane peroxidation and luminescence. *Biochemical and Biophysical Research Communications*, 206, 1: 238–245
- Mahnič-Kalamiza S., Miklavčič D. 2020. Scratching the electrode surface: Insights into a high-voltage pulsed-field application from in vitro & in silico studies in indifferent fluid. *Electrochimica Acta*, 363: 137187, doi: 10.1016/j.electacta.2020.137187: 15 p.
- Mahnič-Kalamiza S., Vorobiev E., Miklavčič D. 2014. Electroporation in Food Processing and Biorefinery. *The Journal of Membrane Biology*, 247, 12: 1279–1304
- Makovec T. 2019. Cisplatin and beyond: Molecular mechanisms of action and drug resistance development in cancer chemotherapy. *Radiology and Oncology*, 53, 2: 148–158
- Marty M., Sersa G., Garbay J.R., Gehl J., Collins C.G., Snoj M., Billard V., Geertsens P.F., Larkin J.O., Miklavcic D., Pavlovic I., Paulin-Kosir S.M., Cemazar M., Morsli N., Soden D.M., Rudolf Z., Robert C., O’Sullivan G.C., Mir L.M. 2006. Electrochemotherapy – An easy, highly effective and safe treatment of cutaneous and subcutaneous metastases: Results of ESOPE (European Standard Operating Procedures of Electrochemotherapy) study. *European Journal of Cancer Supplements*, 4, 11: 3–13

- Marullo R., Werner E., Degtyareva N., Moore B., Altavilla G., Ramalingam S.S., Doetsch P.W. 2013. Cisplatin induces a mitochondrial-ros response that contributes to cytotoxicity depending on mitochondrial redox status and bioenergetic functions. *PLoS ONE*, 8, 11: e81162, doi: 10.1371/journal.pone.0081162 15 p.
- Meakin W.S., Edgerton J., Wharton C.W., Meldrum R.A. 1995. Electroporation-induced damage in mammalian cell DNA. *Biochimica et Biophysica Acta (BBA) - Gene Structure and Expression*, 1264, 3: 357–362
- Michel O., Kulbacka J., Saczko J., Mączyńska J., Błasiak P., Rossowska J., Rzechonek A. 2018. Electroporation with Cisplatin against Metastatic Pancreatic Cancer: In Vitro Study on Human Primary Cell Culture. *BioMed research international*, 2018: 7364539, doi: 10.1155/2018/7364539: 12 p.
- Michel O., Pakhomov A.G., Casciola M., Saczko J., Kulbacka J., Pakhomova O.N. 2020. Electroporation does not correlate with plasma membrane lipid oxidation. *Bioelectrochemistry*, 132: 107433, doi: 10.1016/j.bioelechem.2019.107433: 12 p.
- Miklavčič D., Mali B., Kos B., Heller R., Serša G. 2014. Electrochemotherapy: From the drawing board into medical practice. *BioMedical Engineering Online*, 13, 1: 1–20
- Miklavčič D., Snoj M., Županič A., Kos B., Čemažar M., Kropivnik M., Bracko M., Pečnik T., Gadzišev E., Serša G. 2010. Towards treatment planning and treatment of deep-seated solid tumors by electrochemotherapy. *BioMedical Engineering OnLine*, 9, 1: 10, doi: 10.1186/1475-925x-9-10, 12 p.
- Mir L.M., Gehl J., Sersa G., Collins C.G., Garbay J.R., Billard V., Geertsens P.F., Rudolf Z., O'Sullivan G.C., Marty M. 2006. Standard operating procedures of the electrochemotherapy: Instructions for the use of bleomycin or cisplatin administered either systemically or locally and electric pulses delivered by the Cliniporator™ by means of invasive or non-invasive electrodes. *European Journal of Cancer - Supplement*, 4, 11: 14–25
- Mir L.M., Orlowski S., Belehradek J.J., Paoletti C. 1991. Electrochemotherapy potentiation of antitumour effect of bleomycin by local electric pulses. *European journal of cancer*, 27, 1: 68–72
- Morren J., Roodenburg B., de Haan S.W.H. 2003. Electrochemical reactions and electrode corrosion in pulsed electric field (PEF) treatment chambers. *Innovative Food Science & Emerging Technologies*, 4, 3: 285–295
- Muralidharan A., Rems L., Kreutzer M.T., Boukany P.E. 2021. Actin networks regulate the cell membrane permeability during electroporation. *Biochimica et Biophysica Acta (BBA) - Biomembranes*, 1863, 1: 183468, doi: 10.1016/j.bbamem.2020.183468: 10 p.
- Novickij V., Malyško V., Želvys A., Balevičiūtė A., Zinkevičiūtė A., Novickij J., Girkontaitė I. 2020. Electrochemotherapy using doxorubicin and nanosecond electric field pulses: A pilot in vivo study. *Molecules*, 25, 20: 4601, doi: 10.3390/molecules25204601: 12 p.
- Nuccitelli R., Lui K., Kreis M., Athos B., Nuccitelli P. 2013. Nanosecond pulsed electric field stimulation of reactive oxygen species in human pancreatic cancer cells is Ca²⁺-dependent. *Biochemical and Biophysical Research Communications*, 435, 4: 580–585
- Nuccitelli R., McDaniel A., Connolly R., Zelickson B., Hartman H. 2020. Nano-Pulse Stimulation Induces Changes in the Intracellular Organelles in Rat Liver Tumors Treated In Situ. *Lasers in Surgery and Medicine*, 52, 9: 882–889

- Nuccitelli R., Pliquett U., Chen X., Ford W., James Swanson R., Beebe S.J., Kolb J.F., Schoenbach K.H. 2006. Nanosecond pulsed electric fields cause melanomas to self-destruct. *Biochemical and Biophysical Research Communications*, 343, 2: 351–360
- O'Brien T.J., Passeri M., Lorenzo M.F., Sulzer J.K., Lyman W.B., Swet J.H., Vrochides D., Baker E.H., Iannitti D.A., Davalos R. V., McKillop I.H. 2019. Experimental high-frequency irreversible electroporation using a single-needle delivery approach for nonthermal pancreatic ablation in vivo. *Journal of Vascular and Interventional Radiology*, 30, 6: 854–862
- Pakhomov A.G., Bowman A.M., Ibey B.L., Andre F.M., Pakhomova O.N., Schoenbach K.H. 2009. Lipid nanopores can form a stable, ion channel-like conduction pathway in cell membrane. *Biochemical and biophysical research communications*, 385, 2: 181–186
- Pakhomov A.G., Kolb J.F., White J.A., Joshi R.P., Xiao S., Schoenbach K.H. 2007a. Long-lasting plasma membrane permeabilization in mammalian cells by nanosecond Pulsed Electric Field (nsPEF). *Bioelectromagnetics*, 28, 8: 655–663
- Pakhomov A.G., Pakhomova O.N. 2020. The interplay of excitation and electroporation in nanosecond pulse stimulation. *Bioelectrochemistry*, 136: 107598, doi: 10.1016/j.bioelechem.2020.107598: 8 p.
- Pakhomov A.G., Shevin R., White J.A., Kolb J.F., Pakhomova O.N., Joshi R.P., Schoenbach K.H. 2007b. Membrane permeabilization and cell damage by ultrashort electric field shocks. *Archives of Biochemistry and Biophysics*, 465, 1: 109–118
- Pakhomova O.N., Gregory B.W., Khorokhorina V.A., Bowman A.M., Xiao S., Pakhomov A.G. 2011. Electroporation-induced electrosensitization. *PLoS ONE*, 6, 2: e17100, doi: 10.1371/journal.pone.0017100: 10 p.
- Pakhomova O.N., Khorokhorina V.A., Bowman A.M., Rodaite-Riševičienė R., Saulis G., Xiao S., Pakhomov A.G. 2012. Oxidative effects of nanosecond pulsed electric field exposure in cells and cell-free media. *Archives of Biochemistry and Biophysics*, 527, 1: 55–64
- Pataro G., Ferrari G. 2020. Limitations of pulsed electric field utilization in food industry. In: *Pulsed Electric Fields to Obtain Healthier and Sustainable Food for Tomorrow*. Barba F.J., Parniakov O., Wiktor A. (eds.). Amsterdam, Academic Press: 283–310
- Pirc E., Miklavčič D., Uršič K., Serša G., Reberšek M. 2021. High-frequency and high-voltage asymmetric bipolar pulse generator for electroporation based technologies and therapies. *Electronics*, 10, 10: 1203, doi: 10.3390/electronics10101203: 19 p.
- Pliquett U.F., Gusbeth C.A. 2000. Overcoming electrically induced artifacts in penetration studies with fluorescent tracers. *Bioelectrochemistry*, 51, 1: 75–79
- Pucihar G., Kotnik T., Miklavčič D., Teissié J. 2008. Kinetics of transmembrane transport of small molecules into electroporated cells. *Biophysical Journal*, 95, 6: 2837–2848
- Pucihar G., Krmelj J., Reberšek M., Batista Napotnik T., Miklavčič D. 2011. Equivalent Pulse Parameters for Electroporation. *IEEE Transactions on Biomedical Engineering*, 58, 11: 3279–3288
- Pucihar G., Mir L.M., Miklavčič D. 2002. The effect of pulse repetition frequency on the uptake into electroporated cells in vitro with possible applications in electrochemotherapy. *Bioelectrochemistry*, 57, 2: 167–172

- Reberšek M., Miklavčič D. 2010. Concepts of Electroporation Pulse Generation and Overview of Electric Pulse Generators for Cell and Tissue Electroporation. In: Advanced Electroporation Techniques in Biology and Medicine. Pakhomov A.G., Miklavčič D., Markov M.S. (eds.). Boca Raton, CRC Press, 323–339
- Reberšek M., Miklavčič D., Bertacchini C., Sack M. 2014. Cell membrane electroporation- Part 3: the equipment. IEEE Electrical Insulation Magazine, 30, 3: 8–18
- Rembiałkowska N., Novickij V., Baczyńska D., Dubińska-Magiera M., Saczko J., Rudno-Rudzińska J., Maciejewska M., Kulbacka J. 2022. Micro-and Nanosecond Pulses Used in Doxorubicin Electrochemotherapy in Human Breast and Colon Cancer Cells with Drug Resistance. Molecules, 27, 7: 2052, doi: 10.3390/molecules27072052: 14 p.
- Rems L., Kasimova M.A., Testa I., Delemotte L. 2020. Pulsed Electric Fields Can Create Pores in the Voltage Sensors of Voltage-Gated Ion Channels. Biophysical Journal, 119, 1: 190–205
- Rems L., Miklavčič D. 2016. Tutorial: Electroporation of cells in complex materials and tissue. Journal of Applied Physics, 119, 20: 201101, doi: 10.1063/1.4949264: 22 p.
- Rems L., Viano M., Kasimova M.A., Miklavčič D., Tarek M. 2019. The contribution of lipid peroxidation to membrane permeability in electroporation: A molecular dynamics study. Bioelectrochemistry, 125: 46–57
- Ren Z., Chen X., Cui G., Yin S., Chen L., Jiang J., Hu Z., Xie H., Zheng S., Zhou L. 2013. Nanosecond pulsed electric field inhibits cancer growth followed by alteration in expressions of NF- κ B and Wnt/ β -catenin signaling molecules. PloS one, 8, 9: e74322, doi: 10.1371/journal.pone.0074322: 13 p.
- Ringel-Scaia V.M., Beitel-White N., Lorenzo M.F., Brock R.M., Huie K.E., Coutermarsh-Ott S., Eden K., McDaniel D.K., Verbridge S.S., Rossmeisl J.H.J., Oestreich K.J., Davalos R. V., Allen I.C. 2019. High-frequency irreversible electroporation is an effective tumor ablation strategy that induces immunologic cell death and promotes systemic anti-tumor immunity. EBioMedicine, 44: 112–125
- Rogers W.R., Merritt J.H., Comeaux J.A., Kuhnel C.T., Moreland D.F., Teltschik D.G., Lucas J.H., Murphy M.R. 2004. Strength-duration curve an electrically excitable tissue extended down to near 1 nanosecond. IEEE Transactions on Plasma Science, 32, 4: 1587–1599
- Rols M.-P., Teissié J. 1998. Electroporation of Mammalian Cells to Macromolecules: Control by Pulse Duration. Biophysical Journal, 75, 3: 1415–1423
- Roodenburg B., Morren J., Berg H.E. I., Haan S.W.H. De, de Haan S.W.H. 2005a. Metal release in a stainless steel Pulsed Electric Field (PEF) system: Part I. Effect of different pulse shapes; theory and experimental method. Innovative Food Science & Emerging Technologies, 6, 3: 327–336
- Roodenburg B., Morren J., Berg H.E. I., Haan S.W.H. De, de Haan S.W.H. 2005b. Metal release in a stainless steel pulsed electric field (PEF) system: Part II. The treatment of orange juice; related to legislation and treatment chamber lifetime. Innovative Food Science & Emerging Technologies, 6, 3: 337–345
- Ruiz-Fernández A.R., Campos L., Villanelo F., Gutiérrez-Maldonado S.E., Perez-Acle T. 2021. Exploring the conformational changes induced by nanosecond pulsed electric fields on the voltage sensing domain of a Ca²⁺ channel. Membranes, 11, 7: 473, doi: 10.3390/membranes11070473: 21 p.

- Runas K.A., Malmstadt N. 2015. Low levels of lipid oxidation radically increase the passive permeability of lipid bilayers. *Soft matter*, 11, 3: 499–505
- Sabatini K., Mattila J.-P., Megli F.M., Kinnunen P.K.J. 2006. Characterization of two oxidatively modified phospholipids in mixed monolayers with DPPC. *Biophysical journal*, 90, 12: 4488–4499
- Sano M.B., Arena C.B., DeWitt M.R., Saur D., Davalos R. V. 2014. In-vitro bipolar nano- and microsecond electro-pulse bursts for irreversible electroporation therapies. *Bioelectrochemistry*, 100: 69–79
- Šatkauskas S., Jakštys B., Ruzgys P., Jakutavičiūtė M. 2017. Different Cell Viability Assays Following Electroporation In Vitro. In: *Handbook of Electroporation*. Miklavčič D. (ed.). Cham, Springer: 1411–1424
- Saulis G., Rodaite R., Rodaitė-Riševičienė R., Dainauskaitė V.S., Saulė R. 2015. Electrochemical processes during high-voltage electric pulses and their importance in food processing technology. In: *Advances in Food Biotechnology*. Rai V. R. (ed.). Weinheim, John Wiley & Sons, doi: 10.1002/9781118864463: 575–592
- Schoenbach K.H., Abou-Ghazala A., Vithoulkas T., Alden R.W., Turner R., Beebe S. 1997. The effect of pulsed electrical fields on biological cells. In: *Digest of Technical Papers of 11th IEEE International Pulsed Power Conference, Baltimore, 29 June 1997 - 2 July 1997*. Cooperstein G., Vitkovitsky I. (eds.). New York, IEEE: 73–78
- Schoenbach K.H., Beebe S.J., Buescher E.S. 2001. Intracellular effect of ultrashort electrical pulses. *Bioelectromagnetics*, 22, 6: 440–448
- Scuderi M., Reberšek M., Miklavčič D., Dermol-Černe J. 2019. The use of high-frequency short bipolar pulses in cisplatin electrochemotherapy in vitro. *Radiology and oncology*, 53, 2: 194–205
- Semenov I., Xiao S., Kang D., Schoenbach K.H., Pakhomov A.G. 2015. Cell stimulation and calcium mobilization by picosecond electric pulses. *Bioelectrochemistry*, 105: 65–71
- Semenov I., Xiao S., Pakhomov A.G. 2013. Primary pathways of intracellular Ca²⁺ mobilization by nanosecond pulsed electric field. *Biochimica et Biophysica Acta - Biomembranes*, 1828, 3: 981–989
- Serša G., Čemažar M., Miklavčič D. 1995. Antitumor effectiveness of electrochemotherapy with cis-diamminedichloroplatinum(II) in mice. *Cancer research*, 55, 15: 3450–3455
- Serša G., Kranjc S., Ščančar J., Kržan M., Čemažar M. 2010. Electrochemotherapy of mouse sarcoma tumors using electric pulse trains with repetition frequencies of 1 Hz and 5 kHz. *The Journal of Membrane Biology*, 236, 1: 155–162
- Serša G., Štabuc B., Čemažar M., Jančar B., Miklavčič D., Rudolf Z. 1998. Electrochemotherapy with cisplatin: Potentiation of local cisplatin antitumour effectiveness by application of electric pulses in cancer patients. *European Journal of Cancer*, 34, 8: 1213–1218
- Siddiqui I.A., Latouche E.L., Dewitt M.R., Swet J.H., Kirks R.C., Baker E.H., Iannitti D.A., Vrochides D., Davalos R. V, McKillop I.H. 2016. Induction of rapid, reproducible hepatic ablations using next-generation, high frequency irreversible electroporation (H-FIRE) in vivo. *HPB*, 18, 9: 726–734
- Silve A., Leray I., Mir L.M. 2012. Demonstration of cell membrane permeabilization to medium-sized molecules caused by a single 10 ns electric pulse. *Bioelectrochemistry*, 87: 260–264

- Sözer E.B., Levine Z.A., Vernier P.T. 2017. Quantitative limits on small molecule transport via the electropore measuring and modeling single nanosecond perturbations. *Scientific Reports*, 7, 1: 1–13
- Speelmans G., Sips W.H.H.M., Grisel R.J.H., Staffhorst R.W.H.M., Fichtinger-Schepman A.M.J., Reedijk J., De Kruijff B. 1996. The interaction of the anti-cancer drug cisplatin with phospholipids is specific for negatively charged phospholipids and takes place at low chloride ion concentration. *Biochimica et Biophysica Acta - Biomembranes*, 1283, 1: 60–66
- Stacey M., Fox P., Buescher S., Kolb J. 2011. Nanosecond pulsed electric field induced cytoskeleton, nuclear membrane and telomere damage adversely impact cell survival. *Bioelectrochemistry*, 82, 2: 131–134
- Stacey M., Stickley J., Fox P., Statler V., Schoenbach K., Beebe S.J., Buescher S. 2003. Differential effects in cells exposed to ultra-short, high intensity electric fields: cell survival, DNA damage, and cell cycle analysis. *Mutation Research/Genetic Toxicology and Environmental Mutagenesis*, 542, 1–2: 65–75
- Stapulionis R. 1999. Electric pulse-induced precipitation of biological macromolecules in electroporation. *Bioelectrochemistry and Bioenergetics*, 48, 1: 249–254
- Sugrue A., Vaidya V., Witt C., DeSimone C. V., Yasin O., Maor E., Killu A.M., Kapa S., McLeod C.J., Miklavčič D., Asirvatham S.J. 2019. Irreversible electroporation for catheter-based cardiac ablation: a systematic review of the preclinical experience. *Journal of interventional cardiac electrophysiology*, 55, 3: 251–265
- Sweeney D.C., Reberšek M., Dermol J., Rems L., Miklavčič D., Davalos R. V. 2016. Quantification of cell membrane permeability induced by monopolar and high-frequency bipolar bursts of electrical pulses. *Biochimica et Biophysica Acta (BBA) - Biomembranes*, 1858, 11: 2689–2698
- Szlasa W., Kiełbik A., Szewczyk A., Rembiałkowska N., Novickij V., Tarek M., Saczko J., Kulbacka J. 2021. Oxidative Effects during Irreversible Electroporation of Melanoma Cells—In Vitro Study. *Molecules*, 26: 154, doi: 10.3390/molecules26010154: 17 p.
- Tarek M. 2005. Membrane electroporation: a molecular dynamics simulation. *Biophysical journal*, 88, 6: 4045–4053
- Teissié J., Rols. 1994. Manipulation of Cell Cytoskeleton Affects the Lifetime of Cell Membrane Electroporation. *Annals of the New York Academy of Sciences*, 720, 1: 98–110
- Tekle E., Oubrahim H., Dzekunov S.M., Kolb J.F., Chock P.B. 2005. Selective Field Effects on Intracellular Vacuoles and Vesicle Membranes with Nanosecond Electric Pulses. *Biophysical Journal*, 89, 1: 274–284
- Thompson G.L., Beier H.T., Ibey B.L. 2018. Tracking lysosome migration within Chinese Hamster Ovary (CHO) cells following exposure to nanosecond pulsed electric fields. *Bioengineering*, 5, 4: 103, doi: 10.3390/bioengineering5040103: 8 p.
- Thompson G.L., Roth C.C., Dalzell D.R., Kuipers M.A., Ibey B.L. 2014. Calcium influx affects intracellular transport and membrane repair following nanosecond pulsed electric field exposure. *Journal of Biomedical Optics*, 19, 5: 055005, doi: 10.1117/1.JBO.19.5.055005: 12 p.
- Tieleman D.P. 2004. The molecular basis of electroporation. *BMC Biochemistry*, 5, 10, doi: 10.1186/1471-2091-5-10, 12 p.

- Tomov T., Tsoneva I. 2000. Are the stainless steel electrodes inert? *Bioelectrochemistry*, 51, 2: 207–209
- Tounekti O., Kenani A., Foray N., Orlowski S., Mir L.M. 2001. The ratio of single- to double-strand DNA breaks and their absolute values determine cell death pathway. *British Journal of Cancer*, 84, 9: 1272–1279
- Tounekti O., Pron G., Belehradek J., Mir L.M. 1993. Bleomycin, an Apoptosis-mimetic Drug That Induces Two Types of Cell Death Depending on the Number of Molecules Internalized. *Cancer Research*, 53, 22: 5462–5469
- Tunikowska J., Antończyk A., Rembiałkowska N., Jóźwiak Ł., Novickij V., Kulbacka J. 2020. The first application of nanoelectrochemotherapy in feline oral malignant melanoma treatment— case study. *Animals*, 10, 4: 556, doi: 10.3390/ani10040556: 6 p.
- Ursic K., Kos S., Kamensek U., Cemazar M., Scancar J., Bucek S., Kranjc S., Staresinic B., Sersa G. 2018. Comparable effectiveness and immunomodulatory actions of oxaliplatin and cisplatin in electrochemotherapy of murine melanoma. *Bioelectrochemistry*, 119: 161–171
- Van der Paal J., Neyts E.C., Verlact C.C.W., Bogaerts A. 2016. Effect of lipid peroxidation on membrane permeability of cancer and normal cells subjected to oxidative stress. *Chemical Science*, 7, 1: 489–498
- Vernier P.T., Levine Z.A., Wu Y.H., Joubert V., Ziegler M.J., Mir L.M., Tieleman D.P. 2009. Electroporating fields target oxidatively damaged areas in the cell membrane. *PLoS ONE*, 4, 11: e7966, doi: 10.1371/journal.pone.0007966: 8 p.
- Vernier P.T., Sun Y., Gundersen M.A. 2006. Nanoelectropulse-driven membrane perturbation and small molecule permeabilization. *BMC Cell Biology*, 7: 37, doi: 10.1186/1471-2121-7-37: 16 p.
- Vižintin A., Marković S., Ščančar J., Kladnik J., Turel I., Miklavčič D. 2022. Nanosecond electric pulses are equally effective in electrochemotherapy with cisplatin as microsecond pulses. *Radiology and Oncology*, 56, 3: 326–335
- Vižintin A., Marković S., Ščančar J., Miklavčič D. 2021. Electroporation with nanosecond pulses and bleomycin or cisplatin results in efficient cell kill and low metal release from electrodes. *Bioelectrochemistry*, 140: 107798, doi: 10.1016/j.bioelechem.2021.107798: 12 p.
- Vižintin A., Vidmar J., Ščančar J., Miklavčič D. 2020. Effect of interphase and interpulse delay in high-frequency irreversible electroporation pulses on cell survival, membrane permeabilization and electrode material release. *Bioelectrochemistry*, 134: 107523, doi: 10.1016/j.bioelechem.2020.107523: 14 p.
- White J.A., Blackmore P.F., Schoenbach K.H., Beebe S.J. 2004. Stimulation of capacitative calcium entry in HL-60 cells by nanosecond pulsed electric fields. *The Journal of biological chemistry*, 279, 22: 22964–22972
- Wiczew D., Szulc N., Tarek M. 2021. Molecular dynamics simulations of the effects of lipid oxidation on the permeability of cell membranes. *Bioelectrochemistry*, 141: 107869, doi: 10.1016/j.bioelechem.2021.107869: 14 p.
- Wong-Ekkabut J., Xu Z., Triampo W., Tang I.-M., Tieleman D.P., Monticelli L. 2007. Effect of lipid peroxidation on the properties of lipid bilayers: a molecular dynamics study. *Biophysical journal*, 93, 12: 4225–4236

- Yao C., Dong S., Zhao Y., Lv Y., Liu H., Gong L., Ma J., Wang H., Sun Y. 2017. Bipolar microsecond pulses and insulated needle electrodes for reducing muscle contractions during irreversible electroporation. *IEEE Transactions on Biomedical Engineering*, 64, 12: 2924–2937
- Zakelj M.N., Prevc A., Kranjc S., Cemazar M., Todorovic V., Savarin M., Scancar J., Kosjek T., Groselj B., Strojani P., Sersa G. 2019. Electrochemotherapy of radioresistant head and neck squamous cell carcinoma cells and tumor xenografts. *Oncology Reports*, 41, 3: 1658–1668
- Zhang L., Ye Y., Zhang X., Li X., Chen Q., Sun J.C.W. 2020. Cisplatin under oriented external electric fields: A deeper insight into electrochemotherapy at the molecular level. *International Journal of Quantum Chemistry*, 121, e26578, doi: 10.1002/qua.26578: 9 p.
- Zou H., Gan X.L., Linghu L.J., Chen C., Hu L.N., Zhang Y. 2013. Intense nanosecond pulsed electric fields promote cancer cell apoptosis through centrosome-dependent pathway involving reduced level of PLK1. *European Review for Medical and Pharmacological Sciences*, 17, 2: 152–160
- Županič A., Kos B., Miklavčič D. 2012. Treatment planning of electroporation-based medical interventions: electrochemotherapy, gene electrotransfer and irreversible electroporation. *Physics in Medicine & Biology*, 57, 17: 5425–5440

ACKNOWLEDGEMENTS

I would like to express my sincere gratitude to everyone who contributed to this thesis. First of all, I would like to express my deepest gratitude to my PhD supervisor, Prof. Dr. Damijan Miklavčič, for his guidance, feedback and personal support. Many thanks to all colleagues from the Laboratory of Biocybernetics who unselfishly shared their knowledge with me, for their help with practical matters and for all the friendly chats. I would also like to acknowledge the contribution of other research colleagues with whom I have had the pleasure to collaborate on this journey.

I would like to thank the members of the thesis evaluation committee for their constructive feedback, fruitful discussions, and timely completion of all work.

I am very grateful to my family and friends for their support throughout my studies.

Special thanks to Alexnadra Asanovna Elbakyan for her contribution to open science.

ZAHVALA

Iskrena zahvala vsem, ki so prispevale_i k nastanku te doktorske disertacije. Posebej bi se rada zahvalila mentorju prof. dr. Damijanu Miklavčiču za usmerjanje, povratne informacije in vso podporo. Najlepša hvala kolegicam in kolegom iz Laboratorija za biokibernetiko za vse znanje, ki so ga nesebično delile_i z menoj, pomoč pri praktičnih zagatah in prijetno vzdušje v službi. Rada bi se zahvalila tudi ostalim kolegicam in kolegom, s katerimi mi je bilo v veselje sodelovati pri raziskavah.

Članom komisije za oceno doktorske disertacije se zahvaljujem za konstruktivne komentarje, plodne razprave in pravočasno opravljeno delo.

Zelo sem hvaležna svoji družini in prijateljicam_em za vso podporo v času študija.

Posebna zahvala Aleksandri Asanovni Elbakjan za njen prispevek k odprti znanosti.

ANNEX A

Consent from publishers for the re-publication of Figure 1 from the journal article entitled *Membrane Electroporation and Electroporability: Mechanisms and Models*

19. 08. 22, 15:30 <https://marketplace.copyright.com/rs-ui-web/mp/license/778ac517-0ef1-4e77-85c5-a8ff321d4ac8/73b9fc72-9ef6-4907-b169-2...>



This is a License Agreement between Angelika Vizintin ("User") and Copyright Clearance Center, Inc. ("CCC") on behalf of the Rightsholder identified in the order details below. The license consists of the order details, the Marketplace Order General Terms and Conditions below, and any Rightsholder Terms and Conditions which are included below.

All payments must be made in full to CCC in accordance with the Marketplace Order General Terms and Conditions below.

Order Date	16-Aug-2022	Type of Use	Republish in a
Order License ID	1258423-1	Publisher	thesis/dissertation
ISSN	1936-1238	Portion	Annual Reviews
			Chart/graph/table/figure

LICENSED CONTENT

Publication Title	Annual review of biophysics	Rightsholder	Annual Reviews, Inc.
Date	01/01/2008	Publication Type	e-Journal
Language	English	URL	http://arjournals.annualreviews.org/loi/biophys
Country	United States of America		

REQUEST DETAILS

Portion Type	Chart/graph/table/figure	Distribution	Worldwide
Number of charts / graphs / tables / figures requested	1	Translation	Original language of publication
Format (select all that apply)	Print, Electronic	Copies for the disabled?	No
Who will republish the content?	Academic institution	Minor editing privileges?	No
Duration of Use	Life of current edition	Incidental promotional use?	No
Lifetime Unit Quantity	Up to 499	Currency	EUR
Rights Requested	Main product		

NEW WORK DETAILS

Title	Alternative Pulse Waveforms In Electroporation-based Technologies	Institution name	University of Ljubljana
Instructor name	Angelika Vizintin	Expected presentation date	2022-12-23

ADDITIONAL DETAILS

Order reference number	N/A	The requesting person / organization to appear on the license	Angelika Vizintin
------------------------	-----	---	-------------------

REUSE CONTENT DETAILS

Title, description or numeric reference of the portion(s)	Figure 1	Title of the article/chapter the portion is from	Membrane Electroporation and Electroporability: Mechanisms and Models
---	----------	--	---

19. 08. 22, 15:30	https://marketplace.copyright.com/rs-ui-web/mp/license/778ac517-0ef1-4e77-85c5-a8ff321d4ac8/73b9fc72-9ef6-4907-b169-2...		
Editor of portion(s)	N/A	Author of portion(s)	Tadej Kotnik, Lea Rems, Mounir Tarek, and Damijan Miklavčič
Volume of serial or monograph	48		
Page or page range of portion	65	Issue, if republishing an article from a serial	N/A
		Publication date of portion	2019-02-20

Marketplace Order General Terms and Conditions

The following terms and conditions ("General Terms"), together with any applicable Publisher Terms and Conditions, govern User's use of Works pursuant to the Licenses granted by Copyright Clearance Center, Inc. ("CCC") on behalf of the applicable Rightsholders of such Works through CCC's applicable Marketplace transactional licensing services (each, a "Service").

1) **Definitions.** For purposes of these General Terms, the following definitions apply:

"License" is the licensed use the User obtains via the Marketplace platform in a particular licensing transaction, as set forth in the Order Confirmation.

"Order Confirmation" is the confirmation CCC provides to the User at the conclusion of each Marketplace transaction. "Order Confirmation Terms" are additional terms set forth on specific Order Confirmations not set forth in the General Terms that can include terms applicable to a particular CCC transactional licensing service and/or any Rightsholder-specific terms.

"Rightsholder(s)" are the holders of copyright rights in the Works for which a User obtains licenses via the Marketplace platform, which are displayed on specific Order Confirmations.

"Terms" means the terms and conditions set forth in these General Terms and any additional Order Confirmation Terms collectively.

"User" or "you" is the person or entity making the use granted under the relevant License. Where the person accepting the Terms on behalf of a User is a freelancer or other third party who the User authorized to accept the General Terms on the User's behalf, such person shall be deemed jointly a User for purposes of such Terms.

"Work(s)" are the copyright protected works described in relevant Order Confirmations.

2) **Description of Service.** CCC's Marketplace enables Users to obtain Licenses to use one or more Works in accordance with all relevant Terms. CCC grants Licenses as an agent on behalf of the copyright rightsholder identified in the relevant Order Confirmation.

3) **Applicability of Terms.** The Terms govern User's use of Works in connection with the relevant License. In the event of any conflict between General Terms and Order Confirmation Terms, the latter shall govern. User acknowledges that Rightsholders have complete discretion whether to grant any permission, and whether to place any limitations on any grant, and that CCC has no right to supersede or to modify any such discretionary act by a Rightsholder.

4) **Representations; Acceptance.** By using the Service, User represents and warrants that User has been duly authorized by the User to accept, and hereby does accept, all Terms.

5) **Scope of License; Limitations and Obligations.** All Works and all rights therein, including copyright rights, remain the sole and exclusive property of the Rightsholder. The License provides only those rights expressly set forth in the terms and conveys no other rights in any Works

6) **General Payment Terms.** User may pay at time of checkout by credit card or choose to be invoiced. If the User chooses to be invoiced, the User shall: (i) remit payments in the manner identified on specific invoices, (ii) unless otherwise specifically stated in an Order Confirmation or separate written agreement, Users shall remit payments upon receipt of the relevant invoice from CCC, either by delivery or notification of availability of the invoice via the Marketplace platform, and (iii) if the User does not pay the invoice within 30 days of receipt, the User may incur a service charge of 1.5% per month or the maximum rate allowed by applicable law, whichever is less. While User may exercise the rights in the License immediately upon receiving the Order Confirmation, the License is automatically revoked and is null and void, as if it had never been issued, if CCC does not receive complete payment on a timely basis.

7) **General Limits on Use.** Unless otherwise provided in the Order Confirmation, any grant of rights to User only the rights set forth in the Terms and does not include subsequent or additional uses, (ii) is non-exclusive, transferable, and (iii) is subject to any and all limitations and restrictions (such as, but not limited to, 137 sec duration of use or circulation) included in the Terms. Upon completion of the licensed use as set forth in the Order

19. 08. 22, 15:30 <https://marketplace.copyright.com/rs-ui-web/mp/license/778ac517-0ef1-4e77-85c5-a8ff321d4ac8/73b9fc72-9ef6-4907-b169-2...>

Confirmation, User shall either secure a new permission for further use of the Work(s) or immediately cease any new use of the Work(s) and shall render inaccessible (such as by deleting or by removing or severing links or other locators) any further copies of the Work. User may only make alterations to the Work if and as expressly set forth in the Order Confirmation. No Work may be used in any way that is defamatory, violates the rights of third parties (including such third parties' rights of copyright, privacy, publicity, or other tangible or intangible property), or is otherwise illegal, sexually explicit, or obscene. In addition, User may not conjoin a Work with any other material that may result in damage to the reputation of the Rightsholder. User agrees to inform CCC if it becomes aware of any infringement of any rights in a Work and to cooperate with any reasonable request of CCC or the Rightsholder in connection therewith.

8) **Third Party Materials.** In the event that the material for which a License is sought includes third party materials (such as photographs, illustrations, graphs, inserts and similar materials) that are identified in such material as having been used by permission (or a similar indicator), User is responsible for identifying, and seeking separate licenses (under this Service, if available, or otherwise) for any of such third party materials; without a separate license, User may not use such third party materials via the License.

9) **Copyright Notice.** Use of proper copyright notice for a Work is required as a condition of any License granted under the Service. Unless otherwise provided in the Order Confirmation, a proper copyright notice will read substantially as follows: "Used with permission of [Rightsholder's name], from [Work's title, author, volume, edition number and year of copyright]; permission conveyed through Copyright Clearance Center, Inc." Such notice must be provided in a reasonably legible font size and must be placed either on a cover page or in another location that any person, upon gaining access to the material which is the subject of a permission, shall see, or in the case of republication Licenses, immediately adjacent to the Work as used (for example, as part of a by-line or footnote) or in the place where substantially all other credits or notices for the new work containing the republished Work are located. Failure to include the required notice results in loss to the Rightsholder and CCC, and the User shall be liable to pay liquidated damages for each such failure equal to twice the use fee specified in the Order Confirmation, in addition to the use fee itself and any other fees and charges specified.

10) **Indemnity.** User hereby indemnifies and agrees to defend the Rightsholder and CCC, and their respective employees and directors, against all claims, liability, damages, costs, and expenses, including legal fees and expenses, arising out of any use of a Work beyond the scope of the rights granted herein and in the Order Confirmation, or any use of a Work which has been altered in any unauthorized way by User, including claims of defamation or infringement of rights of copyright, publicity, privacy, or other tangible or intangible property.

11) **Limitation of Liability.** UNDER NO CIRCUMSTANCES WILL CCC OR THE RIGHTSHOLDER BE LIABLE FOR ANY DIRECT, INDIRECT, CONSEQUENTIAL, OR INCIDENTAL DAMAGES (INCLUDING WITHOUT LIMITATION DAMAGES FOR LOSS OF BUSINESS PROFITS OR INFORMATION, OR FOR BUSINESS INTERRUPTION) ARISING OUT OF THE USE OR INABILITY TO USE A WORK, EVEN IF ONE OR BOTH OF THEM HAS BEEN ADVISED OF THE POSSIBILITY OF SUCH DAMAGES. In any event, the total liability of the Rightsholder and CCC (including their respective employees and directors) shall not exceed the total amount actually paid by User for the relevant License. User assumes full liability for the actions and omissions of its principals, employees, agents, affiliates, successors, and assigns.

12) **Limited Warranties.** THE WORK(S) AND RIGHT(S) ARE PROVIDED "AS IS." CCC HAS THE RIGHT TO GRANT TO USER THE RIGHTS GRANTED IN THE ORDER CONFIRMATION DOCUMENT. CCC AND THE RIGHTSHOLDER DISCLAIM ALL OTHER WARRANTIES RELATING TO THE WORK(S) AND RIGHT(S), EITHER EXPRESS OR IMPLIED, INCLUDING WITHOUT LIMITATION IMPLIED WARRANTIES OF MERCHANTABILITY OR FITNESS FOR A PARTICULAR PURPOSE. ADDITIONAL RIGHTS MAY BE REQUIRED TO USE ILLUSTRATIONS, GRAPHS, PHOTOGRAPHS, ABSTRACTS, INSERTS, OR OTHER PORTIONS OF THE WORK (AS OPPOSED TO THE ENTIRE WORK) IN A MANNER CONTEMPLATED BY USER; USER UNDERSTANDS AND AGREES THAT NEITHER CCC NOR THE RIGHTSHOLDER MAY HAVE SUCH ADDITIONAL RIGHTS TO GRANT.

13) **Effect of Breach.** Any failure by User to pay any amount when due, or any use by User of a Work beyond the scope of the License set forth in the Order Confirmation and/or the Terms, shall be a material breach of such License. Any breach not cured within 10 days of written notice thereof shall result in immediate termination of such License without further notice. Any unauthorized (but licensable) use of a Work that is terminated immediately upon notice thereof may be liquidated by payment of the Rightsholder's ordinary license price therefor; any unauthorized (and unlicensable) use that is not terminated immediately for any reason (including, for example, because materials containing the Work cannot reasonably be recalled) will be subject to all remedies available at law or in equity, but in no event to a payment of less than three times the Rightsholder's ordinary license price for the most closely analogous licensable use plus Rightsholder's and/or CCC's costs and expenses incurred in collecting such payment.

14) **Additional Terms for Specific Products and Services.** If a User is making one of the uses described in this Section 14, the additional terms and conditions apply:

a) **Print Uses of Academic Course Content and Materials** (*photocopies for academic coursepacks* & *handouts*). For photocopies for academic coursepacks or classroom handouts the following additional te



i) The copies and anthologies created under this License may be made and assembled by faculty ¹³⁷sec individually or at their request by on-campus bookstores or copy centers, or by off-campus copy shops and other

19. 08. 22, 15:30 <https://marketplace.copyright.com/rs-ui-web/mp/license/778ac517-0ef1-4e77-85c5-a8ff321d4ac8/73b9fc72-9ef6-4907-b169-2...>

similar entities.

ii) No License granted shall in any way: (i) include any right by User to create a substantively non-identical copy of the Work or to edit or in any other way modify the Work (except by means of deleting material immediately preceding or following the entire portion of the Work copied) (ii) permit "publishing ventures" where any particular anthology would be systematically marketed at multiple institutions.

iii) Subject to any Publisher Terms (and notwithstanding any apparent contradiction in the Order Confirmation arising from data provided by User), any use authorized under the academic pay-per-use service is limited as follows:

A) any License granted shall apply to only one class (bearing a unique identifier as assigned by the institution, and thereby including all sections or other subparts of the class) at one institution;

B) use is limited to not more than 25% of the text of a book or of the items in a published collection of essays, poems or articles;

C) use is limited to no more than the greater of (a) 25% of the text of an issue of a journal or other periodical or (b) two articles from such an issue;

D) no User may sell or distribute any particular anthology, whether photocopied or electronic, at more than one institution of learning;

E) in the case of a photocopy permission, no materials may be entered into electronic memory by User except in order to produce an identical copy of a Work before or during the academic term (or analogous period) as to which any particular permission is granted. In the event that User shall choose to retain materials that are the subject of a photocopy permission in electronic memory for purposes of producing identical copies more than one day after such retention (but still within the scope of any permission granted), User must notify CCC of such fact in the applicable permission request and such retention shall constitute one copy actually sold for purposes of calculating permission fees due; and

F) any permission granted shall expire at the end of the class. No permission granted shall in any way include any right by User to create a substantively non-identical copy of the Work or to edit or in any other way modify the Work (except by means of deleting material immediately preceding or following the entire portion of the Work copied).

iv) Books and Records; Right to Audit. As to each permission granted under the academic pay-per-use Service, User shall maintain for at least four full calendar years books and records sufficient for CCC to determine the numbers of copies made by User under such permission. CCC and any representatives it may designate shall have the right to audit such books and records at any time during User's ordinary business hours, upon two days' prior notice. If any such audit shall determine that User shall have underpaid for, or underreported, any photocopies sold or by three percent (3%) or more, then User shall bear all the costs of any such audit; otherwise, CCC shall bear the costs of any such audit. Any amount determined by such audit to have been underpaid by User shall immediately be paid to CCC by User, together with interest thereon at the rate of 10% per annum from the date such amount was originally due. The provisions of this paragraph shall survive the termination of this License for any reason.

b) **Digital Pay-Per-Uses of Academic Course Content and Materials (e-coursepacks, electronic reserves, learning management systems, academic institution intranets).** For uses in e-coursepacks, posts in electronic reserves, posts in learning management systems, or posts on academic institution intranets, the following additional terms apply:

i) The pay-per-uses subject to this Section 14(b) include:

A) Posting e-reserves, course management systems, e-coursepacks for text-based content, which grants authorizations to import requested material in electronic format, and allows electronic access to this material to members of a designated college or university class, under the direction of an instructor designated by the college or university, accessible only under appropriate electronic controls (e.g., password);

B) Posting e-reserves, course management systems, e-coursepacks for material consisting of photographs or other still images not embedded in text, which grants not only the authorizations described in Section 14(b)(i)(A) above, but also the following authorization: to include the requested material in course materials for use consistent with Section 14(b)(i)(A) above, including any necessary resizing, reformatting or modification of the resolution of such requested material (provided that such modification does not alter the underlying editorial content or meaning of the requested material, and provided that the resulting modification is used solely within the scope of, and in a manner consistent with, the particular authorization described in the Order Confirmation and the Terms), but not including any other form of manipulation, alteration, or reproduction of the requested material;



137 sec

19. 08. 22, 15:30

<https://marketplace.copyright.com/rs-ui-web/mp/license/778ac517-0ef1-4e77-85c5-a8ff321d4ac8/73b9fc72-9ef6-4907-b169-2...>

C) Posting e-reserves, course management systems, e-coursepacks or other academic distribution for audiovisual content, which grants not only the authorizations described in Section 14(b)(i)(A) above, but also the following authorizations: (i) to include the requested material in course materials for use consistent with Section 14(b)(i)(A) above; (ii) to display and perform the requested material to such members of such class in the physical classroom or remotely by means of streaming media or other video formats; and (iii) to "clip" or reformat the requested material for purposes of time or content management or ease of delivery, provided that such "clipping" or reformatting does not alter the underlying editorial content or meaning of the requested material and that the resulting material is used solely within the scope of, and in a manner consistent with, the particular authorization described in the Order Confirmation and the Terms. Unless expressly set forth in the relevant Order Confirmation, the License does not authorize any other form of manipulation, alteration or editing of the requested material.

ii) Unless expressly set forth in the relevant Order Confirmation, no License granted shall in any way: (i) include any right by User to create a substantively non-identical copy of the Work or to edit or in any other way modify the Work (except by means of deleting material immediately preceding or following the entire portion of the Work copied or, in the case of Works subject to Sections 14(b)(1)(B) or (C) above, as described in such Sections) (ii) permit "publishing ventures" where any particular course materials would be systematically marketed at multiple institutions.

iii) Subject to any further limitations determined in the Rightsholder Terms (and notwithstanding any apparent contradiction in the Order Confirmation arising from data provided by User), any use authorized under the electronic course content pay-per-use service is limited as follows:

A) any License granted shall apply to only one class (bearing a unique identifier as assigned by the institution, and thereby including all sections or other subparts of the class) at one institution;

B) use is limited to not more than 25% of the text of a book or of the items in a published collection of essays, poems or articles;

C) use is limited to not more than the greater of (a) 25% of the text of an issue of a journal or other periodical or (b) two articles from such an issue;

D) no User may sell or distribute any particular materials, whether photocopied or electronic, at more than one institution of learning;

E) electronic access to material which is the subject of an electronic-use permission must be limited by means of electronic password, student identification or other control permitting access solely to students and instructors in the class;

F) User must ensure (through use of an electronic cover page or other appropriate means) that any person, upon gaining electronic access to the material, which is the subject of a permission, shall see:

- o a proper copyright notice, identifying the Rightsholder in whose name CCC has granted permission,
- o a statement to the effect that such copy was made pursuant to permission,
- o a statement identifying the class to which the material applies and notifying the reader that the material has been made available electronically solely for use in the class, and
- o a statement to the effect that the material may not be further distributed to any person outside the class, whether by copying or by transmission and whether electronically or in paper form, and User must also ensure that such cover page or other means will print out in the event that the person accessing the material chooses to print out the material or any part thereof.

G) any permission granted shall expire at the end of the class and, absent some other form of authorization, User is thereupon required to delete the applicable material from any electronic storage or to block electronic access to the applicable material.

iv) Uses of separate portions of a Work, even if they are to be included in the same course material or the same university or college class, require separate permissions under the electronic course content pay-per-use Service. Unless otherwise provided in the Order Confirmation, any grant of rights to User is limited to use completed no later than the end of the academic term (or analogous period) as to which any particular permission is granted.

v) Books and Records; Right to Audit. As to each permission granted under the electronic course content pay-per-use Service, User shall maintain for at least four full calendar years books and records sufficient for CCC to determine the numbers of copies made by User under such permission. CCC and any representatives it may designate shall have the right to audit such books and records at any time during User's ordinary business hours, upon two weeks prior written notice.



19. 08. 22, 15:30 <https://marketplace.copyright.com/rs-ui-web/mp/license/778ac517-0ef1-4e77-85c5-a8ff321d4ac8/73b9fc72-9ef6-4907-b169-2...>

notice. If any such audit shall determine that User shall have underpaid for, or underreported, any electronic copies used by three percent (3%) or more, then User shall bear all the costs of any such audit; otherwise, CCC shall bear the costs of any such audit. Any amount determined by such audit to have been underpaid by User shall immediately be paid to CCC by User, together with interest thereon at the rate of 10% per annum from the date such amount was originally due. The provisions of this paragraph shall survive the termination of this license for any reason.

c) **Pay-Per-Use Permissions for Certain Reproductions (Academic photocopies for library reserves and interlibrary loan reporting) (Non-academic internal/external business uses and commercial document delivery).** The License expressly excludes the uses listed in Section (c)(i)-(v) below (which must be subject to separate license from the applicable Rightsholder) for: academic photocopies for library reserves and interlibrary loan reporting; and non-academic internal/external business uses and commercial document delivery.

- i) electronic storage of any reproduction (whether in plain-text, PDF, or any other format) other than on a transitory basis;
- ii) the input of Works or reproductions thereof into any computerized database;
- iii) reproduction of an entire Work (cover-to-cover copying) except where the Work is a single article;
- iv) reproduction for resale to anyone other than a specific customer of User;
- v) republication in any different form. Please obtain authorizations for these uses through other CCC services or directly from the rightsholder.

Any license granted is further limited as set forth in any restrictions included in the Order Confirmation and/or in these Terms.

d) **Electronic Reproductions in Online Environments (Non-Academic-email, intranet, internet and extranet).** For "electronic reproductions", which generally includes e-mail use (including instant messaging or other electronic transmission to a defined group of recipients) or posting on an intranet, extranet or Intranet site (including any display or performance incidental thereto), the following additional terms apply:


- i) Unless otherwise set forth in the Order Confirmation, the License is limited to use completed within 30 days for any use on the Internet, 60 days for any use on an intranet or extranet and one year for any other use, all as measured from the "republication date" as identified in the Order Confirmation, if any, and otherwise from the date of the Order Confirmation.
- ii) User may not make or permit any alterations to the Work, unless expressly set forth in the Order Confirmation (after request by User and approval by Rightsholder); provided, however, that a Work consisting of photographs or other still images not embedded in text may, if necessary, be resized, reformatted or have its resolution modified without additional express permission, and a Work consisting of audiovisual content may, if necessary, be "clipped" or reformatted for purposes of time or content management or ease of delivery (provided that any such resizing, reformatting, resolution modification or "clipping" does not alter the underlying editorial content or meaning of the Work used, and that the resulting material is used solely within the scope of, and in a manner consistent with, the particular License described in the Order Confirmation and the Terms.

15) Miscellaneous.

a) User acknowledges that CCC may, from time to time, make changes or additions to the Service or to the Terms, and that Rightsholder may make changes or additions to the Rightsholder Terms. Such updated Terms will replace the prior terms and conditions in the order workflow and shall be effective as to any subsequent Licenses but shall not apply to Licenses already granted and paid for under a prior set of terms.

b) Use of User-related information collected through the Service is governed by CCC's privacy policy, available online at www.copyright.com/about/privacy-policy/.

c) The License is personal to User. Therefore, User may not assign or transfer to any other person (whether a natural person or an organization of any kind) the License or any rights granted thereunder; provided, however, that, where applicable, User may assign such License in its entirety on written notice to CCC in the event of a transfer of all or substantially all of User's rights in any new material which includes the Work(s) licensed under this Service.

d) No amendment or waiver of any Terms is binding unless set forth in writing and signed by the appropriate parties including, where applicable, the Rightsholder. The Rightsholder and CCC hereby object to any terms containing writing prepared by or on behalf of the User or its principals, employees, agents or affiliates and purporting to otherwise relate to the License described in the Order Confirmation, which terms are in any way inconsistent with any Terms set forth in the Order Confirmation, and/or in CCC's standard operating procedures, whether  137 sec

19. 08. 22, 15:30 <https://marketplace.copyright.com/rs-ui-web/mp/license/778ac517-0ef1-4e77-85c5-a8ff321d4ac8/73b9fc72-9ef6-4907-b169-2...>

is prepared prior to, simultaneously with or subsequent to the Order Confirmation, and whether such writing appears on a copy of the Order Confirmation or in a separate instrument.

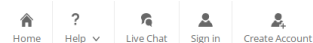
e) The License described in the Order Confirmation shall be governed by and construed under the law of the State of New York, USA, without regard to the principles thereof of conflicts of law. Any case, controversy, suit, action, or proceeding arising out of, in connection with, or related to such License shall be brought, at CCC's sole discretion, in any federal or state court located in the County of New York, State of New York, USA, or in any federal or state court whose geographical jurisdiction covers the location of the Rightsholder set forth in the Order Confirmation. The parties expressly submit to the personal jurisdiction and venue of each such federal or state court.



137 sec

ANNEX B

Consent from publishers for the re-publication of the article entitled *Effect of interphase and interpulse delay in high-frequency irreversible electroporation pulses on cell survival, membrane permeabilization and electrode material release*



Effect of interphase and interpulse delay in high-frequency irreversible electroporation pulses on cell survival, membrane permeabilization and electrode material release

Author: Angelika Vizintin, Janja Vidmar, Janez Ščančar, Damijan Miklavčič

Publication: Bioelectrochemistry

Publisher: Elsevier

Date: August 2020

© 2020 Elsevier B.V. All rights reserved.

Journal Author Rights

Please note that, as the author of this Elsevier article, you retain the right to include it in a thesis or dissertation, provided it is not published commercially. Permission is not required, but please ensure that you reference the journal as the original source. For more information on this and on your other retained rights, please visit: <https://www.elsevier.com/about/our-business/policies/copyright#Author-rights>

BACK

CLOSE WINDOW